

## **NOTE TO USERS**

**This reproduction is the best copy available.**

UMI<sup>®</sup>



**INTEGRATION OF BOREHOLE AND SEISMIC DATA TO  
UNRAVEL COMPLEX STRATIGRAPHY:  
CASE STUDIES FROM THE MANNVILLE GROUP,  
WESTERN CANADA**

Sabrina Esther Sarzalejo Silva

Department of Earth and Planetary Sciences

McGill University, Montreal

February 2009

Thesis submitted to McGill University in partial fulfillment of the requirements  
of the degree of Doctor of Philosophy

©Sabrina Esther Sarzalejo Silva, 2009



Library and Archives  
Canada

Published Heritage  
Branch

395 Wellington Street  
Ottawa ON K1A 0N4  
Canada

Bibliothèque et  
Archives Canada

Direction du  
Patrimoine de l'édition

395, rue Wellington  
Ottawa ON K1A 0N4  
Canada

*Your file* *Votre référence*  
ISBN: 978-0-494-66559-6  
*Our file* *Notre référence*  
ISBN: 978-0-494-66559-6

**NOTICE:**

The author has granted a non-exclusive license allowing Library and Archives Canada to reproduce, publish, archive, preserve, conserve, communicate to the public by telecommunication or on the Internet, loan, distribute and sell theses worldwide, for commercial or non-commercial purposes, in microform, paper, electronic and/or any other formats.

The author retains copyright ownership and moral rights in this thesis. Neither the thesis nor substantial extracts from it may be printed or otherwise reproduced without the author's permission.

---

In compliance with the Canadian Privacy Act some supporting forms may have been removed from this thesis.

While these forms may be included in the document page count, their removal does not represent any loss of content from the thesis.

**AVIS:**

L'auteur a accordé une licence non exclusive permettant à la Bibliothèque et Archives Canada de reproduire, publier, archiver, sauvegarder, conserver, transmettre au public par télécommunication ou par l'Internet, prêter, distribuer et vendre des thèses partout dans le monde, à des fins commerciales ou autres, sur support microforme, papier, électronique et/ou autres formats.

L'auteur conserve la propriété du droit d'auteur et des droits moraux qui protègent cette thèse. Ni la thèse ni des extraits substantiels de celle-ci ne doivent être imprimés ou autrement reproduits sans son autorisation.

---

Conformément à la loi canadienne sur la protection de la vie privée, quelques formulaires secondaires ont été enlevés de cette thèse.

Bien que ces formulaires aient inclus dans la pagination, il n'y aura aucun contenu manquant.

  
**Canada**

## Table of Contents

Table of Contents .....	2
Abstract .....	6
Résumé.....	8
Contributions of Authors .....	10
Acknowledgements.....	11
1. General Introduction .....	13
1.1 Introduction.....	13
1.2 Overview of integrated geological and geophysical studies.....	16
1.3 Motivation and Goals.....	19
1.4 Thesis Organization .....	20
1.5 References.....	23
INTRODUCTION TO CHAPTER 2.....	30
2. Stratigraphy and Lithologic Heterogeneity in the Mannville Group (Southeast Saskatchewan) Defined by Integrating 3-D Seismic and Log Data .....	31
2.1 Abstract.....	32
2.2 Introduction.....	33
2.3 Geological Setting.....	34
2.4 Database and Methodology.....	36
2.5 Interpretation.....	38
2.5.1.a Unit A – Description .....	40
2.5.1.b Unit A – Interpretation.....	40
2.5.2.a Unit B – Description .....	41

2.5.2.b Unit B – Interpretation .....	41
2.5.3.a Unit C – Description .....	43
2.5.3.b Unit C – Interpretation .....	43
2.5.4.a Unit D – Description .....	44
2.5.4.b Unit D – Interpretation.....	44
2.6 Discussion .....	45
2.7 Conclusions.....	49
2.8 Acknowledgements.....	51
2.9 References.....	52
2.10 List of Figures .....	57
INTRODUCTION TO CHAPTER 3.....	61
3. 3-Dimensional Distribution of Channels in a Lower Cretaceous (Mannville Group) Heavy Oil Reservoir in west-central Saskatchewan; Part 1: Seismic Attribute-Based Generation of a Pseudo-Lithology Volume.....	62
3.1 Abstract.....	62
3.2 Introduction.....	63
3.3 Geological Overview .....	65
3.4 Database and Methodology.....	66
3.5 Results.....	68
3.5.1 Stratigraphic correlation.....	68
3.5.2 Attribute Study.....	71
3.6 Discussion .....	76
3.7 Conclusions.....	85
3.8 Acknowledgements.....	87

3.9 References.....	88
3.10 List of Figures.....	93
INTRODUCTION TO CHAPTER 4.....	99
4.3 3-Dimensional Distribution of Channels in a Lower Cretaceous Mannville Heavy Oil Reservoir in west-central Saskatchewan; Part 2: Integration of Borehole and Seismic Data.....	100
4.1 Abstract.....	100
4.2 Introduction.....	102
4.3 Geological Overview.....	103
4.4 Database and General Methodology.....	105
4.5 Detail stratigraphic interpretation.....	107
4.5.1. Key stratigraphic surfaces.....	107
4.5.1. Combined seismic vertical and horizontal views.....	109
4.6 Lithofacies analysis.....	111
4.7 Stratigraphic Units.....	112
4.7.1.a Unit Z description.....	113
4.7.1.b Unit Z interpretation.....	113
4.7.2.a Unit Y description.....	114
4.7.2.b Unit Y interpretation.....	115
4.7.3.a Unit X description.....	115
4.7.3.b Unit X interpretation.....	115
4.7.4.a Unit W Description.....	116
4.7.5.a Unit V Description.....	117
4.7.5.b Unit V Interpretation.....	117

4.7.6.a Unit U Description .....	118
4.7.6.b Unit U Interpretation.....	119
4.7.7.a Units T and S description.....	119
4.7.7.b Unit T and S Interpretation .....	120
4.8 Integration.....	120
4.9 Discussion.....	126
4.10 Conclusions.....	128
4.11 Acknowledgements.....	130
4.12 References.....	131
4.13 List of Tables .....	134
4.14 List of Figures .....	137
5- Conclusions and Recommendations.....	143
Appendix 1:.....	149
Appendix 2:.....	150
Appendix 3:.....	151

## **Abstract**

Understanding the stratigraphic architecture of geologically complex reservoirs, such as the heavy oil deposits of Western Canada, is essential to achieve an efficient hydrocarbon recovery. Borehole and 3-D seismic data were integrated to define the stratigraphic architecture and generate 3-dimensional geological models of the Mannville Group in Saskatchewan. The Mannville is a stratigraphically complex unit formed of fluvial to marine deposits. Two areas in west-central and southern Saskatchewan were examined in this study. In west-central Saskatchewan, the area corresponds to a stratigraphically controlled heavy oil reservoir with production from the undifferentiated Dina-Cummings Members of the Lower Cretaceous Mannville Group. The southern area, although non-prospective for hydrocarbons, shares many similarities with time-equivalent strata in areas of heavy oil production. Seismic sequence stratigraphic principles together with log signatures permitted the subdivision of the Mannville into different packages. An initial geological model was generated integrating seismic and well-log data. Multiattribute analysis and neural networks were used to generate a pseudo-lithology or gamma-ray volume. The incorporation of borehole core data to the model and the subsequent integration with the lithological prediction were crucial to capture the distribution of reservoir and non-reservoir deposits in the study area. The ability to visualize the 3-D seismic data in a variety of ways, including arbitrary lines and stratal or horizon slicing techniques helped the definition of stratigraphic features such as channels and scroll bars that affect fluid flow in hydrocarbon producing areas. Small-scale heterogeneities in the

reservoir were not resolved due to the resolution of the seismic data. Although not undertaken in this study, the resulting stratigraphic framework could be used to help construct a static reservoir model. Because of the small size of the 3-D seismic surveys, horizontal slices through the data volume generally imaged only small portions of the paleogeomorphologic features thought to be present in this area. As such, it was only through the integration of datasets that the geological models were established.

## Résumé

La compréhension de l'architecture stratigraphique de gisements avec une géologie complexe comme celle des dépôts de pétrole lourd de l'Ouest canadien, est essentielle pour récupérer de façon efficiente le pétrole du sous-sol. Les données de puits de pétrole et de sismiques en 3-D ont été intégrées pour définir l'architecture stratigraphique et générer des modèles géologiques en 3 dimensions du Groupe Mannville au Saskatchewan. Le Groupe Mannville est une unité formée de sédiments fluviaux à marins avec une stratigraphie complexe. Deux zones, localisées au Sud et Centre-Ouest du Saskatchewan, ont été examinées dans cette étude. La zone située au Centre-Ouest du Saskatchewan correspond à un gisement de pétrole lourd, dominé par la stratigraphie, dont la production provient des membres, non-différenciés, Dina-Cummings appartenant au Groupe Mannville du Crétacé Inferieur. La zone située au Sud, malgré quelle ne soit pas productrice de pétrole, présente des strates, équivalentes en temps de déposition, qui ont beaucoup de similarités. Les principes de stratigraphie séquentielle sismique avec l'information des signaux des diagraphies différées ont permis de subdiviser le Groupe Mannville en différents paquets. Les données de la sismique et des diagraphies différées ont été utilisés pour la création d'un modèle géologique initial. L'analyse et l'utilisation de plusieurs attributs sismiques et des réseaux neurologiques ont permis la génération d'un volume de prédiction lithologique. L'incorporation des données provenant des carottes, obtenues pendant le forage des puits, dans le modèle et son intégration avec la prédiction

lithologique a été cruciale pour capturer la distribution des sédiments qui contiennent du pétrole et ceux qui n'en contiennent pas dans la zone étudiée. L'habilité de pouvoir visualiser les données sismiques 3-D de différentes façons, qui incluent les techniques de découpage en horizons ou strates et de lignes arbitraires, a aidé à définir les traits stratigraphiques qui affectent la circulation des fluides dans les zones de production de pétrole. Des hétérogénéités de petite échelle dans le gisement n'ont pu être résolues à cause des caractéristiques des données sismiques. La structure stratigraphique obtenue pourrait aider, au-delà de l'objectif entrepris par cette étude, à la construction d'un modèle de gisement statique. Comme l'étude a utilisé une petite levée sismique, les tranches horizontales à travers le volume de données seulement ont pu représenter des petites portions des éléments paléo-géomorphologiques interprétés dans cette étude. Pour cette raison, les modèles géologiques ont été établis à travers l'intégration de toutes les données utilisées.

## **Contributions of Authors**

The research presented in this thesis is the outcome of the collaboration between the author and his advisor Professor Bruce Hart. This thesis is divided into five chapters, one of which has been published (Chapter 2) and two of which are manuscripts intended for publication. The two remaining chapters correspond to the general introduction and conclusions. Each manuscript is co-authored by Prof. Bruce Hart, who provided advice on research methodology, helped assess and interpret the data and made critical reviews of the text. The author is responsible for all the experimental and analytical work involved in the thesis.

## **Acknowledgements**

This thesis is dedicated to my mother Sofia, my husband Patrice and my children Patrice A. and Stephanie. Without their support, patience and love, this work would not have been completed.

I wish to express my sincere gratitude to my advisor Professor Bruce Hart for all the years of scientific guidance, encouragement and support. I am grateful for him offering me the opportunity to be exposed to new and exciting technologies and for patiently reviewing my work. I would like to thank Professor Michael Riedel for his assistance and guidance. Special recognition to my colleagues of the McGill Seismic Research Group for enlightening discussion that contributed to the realization of this study.

I am very grateful for the support received by faculty staff and students of the Earth and Planetary Sciences. Special thanks go to Anne Kosowski and Kristy Thornton. I want also to thank Brigitte Dionne for her support and advice in all the computer related issues. Thanks go to Luis Bayona, Alexandra Kirshner and Jonathan Menivier for their help in drafting some of the figures in this document.

I wish to thank Dr. Dale Leckie for his advice and support throughout the study as well as the team of geologists and geophysicists at Nexen Inc. for constructive discussions, especially Brian Mills, Paul Bessette and Krista Solvason. Special thanks to Chris Gilboy for his support and to James Christopher and Melinda Yurkowski for the discussions that provided key insights into my study during my trips to the Saskatchewan core facility.

I would like to thank all the organizations that supported this research. Nexen Inc. and a NSERC Discovery Grant provided funding for this work to Professor Hart. The seismic and well-log data used in this study were made available by Nexen Inc. and NAL Resources Ltd. Seismic interpretations and analyses described herein were undertaken using software donated by Landmark Graphics Corporation and Veritas/Hampson-Russell software services. I wish to thank the Saskatchewan Subsurface Geological Laboratory for providing me with free access to the well cores.

## **1. General Introduction**

### **1.1 Introduction**

The Lower Cretaceous Mannville and Bullhead Groups of the Western Canadian Sedimentary Basin (WCSB) are Canada's main oil sands and heavy oil reservoirs. The remaining oil reserves in these deposits ( $>173 \times 10^9$  bbl) are among the largest worldwide. As oil is becoming much more difficult to find and extract, the more complicated to produce oil sand and heavy oil reserves of the world have become an important alternative for energy supply. Heavy oil in the WCSB is contained in geologically complex reservoirs with considerable reservoir heterogeneities (spatial variations in lithology, porosity and permeability). The Mannville Group deposits constitute oil reservoirs in British Columbia, Alberta and Saskatchewan. The stratigraphically complex Mannville are unconsolidated reservoirs currently at shallow ( $<1000$  m) depths. Almost all the oil production in the Mannville Group comes from stratigraphic traps; in the Lower Mannville, it occurs in valley-fill sands overlying the Sub-Cretaceous unconformity and in the Upper Mannville the traps result from facies changes due to shifting shorelines (Hayes et al., 1994). Due to the characteristics of the oil (high viscosity), its extraction involves the use of expensive enhanced recovery techniques that require a clear understanding of the reservoir's architecture. Although imaged using seismic data since the early 1980s, detailed Mannville seismic stratigraphy was not documented until the late 1990s when improvements in 3-D seismic resolution and visualization techniques made it possible. In this

project, we will present examples of how 3-D seismic and well data can be integrated at a development-project scale to define stratigraphic architecture and understand the evolution of the Mannville Group complex units.

The areas studied for this project are located in southern and West-Central Saskatchewan. The area in southern Saskatchewan corresponds to a water-saturated region and has no hydrocarbon potential in the Mannville Group interval. The second area corresponds to a heavy oil field located in West-Central Saskatchewan that produces from the Lower Mannville (Dina and Cummings members). This is an area of complex geology exploited using horizontal wells in order to increase its productivity. In addition, this technique reduces drilling costs and environmental damage by decreasing the amount of drilling. A detailed reservoir model for the project area is needed in order to optimize production.

Integration of borehole and seismic data to generate a geological model of the area of interest is today a common practice in the oil industry although the extent and benefits of this integration will depend on the methodology used. The geological models were generated using sequence stratigraphic techniques, which combine seismic facies analysis and well (core and well log) interpretation of facies. Seismic attributes were derived using the geological model combined with the information derived from the seismic traces. These attributes were correlated to borehole physical properties (known from the wells logs and cores) to predict the spatial distribution of the reservoir properties, in this case reservoir and non-reservoir distribution. Although not undertaken in our study, the resulting stratigraphic framework is ready to be used to construct a static (includes petrophysical properties) reservoir model.

## **1.2 Overview of the geology of the Lower Cretaceous Mannville Group.**

The Lower Cretaceous Mannville Group of the Western Canadian Foreland Basin has been studied since the mid 1940s to present. These studies dealt with the understanding of the Mannville deposits in the various basins of Alberta, British Columbia, and Saskatchewan. In Saskatchewan, Christopher (1974, 1984, 1997, 2003) has studied the Mannville Group for decades using well-log, core and outcrop information. His most recent report (2003) described the geology of the Mannville Group everywhere this unit is present in Saskatchewan. Sequence stratigraphic interpretations began during the 1990s (i.e. Banerjee and Kidwell, 1991) in Alberta and Saskatchewan. Cant (1996) proposed a sequence stratigraphic organization defining sequence boundaries and systems tracts for the complete Mannville Group but mainly based on the Alberta units. Leckie et al. (1995a, 1995b, 1997a, 1997b) did the first sequence stratigraphic studies of the Mannville Group in Saskatchewan; they mapped and described the group in South West Saskatchewan. Dwyer (1998) was the first to describe the Mannville deposits in west-central Saskatchewan using sequence stratigraphic techniques. He studied a heavy oil field in the Lloydminster area and established different reservoir architecture for the two Upper Mannville producing sands. The goal of his study was to make an estimation of remaining volume of oil-in-place to establish the hydrocarbon potential of the field. Calver et al. (1999) briefly described the sequence stratigraphy of Upper Mannville deposits of west-central Saskatchewan using both geological and geophysical (seismic) information. Prior

to this study, there had been no comprehensive sequence stratigraphic interpretation of the Lower Mannville deposits in west-central Saskatchewan.

### **1.3 Overview of integrated geological and geophysical studies and methods.**

In this section, I will present a historical overview of the combined use of seismic and well-log data to establish the stratigraphic architecture and depositional history of the Mannville deposits in the Western Canadian Sedimentary Basin. I will describe the initial work done in the basin and then concentrate on the studies done in the Lower Cretaceous Mannville deposits in Saskatchewan.

Many studies were previously carried out on the deposits that host the heavy oil in Alberta (Cant, 1992; Ranger and Pemberton, 1997) and Saskatchewan (Groeneveld and Stasiuk, 1984; Christopher, 1997) to understand the facies distribution of the Mannville Group, but none describes in detail the deposits of this project's study area.

Seismic data have been used to image and explore the Mannville deposits for hydrocarbons since the early 1980s. Dunning et al. (1980) used 2D seismic transects to generate an exploration model in Saskatchewan's heavy oil Lloydminster area. Integration of seismic data and geological information, in the form of boreholes and cores also began at that time (Hermanson et al., 1982; Hopkins et al., 1984) and has evolved thanks to the development of new technology that permits the extraction of better and more detailed information from the seismic and borehole data.

Although the development of seismic stratigraphy occurred in the late 1970s (Vail et al., 1977), there are no records until the late 1980s of studies done using this discipline to understand the stratigraphy of the Mannville deposits. Guidish and Debuyl (1987) and Cederwall (1989) published their studies and seismic transects in atlases dealing with seismic stratigraphy and the Lower Cretaceous Mannville in the Western Canadian hydrocarbon pools respectively. Anderson and Pitman (1988), Hopkins et al. (1987), Anderson and Cederwall (1993) and others used well logs and the seismic signature in 2-dimensional vertical views to locate potential structural and stratigraphic traps in Mannville deposits in Alberta and Saskatchewan. With the advances in reflection seismic technology and the introduction of 3-D seismic techniques in the 1990s, there were several integrated studies (i.e. Farshori and Visser, 1992; Broger et al., 1997; Mawdsley, 1996) that were done mostly on the Mannville deposits of Alberta.

During the 1990s two integrated studies were done in the Mannville deposits in Saskatchewan (Calvert et al., 1999 and Dequirez et al., 1995). These studies are additionally interesting, because they introduced the use of seismic impedance (sometimes considered a seismic attribute) data to generate more accurate geologic and reservoir models. Dequirez et al. (1995) integrated seismic and impedance well-logs, and used stratal slices and seismic facies analysis to generate their reservoir model. Calvert et al. (1999) generated lithological maps from the 3-D impedance volume, but since this work was published as a conference abstract only, the details of the methodology were not available for further review.

More recently (2000 to present) the studies that used seismic data to image Mannville deposits in Saskatchewan (i.e. Lines et al., 2005) have dealt with the use of S-waves vs. the traditional P-waves, and techniques such as Amplitude-Variation with Offset (AVO) to delineate reservoirs and monitor production. McPherson (2005) studied Upper Mannville deposits in Alberta where the channels under investigation were below the resolution of the seismic data, and used new seismic techniques, such as spectral deconvolution and seismic modeling to delineate and predict reservoir properties. Hart et al. (2007) discuss the relationship between seismic stratigraphy and small 3-D seismic surveys and use an example taken from chapter 1 of this manuscript. A small seismic survey can be defined as such either because of the size of the survey (i.e. 6 square km) or because it only images part of the studied stratigraphic sequence.

The discipline of seismic geomorphology evolved at the beginning of the 2000s (Posamentier, 2000) and deals with “the extraction of geomorphic insights using predominantly three-dimensional seismic data” (Posamentier et al., 2007). This discipline when used together with seismic stratigraphy has proven to be a powerful tool to understand the stratigraphy of the deposits. The identification and study of anomalous seismic features is the objective of seismic geomorphology analysis, which includes among other things the use of stratal slicing and seismic attributes to view and analyze them. In this study, I use this discipline to establish the stratigraphic architecture and depositional history of the Mannville deposits in southern and west-central Saskatchewan. The only study that addresses the seismic geomorphology of the Mannville deposits is the one done by Posamentier et al. (2002) published as a conference abstract. It included a case study from

Mannville channels in which the combined use of 3-D seismic plan view images, 2D seismic images and borehole data proved to be very useful in the analysis of depositional systems and unraveling the depositional history of these deposits.

The use of seismic attributes in hydrocarbon determination began in the mid 1970s (Taner and Sheriff, 1977). It was not until the 1990s that seismic attributes were used to predict physical properties from well logs (Ronen et al., 1993; Schultz et al., 1994) by empirically correlating horizon or interval based attributes with physical properties measured by well logs. Later, multiattribute seismic analysis (Russell et al., 1997) and neural networks (Schuelke J. et al., 1998) were introduced to predict physical properties. Hampton et al. (2001) later developed a methodology to use volume-based attributes to estimate physical properties from well logs. This methodology has been successfully applied worldwide by many geoscientist (Leiphart and Hart, 2001; Pramanik et al., 2004; Tebo and Hart, 2006; Calderon and Castagna, 2007; Sheridan, 2007) to predict log response from seismic data. In Alberta, it has been used to predict porosity (Hampton et al., 2001) and lithology (Tonn, 2002) in the Mannville, but has never been used in Saskatchewan to predict any kind of physical property. Tonn (2002) predicted lithology in the Alberta oil sands of the Lower Cretaceous McMurray Fm. of the Bullhead Group, but did not relate the results to the geological model.

#### **1.4 Motivation and Goals**

This study responds to the necessity of understanding the geologically complex heavy oil reservoirs in the Lower Cretaceous Mannville deposits in Saskatchewan. Due to the high viscosity of the oil, the hydrocarbon extraction

involves the use of expensive enhanced recovery techniques that require a thorough understanding of the reservoir's architecture. The goal of this study is to use 3-D seismic and borehole data to generate comprehensive stratigraphic models and to use seismic attributes and core data to predict the distribution of reservoir and non-reservoir deposits. The final 3-D integrated geological model should be able to predict facies distribution as well as the reservoir heterogeneities of the deposits to help improve enhanced recovery strategies and decrease the risk and the costs of the process of reservoir production.

This type of work has never been published for the Mannville and will contribute significantly to the knowledge of these Lower Cretaceous deposits in Saskatchewan. Another important goal of this study is to document the methodology used to perform the integration of the geological and geophysical data so that it would be useful for geoscientists working in any area with similar information (3-D seismic data and boreholes) and objectives.

### **1.5 Thesis Organization**

This thesis is divided into five chapters of which three (Chapters 2 to 4) correspond to manuscripts and the other two (Chapters 1 and 5) are the introduction and conclusions. Chapter 1 states the goal and objectives of the research and gives an overview of the integrated geological and geophysical studies done in the Mannville Group in the Western Canadian Sedimentary Basin.

Chapter 2 describes how integrating 3-D seismic with well-log data served to define stratigraphic units and lithological heterogeneity in the Mannville Group in southern Saskatchewan. In the manuscript I show how the ability to visualize

the data, specifically seismic data in the form of arbitrary lines and stratal or horizon slices techniques, helps define stratigraphic features that affect fluid flow in hydrocarbon producing areas. The Mannville Group is subdivided into three packages and this paper discusses the relationship of the seismically defined units to the formal stratigraphy of the Mannville Group in southern Saskatchewan. This paper, published in 2006, was the first peer-reviewed publication that used 3-D seismic techniques to understand the stratigraphy of the Mannville Group of Saskatchewan.

Chapters 3 and 4 also present a study of the Mannville stratigraphy, but this time located in a heavy oil producing area in west-central Saskatchewan. The stratigraphic interval examined in this chapter zoomed in from the complete Mannville Group examined in Chapter 2, to just the Lower Mannville, where the reservoir is located. The study, divided into two parts, is presented in chapters 3 and 4 respectively.

Chapter 3 focuses on a smaller stratigraphic interval (Lower Mannville Group) than the one described in chapter 2 (Mannville Group) and is located in a heavy oil reservoir in west-central Saskatchewan. This chapter describes how multiattribute analysis and neural network training were used to obtain a relationship between seismic attributes and lithology (gamma-ray response), which was used to predict gamma-ray (GR) response away from well control within the seismic cube. This information, combined with the stratigraphic model obtained from the interpretation of seismic and well data, was used to generate an integrated geological model for the Lower Mannville deposits of the region.

Chapter 4 presents how the integration of borehole and seismic data was used to unravel the stratigraphy and predict the reservoir architecture of the Lower Mannville deposits within the heavy oil field in Central-East Saskatchewan. This chapter illustrates the methodology used to integrate well logs and cores with seismic data (amplitude and pseudo-lithology volumes), and emphasizes the benefits of the use of a particular way of interpreting a combination of vertical and horizontal seismic planes to understand the stratigraphy of the area.

Chapter 5 summarizes the conclusions and recommendations.

## 1.5 References

- Anderson, N. and Pitman, D. 1988. Seismic signature of the lower Mannville channel sandstones at Hayter Field, eastern Alberta, Canada. SEG, Annual Meeting, Anaheim, California, Abstracts, v.1, p. 589-592.
- Anderson, N. L. and Cederwall, D.A. 1993. Westhazel General Petroleum's Pool; case history of a salt-dissolution trap in west-central Saskatchewan, Canada. Geophysics, v. 58, no. 6, p. 889-897.
- Banerjee, I. and Kidwell, S. M. 1991. Significance of molluscan shell beds for sequence stratigraphy; example from the Cretaceous of Canada. Sedimentology, v.38, no.5, p.913-934.
- Broger, E. J., Syhlonyk, K., Garth, E., and Zaitlin, B. A. 1997. Glauconite sandstone exploration; a case study from the Lake Newell Project, southern Alberta. In: Petroleum geology of the Cretaceous Mannville Group, Western Canada. S. G. Pemberton and D. P. James (eds.). Canadian Society of Petroleum Geologists – Memoir, v. 18, p. 140-168.
- Calderon, J. E. and Castagna, J. 2007. Porosity and lithologic estimation using rock physics and multi-attribute transforms in Balcon Field, Colombia: The Leading Edge, v. 26, p. 142-150.
- Calver, E., Doligez, B., Eschard, R., and Torriero, D. 1999. Sequence stratigraphy and stochastic reservoir modeling of an incised valley fill reservoir in the Lower Cretaceous Mannville Group, west central Saskatchewan: AAPG Annual Meeting Expanded Abstracts, p. A20.

- Cant, D. J. 1992. Subsurface Facies Analysis. In: Facies Model response to Sea Level Change. R.G. Walker and N. P. James (eds.). Geological Association of Canada, p. 27-45.
- Cant, D. J. 1996. Sedimentological and sequence stratigraphic organization of a foreland clastic wedge, Mannville Group, Western Canada Basin. *Journal of Sedimentary Research*, v. 66, no. 6, p.1137-1147.
- Cederwall, D. A. 1989. The Lower Cretaceous. In: The CSEG/CSPG geophysical atlas of Western Canadian hydrocarbon pools. N. L. Anderson, Hills, V. Leonard, and D. A., Cederwall, (eds.). p. 217-281.
- Christopher, J. E. 1997. Evolution of the Lower Cretaceous Mannville Sedimentary Basin in Saskatchewan. In: Petroleum geology of the Cretaceous Mannville Group, Western Canada. S. G. Pemberton and D. P. James (eds.). Canadian Society of Petroleum Geologists, Memoir 18, p. 191-210.
- Dwyer, J. 1998. Geology of Golden Lake heavy oil field. In: Oil and gas pools of the Western Canada Sedimentary Basin. J. R. Hogg (ed.). Special Publication - Canadian Society of Petroleum Geologists, v.S-51, p.25-38.
- Dequirez, P. Y., Blanchet, C., Feuchtwanger, T. and Torriero, D.1995. Integrated stratigraphic and lithologic interpretation of the East-Senlac heavy oil pool: SEG Annual Meeting, Houston, Texas, Expanded Technical Program Abstracts with Biographies, v. 65, p. 104-107.
- Dunning, N. E., Henley, H. J., and Lange, A. G.,1980. The Freemont Field: an exploration model for the Lloydminster area, in Lloydminster and beyond; geology of Mannville hydrocarbon reservoirs. L. S. Beck, J. E. Christopher,

- and D. M. Kent (eds.). Saskatchewan Geological Society, Special Publication, no. 5, p.132-148.
- Farshori, M. Z. and Visser, J. 1992. Exploration strategy based on a proven sedimentological model for the Glauconitic Sandstone (Lower Cretaceous) of southern Alberta. AAPG Annual Meeting, Calgary, Alberta, Expanded Abstracts, p. 39.
- Groeneveld, N. A and Stasiuk, L. D. 1984. Depositional environment of the Cummings coal and associated sediments, Winter-Senlac area, Western Saskatchewan. In: Oil and gas in Saskatchewan. J. A. Lorsong and M. A. Wilson, (eds.). Special Publication: Saskatchewan Geological Society, v. 7, p. 135-147.
- Guidish, T. and Debuyt, M. 1987. Delineation of a thin sandstone reservoir using seismic lithologic modeling in the Taber-Turin area, Alberta. In Atlas of seismic stratigraphy. A. Bally (ed.). AAPG Studies in Geology, v. 27, no. 1, p. 96-108.
- Hampson, D., Schuelke, J. and Quirein, J. 2001. Use of multiattribute transforms to predict log properties from seismic data: Geophysics, v. 66, p. 220-236.
- Hayes, B J. R., Christopher, J. E. Rosenthal, L. Los, G. Mckercher, B. Minken, D.F. Tremblay, Y. M. Fennell, J. W. and Smith, D. G. 1994. Cretaceous Mannville Group of the Western Canada sedimentary basin. In: Geological atlas of the Western Canada sedimentary basin. G. Mossop and I. Shetsen (eds.). Canadian Society of Petroleum Geologists and Alberta Research Council, p. 317-334.

- Hermanson, S. W., Hopkins, J. C. Lawton, D. C. 1982. Upper Mannville "glauconitic" channels, Little Bow area, Alberta; geologic models for seismic exploration. *American Association of Petroleum Geologists Bulletin*, v. 66, no. 5, p. 581.
- Hopkins, J. C., Lawton, D. C. and Gunn, J. D. 1984. Evaluation of a complex lower Mannville channel prospect; integrated geological and geophysical models. In: *The Mesozoic of middle North America*, D. F. Stott and D. J. Glass (eds.). -Canadian Society of Petroleum Geologists, Memoir 9, p. 555-556.
- Hopkins, J. C., Lawton, D. C. and Gunn, J. D. 1987. Geological and seismic evaluation of a lower Mannville Valley system; Alderson Prospect, Rolling Hills, southeastern Alberta. *Bulletin of Canadian Petroleum Geology*, v. 35, no. 3, p. 296-315.
- Leckie, D. A., Vanbeselaere, N. and James, D. P. 1995. The Mannville Group of southwestern Saskatchewan; new maps, perspectives and potential. *CSPG Reservoir*, v.22, no.1, p.3-4.
- Leckie, D. A., Vanbeselaere, N. and James, D. P. 1995. Use of Sequence Bounding Surfaces for Correlation and Mapping in Nonmarine, Incised-Valley Reservoirs. *American Association of Petroleum Geologists Bulletin*, v. 79, p. 1728-1729.
- Leckie, D. A., Vanbeselaere, N. and James, D. P. 1997. Regional sedimentology, sequence stratigraphy and petroleum geology of the Mannville Group; southwestern Saskatchewan. In: *Petroleum geology of the Cretaceous*

Mannville Group, Western Canada. S G. Pemberton and D.P. James (eds.).  
Canadian Society of Petroleum Geologists, Memoir 18, p. 211-262.

Leckie, D. A., Vanbeselaere, N. and James, D. P. 1997. Mayhem in the  
Mannville; stratigraphic complexity in southern Alberta and Saskatchewan;  
resolved. CSPG Reservoir, v. 24, no. 9, p.7

Leiphart, D. J. and Hart, B.S. 2001. Case history: Comparison of linear regression  
and a probabilistic neural network to predict porosity from 3-D seismic  
attributes in Lower Brushy Canyon channeled sandstones, southern New  
Mexico: Geophysics, v. 66, p. 1349-1358.

Hart B., Sarzalejo, S. and McCullagh, T. 2007. Seismic stratigraphy and small 3D  
seismic surveys. The Leading Edge, v. 26, no. 7, p. 876-881.

Lines, L., Zou, Y., Zhang, A. Hall, K. Embleton, J. Palmiere, B. Reine, C.  
Bessette, P. Cary, P. and Secord, D. 2005.  $V$  (sub P) /  $V$  (sub S)  
characterization of a heavy-oil reservoir. Leading Edge (Tulsa, OK), v. 24, no.  
11, p. 1134-1136.

Mawdsley, M. J., Eamer, A. L. and Zaitlin, B. A. 1996. Exploration for incised  
valley channel sandstones of the Lower Cretaceous, Alberta, Canada, using  
3D seismic; risks and opportunities. SEG Annual Meeting, Denver, Colorado,  
Expanded Technical Program Abstracts with Biographies, v. 66, p. 295-298.

McPherson, J. M. 2005. Channel boundary delineation and reservoir prediction in  
three stacked glauconitic channel reservoirs using forward seismic modeling,  
spectral decomposition and event similarity prediction Glauconitic Formation,  
southeastern Alberta: Thesis, University of Manitoba, Winnipeg, Canada, 96  
p.

- Posamentier, H. W. 2000. Seismic stratigraphy into the next millennium; a focus on 3D seismic data. AAPG Annual Meeting, New Orleans, Louisiana, Program and Abstracts CD.
- Posamentier, H. W., Byrne, C. Collazos, J. P. Haraldson-Radford, N. Johnson, C. Krentz, D. McLaughlin, R. Miller, M. Mitchelmore, M. and Schoemaker, M. 2002. Analysis of depositional systems based on seismic, geomorphology and stratigraphy integrated with borehole data; case studies from the Western Canadian Sedimentary Basin. AAPG Annual Meeting, Houston, Texas, Expanded Abstracts v. 2002, p. 143.
- Ronen, S., Hattori, M. Hoskins, J. and Schultz, P. 1994. Seismic guided estimation of reservoir properties, 3-D seismology; integrated comprehension of large data volumes. SEG summer research workshop, Society of Exploration Geophysicists, p. 159-162.
- Schuelke, J. S., Quirein, J. A. and Sarg, J. F. 1998. Reservoir architecture and porosity distribution, Pegasus Field, West Texas; an integrated sequence stratigraphic-seismic attribute study using neural networks. Geo-Triad '98 abstracts, plenary oral posters core workshop; rocks, risk and reward, Karel, W., J. Reimer, D. Uffen, and M. Ravlich, Geo-Triad '98, Calgary, AB, Canada, p. 142-145.
- Tebo J.M., and Hart, B.S. 2005. Use of volume-based 3-D seismic attribute analysis to characterize physical property distribution: A case study to delineate reservoir heterogeneity at the Appleton field, SW Alabama: Journal of Sedimentary Research, v. 75, p. 723-735.

Tonn, R., 2002. Neural network seismic reservoir characterization in a heavy oil reservoir: *The Leading Edge*, v. 21, p. 309-312.

Vail, P.R., Mitchum, R.M. Todd, R.G., Widmier, J.M. Thompson, S Sangree, J.B.

Bubb, J.N. and Hatlelid, W.G. 1977. Seismic Stratigraphy and Global Changes of Sea Level. In: *Seismic Stratigraphy-applications to hydrocarbon exploration*: C. E. Payton (ed.). American Association of Petroleum Geologists, Memoir 26, p. 49-212.

## **INTRODUCTION TO CHAPTER 2**

This chapter describes how integrating 3-D seismic data with well-log data served to define stratigraphic units and lithological heterogeneity in the Mannville Group in southern Saskatchewan. We also show how the ability to visualize the data, specifically seismic data in the form of arbitrary lines and stratal or horizon slices techniques, helps define stratigraphic features that affect fluid flow in hydrocarbon producing areas.

**2. Stratigraphy and Lithologic Heterogeneity in the Mannville Group  
(Southeast Saskatchewan) Defined by Integrating 3-D Seismic and Log Data**

**Reprinted by permission of the CSPG whose permission is required for  
further use.**

Sarzalejo S. and Hart B. (2006), Stratigraphy and Lithologic Heterogeneity in the  
Mannville Group (Southeast Saskatchewan) Defined by Integrating 3-D Seismic  
and Log Data. Bulletin of Canadian Petroleum Geology, v. 54, p. 138-151

## 2.1 Abstract

Wireline log and 3-D seismic data were integrated to define stratigraphic units and lithologic heterogeneity in the Mannville Group of southeast Saskatchewan. The Mannville in this area is a stratigraphically complex unit formed of fluvial to marine deposits that, although they are non-prospective for hydrocarbons in this area, share many similarities with time-equivalent strata in areas of heavy oil production. Seismic sequence stratigraphic principles permitted us to subdivide the Mannville into three packages. The ability to visualize the 3-D seismic data in a variety of ways, including arbitrary lines and stratal or horizon slicing techniques, helped us to define stratigraphic features that would affect fluid flow in hydrocarbon producing areas. These features include channels of various sizes and orientations, and channel elements such as scroll bars and lateral accretion surfaces, that are present within specific portions of the Group. Because the effectiveness of enhanced recovery methods such as steam-assisted gravity drainage depends on a development team's ability to recognize reservoir heterogeneity, similar integration of 3-D seismic data, well logs and other data types would assist greatly in developing the Mannville in heavy oil areas. There is close, but not one-to-one correspondence between the stratigraphic units we defined and those established by regional log- and core-based correlations. Seismic resolution problems or log correlation styles could be responsible for the differences.

## 2.2 Introduction

The Lower Cretaceous Mannville Group has been the focus of many previous studies because it is one of the most prolific hydrocarbon intervals within the Western Canadian Sedimentary Basin. To date, geological studies of the Mannville Group in the province of Saskatchewan have been based upon logs and core data. These studies (e.g., Christopher, 2003; Leckie et al., 1997) focused largely on depositional environments and stratigraphy at a regional scale. This paper will illustrate how 3-D seismic and well data may be integrated at a development-project scale to define stratigraphic units and depositional facies in complex units such as the Mannville Group.

Seismic images derived from 3-D volumes have proven to be very useful for imaging stratigraphic units and depositional architecture (e.g., Brown, 1999; Posamentier, 2004). Despite these successes elsewhere, we were unable to find any previous publications that specifically examined the stratigraphic architecture of the Mannville Group using 3-D seismic data. In areas where enhanced recovery methods such as steam-assisted gravity drainage (SAG-D) or other methods are used, it is important to be able to predict lithologic heterogeneity associated with depositional features such as inclined heterolithic strata (IHS) and channel fills because these features potentially affect the movement of hydrocarbons and injected fluids. These features are best defined with the combined use of 3-D seismic and well-log data and can be even better defined in heavy-oil development areas where the wells are closely spaced.

The study area is located in the southeastern region of the province of Saskatchewan, in Townships 6-7, Ranges 9-10. The seismic and well data we present in this paper were collected to explore for, and develop, deeper targets (primarily Mississippian carbonates). The Mannville Group in the study area is wet, and is not considered to be a drilling target for hydrocarbon accumulations. Nevertheless, the seismic data quality is very good at the Mannville level and the data allow us to image depositional features that are analogous to those found in heavy-oil producing areas. As a corollary objective, we established correlations between stratigraphic units defined through our integrated seismic/log interpretations and formations identified by regional correlations (e.g., Christopher, 2003).

### **2.3 Geological Setting**

The study area is in the northern part of the intra-cratonic Williston Basin (Fig. 1). The interval of interest is the Lower Cretaceous Mannville Group, which forms part of the Lower Zuni Sequence that was deposited in the Western Canadian Foreland Basin (Cant, 1989). Previous studies of the Mannville Group divided it into (from oldest to youngest) the Success, Cantuar and Pense formations. Recent studies (Christopher, 2003) excluded the Success Formation (Jurassic to Neocomian) from the group and leave only the Cretaceous Aptian to Albian Cantuar and Pense formations as part of the Mannville Group (Fig. 2).

Cant and Abrahamson (1996) interpreted the Mannville Group as a third-order sequence overlying a second-order sequence boundary that represents a major reorganization of the foreland basin and the Cordillera. This Alberta-based

interpretation divides the succession into transgressive and highstand systems tracts with a maximum flooding surface placed at the base of the Clearwater shales (Fig. 2). The transgressive portion in the Alberta region was defined as the Lower Mannville, Dina and Dina-Cummings members, with units above the Clearwater Formation being assigned to the highstand systems tract

The Williston Basin subsided during the Jurassic then, during Late Jurassic time, the basin was filled and the area experienced regional uplift (Poulton et al., 1994). The S1 Member of the Success Formation was deposited at this time. Neocomian tectonic uplift of the Swift Current Platform and Sweetgrass Arch (Fig. 1) reversed the southerly topographic slope of the Jurassic Williston Basin, forming a major unconformity (Christopher, 1997). The S2 Member of the Success Formation is separated from the S1 Member by this regional sub-Cretaceous unconformity (Fig. 2). The present patchy distribution of the Success Formation is the result of later pre-Mannville erosion (Christopher, 2003).

The Williston Basin did not actively subside during the Cretaceous, and Mannville deposition took place over top of a profound unconformity that truncated Lower Cretaceous to Paleozoic strata (Hayes et al., 1994). During Aptian time, the sea invaded from the north and eventually covered the pre-Mannville topography. The Cantuar Formation, the lowest unit within the Mannville Group in this area, was deposited during late Aptian and early Albian time, and covers the underlying topography of pre-existing valleys and terraces (Christopher, 2003). The Cantuar Formation, comprising six members in southeast Saskatchewan (Fig. 2) with hiatuses and erosional discontinuities, underwent several marine transgressions (Christopher, 2003). Uplift of the

Punnichy Arch terminated Cantuar deposition and marine erosion removed poorly consolidated sediments of the Cantuar in the early Albian. Marine deposits of the Pense Formation were deposited above the Cantuar Formation as the Pense seaway flooded across Saskatchewan during a period of sea-level rise during the middle Albian (Christopher, 1997).

#### **2.4 Database and Methodology**

The database for this project consists of a 3-D seismic survey covering fifty-six km<sup>2</sup>, digital well-logs for 47 wells and paper logs for 16 additional wells (Fig. 3). The 3-D seismic survey has a bin size of 30 m by 30 m, a sample rate of 2 milliseconds, and a trace length of 3 seconds two-way time (TWT). The 30-fold seismic survey was acquired using a dynamite source in 1997. Seismic bandwidth ranges from 10-85 Hz at the Mannville level with a peak frequency of approximately 50 Hz. The vertical resolution of the data (defined as  $\frac{1}{4}$  of the wavelength) is approximately 12 m, calculated using log-derived velocities of 2300 m/s in the interval of interest. Gamma-ray (GR) logs were available for some of the wells, but the majority of the well correlations presented herein are based on spontaneous potential (SP) and resistivity log signatures.

Synthetic seismograms, such as those shown in Figure 4, were generated for the 15 wells that had sonic logs. These well ties allowed stratigraphic units defined in the wells to be correlated to the seismic data and seismically defined surfaces to be identified in the wells. Well-log cross-sections and corresponding seismic transects through the 3-D volume were interpreted throughout the area to generate a stratigraphic framework. Time slices (planes of constant TWT),

horizon slices (images showing amplitude variations along seismic horizons, also known as “amplitude maps”) and stratal slices (slices through the seismic volume that run parallel to overlying or underlying seismic horizons, c.f. Zeng et al., 1998, 2000; stratal slices were termed “flattened time slices” by Posamentier, 2004) were extracted from the data volume to map and observe the spatial geometry of features interpreted on vertical seismic transects and log cross-sections. The horizons used to generate the stratal slices needed to be continuous throughout the 3-D survey and to correspond to depositional surfaces that were originally nearly horizontal (i.e., flooding surfaces can be appropriate choices whereas unconformities or channel bases are poor choices). Because they eliminate the effects of regional dip (or other tectonic disturbance), stratal slices are preferred over simple timeslices for mapping stratigraphic features of interest.

Seismic stratigraphic and sequence stratigraphic principles, described by Mitchum et al. (1977), Vail et al. (1977), Posamentier et al., (1988) Bertram and Milton (1994) and others, were used to define key stratigraphic surfaces such as unconformities and flooding surfaces, and to establish the stratigraphic framework for the integration of seismic and well-log data. As described below, some surfaces were defined seismically as “candidate unconformities” based on truncated and onlapping reflection terminations as shown in Figure 5a, whereas other stratigraphic surfaces were defined based on a combination of well-log and seismic information (Fig. 5b). Although the definition of “candidate unconformities” might seem unusual, a true unconformity is associated with a significant hiatus, something we cannot demonstrate with only log and seismic data. Flooding surfaces were identified within marine shale intervals based on the

combination of high gamma-ray (where present) and low resistivity log signatures.

No core data exist for the water-saturated Mannville Group in the study area. As such, and as illustrated below, we integrated seismic geomorphology techniques (the study of depositional systems using 3D-seismic derived images; Posamentier, 2000), with seismic facies and wireline log shapes to infer lithology and depositional environments in this paper. Posamentier (2004) showed images of sedimentary features interpreted as fluvial scroll bars and channels, which may be identified by their morphology in timeslices and stratal slices. Other authors have also used this approach. For example, Brown (1999) presented examples of meandering channels, point bars and crevasse splays in slices through 3-D seismic volumes.

## **2.5 Interpretation**

Christopher (2003) presented regional correlations of the Mannville Group in Saskatchewan, and his correlations were used in this study to identify the lithostratigraphic units present in our study area. Figure 6 incorporates wells from Christopher's cross-sections C-C' and D-D', with wells from our study area and intervening areas. The type log for the present study area (Fig. 7) shows the relationship between the lithostratigraphy of Christopher and the seismically defined surfaces picked in this study. As defined below, seven main surfaces, labeled I to VII were defined in this study, and each of these surfaces corresponds to a lithologic contact in logs. These changes in lithology are associated with changes in rock physical properties that generated the seismic reflections

identified in this study. Figure 8 shows a representative well-log cross-section and corresponding seismic transect across the study area.

Surfaces I and VII underlie and overlie the Mannville Group respectively. They were picked as stratigraphic markers to “bracket” the Mannville and to generate stratal slices. Our synthetic seismograms show that Surface I corresponds to the top of the Lower Vanguard (part of the Jurassic System shown in Fig. 2). This surface is located at the base of a shale interval (Fig. 7) and is a high-amplitude continuous reflection seen in seismic transects (Fig. 8). Surface VII is a flooding surface in the Joli Fou Formation. In logs this surface corresponds to high gamma-ray log values (where this log is available) and a low-resistivity marker within this shale package. Surfaces II and VI correspond to the base of the Cretaceous section and top of the Mannville Group respectively, according to our synthetic seismograms (Fig. 4) and correlations with the stratigraphic framework established by Christopher (2003; Figs. 6,7). Within the Mannville, the low gamma-ray (GR) or high spontaneous potential (SP) and low (lower than shale) resistivity values seen in the well-logs are interpreted as water-saturated sands.

We identified three seismic packages within the Mannville Group that overlie a fourth Lower Cretaceous package. These packages, labeled Units A to D are shown in Figures 6-8 and their lithologic and stratigraphic character is described next.

### **2.5.1.a Unit A – Description**

Unit A, bounded by Surfaces II and III, is characterized by a parallel to semi-parallel fill reflection pattern (Fig. 8). Surface II, the sub-Cretaceous unconformity (Figs. 2, 6-8) truncates underlying seismic reflections and does not correspond to a continuous seismic reflection. Seismic transects and a time-structure map (Fig. 9) show that Surface II cuts down towards the east, defining the margin of an approximately NNE-SSW striking incision. The amount of incision is estimated to be up to 38 m from well-log data. Logs through Unit A show that the incision is filled with both sand and shale. Figure 8 and 5b show the seismic and wireline log criteria, including truncation of underlying reflections and sharp-based sands in logs, used to define Surface II as a candidate unconformity. Surface III is defined by the top of a discontinuous trough on the seismic data and by the well-log signature (see the base of blocky sands in Figs. 7 and 8). Surface III overlies Surface II in the incision, but the two surfaces merge outside the incision to the west.

### **2.5.1.b Unit A – Interpretation**

Unit A, bounded by Surfaces II and III, is interpreted to be the Success (S2) Formation. This formation has a patchy distribution in the basin due to the unconformities that affected the region (Christopher, 2003) and its presence within the incision observed in the study area seems reasonable. The incision at the base of the unit (delineated by Surface II) is probably part of the Assiniboia drainage pattern that generated the pre-Mannville topography (Christopher, 1984) and our 3-D survey appears to image part of the western margin of a larger

incision. Surface III (Fig 8) corresponds with the erosional surface that caps the Success S2 Member (Fig 2), which has been observed in cores in southern Saskatchewan and was described by Christopher (1997) and Leckie et al., (1997).

#### **2.5.2.a Unit B – Description**

Unit B (Figs.6-8) is bounded by Horizons III and IV and shows a parallel fill in the western region and a more chaotic pattern in the central region of the study area. Logs indicate that it ranges from 56 to 86 m thick and that the basal part of the section is generally sandy. Well logs near the top of this package show a heterolithic fill consisting of sands interbedded with shales, and some intervals show bell-shaped log profiles. The lithology changes laterally, in places over distances of hundreds of meters. A stratal slice in the middle of this unit (Fig. 10) shows amplitude lineaments that have variable widths (typically < 300 m) and run in several directions. The lineaments correspond to the stratigraphic level of the lithologic variability seen in the logs.

Another stratal slice through the middle of Unit B shows a series of arcuate features in the northeast part of the survey that correspond to subtle north-dipping reflections in seismic transects (Fig. 11). These features are traceable for approximately three kilometers in the stratal slice.

#### **2.5.2.b Unit B – Interpretation**

Unit B encompasses the Dina and Lloydminster Members of the Cantuar Formation (the Cummings Member is generally absent in this area; Fig. 6) and

part of the Rex Member. Surface IV falls within the Rex, as seen in Figures 6 and 7.

We interpret many of the features visible in the stratal slices to be channels or channel elements. Posamentier (2004) showed channels with morphologies similar to those seen in this unit that he interpreted as Cretaceous fluvial systems in the Western Canadian Sedimentary Basin. Zeng et al. (1998, 2000), Hardage and Remington (1999) and Miall (2002) have also shown 3-D seismic images of channel systems. The non-marine nature of the lower part of the Mannville Group has been established both in Saskatchewan (Christopher, 1997; Leckie 1997; Smith, 1994) and Alberta (Cant and Abrahamson 1996) and so the presence of fluvial channels at this level is reasonable.

The arcuate features shown in Figure 11 are interpreted as scroll bars produced by point bar migration in a meandering river system. This interpretation is consistent with the dipping reflections seen in the seismic transect that are interpretable as lateral accretion surfaces. The curvature of the features seen in the horizon slice together with the dip in the reflections in the seismic line, indicate point bar migration to the north. Well logs that cut the feature (Fig. 11) show a bell-shaped log signature (abrupt base and fining upward) 15 m thick (i.e., at or slightly above tuning thickness), that is typical of point bar deposits (Cant, 1992). The presence of point bar deposits (lateral accretion surfaces, scroll bars) in the upper part of the unit is consistent with the observations of Leckie et al. (1997) who noted that the upper portion of the Cantuar comprises meander belt, floodplain and estuarine deposits in southwestern Saskatchewan.

Seismic data show incision associated with Surface IV that would be consistent with its being an unconformity (Figs. 5, 8) close to the top of the Rex Member. No unconformity has been recognized at this level on a regional basis (e.g., Christopher, 2003), and so it appears that Surface IV corresponds to a local erosional surface of relatively minor stratigraphic significance.

### **2.5.3.a Unit C – Description**

Unit C, between Surfaces IV and V, shows a parallel fill pattern in some areas but in other areas (e.g., Fig. 12) it is characterized by an oblique-tangential reflection pattern. A stratal slice through Unit C (Fig. 12) displays several arcuate, semicircular features that are approximately 5 km in length, at least 2.5 km across, and correspond to an oblique-tangential reflection configuration on seismic transects that cross them. Figure 13 shows a NW-SE to E-W oriented curvilinear amplitude anomaly, approximately 400 meters wide, that is present near the top of this unit in the southwestern part of the 3-D survey. The anomaly is penetrated by a single well that is filled with sand at this interval. Elsewhere, this stratigraphic level is shaly.

### **2.5.3.b Unit C – Interpretation**

Unit C encompasses the top of the Rex Member, the General Petroleum Member and part of the Waseca Member (Figs. 6-8). As for the underlying Unit B, the seismic and well-log data for this interval indicate a heterolithic fill dominated by channel deposits of various types. The stratal slice and east-dipping reflections in the seismic transect (Fig. 12) suggest eastward migration of a point

bar. Note that the log of the well in the west indicates that the base of this unit is sandy in the area of the scroll bars, whereas the well to the east shows the base of the unit to be shaly in that area. The feature shown in Figure 13 is interpretable as a small channel. The channel has a positive relief that is probably the result of differential compaction between a sandy fill and the shales around it.

Surface V corresponds to an unconformity close to the top of the Cantuar in our lithostratigraphic correlation (Fig. 6, 7). Although it does not correspond exactly with the Pense/Cantuar contact, it is close and so Surface V could correspond to the unconformity of Christopher (2003) that locally eroded the entire Cantuar Formation. Wallace-Dudley et al. (1998) suggested that it is a ravinement surface or a sequence boundary. Toplap seen in Figure 12 supports the interpretation of this surface as an erosional unconformity.

#### **2.5.4.a Unit D – Description**

Unit D, between Surfaces V and VI, displays a nearly parallel fill in some areas but also shows areas that are reflection free (Mitchum, 1977). Unit D does not show significant amplitude trends in time slices or stratal slices, although a small, approximately north-south oriented, meandering channel is observed near the base of the unit (Fig. 14).

#### **2.5.4.b Unit D – Interpretation**

According to correlations presented here (Figs. 6-8), Unit D corresponds to the Pense and upper part of the Waseca Formations. The parallel to transparent fill, and general lack of channel features in seismic profiles through most of this

interval are consistent with a shaly, shallow-marine depositional setting where stratification is more continuous than in fluvial or estuarine deposits. Wallace-Dudley et al. (1998) interpreted a maximum flooding surface in the lower part of the Pense Formation. The channel observed at the base of the unit must be below that surface and the overlying shallow-marine Pense deposits.

Surface VI corresponds to the top of the Mannville Group. According to Christopher (1997, 2003) there is a hiatus at the top of the Mannville (Fig. 2) which corresponds to a regional unconformity that can be observed over all the Western Canadian Sedimentary Basin. However, Wallace-Dudley et al. (1998) described the surface at the top of the Mannville (our Surface VI) as a major flooding surface at the top of a regressive (highstand) systems tract. Our small 3-D seismic survey does not show evidence (e.g., erosional truncation, onlapping reflections) that would support either interpretation.

## **2.6 Discussion**

The data presented in this paper illustrate the value of 3-D seismic data for pool-scale stratigraphic correlation and mapping of depositional features, especially in heavy-oil exploration and development areas where our results have most relevance. Although the Mannville is water saturated in our study area, the seismic images and log profiles presented in this paper show stratigraphic features similar to those that have been interpreted from well logs and cores in heavy oil and oil sands areas (e.g., Van Hulten, 1984; Strobl et al., 1997). Additionally, the size of the 3-D seismic survey studied in this paper is comparable to the size of SAG-D development projects. We frame the remainder of the discussion in

terms of the utility of: a) integrating 3-D seismic data into stratigraphic studies, and b) using 3-D seismic data for definition of stratigraphic features.

Leckie et al. (1995) stated that, in southern Saskatchewan, detailed stratigraphic correlations within the Mannville Group based on well-log control alone are imprecise and highly suspect. It is clear that, given the lateral facies variability seen in channelized deposits of the Cantuar Formation, detailed log-based correlations in the current study area would be ambiguous at best. The seismically defined stratigraphic packages show considerable internal lithologic heterogeneity and stratal slices show many stratigraphic features (e.g., channels) that are too narrow and sinuous to be accurately mapped with logs.

There appears to be close, but not one-to-one, correspondence between the surfaces we defined, by integrating seismic and log data, and those defined through correlations with the regional stratigraphic framework of Christopher (2003). Possible reasons for these differences include:

a) Problems with log-based correlations. Like Leckie et al. (1995), our experience suggests that log-based correlations of the Mannville can be ambiguous in this area, especially when they are based on different vintages and qualities of logs, and no corroborating core is present. Different correlations than those presented in Figure 6 are possible using available well control and log quality, but we have attempted to follow the correlation style of Christopher (2003). If our log picks can be changed, the stratigraphic units shown in that figure become less tabular (perhaps more realistic for fluvial/estuarine systems?) and all of our surfaces can be tied to those of Christopher (2003). Arguably, the

stratigraphic geometries seen in the 3-D seismic data should influence correlation styles outside the seismic survey area.

b) Seismic resolution problems. Regardless of correlation styles, it is clear that at least one of our units, defined by integrating 3-D seismic and log data, corresponds to more than one lithostratigraphically defined unit of the Mannville Group in this area (i.e., Unit C corresponds to several members of the Cantuar Formation). It is possible that the relative thinness of the members and low acoustic-impedance contrasts between the deposits of some members combine to make the units unmappable using seismic data.

We argue that integration of 3-D seismic and log data allows the identification and stratigraphic mapping of bounding surfaces in the Mannville with much more confidence than is possible using either data type alone. Seismic surfaces and reflection configurations put constraints on and suggest log correlation options. We note that, because of its small size, the 3-D survey we used in this survey may not show all of the diagnostic reflection terminations that are useful for seismic-based sequence stratigraphy (e.g., Mitchum et al., 1977; Emery and Myers, 1996). This will be a problem for other stratigraphic studies that use similar-size 3-D seismic surveys. Regional log correlations help to constrain whether erosion surfaces observed in these data represent local incision or stratigraphically significant surfaces (unconformities). Whatever their origin, and because any of these surfaces can juxtapose depositional facies associated with differing porosity and permeability, their recognition would be relevant as they could be associated with flow-unit boundaries in producing areas (e.g., Reynolds, 1996). The addition of core control would provide further insights, by

aiding in the interpretation of depositional facies (e.g., distinction between estuarine and fluvial channels), providing (possibly) biostratigraphic control, and recognition of key stratigraphic surfaces. Unfortunately no core exists from the Mannville Group in the study area.

The other benefit of 3-D seismic data is the possibility of using seismic geomorphology and well logs to define and map stratigraphic features that can act as lateral barriers, baffles or conduits for fluid flow. 3-D interpretation technology allows the user to pick the orientation of seismic profiles that best image the stratigraphic features of interest. For example, lateral accretion surfaces are best imaged in seismic profiles that are perpendicular to them, and can be missed on profiles that have other orientations. Stratal slices showing scroll bars can be used to determine the optimum orientation for examining vertical transects. The lateral accretion surfaces illustrated in this paper have multiple orientations and are subtle in vertical transects through the 3-D volume. However their presence is supported by stratal slices showing scroll bars, and by the characteristic bell-shaped log signatures that are typical of point bar deposits. If a grid of 2-D seismic lines is available from an area that has multiple orientations of point bars, it is highly probable that not all of the lateral accretion surfaces would be oriented perpendicular to the seismic lines, making their identification more difficult. The ability to extract time slices and stratal slices through 3-D volumes allows the interpreter to identify channels and morphologic features associated with channels, of various dimensions, that would probably be missed using logs or 2-D seismic data. These stratigraphic features are likely to have an impact on fluid flow (steam, hydrocarbons, etc.) in the subsurface.

## 2.7 Conclusions

The integration of 3-D seismic and well-log data proved to be an excellent tool to display and interpret the complex stratigraphy of the Mannville Group in southeastern Saskatchewan. Four candidate unconformities and one flooding surface were recognized and mapped for the Mannville Group and adjacent stratigraphic units. Definition of these surfaces allowed us to divide the Mannville into three stratigraphic units, with the S2 member of the Success Formation forming a fourth unit. Each unit displays different types of seismic facies that include parallel, semi-parallel, oblique-tangential, chaotic and reflection-free reflection patterns. Seismic facies from the vertical displays (traces and arbitrary lines) were combined with seismic geomorphology analysis of features seen in the horizontal slices (time slices and stratal slices) and log facies to interpret depositional features. Dimensions and aerial distribution of these features were obtained from the integrated dataset. For example, meandering channels in the Mannville are interpreted to vary in width between 100 and 600 m, and can be up to 30 m thick. Three kilometers of point bar migration, which generates stratigraphic features that can strongly affect hydrocarbon movement, were recognized in the north-east corner of the study area. A maze of channels that run in several directions through the study area, which characterize the middle strata of the Mannville Group, was interpreted from seismic time slices and well-logs.

The channels, point bars, unconformities and other stratigraphic features identified in this study can affect the distribution and movement of fluids in the subsurface. Detecting and mapping similar features is especially important in

heavy oil areas where enhanced recovery techniques are employed to stimulate production from the Mannville. It is important to point out that integration of 3-D seismic and log datasets with core and production information would make the resultant reservoir models even more robust. Unfortunately, such integration was not possible in this study.

Although the primary goal of this study was to focus on reservoir-scale definition of stratigraphic features, our results have significance for the stratigraphy of the Mannville Group in this area. The surfaces and units we defined using our integrated dataset do not correspond exactly to those defined through regional mapping. Although it is possible that seismic-resolution problems prevent us from identifying and mapping existing stratigraphic units, it is also possible that the stratigraphic framework of the Mannville in this area needs to be revisited.

## **2.8 Acknowledgements**

The seismic and well-log data used in this study were made available by NAL Resources Ltd. Seismic and log interpretations were undertaken using software donated by Landmark Graphics Corporation. Funding for this work was partially provided by an NSERC Discovery Grant to Hart. We thank all of these organizations for their continued support of our research.

Reviewers B. Hayes, D Uffen and Bulletin Editor Glen Stockmal are thanked for their detailed and constructive reviews which helped improve the quality of this manuscript.

## 2.9 References

- Bertram, G. T. and Milton, N.J. 1994. Seismic stratigraphy. In: Sequence Stratigraphy. D. Emery and K. J. Meyers (eds.). Blackwell, p. 45-60.
- Brown, A. R. 1999. Interpretation of three-dimensional seismic data. American Association of Petroleum Geologists, Memoir 42, 514 p.
- Cant, D. J. 1989. Zuni Sequence: The Foreland Basin, Lower Zuni Sequence: Middle Jurassic to Middle Cretaceous. In: Western Canada Sedimentary Basin. B. D. Ricketts (ed.). Canadian Society of Petroleum Geologists, p. 251-267.
- Cant, D. J. 1992. Subsurface Facies Analysis. In: Facies Model response to Sea Level Change. R.G. Walker and N. P. James (eds.). Geological Association of Canada, p. 27-45.
- Cant, D. J. and Abrahamson, B. 1996. Regional distribution and internal stratigraphy of the Lower Mannville. Bulletin of Canadian Petroleum Geology, v. 44, p. 508-529.
- Christopher, J. E. 1984. The Lower Cretaceous Mannville Group, northern Williston Basin region, Canada. In: The Mesozoic of middle North America. D.F. Slott and D. J. Glass (eds.). Canadian Society of Petroleum Geologists Memoir 9, p. 109-126.
- Christopher, J. E. 1997. Evolution of the Lower Cretaceous Mannville Sedimentary Basin in Saskatchewan. In: Petroleum geology of the Cretaceous Mannville Group, Western Canada. S. G. Pemberton and D. P. James (eds.). Canadian Society of Petroleum Geologists, Memoir 18, p. 191-210.

- Christopher, J. E. 2003. Jura-Cretaceous Success Formation and Lower Cretaceous Mannville Group of Saskatchewan. Report 223, Saskatchewan Industry and Resources Saskatchewan Geological Survey. p. 128.
- Emery, D. and Myers, K. J. 1996. Sequence Stratigraphy. Blackwell, p. 297.
- Hardage, B. A. and Remington, R. L. 1999. 3-D seismic stratal-surface concepts applied to the interpretation of a fluvial channel system deposited in a high-accommodation environment. *Geophysics*, v. 64, p. 609-620.
- Hayes, B J. R., Christopher, J. E., Rosenthal, L., Los, G., Mckercher, B., Minken, D.F., Tremblay, Y. M., Fennell, J. W. and Smith, D. G. 1994. Cretaceous Mannville Group of the Western Canada sedimentary basin. In: Geological atlas of the Western Canada sedimentary basin. G. Mossop and I. Shetsen (eds.). Canadian Society of Petroleum Geologists and Alberta Research Council, p. 317-334.
- Leckie, D. A., Vanbeselaere, N. and James, D. P. 1995. Use of sequence bounding surfaces for correlation and mapping in nonmarine, incised-valley reservoirs. *American Association of Petroleum Geologists Bulletin*, v. 79, p. 1728-1729.
- Leckie, D. A., Vanbeselaere, N. and James, D. P. 1997. Regional sedimentology, sequence stratigraphy and petroleum geology of the Mannville Group; southwestern Saskatchewan. In: Petroleum geology of the Cretaceous Mannville Group, Western Canada. S G. Pemberton and D. P. James (eds.). Canadian Society of Petroleum Geologists, Memoir 18, p. 211-262.
- Miall, A.D. 2002. Architecture and sequence stratigraphy of Pleistocene fluvial systems in the Malay Basin, based on seismic time slice analysis. *American Association of Petroleum Geologists Bulletin*, v. 86, p. 1201-1215.

- Mitchum, R. M, Vail, P. R. and Thompson, S. 1977. Seismic stratigraphy and global changes of sea level; Part 2, The depositional sequence as a basic unit for stratigraphic analysis. In: Seismic stratigraphy; applications to hydrocarbon exploration. C. E. Payton (ed.). American Association of Petroleum Geologists, Memoir 26, p. 53-62.
- Posamentier, H. W., Jervey, M. T. and Vail, P. R. 1988. Eustatic controls on clastic deposition. I. Conceptual framework. In: C. K. Wilgus, B. S. Hastings, Christopher. G. St. C. Kendall, H. W. Posamentier, C. A. Ross and J. C. Van Wagoner, (eds.), Sea Level Changes—An Integrated Approach, vol. 42. Society for Sedimentary Geology, Special Publication, p. 109 -124.
- Posamentier, H. W. 2000. Seismic stratigraphy into the next millennium; a focus on 3D seismic data. AAPG Annual Conference, New Orleans, Louisiana, Program and Abstracts CD.
- Posamentier, H. W. 2004. Seismic geomorphology: imaging elements of depositional systems from shelf to deep basin using 3D seismic data: implications for exploration and development. In: 3D Seismic Technology: Application to the Exploration of Sedimentary Basins. R. J. Davies, J. A. Cartwright, S.A. Stewart, M. Lappin, and J. R. Underhill (eds.) Geological Society, Memoir 29, p. 11-24.
- Poulton, T. P, Christopher, J. E., Hayes, B. J. R., Losert, L. Tittlemore, J., Gilchrist, R., Bezy, S., R. and McCabe, H. R. 1994. Jurassic and lowermost Cretaceous strata of the Western Canada sedimentary basin. In: Geological atlas of the Western Canada sedimentary basin, G. Mossop and I. Shetsen

- (eds.). Canadian Society of Petroleum Geologists and Alberta Research Council, p. 297-316.
- Reynolds, A.D. 1996. Paralic successions. In: Sequence Stratigraphy, D. Emery and K. J. Myers (eds.). Blackwell, p. 134-177.
- Smith, D. G. 1994. Paleogeographic evolution of the Western Canadian Foreland Basin. In: Geological atlas of the Western Canada sedimentary basin. G. Mossop and I. Shetsen (eds.). Canadian Society of Petroleum Geologists and Alberta Research Council, p. 297-316.
- Strobl, R. S., Wightman D. M., Walid K. M., Darrell K. C. and LiPing Y. 1997. Application of Outcrop Analogues and detailed reservoir characterization to the AOSTRA underground test facilities, McMurray Formation, North Eastern Alberta. In: Petroleum geology of the Cretaceous Mannville Group, Western Canada. S G. Pemberton and D. P. James (eds.). Canadian Society of Petroleum Geologists, Memoir 18, p. 375-391.
- Vail, P. R., Mitchum, R. M., Todd, R. G., Widmier, J. M., Thompson, S., Sangree, J. B., Bubb, J. N., and Hatlelid, W. G. 1977. Seismic Stratigraphy and Global Changes of Sea Level. In: Seismic Stratigraphy-applications to hydrocarbon exploration. C. E. Payton (ed.). American Association of Petroleum Geologists, Memoir 26, p. 49-212.
- Wallace-Dudley, K. E., Leckie, D. A, Vanbeselaere, N. A. and James, D. P. 1998. Regional geology, sedimentary and sequence stratigraphic framework of the Albian Pense Formation, southwestern Saskatchewan. Bulletin of Canadian Petroleum Geology, v. 46, p. 599-632.

- Van Hulst, F. F. N. 1984. Petroleum geology of Pikes Peak heavy oil field, Waseca Formation, Lower Cretaceous, Saskatchewan. In: The Mesozoic of middle North America. D. F. Stott and D. J. Glass (eds.). Canadian Society of Petroleum Geologists, Memoir 9, p. 441-454.
- Zeng, H., Backus, M.M., Barrow, K.T. and Tyler, N. 1998. Stratal slicing, part I: realistic 3-D seismic model. *Geophysics*, v. 63, p. 502-513.
- Zeng, H., Tucker, F. H. and Wood, L. J. 2000. Three-D Seismic Facies Imaging by Stratal Slicing of Miocene-Pliocene Sediments in Vermilion Block 50-Tiger Shoal Area, Offshore Louisiana. AAPG Annual Meeting, New Orleans, Louisiana, Program and Abstracts CD.

## 2.10 List of Figures

**Figure 1.** Location of the study area in southeastern Saskatchewan. The figure also shows the location of the main structural elements of the region, including the approximate outline of the Williston Basin.

**Figure 2.** Correlation chart of the Mannville Group (modified from Christopher, 2003). Stratigraphic nomenclature for southeast Saskatchewan is highlighted by box.

**Figure 3.** Base map showing outline of 3-D seismic survey and well locations. Filled dots correspond to the wells used in the study. Location of cross-section A-A' is indicated in the map. Circled filled dots show the wells in cross-section A-A'.

**Figure 4.** Examples of synthetic seismograms used to tie the well logs to the seismic data. Abbreviated formation names shown are: SSPK – Second White Speckled Shale, VKNG – Viking, MNVL – Mannville (corresponds to Surface IV in this study), UVNG – Upper Vanguard (corresponds to Surface II), LVNG – Lower Vanguard (Surface I), LGVB – Lower Gravelbourg, WTRS – Watrous.

**Figure 5.** a- Sample seismic transect showing the use of onlapping reflections to identify an unconformity. This unconformity corresponds to Surface IV (e.g., Fig. 8). b- Example of the combined use of logs and seismic data to define an unconformity. Reflection truncations correspond to the base of a sharp-based

sandbody. This surface (Surface II) corresponds to the sub-Cretaceous unconformity that separates Jurassic rocks from overlying Cretaceous units of the Success Formation and Mannville Group. (e.g., Figs. 6-8).

**Figure 6.** Stratigraphic cross section through southeastern Saskatchewan that shows the relation between the lithostratigraphic units described by Christopher (2003) and the seismic units defined in this paper. The wells used by Christopher are on the extremes of the cross section and the wells from the 3-D seismic study are located in the central part of the correlation. Greytones highlight seismic stratigraphic units defined in this paper. For each well the geophysical logs shown are Spontaneous Potential (left) and Resistivity (right). G. Petro = General Petroleum Member and Lloyd = Lloydminster Member.

**Figure 7.** Type Log for the area showing (to the left of the logs) the relation with the lithostratigraphic units described by Christopher (2003) and (to the right of the logs) the surfaces and units defined in this study.

**Figure 8.** Seismic transect and corresponding stratigraphic cross section A-A'. The seismic and well-log profiles shows the key surfaces interpreted in this study (labeled I to VII). Surfaces VII (a flooding surface in the Joli Fou) and I (a log marker separating the Upper and Lower Vanguard units) are shown, together with Surfaces II to VI and Units A-D. One-sided arrows highlight reflection terminations typical of those used to define stratigraphic surfaces. Location of A-A' is shown in Figure 3. Surface I is the stratigraphic datum in both sections.

**Figure 9.** Time-structure map (top) and perspective view (below) of Surface II, showing what may be the western margin of a valley of the Assiniboia drainage network. Map contours in seconds two-way traveltime (TWT). Coordinates are UTM (Zone 13).

**Figure 10.** Seismic lines C-C' and D-D' show the chaotic and semi-parallel fill reflections of Unit B as well as the location of the stratal slice (dotted line) through sand and shales of Unit B. Note the lateral variability in the log signature in Unit B, testifying to lateral lithologic heterogeneity in this interval. The stratal slice corresponds to a slice through the data 81 ms below Surface VII, and it shows crossing and curvilinear amplitude trends that are interpreted as fluvial channels that run in various directions through the area.

**Figure 11.** Seismic images of a point bar. A) Uninterpreted (left) and interpreted (right) North-South seismic profile E-E' shows a series of shingled troughs (yellow oval) that dip subtly to the right. Interpreted view highlights dipping reflections that represent lateral accretion surfaces. B) Same view as in A but with gamma ray log overlay. Note the fining-upward signature of the logs (arrows) in this interval. C) In a stratal slice, the lateral accretion surfaces correspond to arcuate amplitude trends that are similar in scale and shape to modern scroll bars. D) Example of modern scroll bars on the floodplain between the Apure and Apurito rivers in Venezuela, the distance between the asterisks is 3 kilometers

(Photo courtesy of R.H. Meade, USGS). The level of the stratal slice is indicated by the dashed line in the seismic profiles.

**Figure 12.** Seismic profile F-F' shows the oblique-tangential reflection configuration of Unit C and the location of a stratal slice that cuts across the features at its base. The stratal slice (53 ms below Surface VII) displays arcuate figures in the western part of the survey that are interpreted to be scroll bars (e.g., Fig. 11) of a meandering channel system. The upper arrow highlights possible toplap below surface V. Unit C is located between Surfaces V and IV.

**Figure 13.** Sequential seismic transects crossing a positive-relief, arcuate channel in Unit C. Channel location is circled in all transects. One well (shown in transect c-c') penetrates the channel and it shows the channel to be sandy at that location. Elsewhere the equivalent stratigraphic level is shaly (e.g., logs in transects b-b' and d-d'). The positive relief is therefore thought to be associated with differential compaction between the sand-filled channel and the surrounding shales. The stratal slice location is shown with a dashed line in the seismic profiles. Unit C is located between Surfaces V and IV.

**Figure 14.** Stratal slice 5 ms above Surface V showing a curvilinear feature interpreted to be a channel around 140 m wide at the eastern region of the seismic survey. The stratigraphic location of the stratal slice and the feature are displayed in the seismic profile G-G'.

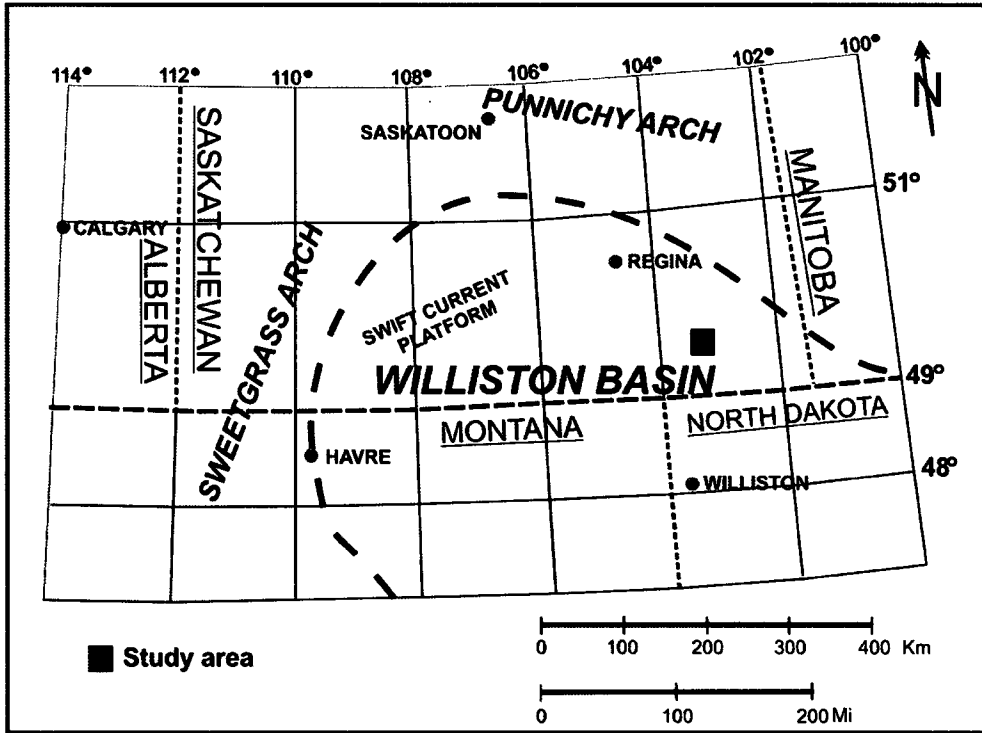


Fig 1

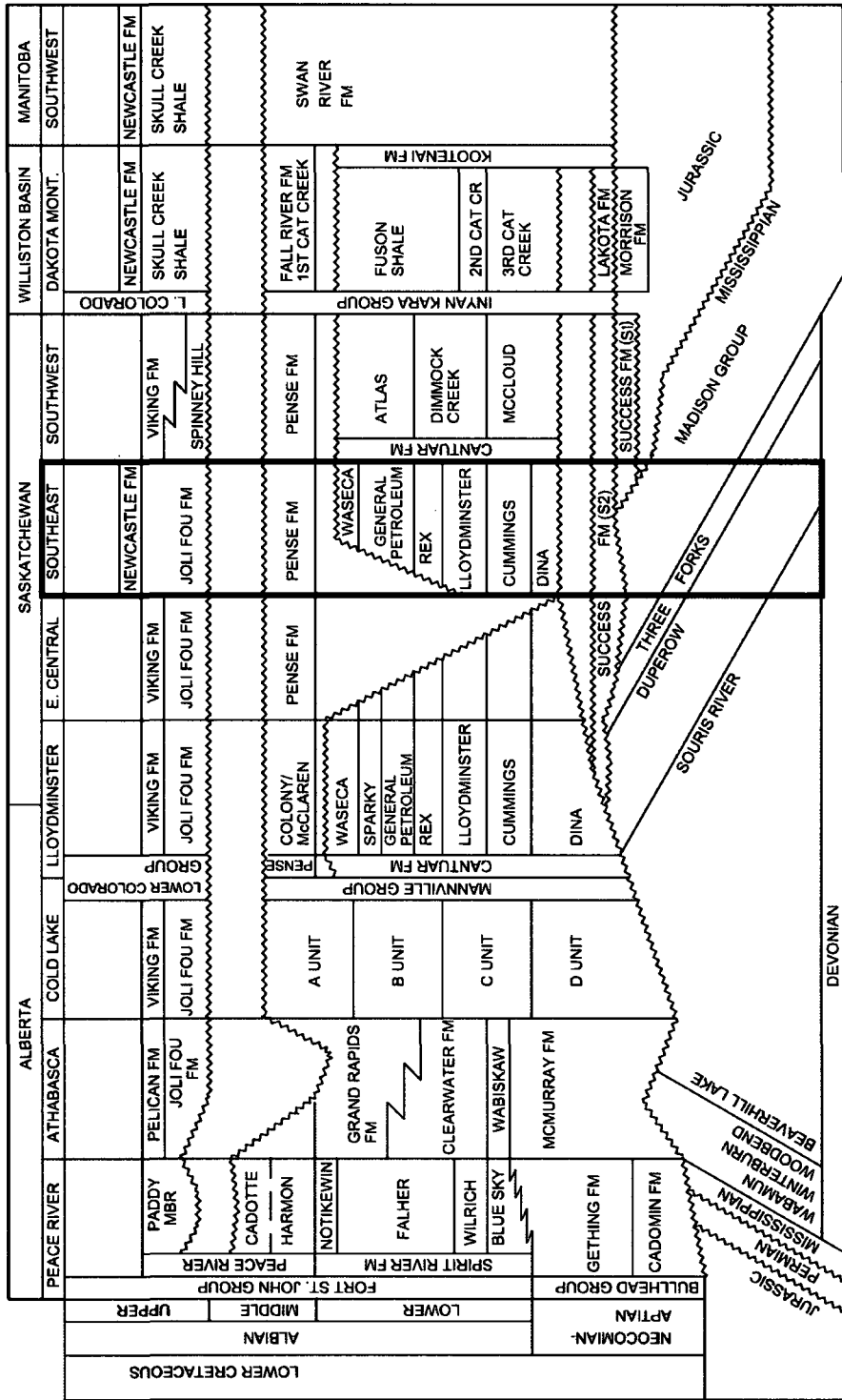


Fig 2

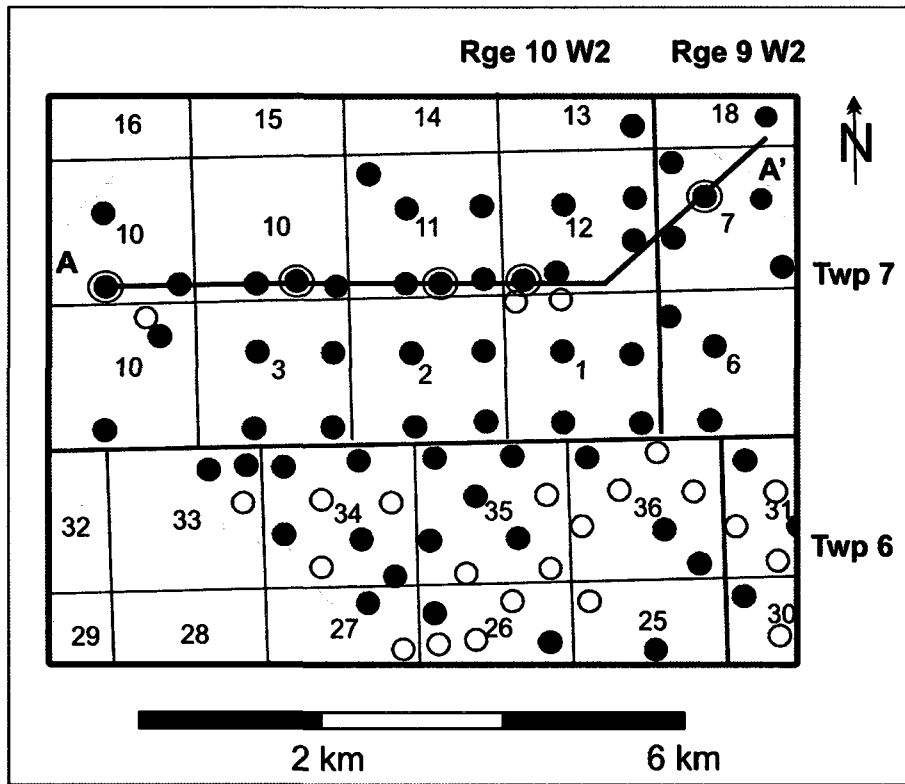


Fig 3

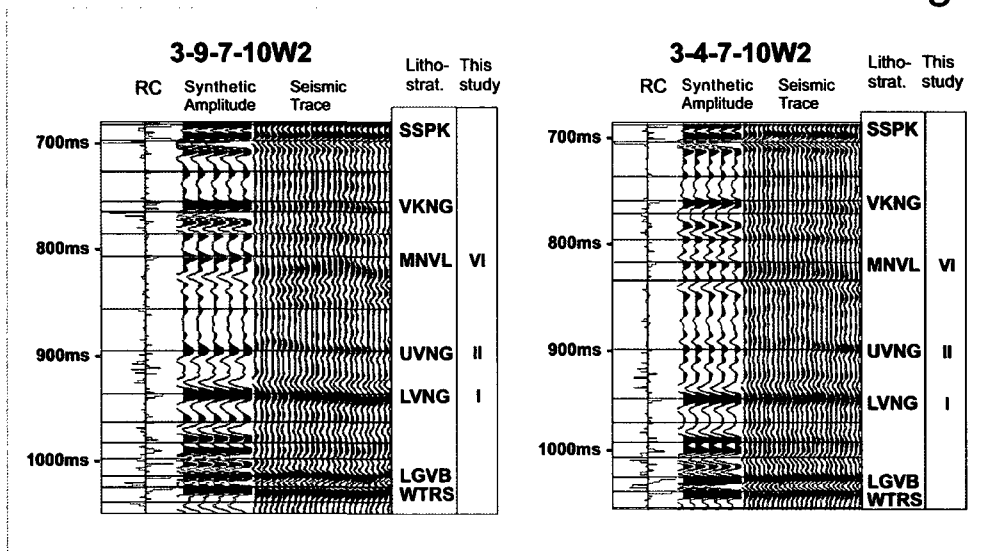


Fig 4

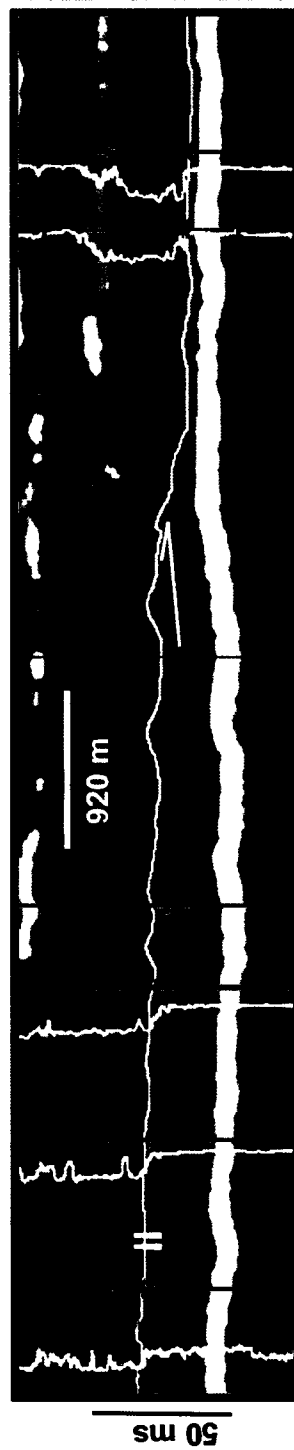
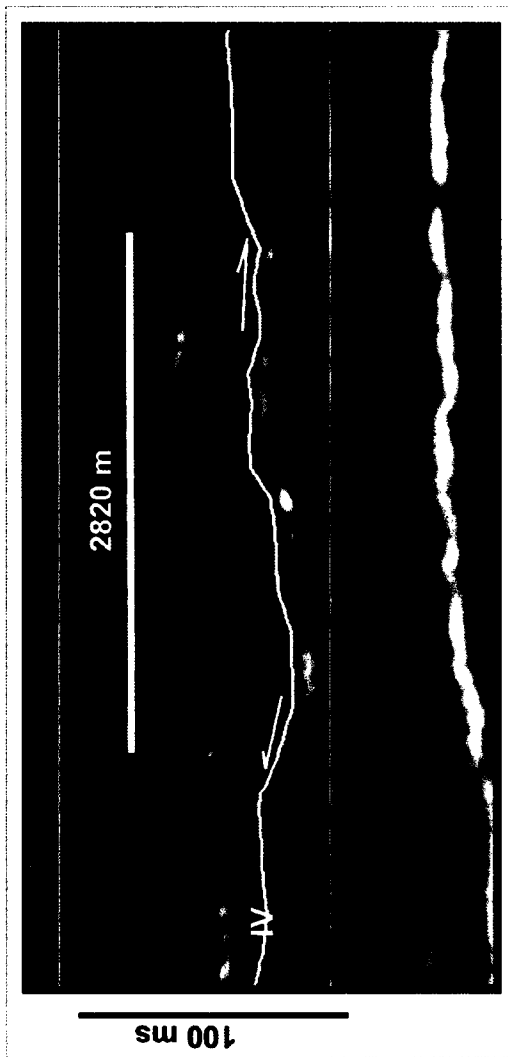


Fig 5

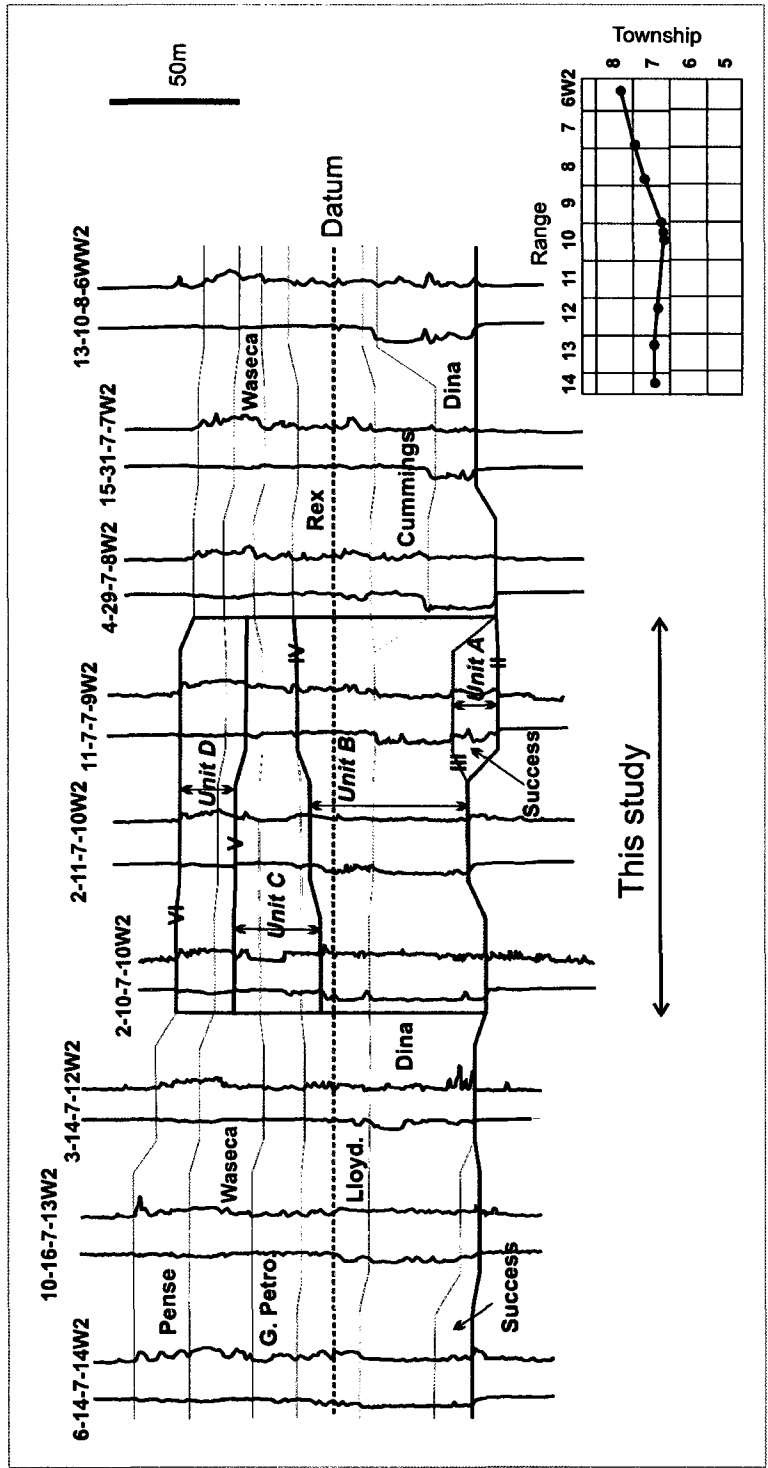


Fig 6

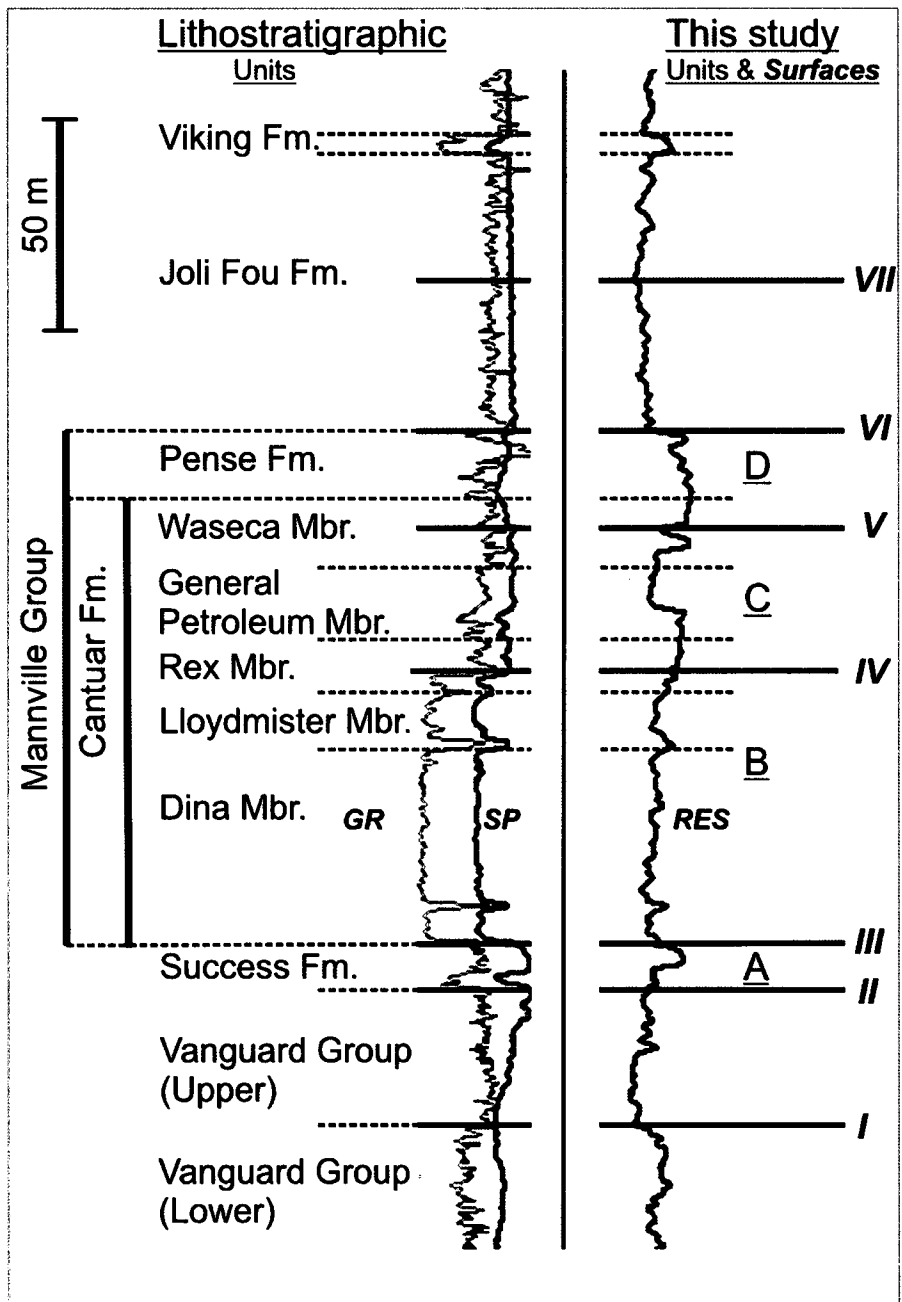


Fig 7

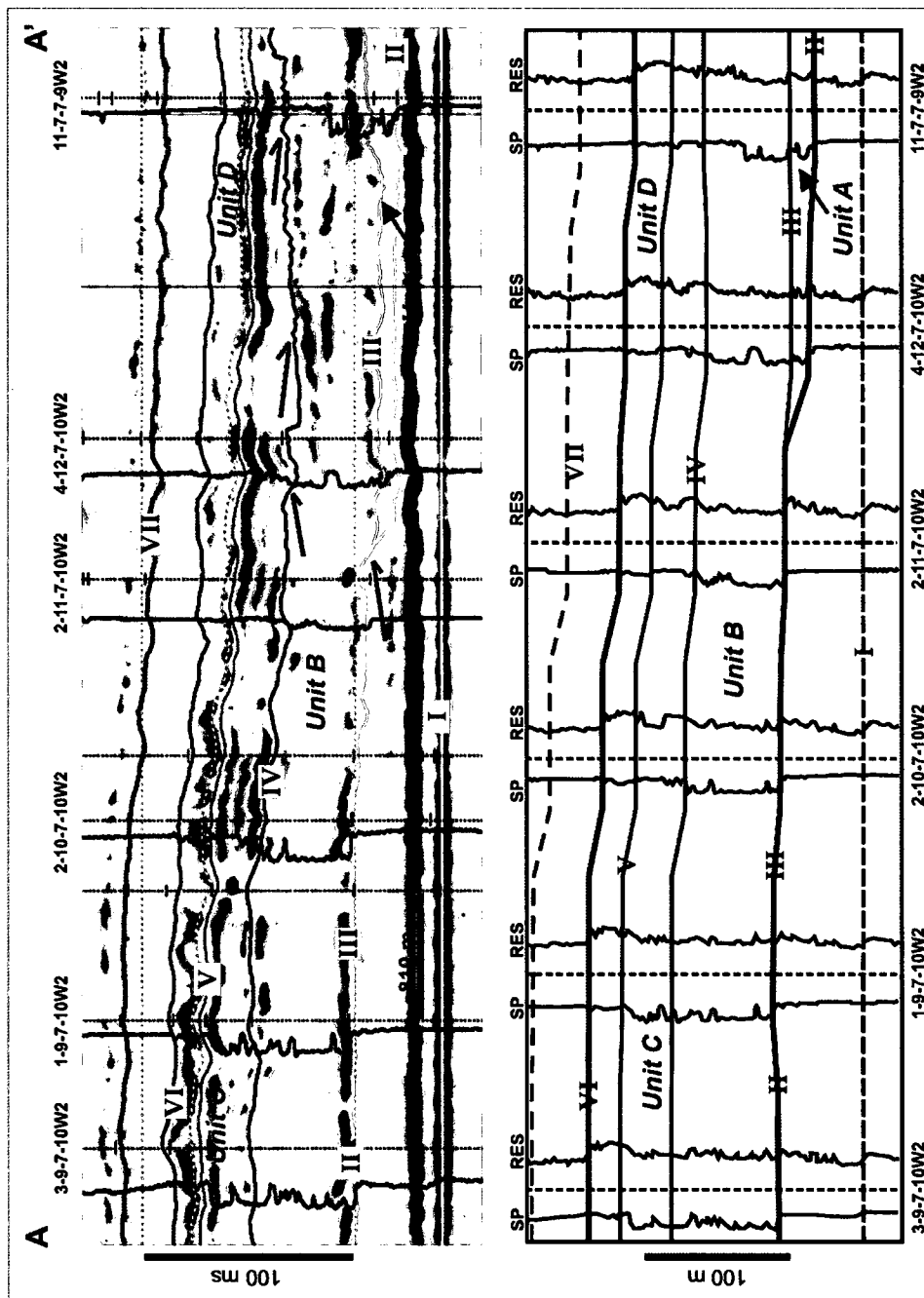


Fig 8

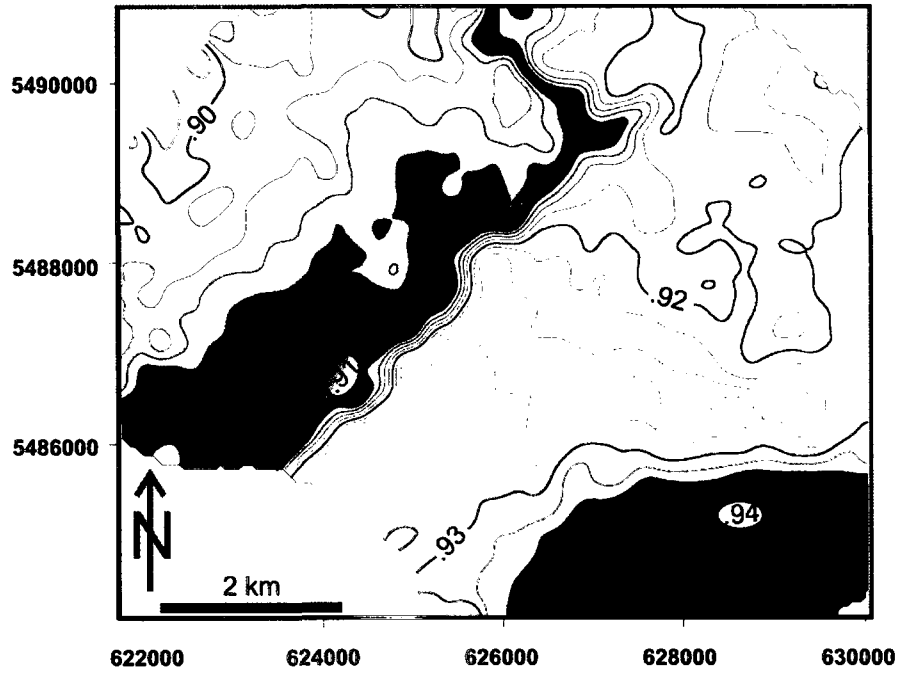


Fig 9

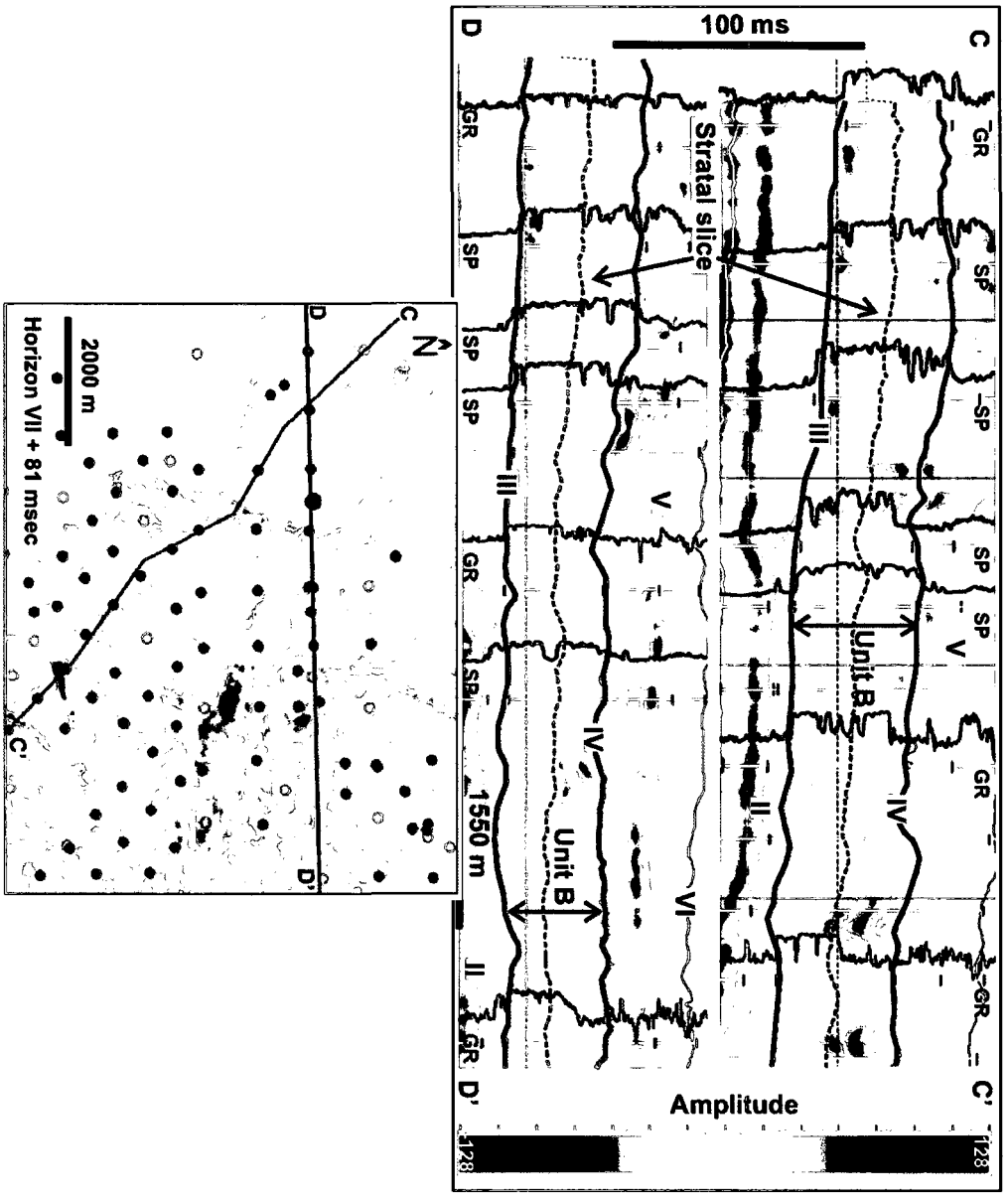


Fig 10

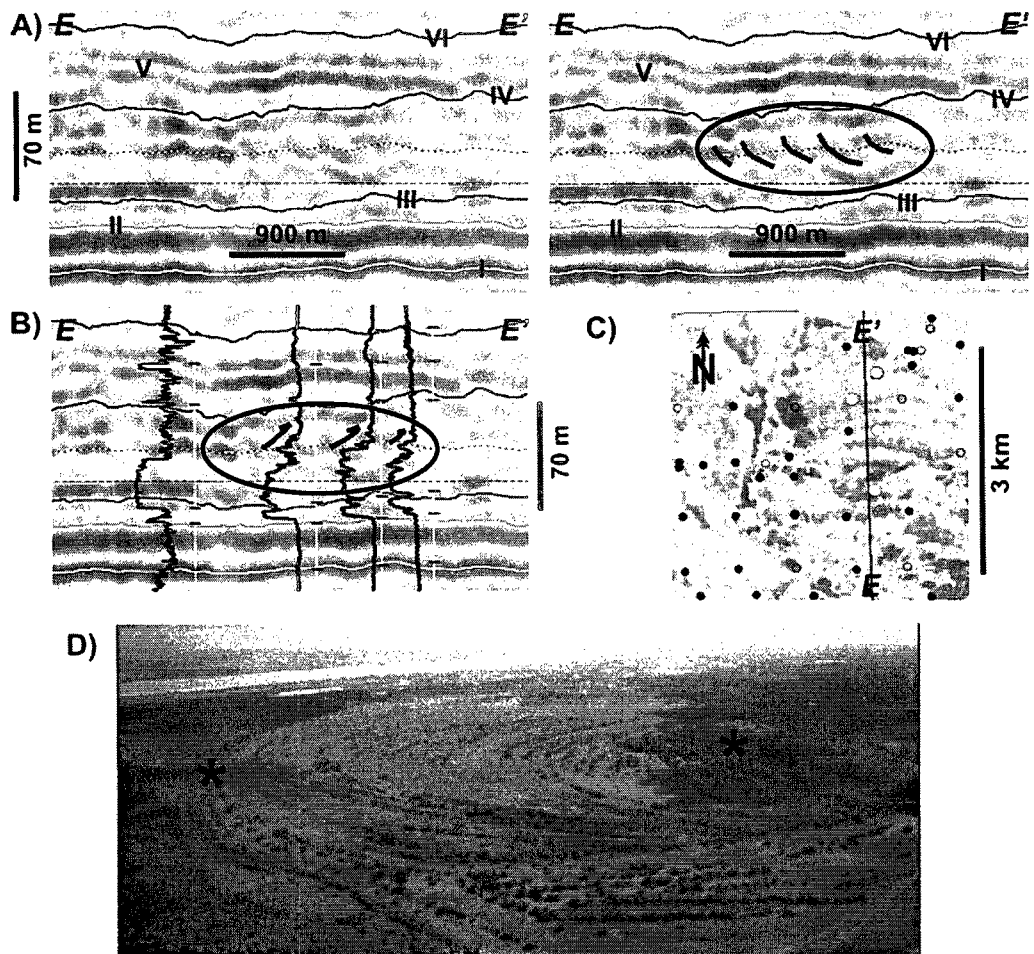


Fig 11

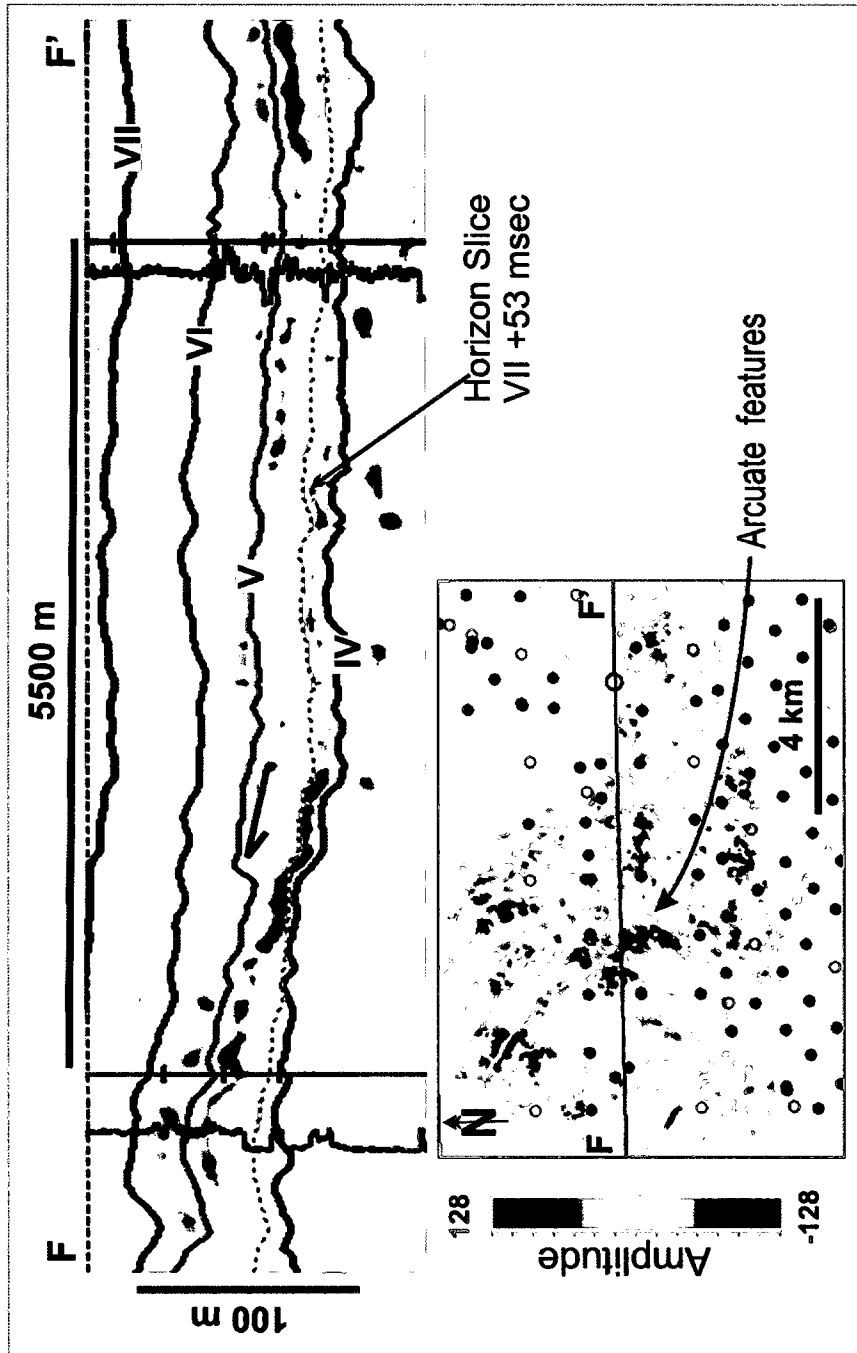


Fig 12

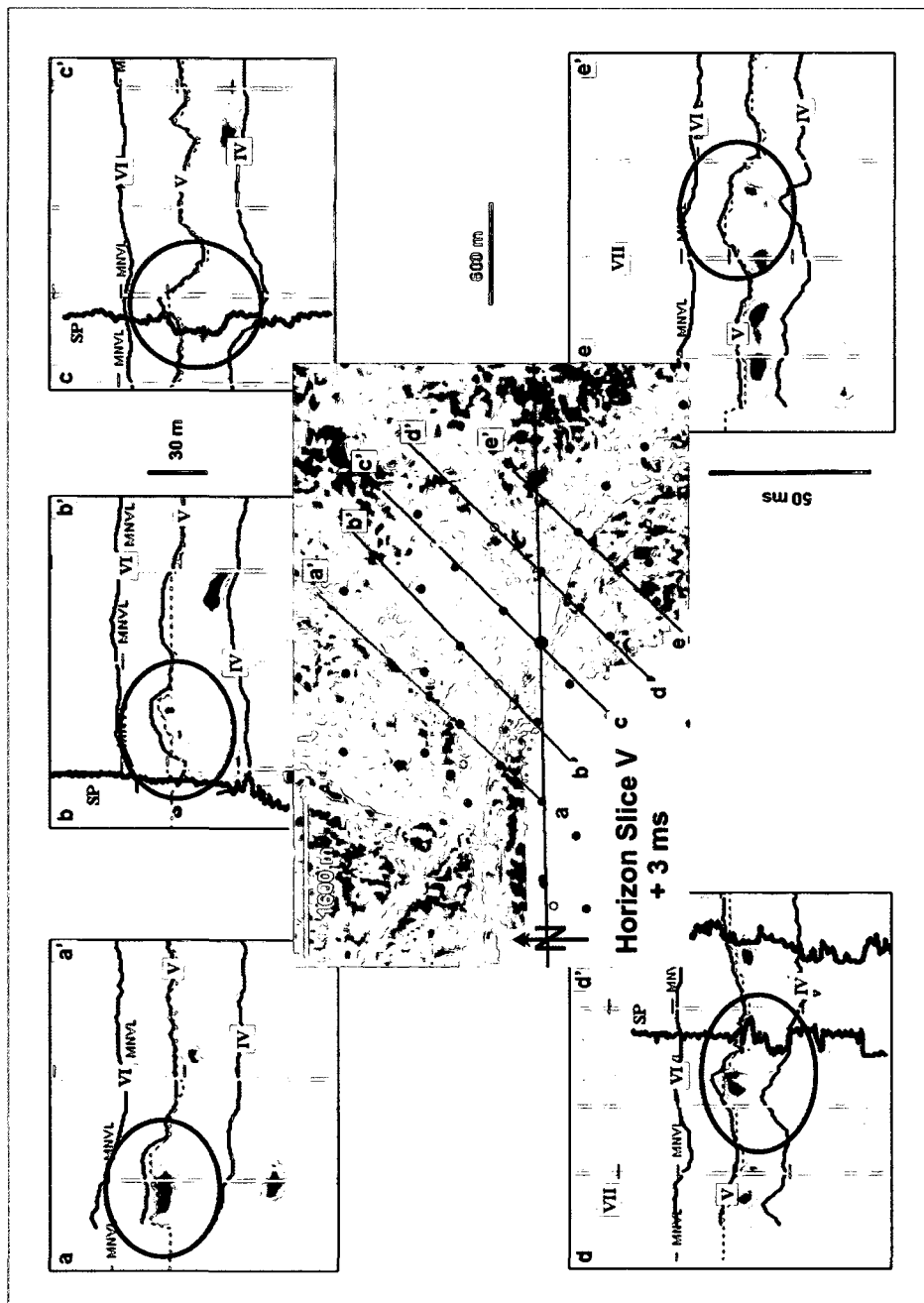


Fig 13

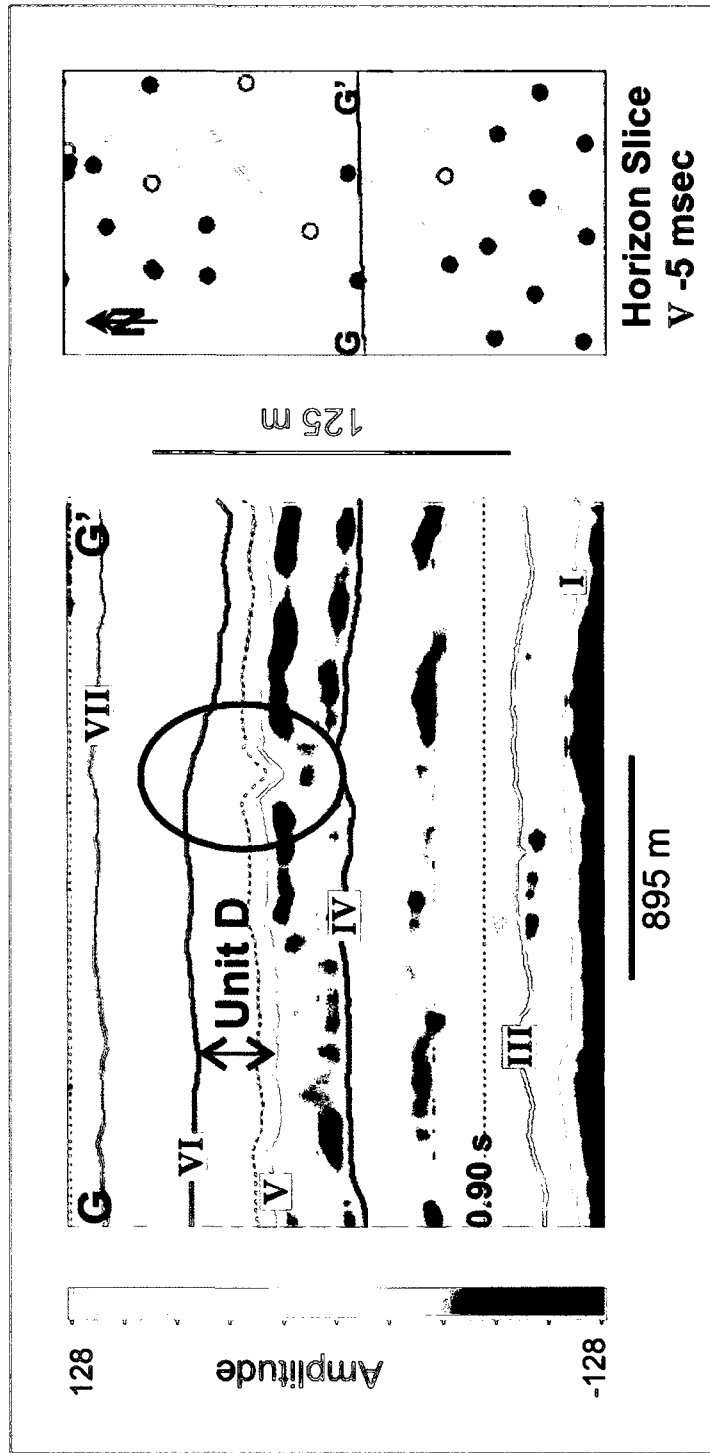


Fig 14

### **INTRODUCTION TO CHAPTER 3**

The following chapter focuses on a smaller stratigraphic interval (Lower Mannville Group) than the one described in chapter 2 (Mannville Group), located in a heavy oil reservoir in west-central Saskatchewan. This chapter describes how multiattribute analysis and neural network training are used to obtain a relationship between seismic attributes and lithology (gamma-ray response), which is used to predict gamma-ray (GR) response away from well control within the seismic cube. This information combined with the stratigraphic model obtained from the interpretation of seismic and well data is used to generate an integrated geological model for the Lower Mannville deposits of the region.

### **3. Dimensional Distribution of Channels in a Lower Cretaceous (Mannville Group) Heavy Oil Reservoir in West-Central Saskatchewan; Part 1: Seismic Attribute-Based Generation of a Pseudo-Lithology Volume**

#### **3.1 Abstract**

The Winter Field is a stratigraphically controlled heavy oil reservoir with production from the undifferentiated Dina-Cummings Members of the Lower Cretaceous Mannville Group. As in other heavy oil reservoirs, stratigraphic heterogeneities and structural elements are potentially responsible for hydrocarbon trapping and can act as baffles or barriers to fluid flow. In order to effectively drain the reservoir, its stratigraphic architecture needs to be established. In this study, we integrated seismic and well-log data to generate a pseudo-lithology or GR volume that seeks to capture the distribution of reservoir and non-reservoir deposits in the study area. Neural networks were used to obtain a relationship between seismic attributes and lithology (gamma-ray response) at well locations. The neural networks then used that relationship to predict GR response away from well control within the seismic volume. We then used both the original seismic and GR volumes to define stratigraphic features and assign lithologies to them. Although not undertaken in this study, the resulting stratigraphic framework could be used to help construct a static reservoir model.

### 3.2 Introduction

The Western Canadian Sedimentary Basin is well known for its large unconventional hydrocarbon resource base, in particular the oil sands and the heavy oil deposits of the provinces of Alberta and Saskatchewan (Fig. 1). These reservoirs are located in Lower Cretaceous clastic deposits of the Mannville and the Bullhead Groups (Fig 2) which unconformably overlie Devonian to Jurassic deposits. These stratigraphically complex reservoirs formed in the initial stages of development of the Western Canadian Foreland Basin. The complexity of the reservoir is due to the nature of the deposits. These, simplistically, progressively change from fluvial at the base to shallow marine at the top, and to the irregular topography of the Paleozoic terrain over which they were deposited.

Many geological (cores, outcrop etc.) and geophysical tools (well logs, seismic data, etc.) have been used, either alone (e.g. Groenneveld & Stasiuk, 1984; Zaitlin & Shultz, 1984; Leckie et al., 1997; Christopher, 2003) or together (e.g.; Dequierez et al., 1995; Sarzalejo and Hart, 2006) to examine the stratigraphic architecture of the Mannville. The type(s) of data used by these authors is determined by their interests (e.g., geologists *versus* geophysicists) and by data availability and quality. Data quality is largely a function of the physical properties of the strata being studied (e.g. degree of consolidation affects borehole stability, thereby affecting logging response). Well logs and cores were originally used to understand and map the reservoir units. Later, the introduction of 3-D seismic data, including the application of seismic geomorphology (e.g. Posamentier, 2001; Wood, 2003; Sarzalejo and Hart, 2006) provided a powerful way of imaging the spatial distribution of depositional features, which in turn can

be associated to reservoir lithofacies. Seismic displays of attributes like coherence, instantaneous frequency, etc., also provide new insights into what the conventional amplitude displays were able to offer. Seismic attributes, seismic inversion, multiattribute analysis and neural networks are now increasingly used to predict reservoir physical properties (e.g., porosity, lithology), thereby contributing towards a better understanding of the reservoir. These methods are increasingly applied to study the complex heavy oil deposits (e.g., Calver et al., 1999; Tonn, 2002, Takahashi et al., 2006).

The study area, a portion of the Winter Field in Saskatchewan, is characterized by a high water-oil ratio of the produced fluids. The reservoir is located between 600 and 700 meters below the ground surface and produces through horizontal wells. The oil pool that has produced mainly by reservoir water drive has no gas cap. Water injection is used to enhance recovery in this pool. The decrease of pressure associated with the water production has strongly affected secondary production. Although many different factors (e.g., completion methods) affect reservoir performance, a better understanding of the reservoir architecture is needed in order to produce the heavy oil that is left behind. Mapping the top of the reservoir using seismic data is challenging but possible with the aid of the boreholes, but no previous attempt has been made to define the detailed stratigraphic architecture of the reservoir using 3-D seismic data.

In this paper we describe how we predicted the 3-D distribution of lithofacies in the reservoir by integrating borehole logs and 3-D seismic data. The seismic data were used to map stratigraphic horizons identified in the boreholes, to identify and map stratigraphic features in the area and to predict lithology (GR

log response) by integrating seismic attributes with borehole information. Ultimately, we sought to generate a robust geological model of the area that can be used in the design of a production strategy that will lead to higher recovery rates. In the companion paper (Sarzalajo and Hart, chapter 4) we integrate the attribute-based lithology prediction with sedimentologic core descriptions to define the depositional environment and history of the Mannville Group in this area.

### **3.3 Geological Overview**

The study area is part of the Winter Field, located in Township 42 and Range 25 of west-central Saskatchewan (Fig. 1). The stratigraphic interval of interest includes the Dina-Cummings Members of the Cantuar Formation (Fig. 2) within the Lower Cretaceous Mannville Group. In the study area, no clear boundary can be established between the two members that produce together in an oil reservoir called the Winter Cummings Pool. The reservoir rests on top of the Sub-Cretaceous unconformity that separates Devonian carbonates of the Duperow Formation from the overlying Cretaceous clastics of the Mannville Group.

Few geological studies have examined the stratigraphy of the Mannville in the current study area. Groeneveld and Stasiuk (1984) studied the Dina-Cummings interval, and more specifically the Cummings coal, which constitutes an important correlation marker within the reservoir. They interpreted a fluvial to marginal marine origin for the Dina-Cummings unit and established that the coal was formed from marsh peat. The marine Lloydminster Member, which overlies

the Cummings Member, contains a shaly interval that is a regional seal for the Cretaceous Lower Mannville reservoirs.

### **3.4 Database and Methodology**

The database for this project consists of a 3-D seismic survey covering approximately 15 km<sup>2</sup> and digital well-logs for 17 wells (Fig. 3). This survey was selected from amongst several other 3-D surveys that cover parts of Winter Field because of the relatively high number of wells (14) in the survey area with sonic and density logs, data considered key for the analysis. The 3-D seismic survey we used has a bin size of 20 m by 20 m, a sample rate of 2 milliseconds, and the depth to the Mannville ranged from 466 to 866 ms two-way time (TWT). The survey has a dominant frequency of approximately 50 Hz at the reservoir level (Figure 4). The vertical resolution of the data (defined as  $\frac{1}{4}$  of the wavelength) is approximately 15 m, calculated using log-derived velocities of 2970 m/s in the interval of interest. If, following Brown (2003), we can define detection limits of  $\lambda/20$  to  $\lambda/30$  for the good- to excellent-quality seismic data we worked with, then the seismic data should be able to detect beds 2 to 3 m thick, provided that there is a significant enough acoustic impedance contrast to generate a reflection. GR logs were available for the majority of the wells and were used as a stratigraphic correlation tool together with the resistivity, sonic and density logs for each well.

The workflow for this study is shown in Figure 5. The basic information used was well and 3-D seismic data. This information allowed us to establish a stratigraphic framework for the study area. Sonic and density logs were used to generate synthetic seismograms to tie the 14 wells to the seismic data. Key

stratigraphic surfaces such as unconformities and flooding surfaces were defined in logs and in the seismic data using the seismic stratigraphic and sequence stratigraphic principles described by Mitchum et al. (1977), Vail et al., (1977), Posamentier et al. (1988), Bertram and Milton (1994) and others. Because of the small area covered by the seismic data volume, and in the absence of good age control from microfossils, we recognize that it can be difficult to identify diagnostic reflection terminations or other seismic and/or well-based criteria for defining key stratigraphic surfaces. In this small area it is also difficult to distinguish localized erosion surfaces (e.g. channel bases) from regionally significant sequence boundaries (Sarzalajo and Hart, 2006; Hart et al., 2007). As such, building a complete sequence stratigraphic model for the study area was beyond the scope of this project.

We began by tying the wells to the seismic data using synthetic seismograms. After the well ties had been made, wireline log and seismic correlations could be made simultaneously, with the aid of computer packages, so that the picks were selected to honor both data sets by giving more weight during the interpretation to the most reliable data source at each location. This procedure was necessary because the log and seismic correlations could be ambiguous in places, and using both datasets to correlate significantly reduced the level of ambiguity. Wherever seismic resolution permitted, the log-based stratigraphic picks were transferred to the seismic data via the synthetic seismograms and correlated throughout the seismic volume. The initial horizon picks were made to define top and bottom horizons that were used to constrain the analysis interval for the volume-based attribute study.

The attribute study was carried out after the stratigraphic framework had been established in order to generate a GR (pseudo-lithology) volume for the Dina-Cummings interval in the study area. We selected a volume-based approach (Hampson et al., 2001; Leiphart and Hart, 2001; Sagan and Hart, 2006) over a horizon-based study (e.g., Pearson and Hart, 2004) because of the thickness (45-70 m) and expected geological complexity of the interval under study. As described below, the methodology of Hampson et al. (2001) identifies the best combination of seismic attributes to predict the log-based physical property of interest. The analysis was performed using only the wells that could be adequately tied to the seismic data via a synthetic seismogram. Various techniques were used to evaluate the lithology prediction.

### **3.5 Results**

#### **3.5.1 Stratigraphic correlation**

A type log showing some of the members of the Cantuar Formation is displayed in Figure 6. The Dina-Cummings unit forms the reservoir here. The strong contrast in physical properties between the Cretaceous clastics of the Mannville and the underlying Devonian carbonates generates a diagnostic signature in the logs shown in Figure 6. The upward change from higher to lower density, resistivity and higher spontaneous potential indicates the change from non-permeable carbonate to water-saturated sand. The Dina-Cummings unit contains blocky sand at the base that is usually more than 20 m thick and ranges between 6 and 40 m thick. The blocky sand is not all oil charged, and an oil-water

contact is easily observed in the resistivity logs. The blocky sand, which can contain shale layers up to 0.25 m thick (core data), is overlain by marginal-marine deposits that generally include a coal referred to as the Cummings coal. The marginal marine succession of the Cummings Member grades upward into marine shale (Figure 6) of the Lloydminster Member. This shale interval, which corresponds to the regional seal for the Lower Cretaceous reservoir sands, contains a maximum flooding surface (MFS) that constitutes an excellent stratigraphic marker for the well correlations.

Detailed inter-well correlations of the Dina-Cummings interval cannot be made confidently because of the complicated stratigraphy of these fluvial to marginal-marine channels (c.f. Sarzalejo and Hart, 2006). The top of the Duperow carbonates (DPRW pick; i.e. sub-Cretaceous unconformity), the Cummings coal (CMGS\_C) and the maximum flooding surface (MFS) above the reservoir are the best markers for the well correlation. Other picks included the tops of the Cummings (CMGS), Lloydminster (LDMR), and Rex (REX) Members of the Cantuar Formation.

Well and seismic data were tied using synthetic seismograms. Figure 7 shows an example of a “good” and a “bad” synthetic seismogram. The first synthetic seismogram has a high correlation coefficient (0.94) and the second one has a low correlation coefficient (0.82) when compared to the seismic trace in the well location. A vertical transect through the 3-D seismic data (Fig. 8) shows four wells penetrating the section of interest that were tied to the seismic data using synthetic seismograms. The seismic data show a high-amplitude positive reflection which corresponds to the Duperow/Mannville interface (DPRW). This

reflection was tied to a high-amplitude peak in the synthetic seismograms and corresponds to the base of the interval chosen for the attribute study. The reflections that correspond to the Dina-Cummings interval above the unconformity show a more discontinuous nature and at well sites, the seismic traces generally do not match the synthetic seismograms. Correlating the reflections within the reservoir interval was a difficult task because they lack continuity. As such, we searched for another continuous reflector higher in the section that could be used to constrain the attribute analysis window. This reflector, located above the reservoir level and henceforth referred to as the Intra-Rex horizon (IREX), corresponds to a positive reflection within the Rex Member of the Cantuar Formation. This reflector was recognized throughout the current study area and in neighboring 3-D seismic surveys not reported in this paper. The IREX corresponds to fine-grained deposits (shales and silts) with higher density than the surrounding sandy deposits. Figure 8 shows how the top (IREX) and bottom (DPRW) horizons constrain the attribute analysis window.

The two cross-sections; seismic and stratigraphic, shown in Figure 9 illustrate the interpreted IREX and DPRW horizons. The well-log cross-section is hung on the MFS and shows the blocky sand reservoir package that overlies the unconformity, the overlying thinner coarsening upward package of shale, coal and sand, and the overlying marine shale containing the datum (MFS). A coarsening upward sequence deposited over the shale completes the interval that will be used for the lithology prediction. The attribute analysis window, bounded by continuous relatively high-amplitude reflections, is composed of a variety of

lithologies of different thickness that correspond to discontinuous reflections in the seismic data.

A 3-D representation of the two surfaces (IREX and DPRW) is shown in Figure 10. The IREX surface shows some significant features, such as a N-S incision cutting through the center of the area, two SW-NE incisions to the west and some minor elongated lows in the east. The unconformity (DPRW) is relatively smooth in this area with the exception of a couple of circular lows that penetrate the underlying carbonates. We interpret these lows to represent collapsed sections due to karsting in these Devonian carbonates.

### **3.5.2 Attribute Study**

Having defined the broad-scale stratigraphic framework, the next step was to predict the distribution of lithology by integrating seismic attributes with wireline logs. This attribute study sought to establish an empirical correlation between seismic attributes and GR logs at well locations. If a statistically significant correlation could be established, this correlation would be used to predict lithology elsewhere in the seismic volume where logs are lacking.

Cross-plots of acoustic impedance (AI) vs. gamma-ray (GR) were generated to see whether a relationship between the seismic data and lithology might be expected. Figure 11 shows one such cross-plot generated using all the wells with sonic and density logs. This figure shows that even though there is no clear linear relationship between the two variables, the diverse lithologies are clustered and occur in different locations within the plot. In general, the values of AI for the reservoir sands are slightly lower than those for finer-grained non-

reservoir strata, although there is considerable overlap. Some wells show a slight difference in AI between the oil and water bearing sands. Cross-plots of AI vs. porosity were also generated but did not show significant trends or correlations.

The next part of the attribute study involved the generation of attributes from the seismic data. These were combined and ranked by their ability to predict the targeted log property. One hundred and forty-five GR data points from the fourteen wells with synthetic seismograms were used as input for the attribute analysis. Eighteen attributes, including the results of an acoustic impedance inversion, were calculated and used in the regression exercise. Following the methods of Hampson et al. (2001), stepwise linear regression and validation testing were used to determine that a combination of three attributes, the integrated trace, apparent polarity and filter 25/30-35/40 (all described in the Discussion section), gave the best prediction. The validation testing systematically excluded one well at a time from the correlation exercise, and then predicted the log response of the excluded well based on the correlation between attributes and log properties derived from the other wells. Figure 12 shows that the validation error increases with more than three attributes, meaning that the additional attributes are over-fitting the data. Using multivariate linear regression, this combination of three attributes could be used to predict the gamma-ray log in the training data set, i.e. the wells with GR curves, with a correlation coefficient of 0.82 (Fig. 13) and an average error of 17 American Petroleum Institute (API) units (8.5%). API units are a measure of natural radioactivity of the rocks based on an artificially radioactive concrete block located at the University of Houston, Texas, USA. This reference block is defined to have a radioactivity that

corresponds to 200 API units. Figure 11 shows values of GR that range from 20-30 API for clean reservoir sands to 70- 140 API for shales.

Having identified the three best attributes, a neural network was trained to predict GR logs from the three selected seismic attributes. Because they can capture non-linear relationships between variables, the use of neural networks often provides a statistically better and a more geologically reasonable result than linear regression (e.g., Leiphart and Hart, 2001). The application of the neural networks to predict the GR values resulted in better correlation values than the multiattribute regression (Fig. 13) as expected. The correlation coefficient for the application of neural networks to predict the GR was 0.90 and the prediction error 13 API units (6.5%). Figure 14 shows the result of applying the non-linear relationship to predict the target GR log. Validation testing of the neural networks results using the validation method described above gave an average correlation coefficient of 0.79 and an error of 19 API units (9.5%), thereby indicating that neural networks could satisfactorily, but not perfectly, predict lithology at locations not included in the correlation exercise.

The type of neural network used for the analysis (specifically for the mapping component) was the probabilistic neural network (Masters, 1995; Specht, 1990, 1991). Hampson et al. (2001) define the probabilistic neural network (PNN) as a mathematical interpolation scheme that uses neural network architecture for its implementation.

The training dataset consisted of a series of values that exist for each seismic sample within the analysis windows in the location of all the wells used in the exercise. For seismic sample 1, the training values comprise the values of the

attributes  $A_{11}$ ,  $A_{21}$ ,  $A_{31}$ , (in the case of three attributes) and  $L_1$ , the measured target log value. The PPN assumes that it is possible to write each new output log value as a linear combination of the log values in the training data. If  $x = \{A_{1j}, A_{2j}, A_{3j}\}$  for a new data sample, and  $L_i$  corresponds to the measured target log values for each of the data points, the new log value  $\hat{L}(x)$  can be obtained from an expression that is a function of  $L_i$  and  $D(x, x_i)$ . This last value,  $D$ , corresponds to the distance between the input point and each of the training points  $x_i$ . This distance is scaled by  $\sigma_j$  (which could be different for each attribute) which basically functions like a smoothing operator (reduction in curvature of the function relating attributes to predict the log value). Searching for the optimal set of these smoothing parameters  $\sigma_j$  constitutes the training of the network. The resulting network is the one with the  $\sigma_j$  values that generate the lowest validation error.

The validation process consists in predicting a specific  $L_m$  value without using sample  $m$ 's values in the training and later comparing the result with the known value. A validation or prediction error is calculated for the sample and the process is repeated for all of the training samples to obtain a total prediction error for the training data. Hampson et al. (2001) in their description of the neural network process emphasize that the prediction error depends on the choice of the parameters  $\sigma_j$ . The resulting network has a minimized validation error.

The neural network training done to generate the lithological prediction presented here tried 25  $\sigma$  values that ranged from 0.1 to 3. Well by well was the

type of validation implemented and the number of conjugate-gradient iterations was set to 20.

The non-linear function from the neural network was applied to the seismic data to generate the GR (pseudo-lithology) volume. Figure 15 shows a vertical transect through the resulting gamma-ray volume, the colors representing the predicted API values at the trace location. The GR curve for one of the wells is superimposed on the image. Note how the shaly and sandy intervals seen in the GR log of the well correspond to the attribute-based predictions. In general, three main units are observed in this volume: a lower sandy zone (Dina-Cummings interval), a middle shale zone (including the MFS) and an upper zone that is somewhat sandier (Lloydminster and Rex interval). The shale (~7 m thick) corresponding to the MFS in the middle of the interval is well imaged, whereas the thin shale layers of the Dina-Cummings interval are not recognized because they are below the limits of seismic detection (as predicted above). The top of the Dina-Cummings reservoir in this location is well imaged by the prediction. Figure 16 shows another vertical transect through the GR (pseudo-lithology) volume with the same wells as Figure 9. In this display, the amplitude traces (in gray) are overlaid on the GR volume (shown in color). Low GR values are displayed in yellow, intermediate values in light brown and the high gamma in green. As discussed below and in the companion paper (Sarzalajo and Hart, chapter 4) the GR volume was subsequently integrated with core and other data to establish a geological model for the study area.

### 3.6 Discussion

Hart (1999), Hampson et al. (2001) and others have defined a series of necessary steps for undertaking seismic attribute studies. These steps are: ensuring that the wells are adequately tied to the seismic data to establish a proper stratigraphic framework, defining the best combination of seismic attributes to predict the physical property of interest (statistically testing the correlation), examining the physical basis for the relationships between attributes and the property of interest, and performing a geologic evaluation of the results. Here we examine each of these points in succession in order to evaluate the validity of the attribute-based lithology prediction.

Well and seismic data were confidently tied with synthetic seismograms in the interval of interest. High correlation values were obtained within a 100 ms window between the synthetic seismogram and the trace at the well location. The tie to the two surfaces IREX and DPRW (11 of 14 wells) was generally good, similar to the one shown in Figure 7a. The problems seen in some wells could be due to the low AI contrast between reservoir sands and non-reservoir units that is seen in Figure 11. The resolution of the seismic ( $1/4 \lambda$ ) is 15 m and therefore, because the interval of interest is between 45 and 70 m thick, we expected to observe some of the internal configuration of the interval. It is possible to detect layers down to approximately 10 m thick as seen in Figure 17 where a shale at 686 ms is seen to correspond to a peak. Thinner shales in the Dina-Cummings interval cannot be mapped, even if detection limits should theoretically be 2 – 3 m. The low acoustic impedance contrast between the shales and sands (Fig. 11) is

probably responsible for this problem. The transition between the sandy reservoir facies in the bottom of the interval and the shalier facies on top is imaged, probably due to the presence of the coal at the top of the sandy interval.

The seismic correlation (Fig 9) of the two surfaces chosen to constrain the attribute analysis window was relatively easy due to the continuity and amplitude of the reflections associated with these events. The stratigraphic correlation of the unconformity (Fig. 9) was carried out with no difficulty due to the log character associated with the clastics/carbonate contact. The blocky sand at the base of the interval shown in Figure 9 corresponds to the fluvial (Groeneveld and Stasiuk, 1984) Dina-Cummings reservoir. The fluvial sands are overlain by the estuarine succession that contains the Cummings coal and by the shaly Lloydminster marine deposits. These deposits contain the maximum flooding surface (MFS) that was used as a datum in the stratigraphic correlation. Unfortunately this surface, present in the great majority of the wells, could not be identified everywhere in the seismic volume for two reasons. The first is that it has been eroded in several locations, and the second is because the shaly Lloydminster interval that contains it becomes thinner in certain areas and therefore drops below the resolution of the seismic data.

Acoustic impedance and lithology (GR) do not show a linear relationship (Fig.11) but, as seen in the crossplot the different lithologies tend to cluster in different areas within the plot. This observation suggested that it would be important to look for non-linear relationships between the seismic data and lithology. Neural networks can be useful for establishing and exploiting these types of non-linear relationship between attributes and log-derived physical

properties (Hampson et al., 2001; Hart and Chen, 2004). Stepwise linear regression and validation testing indicated (Fig.12) that we needed three attributes to effectively predict GR from the seismic data. From the multiattribute analysis we found that integrated trace, apparent polarity and filter 25/30-35/40 represented the best combination of attributes for the prediction.

Figure 13a shows the result of combining these attributes to predict the GR. The 81% regression correlation coefficient could be considered a statistically good result, but in order to reduce the 17 API units error obtained (8.5%) in the prediction a neural network training was performed. The prediction of the GR was obviously improved by the application of neural networks, because it captures the non-linear nature of the relationship better than the multiattribute analysis (Figure 13b). Figure 14 shows a display of the wells involved in the analysis. The actual GR is displayed in black and the GR predicted using the neural network is shown in red. The correlation between the real and predicted GR is 0.9 and the average error is 13 API units (6.5%), which is considered statistically acceptable although not perfect. This error will allow the differentiation between the lithologies pursued in this study. Note how the predicted GR captures the changes in lithology within the study interval in most of the wells. In general, the predicted GR can be used to distinguish the sandy reservoir from the shalier non-reservoir deposits.

At least some of the difference between real and predicted GR observed in some wells is probably due to noise in the seismic data. Figure 18 shows a time slice that displays the low frequency (6-10 Hz) noise at two different levels in the volume, above the interval of interest (at 476 ms) and within the interval (at 684

ms). The noise at 476 ms is random (Fig. 18A) but at 684 ms, it shows the acquisition footprint (Fig. 18B). The noise seems to be somewhat stronger toward the west of the survey but the wells with discrepancies between real and predicted GR are distributed throughout the area.

Seismic attribute responses are controlled by changes in physical properties (e.g., acoustic impedance) and changes in the arrangement of the layers with different physical properties (i.e. the stratigraphy). Hart (2008) defined "stratigraphically significant attributes" as attributes that capture changes in waveform shape produced by changes in bed thickness and physical properties that are related to depositional or diagenetic processes. As described below, we believe that the three attributes we used to predict lithology have both physical and stratigraphic significance.

Guidelines for undertaking a seismic attribute study have been presented by Schultz et al. (1994), Kalkomey, (1997), Hart (1999) and others. Among these guidelines, we note that the statistical significance of the empirical relationship between attributes and physical properties needs to be clear, the reasons for the observed relationships between attributes and physical properties need to be understood, and the results must make geologic sense. Some interpreters focus on attributes that are thought to have physical significance in the study of interest, but Hart (2008) made a case for seeking stratigraphically significant attributes as well.

The most significant attribute in the regression relationship was the integrated trace. This attribute is calculated by integrating the seismic trace and is in reality a very crude type of inversion. As such, it can help to define the broad-

scale acoustic impedance structure. We note that, although the integrated trace was selected, the acoustic impedance inversion result (used as an attribute in the study) was not one of the attributes selected to predict lithology. Because the relationship between lithology (GR) and acoustic impedance in the Dina-Cummings interval derived from Figure 11 is not obvious, we could speculate that the inversion result was too detailed in its impedance prediction and that the relative impedance trends provided by the integrated trace were more useful for capturing general trends.

The second attribute in significance was apparent polarity, which is calculated by multiplying the amplitude envelope (also known as reflection strength) by the sign of the seismic sample at its peak value, applied in a segment between the troughs on either side of this peak. No clear relation between the attribute and the lithology can be found apart from the fact that the reflection strength is related to the acoustic impedance and we can again speculate again that the relative impedance trends provided by the apparent polarity were useful for capturing general trends.

Finally, the third attribute is a narrow band filter slice attribute; the slice that seems to have correlation with the GR is the 25/30-35/40 Hz. The filter 25-30/35-40 is a frequency attribute related to the characteristics of the seismic trace within that frequency slice. The frequency attribute (filter 25-30/35-40) indicates seismic frequency, which could be viewed as a function of the “geological frequency” and thus of the layering and thicknesses of the units involved. Geological frequency (Brown, 1999) is the number of reflecting layers within a unit thickness of rock. This filter attribute can be related to the thicknesses of the

packages that can be resolved in the seismic data. The average thickness of the sandy (reservoir) packages is 26 m and for the shalier (non-reservoir) packages it is 28 m. If we take into account the whole filter slice from 25 to 40 Hz, tuning thickness varies from 30 to 19 m, which encompasses the average thickness of the packages of both reservoir and non-reservoir deposits resolved in the seismic data. This relationship between the range of frequencies and the thickness of the two packages of distinctly different GR values is picked up by the filter attribute. Calderon and Castagna (2007) using multiattributes analysis as well, obtained a similar filter (15-20/25-30) as one of the best attributes to predict the GR curve and consequentially lithology.

The methodology we used integrates stepwise linear regression and validation testing to identify a combination of attributes that best predicts the gamma-ray curve at well locations. In essence, the method finds the combination of attributes that best predicts the gamma-ray response at well locations. In this case, the problem is four-dimensional: the three attributes and gamma-ray value as the fourth dimension. Marroquin and Hart (2004) previously showed how attributes could combine to fit non-linear data trends in the n-dimensional space spanned by the attributes and a physical property of interest (in their case, the thickness of a coal layer). In a similar way, and as described next, we suggest that the three attributes identified in this study were selected because, when combined, they closely fit a curve to the four-dimensional cloud of points that served as the input data to this study.

Although some relationship has been found between the attributes chosen in multivariate linear regression and the physical property examined, there is no

clear connection between them. It is possible to argue that the three attributes do not have to have a direct connection with the property investigated but that the resulting combination of attributes provides a mathematical fit to the non-linear transform that relates the physical property (GR) with the seismic data. Figure 19 shows vertical transect A-A' through the integrated trace, apparent polarity and filter 25/30-35/40 attribute volumes. These display the distribution of each seismic attribute and in colors the prediction of the GR from each attribute. Yellow denotes low GR that correspond to sands and green denotes high GR that correspond to shaly deposits. As seen in the GR vs. Integrated trace graph, the first attribute in the list obtained from the multivariate linear regression has a positive correlation. This attribute is over-predicting sand as seen in the interval highlighted with the red circle in the GR of well 10-28. The second attribute apparent polarity has a negative correlation and over-predicts shales in the same interval highlighted. This prediction when combined with that of the Integrated trace would compensate for the first attribute's over-prediction of sand. The third attribute (Filter 25/30-35/40) has a very small positive correlation and we could argue that it would be just fine-tuning the combined prediction of the integrated trace and the apparent polarity. We think that this argument would make the case that it is the mathematical combination of the attributes that is found by the multivariate linear regression and not their individual relationship with the physical property that makes them useful for the prediction.

We acknowledge that there are dangers, especially the possibility of finding spurious correlations between attributes and physical properties (e.g., Kalkomey, 1997), associated with using this type of approach. However, in the

current case we argue that the high number of samples in the correlation exercise makes this possibility unlikely, although not impossible.

The correlation between the predicted and observed lithology values improves when a neural network is used compared to multivariate linear regression. Leiphart and Hart (2001) showed that neural networks could generate more geologically realistic predictions of physical properties from attributes than linear regression methods. Hart and Chen (2004) showed that relationships between attributes and physical properties can be clearly non-linear, even in simple geologic settings, and their observations argue in favor of using neural networks to capture non-linear relationships.

The attribute-based GR volume was loaded into a visualization package and colors were assigned to observe the distribution of predicted lithologies. Low GR values are again associated with reservoir sands and are displayed in yellow, intermediate values, associated with non-reservoir silts and shales, are displayed in light brown, and the high GR values, associated with shales, are seen in a darker brown. The GR volume was corendered with another attribute: the coherency (e.g semblance) cube to highlight the discontinuities. Corendering coherence with other attributes has been successfully used (Chopra 2002; Hart, 2008) to identify stratigraphic features from the seismic data. Figure 20 compares two time-slices at 964 ms, one from the combined GR and semblance cube and the other from the corendered amplitude volume and semblance cube. The two time slices show lineations that are interpreted to represent channel features. The GR cube indicates that some of these lineations are associated with sands and others with non-reservoir shales. One lineation, running north-south in the center

of the cube, is interpreted as a mud plug filling part of the incision shown in Figure 10. Figure 21 displays four time-slices of the GR volume. The deeper units (698 and 696 ms) are sandier than the shallower ones (694 and 690 ms) and this observation agrees with the trends seen in the log correlations (e.g., Fig. 9). According to the GR prediction the incision located in the middle of the survey was filled with sand during the fluvial stage of deposition and then with finer-grained sediments during the estuarine or abandonment stages. Another incision, also observed in the structural map of the IREX, is seen in the GR volume as a SW-NE trending shale lineament. Recognition of this type of feature is important because it could constitute a barrier separating reservoir sands, and such a barrier would have an impact on the reservoir's behavior.

In Figure 16 there is a vertical transect through the GR volume.. The colors in the display represent the predicted GR values and in gray superimposed over them are the amplitude traces. In this case, displayed in yellow are low GR values associated with reservoir sands, shown in light brown are non-reservoir (silts and shales) and shown in green are the shales. This figure shows that it is possible to identify the principal stratigraphic units defined in the initial stratigraphic correlation. The boundary between the reservoir sands (in yellow) of the Dina-Cummings and the non-reservoir (in brown) sands, shales, silts and the Cummings coal is observed in the GR volume. The sealing deposits that correspond to the marine shales (including the maximum flooding surface) of the Lloydminster Member are shown in green. Unfortunately, and as noted previously, the GR volume does not detect small-scale details within the reservoir such as the shale partings identified in the GR log. Despite this limitation, the GR

volume can still be useful when combined with a detailed seismic amplitude interpretation and additional well information to establish the stratigraphic architecture of the reservoir at a larger scale. Integration of all the available information from both the seismic data and the boreholes is necessary to generate the geological model of the reservoir in the study area. This integration is important when interpreting possible geomorphologic features from plan-form images (e.g., time slices) because we are dealing with a small survey that can image complete stratigraphic features (e.g., channel, bar, lagoon, etc.) only if they are small. Hart et al. (2007) interpreted the Lower Mannville in a small survey in southern Saskatchewan where only parts of the geomorphology of the deposits were imaged. In that case, the paleo-environmental interpretation was only possible by integrating seismic data and well information, which for this study's area will be addressed in the companion paper (Sarzialejo and Hart, chapter 2).

### **3.7 Conclusions**

This study shows how seismic attributes were used to predict the lithology distribution in the study area, a portion of the Winter Field in west-central Saskatchewan. Two horizons, the sub-Cretaceous unconformity (DPRW horizon) and a continuous fine-grained marine unit above the reservoir (IREX horizon), were mapped through the area using seismic and well-log data. High correlation coefficients between synthetic seismograms and seismic data at well locations allowed a confident tie between the two datasets. Other stratigraphic picks were also correlated in well-log cross-sections to establish a stratigraphic framework for the area. The reservoir, fluvial sands of the Dina-Cummings interval, overlies

an irregular topography of Devonian carbonates (Duperow Formation) and is capped by a widespread coal and its associated marginal marine to marine finer-grained sediments, which constitute the reservoir seal. The maximum flooding surface within the seal was interpreted in all the wells and serves as a good datum for the well-log correlations.

The multiattribute analysis and neural network training were used to generate a GR (pseudo-lithology) volume. The IREX and DPRW horizons were used as the boundaries for the analysis window in the volume-based attribute study. Stepwise linear regression and validation testing indicated that a combination of three attributes, integrated trace, apparent polarity and a band pass filter of 25/30-35/40, would best predict lithology from the seismic data. The use of a neural network, rather than multivariate linear regression, resulted in an improved GR prediction for the area. The physical relationship between the attributes (selected using the stepwise linear regression) and the lithology was found but was not considered strong. We can conclude that, at least in this study, it is the mathematical combination of attributes and not their physical relationship with the searched property that is responsible for the resulting GR prediction. This conclusion is based on examination of the 3-D volumes of the three attributes (Integrated trace, Apparent polarity and Filter 25/30-35/40) and an empirical analysis of their combination. The neural network transform was applied to the seismic volume to generate a geologically reasonable GR (pseudo-lithology) volume. Combination of the GR, seismic amplitude and semblance volumes allows assigning lithologies to stratigraphic features (e.g., fluvial channels) and a more confident interpretation of the architecture of the reservoir.

The resultant GR (pseudo-lithology) volume, which predicts the distribution of lithologies away from the well control, does not resolve small features (e.g. shale partings) but can be used to interpret distribution and configuration of larger features (e.g., channel incisions) within the reservoir. A detailed correlation of both seismic and well-log data integrated with core information is necessary at this stage to combine with the GR volume in order to generate a robust stratigraphic model of the area and understand the reservoir behavior.

### **3.8 Acknowledgements**

The seismic and well-log data used in this study were provided by Nexen Inc. Seismic interpretations and analyses described herein were undertaken using software donated by Landmark Graphics Corporation and Veritas/Hampson-Russell software services. Funding for this work was provided by Nexen Inc. and a NSERC Collaborative Research and Development Grant to Professor Hart. We thank all of these organizations for their continued support of this research.

### 3.9 References

- Bertram, G. T. and Milton, N.J. 1994. Seismic stratigraphy. In: Sequence Stratigraphy. D. Emery and K. J. Meyers (eds.). Blackwell, p. 45-60.
- Brown, A. R. 1999. Interpretation of three-dimensional seismic data. American Association of Petroleum Geologists, Memoir 42, 514 p.
- Chopra, S. 2002. Coherence cube and beyond. *First Break*, v.20 p.27-33.
- Christopher, J. E. 2003. Jura-Cretaceous Success Formation and Lower Cretaceous Mannville Group of Saskatchewan. Report 223, Saskatchewan Industry and Resources Saskatchewan Geological Survey. p. 128.
- Calderon, J. E. and Castagna, J. 2007. Porosity and lithologic estimation using rock physics and multi-attribute transforms in Balcon Field, Colombia: *The Leading Edge*, v. 26, p. 142-150.
- Calver, E., Doligez, B., Eschard, R., and Torriero, D. 1999. Sequence stratigraphy and stochastic reservoir modeling of an incised valley fill reservoir in the Lower Cretaceous Mannville Group, west central Saskatchewan: AAPG Annual Meeting, San Antonio, Texas, Expanded Abstracts, p. A20.
- Cant, D. J. and Abrahamson, B. 1996. Regional distribution and internal stratigraphy of the Lower Mannville. *Bulletin of Canadian Petroleum Geology*, v. 44, p. 508-529.
- Dequierez, P. Y., Blanchet, C. Feuchtwanger, T. and Torriero, D. 1995. Integrated stratigraphic and lithologic interpretation of the East-Senlac heavy oil pool: SEG Annual Meeting, Houston, Texas, Expanded Technical Program Abstracts with Biographies, v. 65, p.104-107.

- Groeneveld, N. A and Stasiuk, L. D. 1984. Depositional environment of the Cummings coal and associated sediments, Winter-Senlac area, Western Saskatchewan. In: Oil and gas in Saskatchewan. J. A. Lorsong and M. A. Wilson, (eds.). Special Publication: Saskatchewan Geological Society, v. 7, p. 135-147.
- Hampson, D., Schuelke, J. and Quirein, J. 2001. Use of multiattribute transforms to predict log properties from seismic data: *Geophysics*, v. 66, p. 220-236.
- Hart, B. S. 2008. Channel detection in 3-D seismic data using sweetness. *American Association of Petroleum Geologists Bulletin*, v. 92, p. 733-742.
- Hart, B. S. 2008. Stratigraphically Significant Attributes: *The Leading Edge*, v. 27, no. 3, p. 320-324.
- Hart, B. S., Sarzalejo, S. and McCullagh, T. 2007. Seismic stratigraphy and small 3D seismic surveys: *The Leading Edge*, v. 26, no. 7, p. 876-881.
- Hart, B. S. and Chen, M. A. 2004. Understanding seismic attributes through forward modeling: *The Leading Edge*, v. 23, p. 834-841.
- Hart, B. S. 1999. Geology plays key in seismic attribute studies: *Oil & Gas Journal*, v.97, p.76-80.
- Kalkomey, C. 1997. Potential risks when using seismic attributes as predictors of reservoir properties: *The Leading Edge*, v. 16, no. 3, p. 247-251.
- Leckie, D. A., Vanbeselaere, N. and James, D. P. 1997. Regional sedimentology, sequence stratigraphy and petroleum geology of the Mannville Group; southwestern Saskatchewan. In: *Petroleum geology of the Cretaceous Mannville Group, Western Canada*. S G. Pemberton and D.P. James (eds.). Canadian Society of Petroleum Geologists, Memoir 18, p. 211-262.

- Leiphart, D. J. and Hart, B.S. 2001. Case history: Comparison of linear regression and a probabilistic neural network to predict porosity from 3-D seismic attributes in Lower Brushy Canyon channeled sandstones, southern New Mexico: *Geophysics*, v. 66, p. 1349-1358.
- Marroquin, I., and Hart, B. S. 2004. Seismic attribute-based characterization of coalbed methane reservoirs; an example from the Fruitland Formation, San Juan Basin, New Mexico. *American Association of Petroleum Geologists Bulletin*, v. 88, no. 11, p. 1603-1621.
- Mitchum, R. M, Vail, P. R. and Thompson, S. 1977. Seismic stratigraphy and global changes of sea level; Part 2, The depositional sequence as a basic unit for stratigraphic analysis. In: *Seismic stratigraphy; applications to hydrocarbon exploration*. C. E. Payton (ed.). American Association of Petroleum Geologists, Memoir 26, p. 53-62.
- Pearson, R. A. and Hart, B. S. 2004. Three-dimensional seismic attributes help define controls on reservoir development: Case study from the Red River Formation, Williston Basin. In: *Seismic imaging of carbonate reservoirs and systems*. G. P. Eberli, J. L. Masferro and J. F. Sarg (eds.), American Association of Petroleum Geologists Memoir 81, p. 43– 57.
- Posamentier, H. W., Jervey, M. T. and Vail, P. R. 1988. Eustatic controls on clastic deposition. I. Conceptual framework. In: C. K. Wilgus, B. S. Hastings, Christopher. G. St. C. Kendall, H. W. Posamentier, C. A. Ross and J. C. Van Wagoner, (eds.), *Sea Level Changes—An Integrated Approach*, vol. 42. Society for Sedimentary Geology, Special Publication, p. 109 -124.

- Sagan, J. A. and Hart, B. S. 2006. Three-dimensional seismic-based definition of fault-related porosity development: Trenton-Black River interval, Saybrook, Ohio: American Association of Petroleum Geologists Bulletin, v.90, p. 1763-1785.
- Sarzalejo, S. and Hart, B. S. 2006. Stratigraphy and lithologic heterogeneity in the Mannville Group (southeast Saskatchewan) defined by integrating 3-D seismic and log data. Bulletin of Canadian Petroleum Geology, v. 54, no. 2, p.138-151.
- Schultz, P. S., Ronen, S., Hattori, H. and Corbett, C. Seismic-guided estimation of log properties; Part 1, A data-driven interpretation methodology: The Leading Edge, v. 13, no. 5, p. 305-310.
- Taner, M. T. Koehler, F., and Sheriff, R. E. 1979. Complex seismic trace analysis: Geophysics, v.44, p.1041-1063.
- Takahashi, A., Torigoe, T., Tsuji, T., Kashihara, K., Nakayama, T., Kose, M., Skinner, L. and Nasen, R. 2006. Geological modeling of oil sands reservoir by integrating the borehole and seismic data in the JACOS Hangingstone SAGD operation area, Athabasca, Canada: Journal of the Japanese Association for Petroleum Technology, v.71 No 1, p. 54-63.
- Tebo J. M. and Hart, B. S. 2005. Use of volume-based 3-D seismic attribute analysis to characterize physical property distribution: A case study to delineate reservoir heterogeneity at the Appleton field, SW Alabama: Journal of Sedimentary Research, v.75, p. 723-735.
- Tonn, R. 2002. Neural network seismic reservoir characterization in a heavy oil reservoir: The Leading Edge, v.21, p. 309-312.

- Vail, P. R., Mitchum, R.M. Todd, R. G., Widmier, J.M. Thompson, S Sangree, J. B. Bubb, J. N. and Hatlelid, W. G. 1977. Seismic Stratigraphy and Global Changes of Sea Level. In: Seismic Stratigraphy-applications to hydrocarbon exploration: C. E. Payton (ed.). American Association of Petroleum Geologists, Memoir 26, p. 49-212.
- Wood, L. J. 2003. Quantitative Seismic Geomorphology and Reservoir Architecture of Clastic Depositional Systems: The Future of Uncertainty Analysis in Exploration and Production: 2003 AAPG Annual Meeting, Salt Lake City, Utah, Program and Abstracts CD.
- Zaitlin, B. A. and Shultz, B. C. 1984. An estuarine-embayment fill model from the Lower Cretaceous Mannville Group, west-central Saskatchewan. In: The Mesozoic of middle North America. D. F. Stott and D. J. Glass (eds.). Canadian Society of Petroleum Geologists, Memoir 9, p.455-469.

### 3.10 List of Figures

**Figure 1.** Location of the study area in west-central Saskatchewan. The figure also shows the location of the oil sands and heavy oil reservoirs in the Western Canadian Sedimentary Basin.

**Figure 2.** Correlation chart of the Mannville Group (modified from Christopher, 2003). Stratigraphic nomenclature for west-central Saskatchewan is under the Lloydminster column.

**Figure 3.** Base map showing outline of the Winter 3-D survey showing well locations. The wells were drilled by Nexen Inc. The location of the west-east seismic transect A-A' is indicated on the map.

**Figure 4.** West-east seismic transect A-A' (location in figure 4) showing the seismic signature of the study area. The high amplitude peak (blue) corresponds to the contact between the carbonate deposits of Devonian Duperow Formation and the clastic deposits of the Cretaceous Lower Mannville. The frequency distribution amplitude between 620 and 720 milliseconds shows that dominant frequency is in the order of 50 Hz. The resolution ( $1/4 \lambda$ ) obtained using a velocity of 2970 m/s is 15 m.

**Figure 5.** Workflow used in this study that begins with well and seismic information that is combined to obtain a GR (pseudo-lithology) volume from seismic attribute analysis.

**Figure 6.** Stratigraphic column and type log of the study area indicating the reservoir interval within the Winter Field.

**Figure 7.** Examples of “good” (A) and “bad” (B) synthetic seismograms. The synthetic seismogram traces are shown in blue and the seismic traces at well locations are shown in red. Several traces are shown in both cases to improve visualization. Synthetic seismogram A has a high correlation coefficient (0.94) and as seen in the figure honors the trace at the well location. Synthetic seismogram B honors the high amplitude events of the trace at the well location but shows discrepancies in the low frequency interval.

**Figure 8.** Seismic transect A-A’ penetrated by four wells. Overlaid in white are the synthetic seismograms used to tie the wells to the seismic data and GR logs are in black.

**Figure 9.** Seismic transect and corresponding stratigraphic cross section A-A’. The seismic data and well-log profiles show the two surfaces (IREX and DPRW) that constitute the top and bottom of the attribute analysis window. Location of A-A’ is shown in Figure 3. The maximum flooding surface MFS is the datum (dashed lines) and other interpreted picks are shown in the stratigraphic cross section.

**Figure 10.** A three dimensional representation of the seismic volume showing the two interpreted horizons. The lower horizon is the top of the Duperow (DPRW) or sub-Cretaceous unconformity and the one on top is the intra Rex (IREX). In the display are several lows interpreted as fluvial incisions.

**Figure 11.** Crossplot (left) of acoustic impedance (AI) vs. gamma-ray (GR) generated with data from all the wells with sonic and/or density logs. To the right a GR log shows with different colors the various lithological packages observed in the wells in the area. The different ellipses comprise the data points that correspond to the stratigraphic level indicated with the same color in the GR log.

**Figure 12.** Plot of the multiattribute stepwise linear regression analysis showing that three is the optimum number of attributes to use for the GR prediction.

**Figure 13.** Two cross-plots that compare the GR prediction results using multiattribute regression (left) and neural networks (right). Note the improved prediction observed using neural networks, indicated by a higher correlation coefficient and a lower API error.

**Figure 14.** Result of validating the neural network transform to the seismic data at the wells to predict the GR log.. The predicted logs are shown in red and the original are shown in black for comparison.

**Figure 15.** Vertical transect B-B' through the gamma-ray volume showing with colors the different GR values obtained within the interval of interest. Greens and yellows correspond to low GR values, light blue and brown correspond to intermediate values and dark blue and pink correspond to high values. A GR log of a well that penetrated the section is displayed in the vertical transect.

**Figure 16.** Vertical transect A-A' through the gamma-ray (GR) volume with the pseudo-lithologies shown in different colors, superimposed in gray are the amplitudes traces. Low GR values corresponding to the reservoir sands are shown in yellow, intermediate GR values of the non-reservoir finer deposits in brown and the high GR shales in green. Also shown are the GR logs of the four wells that penetrate the section.

**Figure 17.** Electrical logs of well 11-28 and the synthetic seismogram (blue) used to tie the well to the seismic data. The dashed line indicates the location of the incipient peak that corresponds to the shale layer containing the MFS in the well. The oil/water contact observed in the well log seems to be imaged by a trough in several boreholes the same occurs with the top of the reservoir (in orange).

**Figure 18.** The noise seen in these two time slices could be held responsible for the error in the prediction of GR log in some boreholes. Time-slices through a low frequency filtered seismic volume show at 476 ms random noise while at 684 ms show the acquisition footprint. Distribution of wells (black circles) is shown in the figure.

**Figure 19.** Seismic transects through seismic attribute volumes: integrated trace (Integrate), apparent polarity and filter 25/30-35/40. A graph displaying the relationship between the attribute and the GR is shown for each seismic attribute. Yellow corresponds to the low GR values associated with sands. The GR curve from well 10-28 shows the lithology at that location that can be compared with the GR predicted by the attribute.

**Figure 20.** Time-slices at 694 ms through the gamma-ray and amplitude volume. In the upper slice the yellow areas correspond to sandy deposits (low GR values) and the orange-brown areas (intermediate and high GR values) to non-reservoir finer-grained sediments. The lineations seen in the figure are associated with channel incisions and their associated lithology can be characterized using the GR prediction. The red lines correspond to boreholes within the survey area.

**Figure 21.** Four data slices through the GR (pseudo-lithology) volume show the distribution of the predicted lithologies through time. In yellow are the low GR values, intermediate GR values are in brown and the high GR are in green. From the data slices, we can interpret that the deposits are sandier at the base (698 ms) and become finer and shalier toward the top (690 ms). Several green shaly lineations are seen and are interpreted as mud filled channel incisions or abandonment shale plugs.



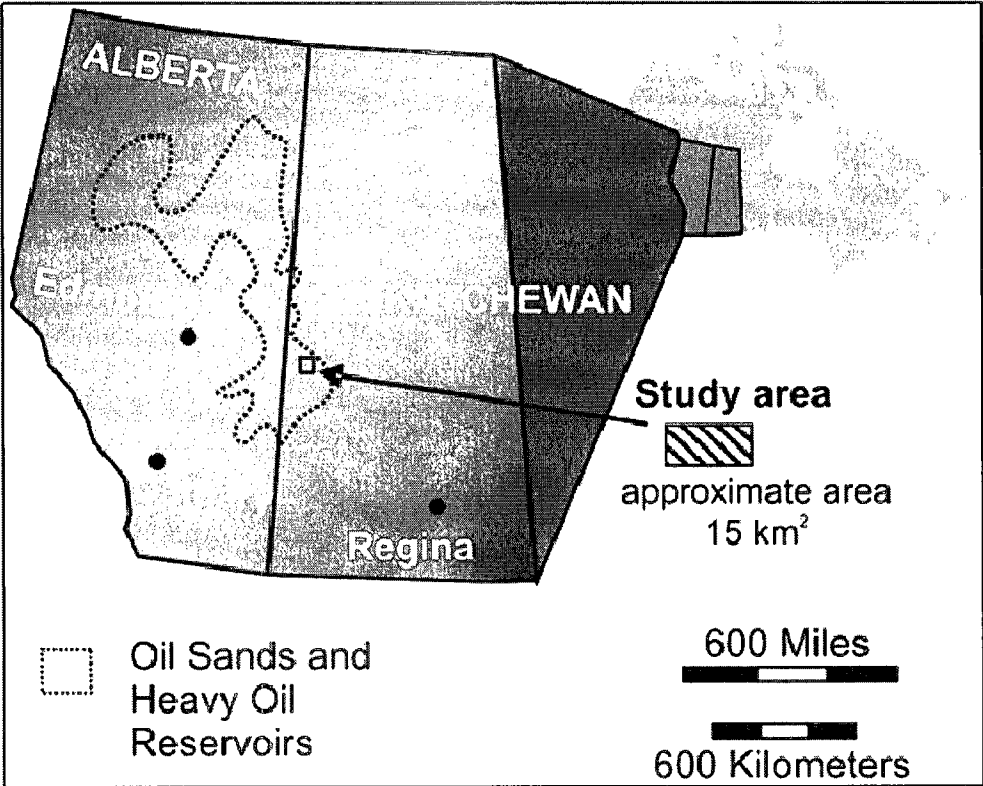


Fig 1



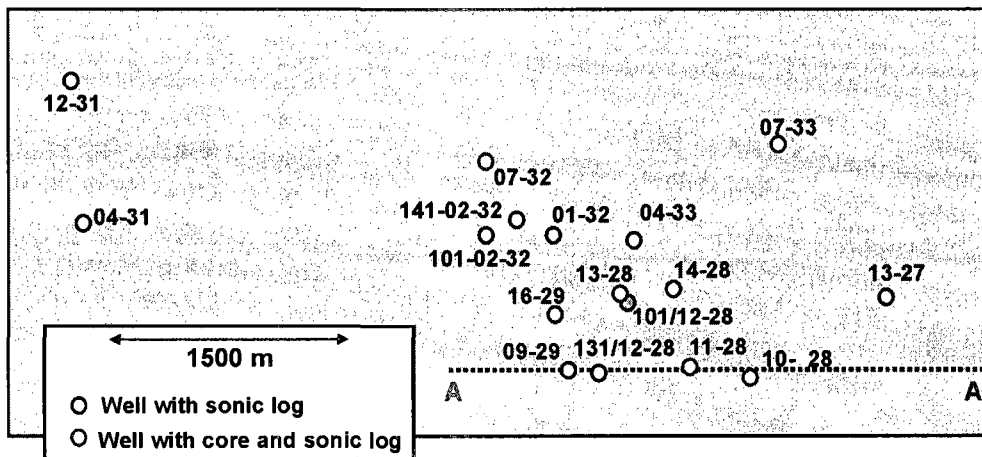


Fig 3

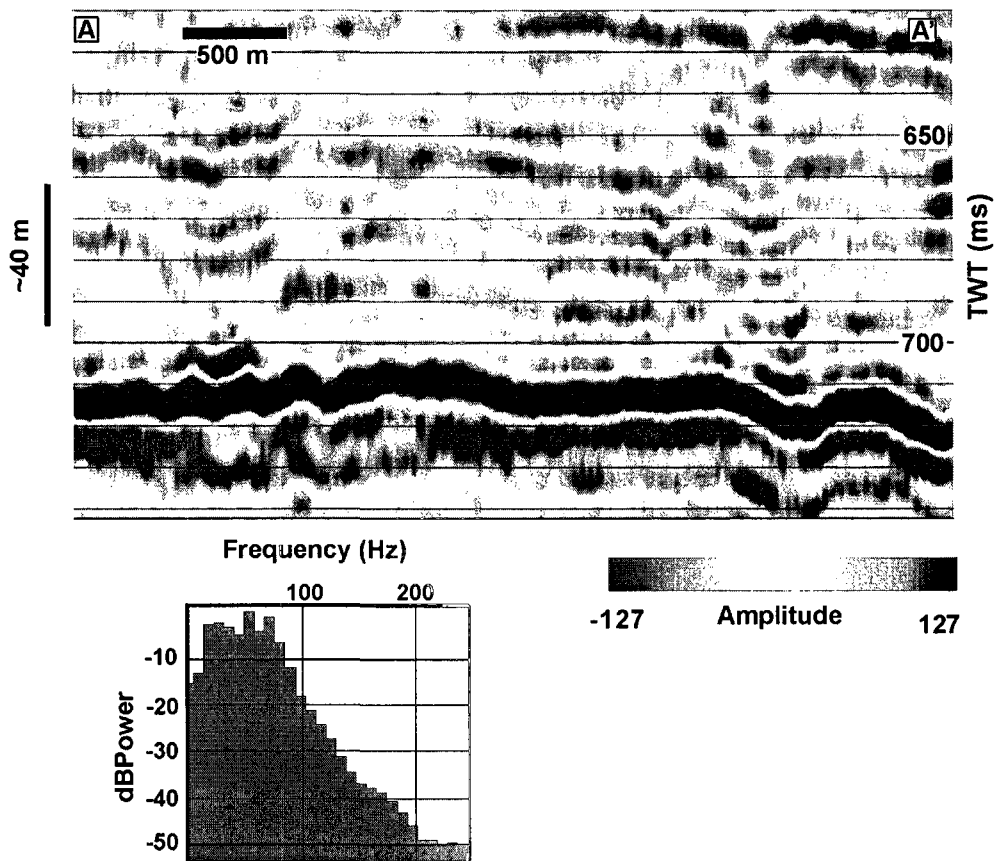


Fig 4

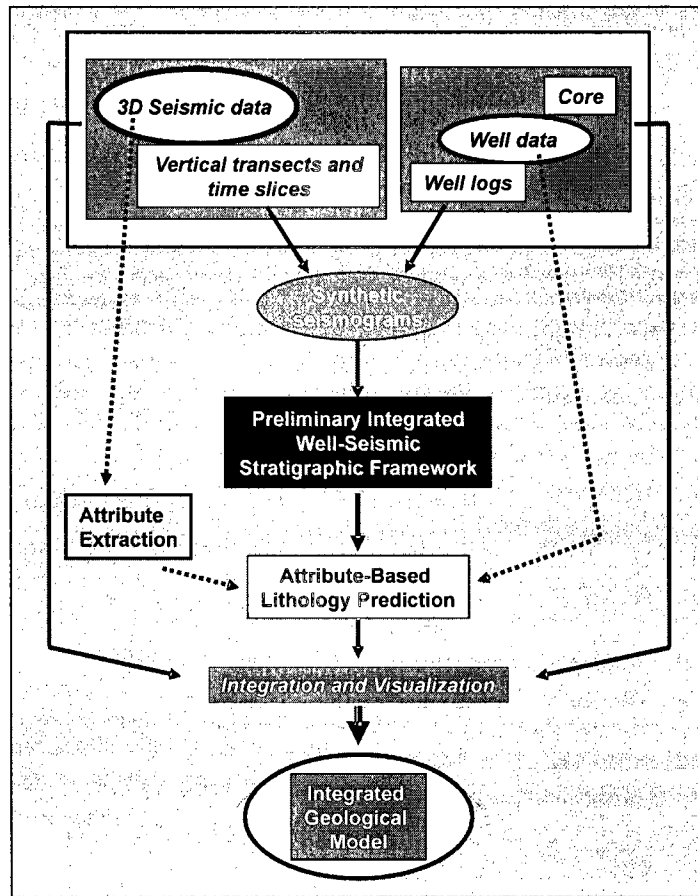


Fig 5

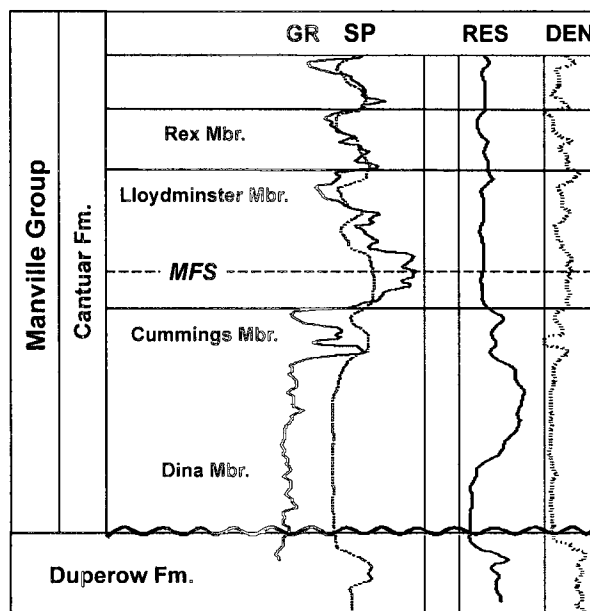


Fig 6

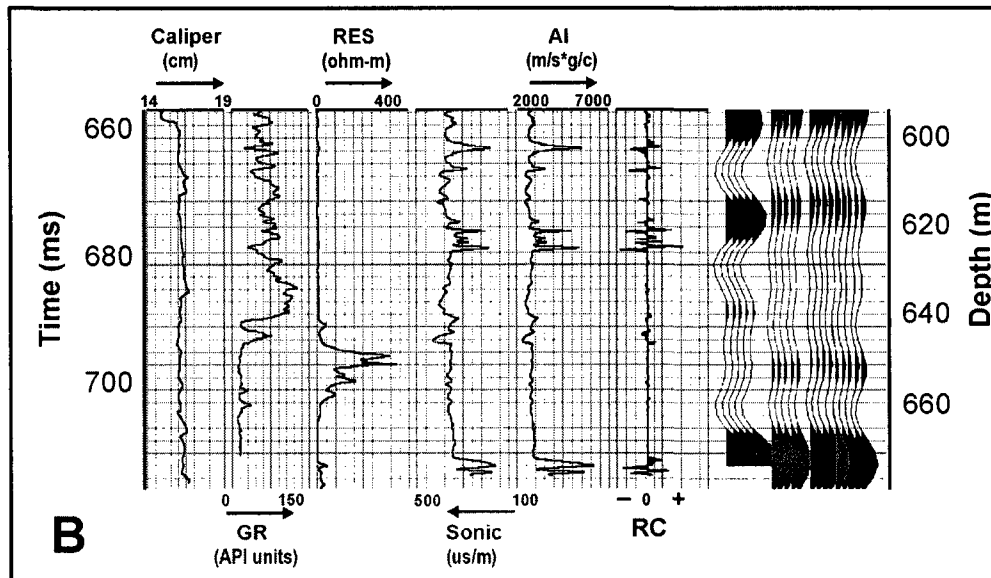
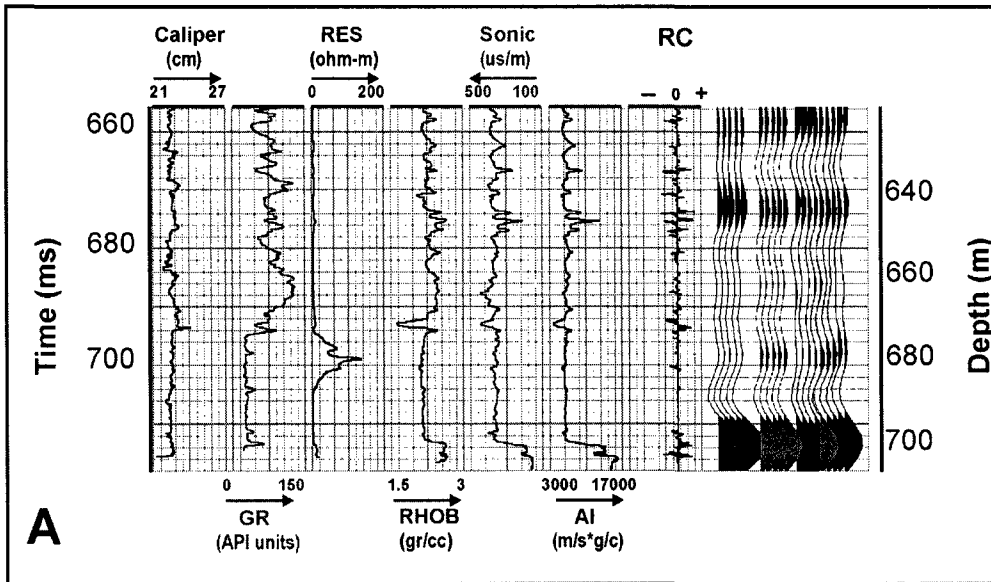


Fig 7

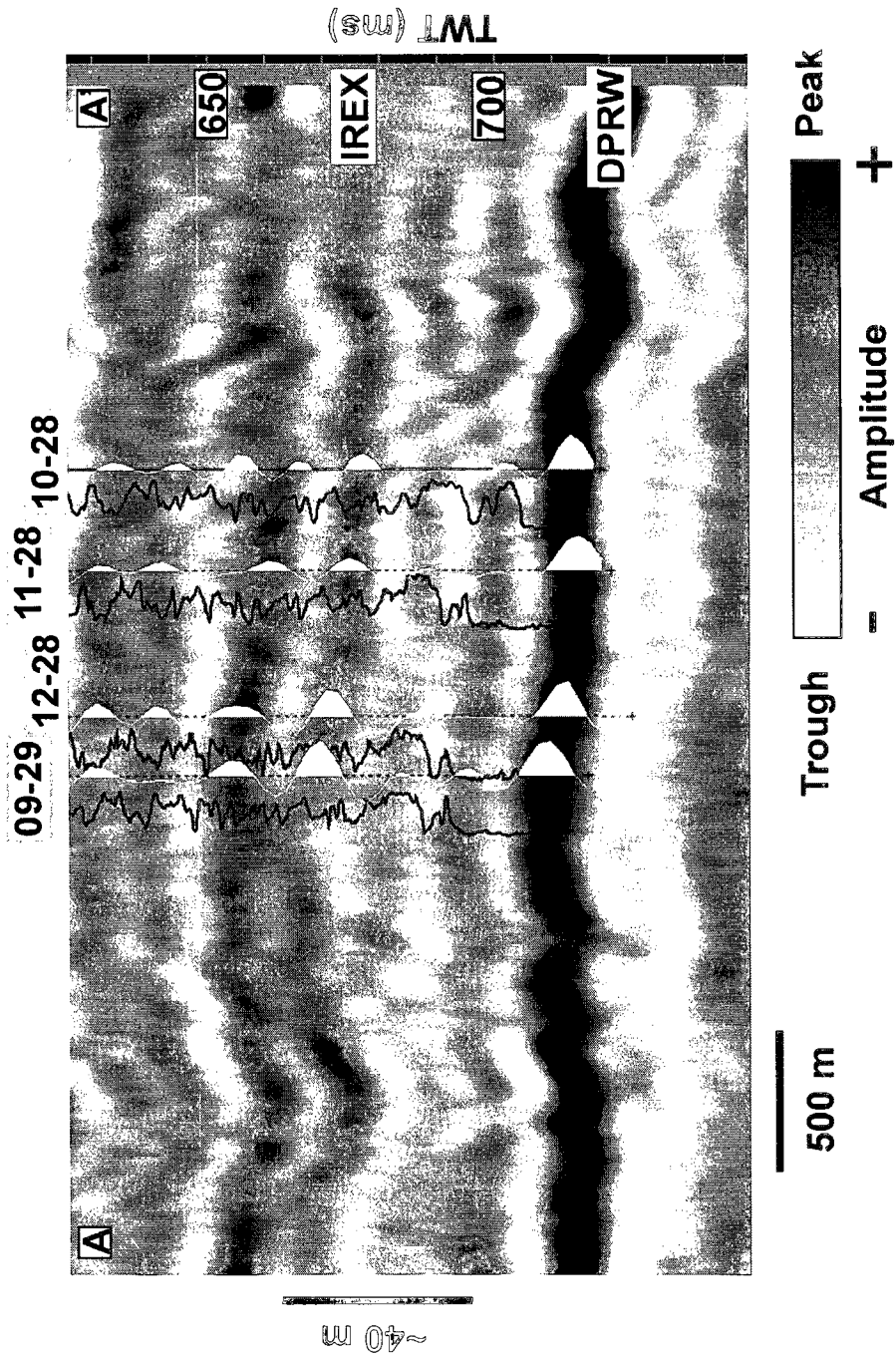


Fig 8

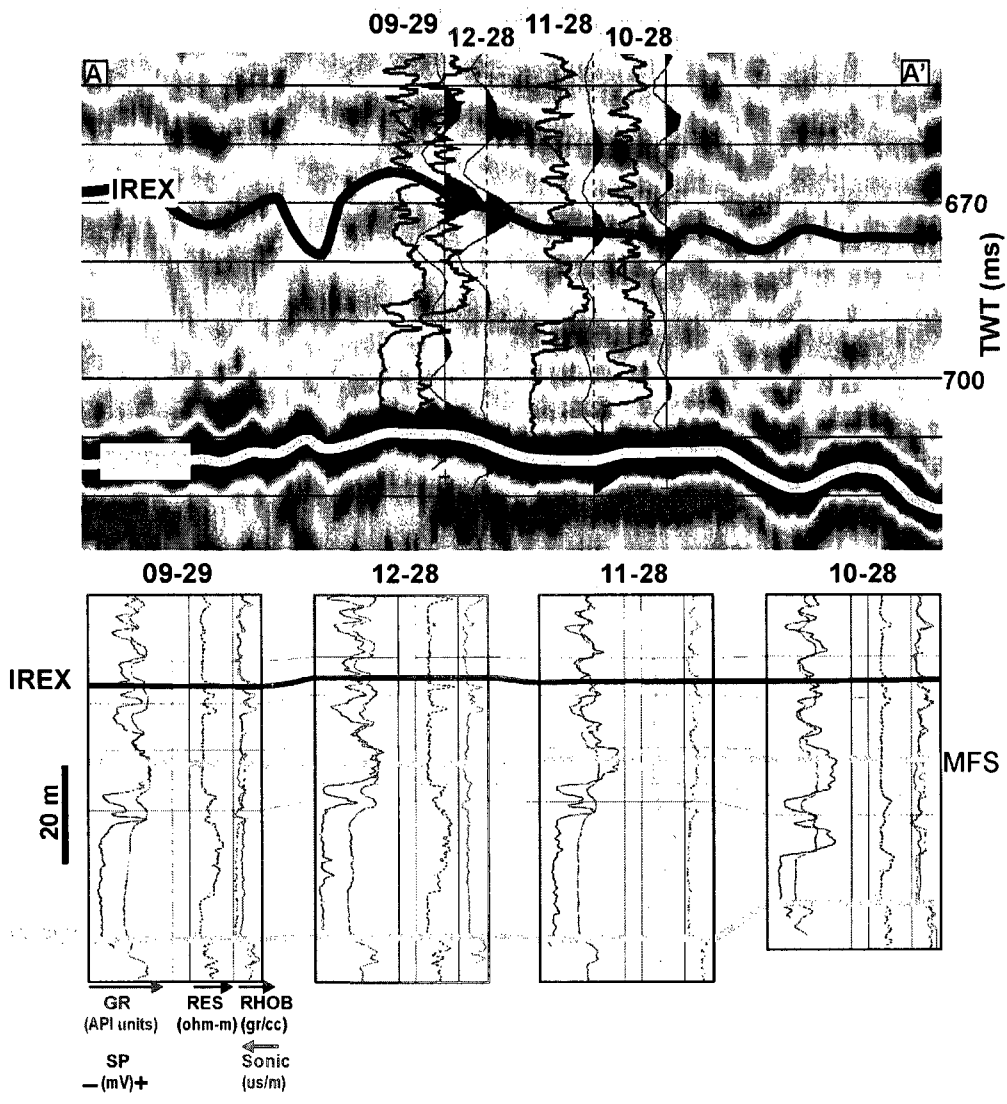


Fig 9

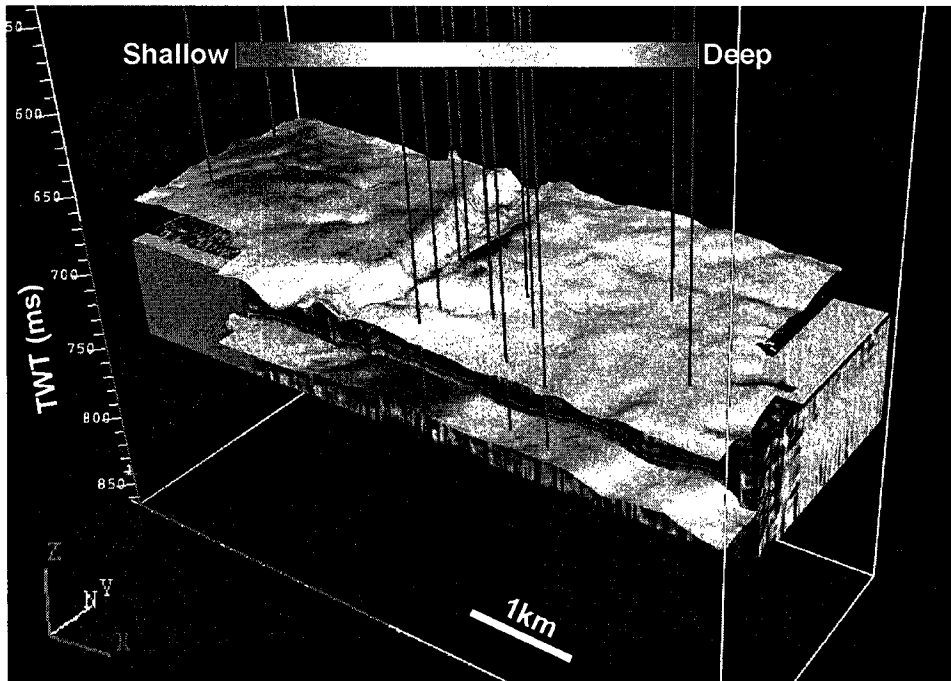


Fig 10

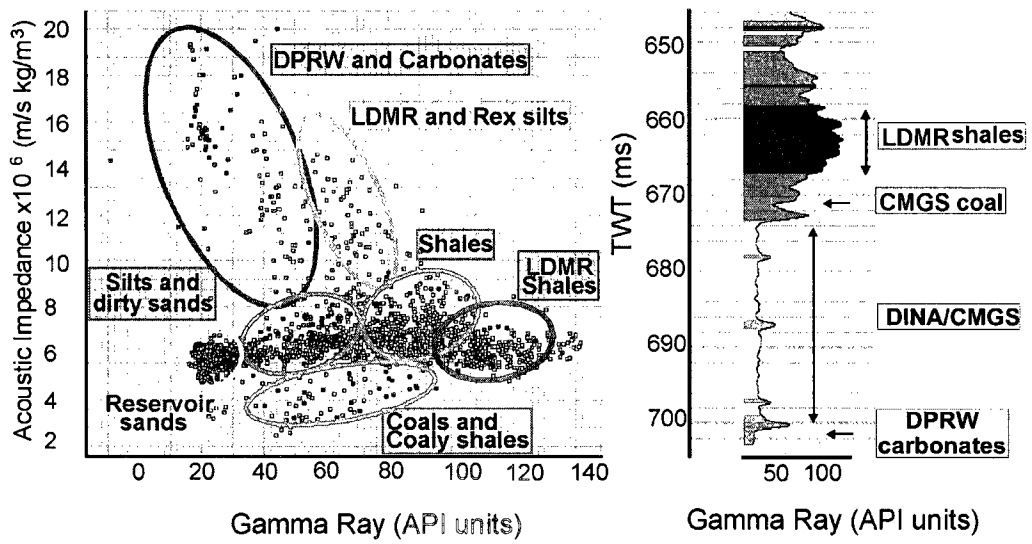


Fig 11

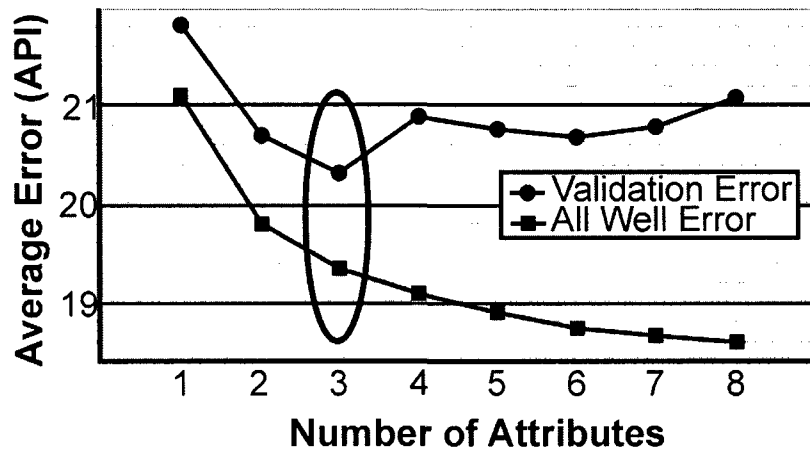


Fig 12

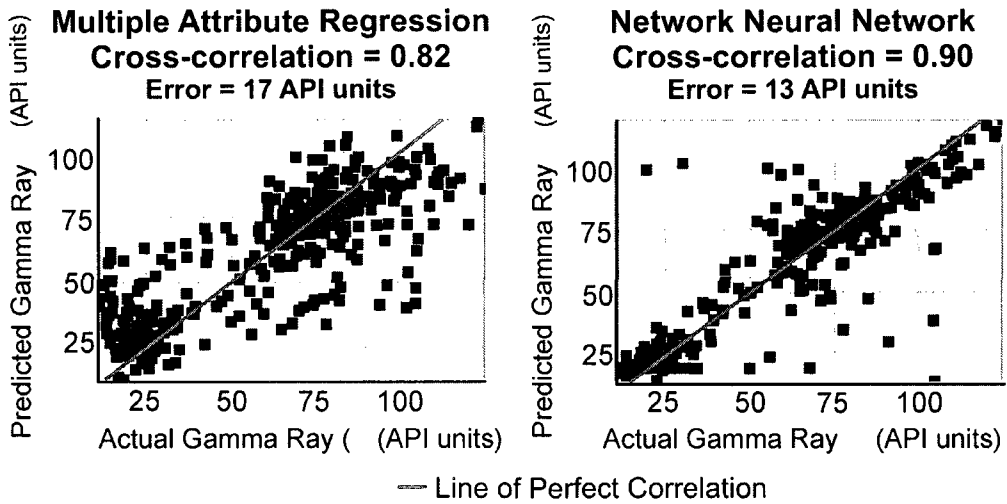


Fig 13

**Validation of Probabilistic Neural Network  
Correlation = 0.79  
Average Error = 18.5 (API units)**

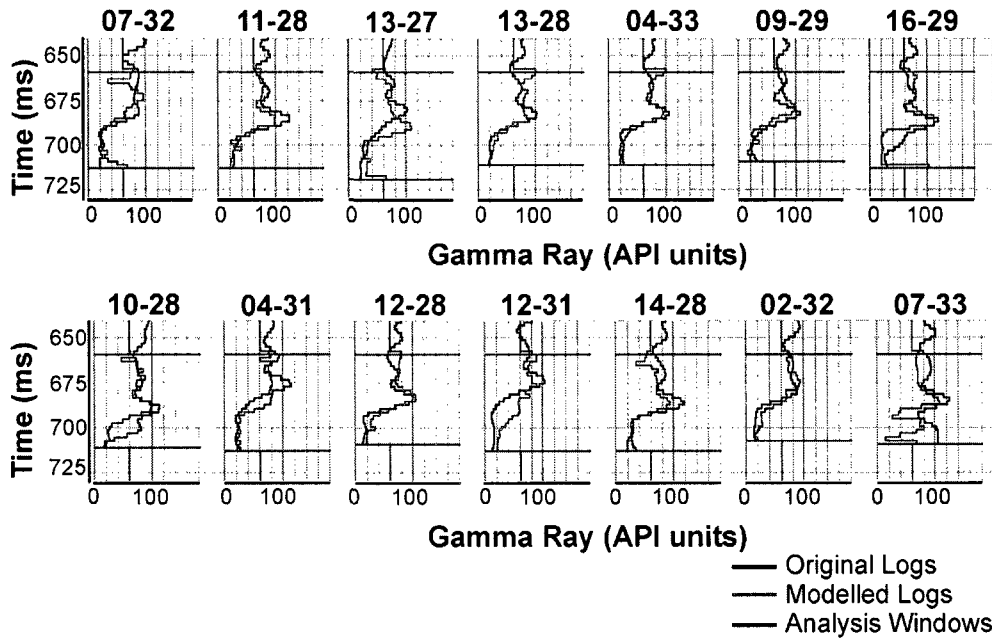


Fig 14

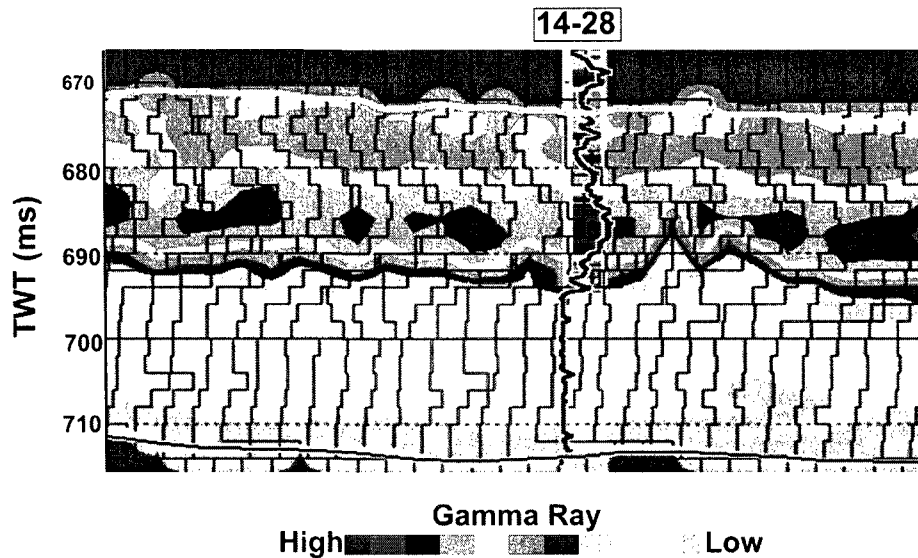


Fig 15

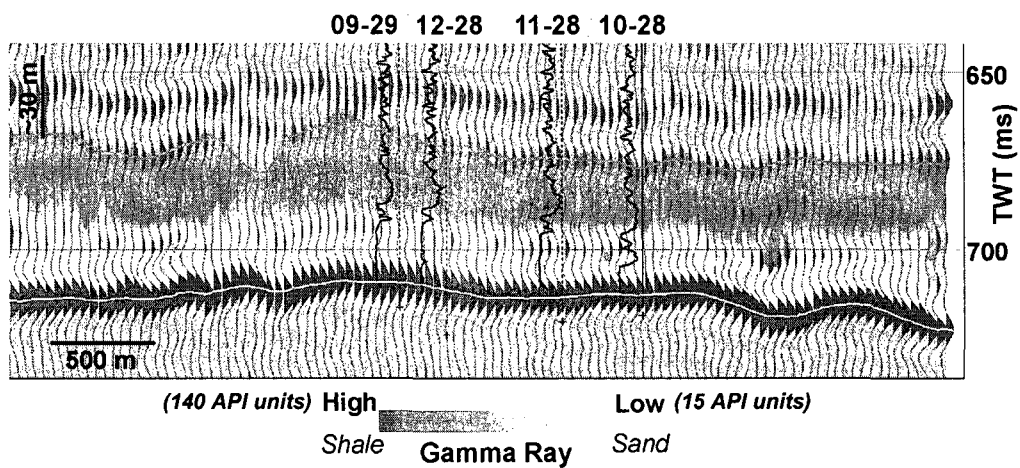


Fig 16

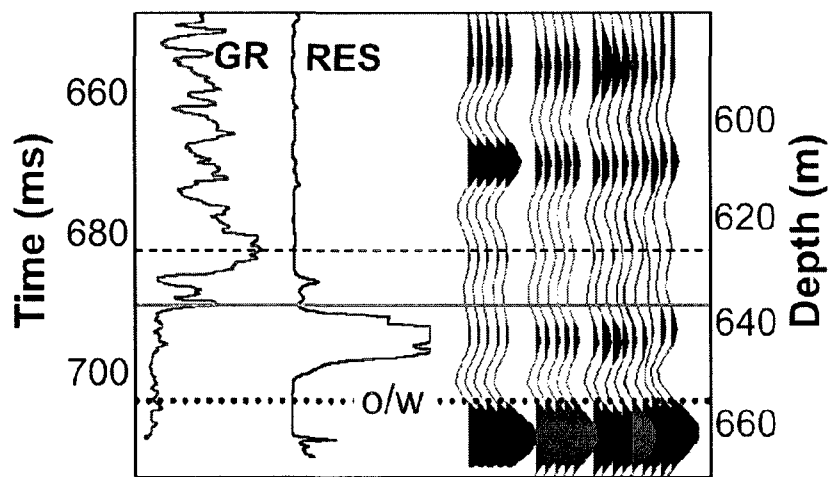


Fig 17

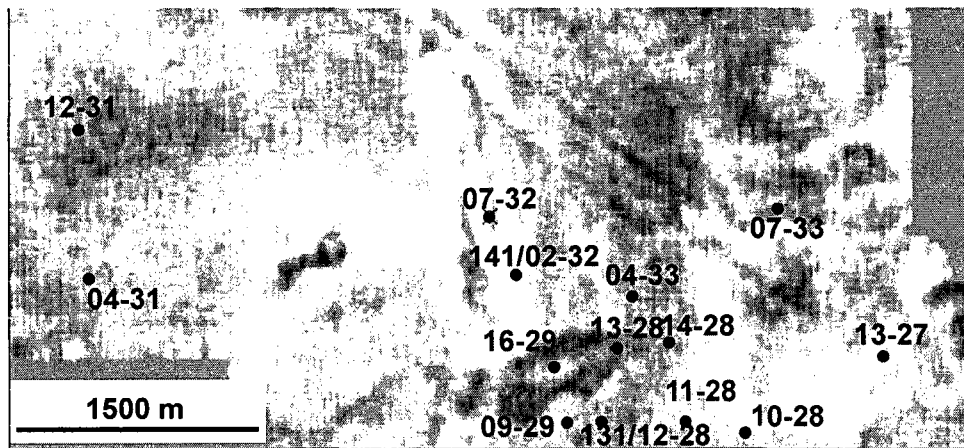
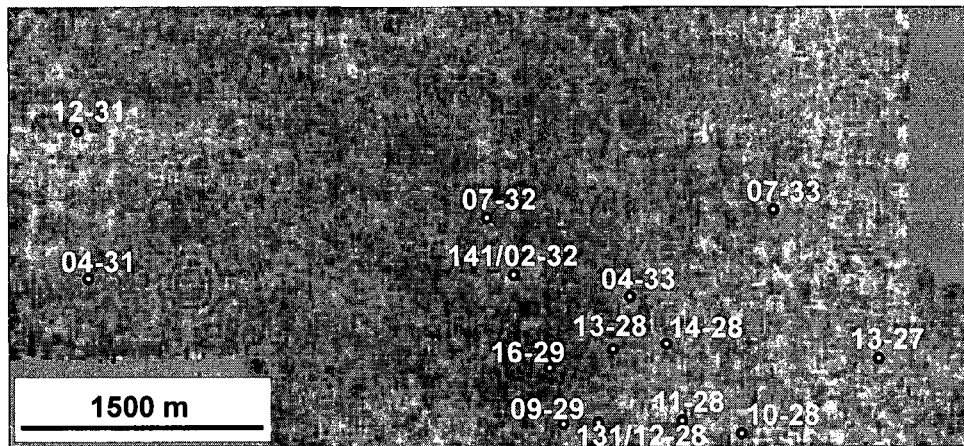


Fig 18

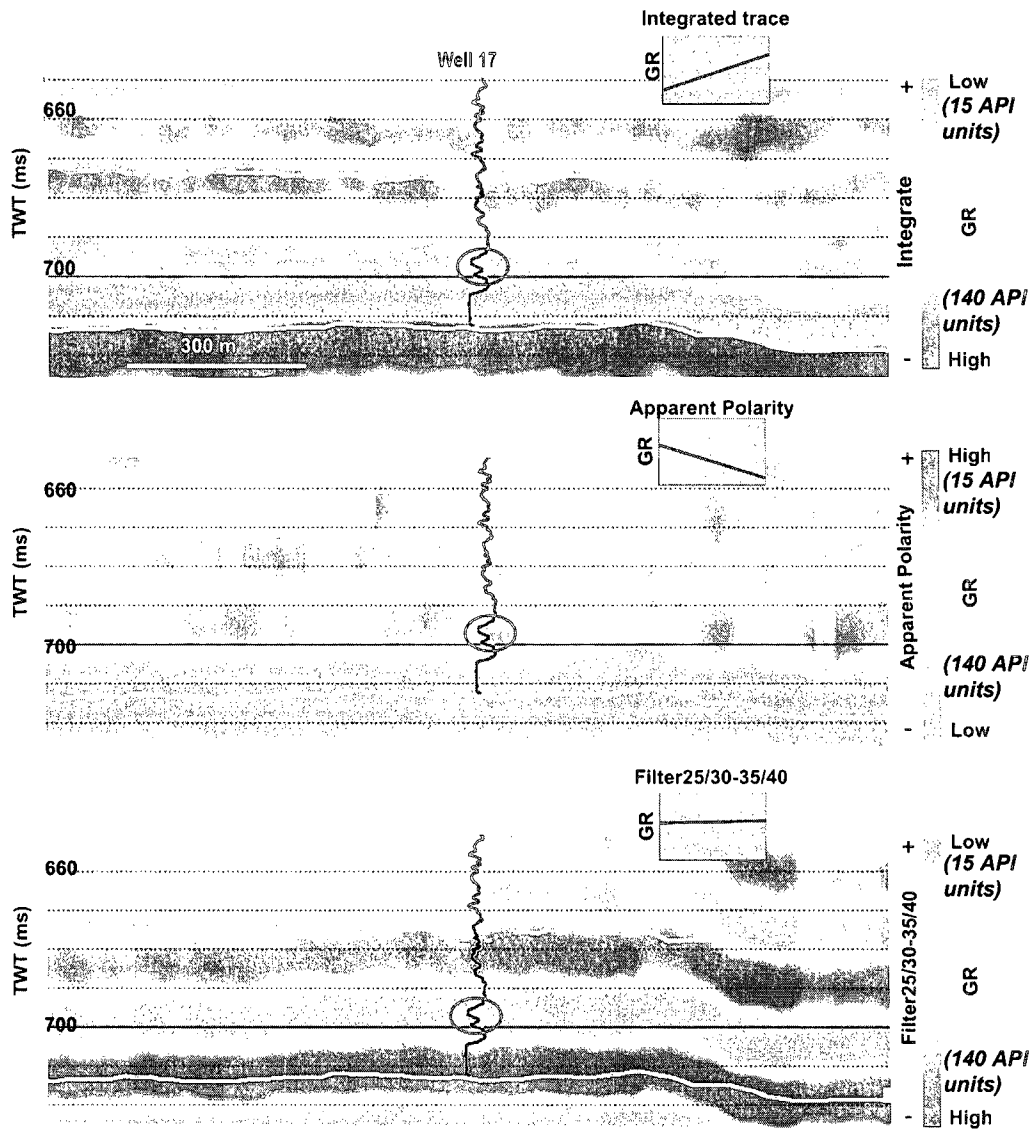
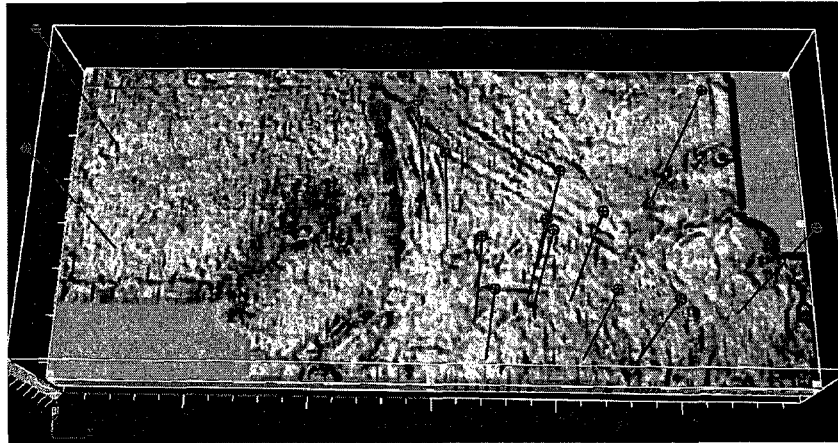


Fig 19

High  
Shale  
(140 API  
units)

Gamma Ray

(15 API  
units)  
Low  
Sand



Peak

Amplitude

Trough



Fig 20

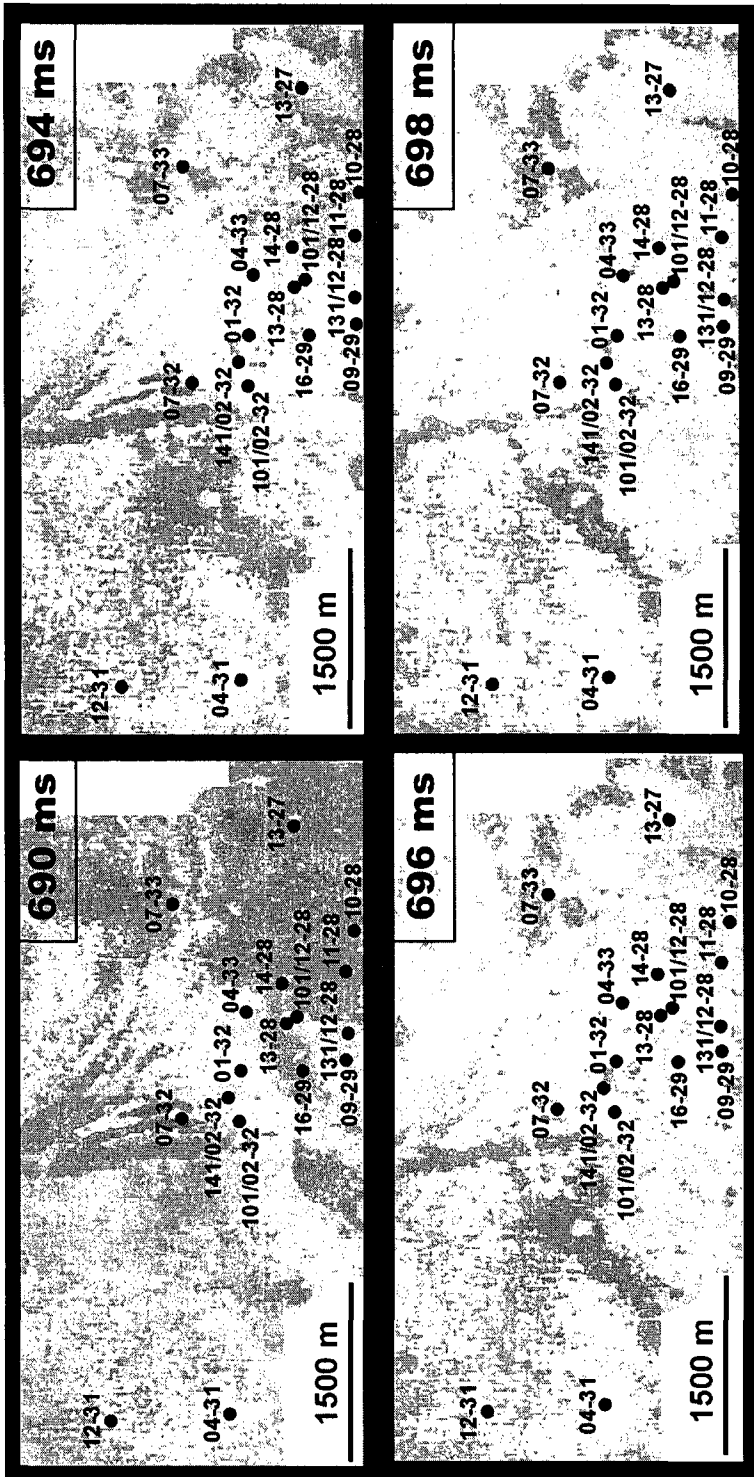


Fig 21

#### **INTRODUCTION TO CHAPTER 4**

Chapter 4 presents how the integration of borehole and seismic data was used to unravel the stratigraphy and predict the reservoir architecture of the Lower Mannville deposits within the heavy oil field in East-Central Saskatchewan. This chapter illustrates the methodology used to integrate well logs and cores with seismic data (amplitude and pseudo-lithology volumes), and emphasizes the benefits of the use of a particular way of interpreting a combination of vertical and horizontal seismic planes to understand the stratigraphy of the area.

## **4. Dimensional Distribution of Channels in a Lower Cretaceous Mannville Heavy Oil Reservoir in West-Central Saskatchewan; Part 2: Integration of Borehole and Seismic Data**

### **4.1 Abstract**

Integration of well and seismic data was used to unravel the stratigraphy and predict the reservoir architecture within the Winter Field in west-central Saskatchewan. The complex deposits of the Lower Cretaceous Mannville's Dina and Cummings Members of the Cantuar Formation are the host to heavy oil deposits in this area. Our approach was to generate a three-dimensional well-validated seismic model and then combine all the available data, including a seismic attribute derived gamma-ray volume and core data, to build on it. The combined use of seismic vertical and plan views (horizon, time and stratal slices) was crucial to trace and define the stratigraphic architecture of the area. Although small scale heterogeneities in the reservoir were not resolved due to the characteristics of the seismic data, we were able to establish the presence of stratigraphic features such as channel incisions filled with reservoir and non-reservoir deposits. Core and borehole data were used to ground proof the seismic-based interpretations. Because of the small size of the 3-D seismic survey horizontal slices through the data volume generally imaged only small portions of the paleogeomorphologic features thought to be present in this area. As such, it was only through the integration of datasets that the depositional setting was established. This paper illustrates the methodology used to integrate well logs and

cores with seismic data (amplitude and gamma-ray or pseudo-lithology volumes), and emphasizes the benefits of the use of a particular way of interpreting a combination of vertical and horizontal seismic planes to unravel the stratigraphy of the area. The integration of this detailed stratigraphic interpretation with the attribute-based lithological prediction was crucial to propose a depositional setting and depositional history in order to generate a coherent geological model of the Winter Field.

## 4.2 Introduction

Production of heavy oil reserves in the Western Canadian Sedimentary Basin is challenging not only because of the nature of the hydrocarbons but also because of the stratigraphic complexity of the host deposits. The extensively studied Lower Cretaceous Mannville and Bullhead Groups contain the majority of the unconventional hydrocarbons in the basin, of which the Dina and Cummings Members of the Cantuar Formation, and time-equivalent deposits, are the richest. We integrated three-dimensional seismic and borehole data to establish the reservoir architecture of a heavy oil field in western Saskatchewan, and thereby help improve the oil production and total recovery. Well logs and seismic data have previously been combined to define stratigraphic units and understand the lithologic heterogeneity of the Mannville in another area (Sarzialejo and Hart, 2006). In the present study, and in order to more precisely calibrate the geologic model and better define the depositional history, we incorporated additional information such as conventional cores and the pseudo-lithology or gamma-ray (GR) volume. This volume predicts the distribution of reservoir and non-reservoir deposits in the area and details of its generation were discussed in Chapter 3. In this chapter, we deal with the methodology applied to integrate all the data, which were used to establish the depositional history and generate the geological model for the area.

The study area shown in Figure 1 is located in Township 42 and Range 25 of west-central Saskatchewan within the Winter Field. The heavy oil (12.9° API gravity) production comes from a stratigraphically controlled reservoir officially named the Winter Cummings Pool and herein referred to as the Winter Field. The

Field. The undifferentiated Dina-Cummings Members of the Cantuar Formation (Fig. 2) are the producing units here. The reservoir, an oil pool with no gas cap, has produced mainly by water drive (natural and induced) and currently produces with a high water/oil ratio. Horizontal wells have been used to produce the reservoir that is located between 630 and 700 meters subsurface depth. In order to understand the water production and to establish strategies to decrease its production thus increasing the oil/water ratio, it is necessary to have a comprehensive three dimensional model of the reservoir. Previous studies in the area (Groeneveld & Stasiuk, 1984) and in the close vicinity (Zaitlin & Shultz, 1984) used well logs and cores to understand the sedimentary environment and stratigraphy of the area. No published study has attempted to integrate well and seismic data to unravel the stratigraphy and generate a geological model of the Winter Field reservoir, and results of similar studies in other areas are not abundant. For example Dequirez et al. (1995) performed a study in the vicinity of our study area that successfully combined borehole and seismic (seismic facies and seismic inversion) data to define an integrated reservoir model.

#### **4.3 Geological Overview**

The sands of the Dina-Cummings Members of the Cantuar Formation form the reservoir of the Winter Field. These clastic deposits unconformably overlie the carbonates of the Devonian Duperow Formation (Fig. 2) and are overlain by the finer-grained deposits of the Cummings and Lloydminster members. The Aptian-Albian Mannville Group has been subdivided into a lower "Transgressive Systems Tract" and an upper "Highstand Systems Tract" (Cant and

Abrahamson, 1996) with the maximum flooding surface (MFS) occurring in the lower Albian. The sub-Cretaceous unconformity constitutes the basal sequence boundary of the stratigraphic unit. In this study, we deal with the transgressive deposits that overlie the sub-Cretaceous unconformity (Fig.3). According to Cant and Abrahamson (1994), the transgressive unit comprises the non-marine to marginal marine Dina Member, and time equivalent units (Fig.2) as well as the overlying sands of the Cummings Member, and its correlative units.

McPhee (1994) studied the Lower Mannville Group in east-central Alberta just west of our study area. He suggested that three major flooding events were present within the Transgressive Systems Tract. The transgression of the Boreal sea caused the first flooding event and fluvial deposits filled the paleo-valleys of the sub-Cretaceous unconformity. A major sea-level drop followed this flooding event and generated incised valleys, which were subsequently drowned during the second inundation. Elongated estuaries formed initially as the river valleys were flooded and then broad estuaries prevailed as the flooding extended. Sandstone sheets were deposited during the following still-stand and flooded during the maximum transgression time when an open marine environment was established in the area.

Groeneveld and Stasiuk (1984) and Zaitlin and Shultz (1984) focused their research on the Dina-Cummings Members in and around our study area. They concluded that they were deposited in a fluvial to nearshore marine to coastal marsh environment. In the Winter Field, they interpreted a tidal channel due to the presence of channel bank collapse conglomerates and abundant marine palynomorphs. The authors reported a lack of clear tidal structures in the Dina-

Cummings cores, which they interpreted to be either due to a real absence or to the presence of the strong oil saturation, which masked the structures. The Dina Member in both the Winter and Senlac areas is described as fluvial deposits infilling paleo-topographic lows that reduced the relief on the sub-Cretaceous unconformity. The Cummings Member is interpreted as a marine sequence deposited during a southward transgression of the Clearwater Sea. The coal is viewed as a product of a brief emergence, formed from marsh vegetation in a marginal marine (average 10% marine palynomorphs) setting. Their interpretation of the valley fill and tidal flat environments is consistent with previous regional interpretations that indicate that the Clearwater Sea flooded river-valley systems creating large estuaries that extended from central Alberta to the Winter-Senlac area.

Zaitlin and Shultz (1994) studied the Mannville Group south of the current study area. They interpreted the succession to represent the progressive change from terrestrial valley-filled deposits (Dina-Cummings Members) to estuarine-embayment fill deposits (Lloydminster Member). A brackish shallow marine ichnofossil suite near the top of the Dina-Cummings sequence was interpreted as indicative of the beginning of a slow southward flooding of the paleo-valley and the tidally influenced rivers that generated estuaries at the end of this time. The major marine transgression is observed within the Lloydminster interval.

#### **4.4 Database and General Methodology**

Our database consists of a 3-D seismic volume, digital well logs for 17 wells (Fig. 4) and cores from 16 wells of which six were within the study area.

The seismic survey covered approximately 15 km<sup>2</sup> with a bin size of 20 m x 20 m, a sample rate of 2 milliseconds, a dominant frequency of 50Hz and a time window from 466 to 866 ms two-way time (TWT). The vertical resolution of the data defined as  $1/4 \lambda$  is approximately 15 m, although thinner units of approximately 10 m are detected.

The workflow used in this study is shown in Figure 5. The methodology was divided into two phases. The workflow of the first phase, described in Chapter 3, is shown in Box A and the workflow of the second phase, which will be described in this chapter, is displayed in Box B. The basic database for both phases of the study consists of borehole (well logs and cores) and seismic (vertical and horizontal slices) data. During the first phase of the study we used vertical transects through the seismic data to make a preliminary seismic and well interpretation that was used to define the top and base of the seismic attribute analysis window. The result of the first phase was an attribute-based lithology prediction that we will denominate from now on the GR volume. The workflow of the second phase begins with the use of well logs and a combination of vertical and horizon slices to generate the detailed interpretation. This was necessary to establish the stratigraphic framework used to understand the reservoir architecture. Key stratigraphic surfaces such as unconformities, parasequence boundaries and flooding surfaces were defined using seismic and sequence stratigraphic principles described by Mitchum et al. (1977), Vail et al. (1977), Posamentier et al. (1988) Bertram and Milton (1994) and others. This interpretation was done simultaneously in both datasets with the aid of the

interpretation software. We applied concepts of seismic geomorphology, which involve the use of time, horizon and stratal slices (Posamentier, 2004), to establish the depositional setting and history. Due to the complex stratigraphy of the area and minimal structural dip, time slices (planes of constant two way time) were preferred over horizon slices (images showing amplitude variations along seismic horizons) and stratal slices (slices through the seismic volume that are parallel to overlying or underlying seismic horizons, cf. Zeng et al., 1998, 2000) are usually preferred for examining depositional features. The details of the stratigraphic integrated interpretation are explained in the following section.

A total of 394 m of cores from 16 wells, of which six were in the current 3-D area were examined for this study. Lithofacies were defined from the core analyses and combined with the well-log correlations to interpret the sedimentary environments of the area. This information was incorporated into the seismic interpretation and combined with the GR volume to generate a robust environmental interpretation, establish the stratigraphic history and generate a geological model for the reservoir within the Winter Field.

## **4.5 Detail stratigraphic interpretation**

### **4.5.1. Key stratigraphic surfaces**

The identification of the key stratigraphic surfaces involved the use of well logs, vertical seismic transects, time and stratal slices across the volume. East-West seismic transect A-A' (Fig. 6) displays the ten seismic horizons that were correlated throughout the area. Well 04-31 is one of the two wells that cut through

the complete section of interest in the western part of the study area. The stratigraphic surfaces correlated in this study include (from bottom to top): the Sub-Cretaceous unconformity or top of the Duperow Formation (DPRW), four horizons within the Dina-Cummings Members (Z, Y, X and W), the top of the Cummings coal (V), the top of the Cummings Member (CMGS), the maximum flooding surface (MFS), an intra Lloyminster horizon (U), close to the top of the Lloyminster Member (T), an intra Rex horizon named IREX (S), and the top of the Rex Member (REX).

As mentioned previously, a combination of the seismic data and well-log information was used to define this study's key stratigraphic surfaces. Figure 7 shows a representative well-log cross-section and corresponding seismic transect across the study area. Sequence stratigraphic methodology (i.e. reflection terminations, well-log signatures, etc.) was again used to identify the surfaces. Nine of the ten tops correlated through the area are shown in the figure. Seismic horizon DPRW corresponds to a continuous and very high amplitude peak in all the study area. Although this reflector generally does not display much irregularity through the study area, U- or V-shaped depressions are seen in a few locations. Horizons Z and Y are also continuous and seem to overlie conformably the DPRW throughout the area. Horizons Z and Y are truncated by younger horizons in certain locations throughout the area. These horizons followed well-log defined flooding surfaces. Seismic terminations, truncation and onlap (Fig. 6, 7) and log signature were used to define erosion surfaces X, W, U, and T. Horizon V corresponds to a low amplitude trough at the top of the Cummings coal that can be followed in boreholes and seismic data through most of the study area. A

distinctive well log signature was used to define the maximum flooding surface (MFS) and although it is clearly observed in the well logs, this surface could not be mapped throughout the seismic volume because it is erosionally truncated in places. Figures 6 and 7 display how several horizons, including the MFS, are truncated by other horizons throughout the area. The top of the Cummings Member is shown in the well correlation in Figure 7 to indicate the location of the top of the lithostratigraphic unit. Surface S corresponds to the horizon IREX that was defined initially in the study to bound the interval of study; this surface was picked because it was the first continuous surface observed above the DPRW in the current study area and in neighboring 3-D seismic surveys not reported on in this paper.

#### **4.5.1. Combined seismic vertical and horizontal views**

Time slices were combined with the vertical transects to do the detailed interpretation. We examined time slices over a time interval of 50 ms (660 to 710 ms) which corresponds to a thickness of approximately 70 m (600 to 700 m TVD *True Vertical Depth*). Horizons such as flooding surfaces, which are considered approximations of depositional timelines, are commonly used to generate stratal slices. However, in the area they have been locally eroded, are discontinuous, and are therefore not appropriate for generating horizon or stratal slices. Figure 8 displays a time slice at 688 ms, which shows several elongated features pointing in different directions. Features like this were identified in all the time slices analyzed. Once identified, the features were delineated in each time slice and overlaid on top of each other. The features observed on several time slices were

traced and were considered to represent probable geomorphologic features. Examination of timeslices in conjunction with the vertical transects showed that some of these features correspond to structural elements (e.g. structural highs and faults) and others to the stratigraphy (incisions). Features that do not show up in several time slices were considered not relevant or noise and were not used in the interpretation.

The initial stratigraphic horizon interpretation was first done in the vertical transects and later improved by combining them with the time slices with the sketched features. Figure 9 shows how the time slices and the vertical transect were set up for the interpretation. The plan view shows the distribution of the units, an approximate (due to the impact of structure) representation of the geomorphology of the deposits. Time slices at 694, 698 and 700 milliseconds were interpreted in this study. These three time slices cover the Dina-Cummings interval of interest. Figure 10 shows the interpreted and un-interpreted slices at 694 ms, the colors indicate the distribution of units S to Z in the study area. These units are each bounded by the stratigraphic surfaces described above and will be described in detail in section 4.7.

Due to the irregular nature of the sub-Cretaceous unconformity (i.e. the DPRW surface), time slices below 700 ms could not be used to image the distribution of amplitudes of the sandy deposits closely overlying the unconformity. In order to image these deposits we generated stratal slices at five and eight milliseconds above the DPRW surface. The ideal surface to generate the stratal slice would be the MFS, which is considered a close representation of a time line, but this surface could not be mapped in the area, as discussed

previously. Because all the interpreted horizons either corresponded to erosion surfaces or are not continuous due to erosion, we considered that the best surface for generating stratal slices in the Dina interval was the sub-Cretaceous unconformity. This horizon is highly diachronous and has significant relief, but it is the only continuous surface (Fig. 9) and is the closest surface to the strata of interest. The distribution of amplitudes in a stratal slice 8 milliseconds above the unconformity (Figure 11) shows the elongated features that were previously seen in the time slices. Seismic transect A-A shows the location of the stratal slice in yellow. The stratal slice in Figure 11 images the amplitudes associated with the lower sandy package as indicated by the GR logs of the wells that penetrate the stratigraphic section displayed in seismic transect A-A'. As was done with the time slices higher in the section, the features observed on the stratal slices were outlined, and then compared with those obtained from the time slice exercise. Only two of the sandy wells seem to be within one of the elongated features.

#### **4.6 Lithofacies analysis**

We described 394 m of conventional core from 16 wells within the Winter Field, but out of these, only 193 m corresponds to the six wells (Fig 4) located in the study area. Details of the all the core descriptions can be found in Appendix 1. The lithofacies analysis was performed and four groups of lithofacies were identified. These are shown in Table 1 and Figure 12. Six different sand lithofacies of Group 1 (crossbedded, structureless, parallel laminated to rippled, parallel bedded, concretionary, and calcite-cemented sands) were identified in the cores within this area. Also in the group and listed in Fig 12 are moderately

bioturbated sands and intraformational mud-clast breccias that were seen only in some cores located south of the seismic study area. Seven heterolithic facies (Group 2) were found within the study area and are described in Table 1. The facies range from interbedded to laminated, and include burrowed siltstones, mudstones and sands. The inclined stratified 2c facies was only found in a core situated to the south, outside the area of this study. The third lithofacies group includes laminated or massive, light or dark gray mudstones and siltstones. The last group is composed of coals and coaly mudstones and rooted siltstones.

#### **4.7 Stratigraphic Units**

The three seismic transects in Figure 13 show the detailed stratigraphic interpretation and the lithofacies interpreted in cores from wells that penetrate the section. Several channel incisions that cut the section at different stratigraphic levels were interpreted throughout the study area. Eight stratigraphic units were defined and named from bottom to top, units Z to S. The correlation between seismically defined units S to Z and the well-derived lithologic units is indicated in Figure 13. The bounding surfaces correspond to seismic boundaries, flooding or erosion surfaces. Figure 14 displays the well logs and core information for the four wells shown in Figure 13.

Integration of the well logs and cores in the area (Fig. 7 and 14) shows that there is a sandy package above the sub-Cretaceous unconformity that is, in turn, capped by an overall fining upwards succession. This fining upwards succession is overlain by radioactive (high gamma-ray) shale interpreted as a maximum flooding surface. The lowermost sandy unit ranges in thickness from 10 to 50 m,

displays a blocky character in the GR logs, and constitutes the reservoir at the Winter Field. The basal sandy package is generally formed of units Z, Y, and X (Fig 14).

#### **4.7.1.a Unit Z description**

Unit Z, bounded by the unconformity at the top of the Duperow (DPRW) and surface Z, is characterized by a fairly continuous, parallel wavy reflection pattern (Fig. 9) and generally drapes the Sub-Cretaceous unconformity. The average (Fig. 13) thickness is relatively constant (12 m) but ranges from 7 (eroded) to 14 m. Surface W is found bounding it in several locations throughout the area (Fig. 13) where it has been incised prior to deposition of Unit V. The six cores that cut this interval show that Unit Z is composed primarily of sands of Lithofacies Group 1, including crossbedded sands (1a), parallel laminated to ripple sands (1b), structureless sands (1d), calcite cemented sands located close to the contact with the Duperow carbonates (1h), concretionary sands that are generally located close to the oil/water contact (1g) and some thin (generally less than 25 cm) silt (3e) and shale (3b) beds. No trace fossils are seen in this unit. The well-log signature of Unit Z corresponds to a blocky sand with minor shale partings (Fig. 7). The resistivity logs indicate that most of the unit is water saturated in the study area.

#### **4.7.1.b Unit Z interpretation**

This combination of facies can be found in many environments but the constant medium to fine sand grain size found in the cores together with the

blocky aggradational character seen in the well log, supports the interpretation of a paleochannel. Both Groeneveld and Stasiuk (1984) and Zaitlin and Shultz (1984) interpreted a fluvial origin for these deposits, and we agree with their interpretations. These deposits would correspond with the initial transgressive fluvial deposits described by McPhee (1994). This interpretation would fit the regional depositional history described by Christopher (1997), Cant and Abrahamson (1996) and others that indicates that the unconformity was initially covered by deposits of non-marine to marginal marine origin. The absence of trace fossils in the cored sections is another argument for the fluvial origin of this unit.

#### **4.7.2.a Unit Y description**

Unit Y (orange) bounded by surfaces Z and Y has a continuous wavy parallel reflection pattern (Fig. 6, 9) and has a relatively constant thickness (Fig. 13) between 5 and 8 m. This unit is sampled in four cores and has the same combination of sandy facies as Unit Z with the exception of the calcite cemented sands (1h) which may be due to its location further above the Devonian carbonates. The fine-grained components of this unit are rippled silty mudstone (2h) and siltstones (3e). No bioturbation is observed in this unit. The same blocky character seen in the underlying Unit Z is observed in this unit (orange) in Figure 14. This unit has been incised in several locations within the area as seen in Figure 13.

#### **4.7.2.b Unit Y interpretation**

Unit Y, like unit Z, is interpreted to be fluvial in origin with the fine-grained intervals indicating periods of inundation within evolving sedimentary systems or autocyclic processes. As in Unit Z the absence of trace fossils in the cored sections is again another argument for its fluvial origin. This unit is water saturated in some regions.

#### **4.7.3.a Unit X description**

Unit X (light green) is bounded by surface Y and by erosion surface X, but due to erosion could be found underlying surfaces W or V. Figure 13 shows how Unit X (light green) thins towards the east, principally due to erosion. This unit shows a parallel reflection pattern and, like the two underlying units, it has a blocky well-log shape. This unit has an apparent divergent reflection pattern (Fig. 6) in the eastern region of the study area. The three cores that sample this unit all show the same lithofacies succession that from bottom to top are structureless sands (1d) parallel laminated or bedded (1c) and composed of crossbedded (1a) sands. The average thickness taken from the well logs of this unit is 8 m but ranges from 12 to 2 m from west to east.

#### **4.7.3.b Unit X interpretation**

In this unit, we see for the first time in the core samples parallel laminated strata, which can be interpreted as deposited by high energy currents in fluvial, tidal or coastal settings, due to the associated high energy lithofacies. The

combination of lithofacies observed as well as the well-log signature indicate that this unit could have been deposited like the previous ones in a fluvial setting and towards the top a transition fluvial-estuarine due to the nature of the overlying deposits. In the eastern region of the study area (Fig. 6, 13) this unit thins and displays a wedge shape and a divergent reflection pattern. This has been interpreted to be a consequence of erosion by the younger unit, although depositional thinning of the unit towards the east cannot be completely ruled out.

#### **4.7.4.a Unit W Description**

Unit W (brown) is bounded by erosion surfaces X and W. As seen in Figure 13, this unit incises Unit X in several locations and so varies in thickness throughout the area. Well-log measurements range from 3m to 9m. It is characterized by a parallel to parallel disrupted and chaotic fill reflection pattern. Three wells penetrate this unit in the study area and show a blocky well-log signature. Core samples indicate that it is composed of structureless sands of lithofacies 1d. This unit is observed incising on the east side of the survey and disappears by erosion and/or non-deposition towards the west of the study area.

#### **4.7.4.b Unit W Interpretation**

The only well that sampled this unit shows that it consists of fine to medium-grained structureless sands. This type of sedimentary deposit is interpreted to be formed by a rapid deposition of sand from suspension as strong currents lose velocity. This information, together with the well-log blocky gamma-ray signature and the seismic images, leads to the interpretation of these

deposits as fluvial or estuarine channel fills. Cant (1992) shows an example of these types of deposit from the Upper Mannville of eastern Alberta.

#### **4.7.5.a Unit V Description**

Unit V (green), between Surfaces W and V, shows a continuous parallel to parallel-disrupted reflection pattern in most of the area but shows a chaotic and complex fill pattern in some locations. Figures 9 and 13 show how this unit incises deeply into Units Z, Y, X and W. All the cores taken in the area sample this unit. It ranges in thickness from 16 m where it is infilling the incisions to 3 m where it drapes the lower units. Sands (1a, d and c), heterolithic deposits (2a, c, d, g and f), shales (3b, c and e) shaly coals (4a,b and c), silty paleosols and coals are all components of this unit. Except for Well 07-32 (Fig. 13) which sampled the incision fill, the cores show (Fig 7, 14) coarser-grained sands or silts at the base that are overlain by finer-grained, interlaminated (locally burrowed) deposits. Well log interpretations indicate that the unit is usually capped by the Cummings coal.

#### **4.7.5.b Unit V Interpretation**

Based on the presence of lithofacies 2a, 2d, 2f, 2g, 3b, 3e and 4a, Unit V is interpreted as deposited in an estuarine and coastal plain environment. These lithofacies can be interpreted to be a product of depositional processes that include: as a series of waning flows at the end of the channel fill episode (2a), mixed energy environment with flooding and weak currents bringing in the sands

(2d), fallout from suspension during flooding in distal coastal plain settings representing fluctuations in energy within a continuous deposition (2f), suspension fallout in low energy environments where sands are brought in periodically to a well-oxygenated environment (2g), suspension fallout in a low energy regime in a relatively oxidized environment (3b) and deposited from rapid suspension fallout during flooding events in coastal plains.

Channels, possibly estuarine, incised the area and were infilled with fining upwards deposits, by abandonment of the channel, a sea level rise or both. After a period of submergence, the paleosols observed in several wells were formed and then the area was flooded, with rising base level generating coal deposits from marsh peat in this marginal marine setting.

#### **4.7.6.a Unit U Description**

Unit U is seen as a series of continuous nearly parallel to parallel-disrupted reflections (Fig 9, 13) between erosional surfaces V and U. The unit is seen continuously blanketing the area. In the eastern region, within the incisions, the signature of surface V at the base of unit indicates erosion of parts of the underlying Unit V. The incision fill shows a chaotic reflection pattern in some locations. Well logs show a fining upward signature and the highest GR deposits of the interval studied. The unit is generally 12 m thick (5 to 14m range) and is composed of crossbedded, parallel laminated and structureless sands and several heterolithic deposits as coarsening upward mudstones and silty sands (2d), rippled silty mudstone (2h), interbedded sandy siltstones and silty mudstones (2e) and

burrowed sandy siltstones (2g). Gray mudstones (3a) burrowed mudstones (3d) and a paleosol are found overlying the sand and heterolithic deposits.

#### **4.7.6.b Unit U Interpretation**

Unit U was deposited after another period of incision and is interpreted as being deposited in a marginal marine to marine setting. This interpretation is based on the well log and core interpretations that show an overall fining upwards from a coarsening upward clean structureless fine-grained sand to a series of burrowed silts and shales all the way up to a burrowed dark gray shale that corresponds to the highest GR shale in the well logs. The MFS, which has been interpreted in all the region's well logs, is located within this shale package. No downlap surface is observed in the seismic data associated with this surface. This could be due to the relatively small size of the survey. This surface, the MFS shown in Figure 7, which is located within the Lloydminster Member, has been interpreted as marine by several authors (e.g. Christopher, 2003). It coincides with the maximum flooding surface interpreted by Cant and Abrahamson (1996) and McPhee (1994).

#### **4.7.7.a Units T and S description**

Units T and S do not form part of the Dina-Cummings reservoir under study and only the first unit has been partially sampled in core. Unit T is located between erosion surfaces U and T and is seen incising units X, W, V and U throughout the area. The biggest channel incision is seen in the central part of the

seismic volume (Fig. 13). Unit T shows mostly continuous parallel reflection pattern and chaotic fill within the incisions in some locations. The thickness of the unit varies between 15 and 8 m with an average of 11 m. The well log shows a coarsening upwards sequence. An incision filled with the units was penetrated by Well 07-33 (Fig. 13, 14). The interval sampled by the cores showed coarsening upwards fine-grained facies (2a) and coaly and rooted silts (4c) and generally finer-grained sediments than the rest of the wells.

Unit S located between erosion surface T and surface S shows a continuous parallel reflection pattern. This unit drapes Unit T and has a thickness of between 2 and 7 m (5 m average).

#### **4.7.7.b Unit T and S Interpretation**

Unit T was deposited after the MFS and shows a well-log signature that can be interpreted as prograding shallow marine bars and surrounding environments. The only samples that exist of Unit T (Well 07-32) correspond to possible estuarine fine-grained deposits filling the incision shown in Figure 13 a. Units T and S do not correspond to sequence stratigraphic units. They are bounded by local erosion surfaces and flooding surfaces generated by autocyclic events affecting the area.

#### **4.8 Integration**

Units Z, Y and X, as seen in the seismic transects in Figure 13, are conformable stratigraphic packages that are incised by the younger units. They are proposed to be the product of a series of episodes of fluvial deposition in the

basin, based on the borehole data. They are interpreted in the sequence stratigraphic framework as the basal part of the transgressive deposits overlying the sequence boundary, the Sub-Cretaceous unconformity, on top of the Duperow Carbonates. In the seismic transects and in the map views we do not see any geomorphologic features that could be interpreted as generated at the time of the sedimentation of units Z, Y and X; this could be explained if we are imaging a large system with the small seismic survey used in this study. Figure 15 shows a map with wells located within and surrounding the study area. If we focus on the basal part of the logs (units Z to X) we could interpret the presence of a large channel or fluvial valley (dotted area) filled with sand. The study area (shown by the red rectangle) is only partially sampling the large feature. This would explain what is observed in the time slices.

Units W to T all incise older units (Fig. 13). These incisions, as mentioned before, were interpreted from the combination of vertical and horizontal seismic images and would have been difficult if not impossible to define based only on well-log interpretations (see also Sarzalejo and Hart, 2006). These units are interpreted as a series of incised fluvial to estuarine valleys.

The geomorphology and timing of the incisions was interpreted by combined study of the horizontal and vertical seismic views. Figure 16 shows the outlines of the incisions interpreted from the time slices at 688, 694 and 700 ms. The channel incisions were colored to represent the time of their generation and infilling. The oldest incisions were filled with deposits from Unit W and have two sets of directions, SW-NE and approximately N-S. Incisions filled with Unit V deposits also show both directions and a channel running SE-NW. Finally we

observe the youngest incisions filled with units U and T which run in the same directions as the older units. We can observe in Figures 13 and 16 how the younger systems tend to re-incise the older valleys and erode part of their fill.

Because we are dealing with a relatively small area the surfaces interpreted on the seismic data may correspond to sequence stratigraphic significant surfaces such as sequence boundaries (e.g. DPRW) and maximum flooding surfaces (MFS) or to surfaces with only local presence and significance. The channel erosion surfaces identified in the vertical transects (e.g., top X or U) could represent periods of sea level fall or could simply represent autocyclic events in fluvial or estuarine settings. Other examples of non-regional surfaces identified and mapped in small surveys are discussed in Sarzalejo and Hart (2006) and Hart et al. (2007).

Groeneveld and Stasiuk (1984) have interpreted fluvial and estuarine environments previously for this area and the surrounding areas. Although no typical tidal sedimentary structures were found, estuarine and coastal plain conditions are suggested by the combined presence of lithofacies 2a, d, e, f, g, 3 and 4. The sandy deposits of units Z, Y, X and W deposits are interpreted as fluvial (channel fill) or as bay-head deposits in an estuarine environment and Unit V is interpreted as coastal plain to estuarine. Due to the absence of clear tidal structures, we suggest that the study area would be in the inner estuary (Darlymple et al., 1992) where fluvial processes predominate. If this area is all within a large estuary, and in this study we are viewing and sampling only part of it, we cannot make many inferences with respect to its overall geometry (bar-built or more open end type). The incised valleys observed in the seismic volume, due

to their elongated morphology and fill, could be interpreted as smaller estuaries of the drowned river valley type (Pritchard, 1952). Figure 17 shows a large modern estuary. If we assume that we are dealing with an estuary of similar scale, because of the size of the survey (white rectangle), we would only be able to use the 3-D seismic data to image small features such as the channel shown in Figure 17.

In terms of the stratigraphic evolution of the area, we could extrapolate the interpretation done by McPhee (1994) in eastern Alberta. The three major flooding events, which he interpreted within the Transgressive Systems Tract, could be present in the current study area. The transgression of the Boreal Sea caused the first flooding event and fluvial deposits filled the paleo-valleys on the sub-Cretaceous unconformity leading to deposition of units Z, Y and X. The incisions observed in this area in unit V may be a product of the sea level fall (McPhee, 1994) or autocyclic depositional processes. A second transgression led to flooding of the river valleys. Small estuaries formed initially but as flooding extended, broad estuaries prevailed. During this time, paleosols and coals formed in the marginal marine setting. The sandstones of Unit U could have been deposited during a sea-level still-stand and were subsequently flooded during the maximum transgression when an open marine environment was established at the end of Unit U.

Figure 18a shows a vertical transect through the GR volume and superimposed on it is the detailed stratigraphic interpretation and the GR logs. From integrating the two data-sets we can see the lithology prediction for the different units displayed in the seismic transect in Figure 18b. Mostly sand (yellow) is predicted for Units Z and Y, while it is possible to observe sands with

some shales and non-reservoir deposits in Unit X. These three units are generally within the undifferentiated Dina-Cummings Members and are interpreted to be of fluvial origin. In Figure 18b we can see a well that cuts these units; the core taken at this well location recovered a thick package of sand (yellow) within units Z, Y and X. For Unit V the predicted sediments are mostly non-reservoir (brown) deposits, this unit is also within the undifferentiated Dina-Cummings Members. The changes observed in this unit both in lithology prediction and in depositional environments (interpreted from cores) together with the presence of the Cummings coal at the top of this unit, lead us to separate this unit from the lower units Z, Y and X and locate it within the Cummings Member. For Unit U (Fig. 18a) the prediction is shales (in green) and non-reservoir silty and shaly deposits (brown). The maximum flooding surface (light green horizon) coincides with the generally continuous area of the highest GR prediction, which constitutes the vertical seal for the reservoir. This unit, based on the core lithofacies, is interpreted as marginal marine to marine. Non-reservoir deposits are predicted for Units T and S. The log character can be seen in the GR logs in Figure 14.

Gamma ray time slices at 688, 694 and 700 ms are shown in Figure 19. Superimposed on the slices are the incision outlines that resulted from the combined interpretation of the seismic map view (time and stratal slices) and vertical views. We can observe that the bottom slice (700 ms) predicts mostly sand throughout the area; non-reservoir and shaly deposits are seen within most of the incisions and in the east-central region. The middle slice at 694 still shows sand especially in the central area but the shallower slice at 688 shows non-reservoir deposits infilling the area together with the shales in the east. In these

images we see the type of lithology that is predicted to infill the incisions. The SW-NE channel incisions located to the south as well as the N-S and the NE-SW incisions are mostly filled with sand at their bases (700 ms). The 688 and 694ms slices show that towards the top non-reservoir silty and shaly deposits would be filling the valleys. Only the SW-NE incision in the west-central region is predicted to be filled with shales from top to bottom. Fine-grained deposits are predicted in the east-central region of the 700 ms slice. Well 07-33 (Fig 20a), located in that area, shows fine-grained deposits affected by slumps, faults and microfaults (lithofacies 2b in Figure 12) at this interval in core. In this location younger deposits have been remobilized into a sinkhole due to collapse of the underlying Duperow carbonate. The linear trends observed in the time slice are most likely related to underlying faults seen in vertical seismic transects that image that area.

The incisions interpreted from the integrated seismic and well data illustrate the type of complexity that is observed in the lower Mannville deposits in the area. This complexity can affect the behavior of the reservoir, and this is important to consider when designing production strategies. Figure 20 displays two (E-E' and F-F') transects from the GR and amplitude volume. In the eastern region of vertical transect E-E (Fig. 20a) we observe an incision filled with shales (green) according to the GR prediction. The same incision is seen further south (Fig. 20b) in seismic transect F-F'. At location F-F' it coincides with one of the sinkholes observed in the area. This incision corresponds to the SW-NE incision located at the west of the area (Fig. 19) predicted to be filled with shales. These shale-filled incisions, depending on their extent and location, could act as barriers

that affect the movement of fluids through the reservoir sands and compartmentalize the accumulations. Locating and understanding the nature of these barriers is essential to the exploitation of the reservoir.

#### **4.9 Discussion**

The methodology of integration of datasets and results just described allowed us to use all the available data to understand the evolution of the deposits of the area, as well as generate a 3-dimensional prediction of the lithology distribution. This methodology can be applied to any area with similar data in order to characterize the deposits. We would like to emphasize the benefits of using the particular form of combining plan and vertical seismic images used in this study. Combining the images and sketching the interpretation simultaneously in vertical and horizontal seismic transects allows the interpreter to examine the features from different perspectives at the same time and generate a more realistic geological interpretation. Two aspects in our methodology that contributed greatly towards the end model were the generation and integration of the attribute-based lithology prediction. Color was a very useful tool for the interpretation during the combined seismic interpretation phase because it enhances the geometry of the stratigraphic elements. Color also was critical later during the integration of the results when visualizing the lithology prediction and geological features.

Figure 21 shows a summary diagram with the major stratigraphic (incised valleys) and structural (karsting) features observed in the area. The colors correspond to and are the same as the predicted facies (reservoir, non-reservoir and seal) from the GR volume. The reservoir package covers the Devonian

Duperow carbonates. The erosion surfaces shown as dotted lines are affecting all the area. They are decapitating some of eastern packages and incising mostly in the center and eastern side of the area. Collapse due to karst dissolution is seen in several locations in the area. These features are predicted to be filled with fine-grained non-reservoir sediments or shales. Sands are predicted all over the area in the bottom of the sequence with a few exceptions. The incisions are filled with both sands and fine-grained sediments. Shale and non-reservoir filled channels or collapsed areas could constitute lateral barriers for the fluids in the reservoir. In our study area we did not see an obvious compartmentalization generated by these features and if it were present, it would be generated by smaller scale heterogeneities or a combination of both. As mentioned before, small-scale heterogeneities could not be resolved in this area due to the physical characteristics of the deposits, which produce small differences in acoustic impedance between the different lithologies (see chapter 2).

A model like the one generated here, which includes a 3-dimensional lithology prediction, should be used to update and re-evaluate the existing reservoir model. Channel directions, lateral continuity of the reservoir facies, the presence of shaly barriers, and relations between structure and reservoir facies, are some of the aspects to consider for production strategies. Stratigraphic and facies models are the first inputs in a reservoir characterization study. The facies model would have the three facies (reservoir, non-reservoir and shale) predicted. Several more steps are necessary to generate a complete geological static model. The next step would be to combine the stratigraphic surfaces and units with the 3-D lithology prediction and generate a 3D geocellular model. This initial model

would have depth horizons (generated from the surfaces) that bound zones; these zones would subsequently be layered and divided into cells. Each cell would carry the lithology information from the 3-dimensional prediction. Pressure data would be introduced to help validate the stratigraphic correlation and to define the heterogeneities that constitute the fluid barriers in the reservoir. Finally, the reservoir static model would be completed when petrophysical data (i.e. porosity, permeability and water saturation) were assigned to each cell of the 3-D grid.

#### **4.10 Conclusions**

A geological model of part of the Winter Field in west-central Saskatchewan was generated through the integration of the geological data (well logs and cores) and geophysical data (amplitude and GR volumes). A detailed correlation was done using a particular way of interpreting the combined vertical and planar views of the seismic amplitude volume. Several stratigraphic units (Z to S) were defined in this study and correlated throughout the area. Lithology was assigned to these units using borehole and core information together with the attribute-based lithology prediction. According to our interpretation, the base of the reservoir was deposited by fluvial processes and formed part of a large system that could not be completely imaged due to survey-size limitations. This initial fluvial episode filled most of the area with medium- to fine-grained sands found in units Z, Y and X. These sands display a blocky signature in GR logs that is characteristic of channel-fill deposits. Following the period of sand aggregation, smaller channels incised the area and deposited units W to S, which cut the underlying sands in several directions. The channels show several periods of

incision. The sandy fluvial deposits were overlain by estuarine and marginal marine sediments that include the denominated Cummings coal. These deposits constitute the top of the reservoir. An overall transgression is seen from the bottom to the top of the reservoir and all the way to the shales containing the maximum flooding surface, which constitutes a regional seal. Some surfaces have regional sequence stratigraphic significance, such as the DPRW (Sequence Boundary) and the MFS, while others are local erosional surfaces tied to autocyclic processes.

This complex interpretation would have been difficult to achieve using only vertical transects without the planar views and even more so with the sole use of well logs. The incorporation of borehole information and the lithology prediction to the seismic interpretation tells us that some of the incisions were filled with sands at the bottom and non-reservoir deposits towards the top, and some were filled only with fine-grained sediments. These incisions filled with impermeable deposits do not constitute barriers in this area because of their relatively small vertical and lateral extent. Unfortunately, the locations and distribution of other possible reservoir barriers, such as thin shale partings within the sandy packages, was beyond the resolution of the seismic data in this study. Integration of all the available information resulted in a comprehensive geological model for the area and contributed to the understanding of the stratigraphy and depositional history of the Lower Mannville deposits. The methodology described in this study to generate the geological model can be applied by both geologists and geophysicists working in any area with similar information.

#### **4.11 Acknowledgements**

The seismic and well-log data used in this study were made available by Nexen Inc. Seismic and log interpretations were undertaken using software donated by Landmark Graphics Corporation. Funding for this work was provided by Nexen Inc. and a NSERC Discovery Grant to Professor Hart. I wish to thank the Saskatchewan Subsurface Geological Laboratory for providing me with free access to the well cores. We thank all of these organizations for their continued support of our research. Crystal Mann is thanked for her detailed and constructive review which improved the quality of this manuscript.

#### 4.12 References

- Bertram, G. T. and Milton, N.J. 1994. Seismic stratigraphy. In: Sequence Stratigraphy. D. Emery and K. J. Meyers (eds.). Blackwell, p. 45-60.
- Brown, A. R. 1999. Interpretation of three-dimensional seismic data. American Association of Petroleum Geologists, Memoir 42, 514 p.
- Cant, D. J. 1992. Subsurface Facies Analysis. In: Facies Model response to Sea Level Change. R.G. Walker and N. P. James (eds.). Geological Association of Canada, p. 27-45
- Cant, D. J. and Abrahamson, B. 1996. Regional distribution and internal stratigraphy of the Lower Mannville. Bulletin of Canadian Petroleum Geology, v. 44, p. 508-529.
- Christopher, J. E. 1997. Evolution of the Lower Cretaceous Mannville Sedimentary Basin in Saskatchewan. In: Petroleum geology of the Cretaceous Mannville Group, Western Canada. S. G. Pemberton and D. P. James (eds.). Canadian Society of Petroleum Geologists, Memoir 18, p. 191-210.
- Dalrymple, R. W., Zaitlin, B. A., and Boyd, R. 1992. Estuarine facies models-- Conceptual basis and stratigraphic implications: Journal of Sedimentary Petrology, v. 62, p. 1,130-1,146.
- Dequirez, P. Y., Blanchet, C. Feuchtwanger, T. and Torriero, D. 1995. Integrated stratigraphic and lithologic interpretation of the East-Senlac heavy oil pool: SEG Annual Meeting, Houston, Texas, Expanded Technical Program Abstracts with Biographies, v. 65, p.104-107.
- Groeneveld, N. A and Stasiuk, L. D. 1984. Depositional environment of the Cummings coal and associated sediments, Winter-Senlac area, Western

- Saskatchewan. In: Oil and gas in Saskatchewan. J. A. Lorsong and M. A. Wilson, (eds.). Special Publication: Saskatchewan Geological Society, v. 7, p. 135-147.
- Hampson, D., Schuelke, J. and Quirein, J. 2001. Use of multiattribute transforms to predict log properties from seismic data: *Geophysics*, v. 66, p. 220-236.
- Hart, B. S., Sarzalejo, S. and McCullagh, T. 2007. Seismic stratigraphy and small 3D seismic surveys: *The Leading Edge*, v. 26, no. 7, p. 876-881.1
- McPhee D. 1994. Sequence stratigraphy of the lower Cretaceous Mannville Group of east-central Alberta. M.Sc. thesis, University of Alberta, 64 p.
- Mitchum, R. M, Vail, P. R. and Thompson, S. 1977. Seismic stratigraphy and global changes of sea level; Part 2, The depositional sequence as a basic unit for stratigraphic analysis. In: *Seismic stratigraphy; applications to hydrocarbon exploration*. C. E. Payton (ed.). American Association of Petroleum Geologists, Memoir 26, p. 53-62.
- Pritchard D. W. 1952. Estuarine hydrography. In: *Advances in geophysics*. Landsberg, H. E. (ed.). vol 1, p. 243-280.
- Posamentier, H. W., Jervey, M. T. and Vail, P. R. 1988. Eustatic controls on clastic deposition. I. Conceptual framework. In: C. K. Wilgus, B. S. Hastings, Christopher. G. St. C. Kendall, H. W. Posamentier, C. A. Ross and J. C. Van Wagoner, (eds.), *Sea Level Changes—An Integrated Approach*, vol. 42. Society for Sedimentary Geology, Special Publication, p. 109 -124.
- Posamentier, H. W. 2000. Seismic stratigraphy into the next millennium; a focus on 3D seismic data. AAPG Annual Conference, New Orleans, Louisiana, Program and Abstracts CD.

- Sarzalejo, S. and Hart, B.S. 2006. Stratigraphy and lithological heterogeneity in the Mannville Group (southeast Saskatchewan) defined by integrating 3-D seismic and log data. *Bulletin of Canadian Petroleum Geology*, v. 54, p. 138-151.
- Vail, P. R., R. M. Mitchum, R. G. Todd, J. M. Widmier, S. Thompson, J. B. Sangree, J. N. Bubbs and W. G. Hatlelid, 1977, *Seismic Stratigraphy and Global Changes of Sea Level*, in C. E. Payton ed. *Seismic Stratigraphy-applications to hydrocarbon exploration: American Association of Petroleum Geologists, Memoir 26*, p. 49-212.
- Zaitlin, B. A. and Shultz, B. C. 1984. An estuarine-embayment fill model from the Lower Cretaceous Mannville Group, west-central Saskatchewan. In: *The Mesozoic of middle North America*. D. F. Stott and D. J. Glass (eds.). *Canadian Society of Petroleum Geologists, Memoir 9*, p.455-469.
- Zeng H., Backus, M. M., Barrow, K. T. and Tyler, N. 1998. Stratal slicing, part I: realistic 3-D seismic model. *Geophysics*, v. 63, p. 502-513.
- Zeng H., Tucker F. H. and Wood, L. J. 2000. Three-D Seismic Facies Imaging by Stratal Slicing of Miocene-Pliocene Sediments in Vermilion Block 50- Tiger Shoal Area, Offshore Louisiana. AAPG Annual Meeting, New Orleans, Louisiana, Program and Abstracts CD.

#### **4.13 List of Tables**

Table 1. Lithofacies summary

Facies	Description	Thickness	Depositional process	Sedimentary Environment	Associations
Sandstone 1a Cross-bedded sands	very fine to medium grained sand with mainly high angle tabular cross-bedding base of sets may contain mud clasts, organic matter laminae may be present, no change of grain size with depth, high bitumen saturation	several centimeters to 10 m	dune migration	fluvial	1d
Sandstone 1b Parallel laminated to rippled sands	very fine to fine grained current rippled and ripple drift sands, sedimentary structures enhanced by bitumen saturation	few centimeters to a meter	deposited from episodic waning flow in relatively weak slow currents	lagoon, point bar, fluvial channel, overbank, or flood channels	2a, 2g, 2d
Sandstone 1c Parallel laminated or bedded sands	fine grained sands associated to structureless and cross-bedded sands	several centimeters to a meter	high energy currents	fluvial, tidal or coastal settings	1a, 1d
Sandstone 1d Structureless sands	fine to medium grained sands, no clear sedimentary structures distinguished, appear structureless, bitumen saturation possibly obscuring existing structures, isolated mud clasts in some cores, no change of grain size with depth	up to 10 m but intervals of 1 m common	rapid deposition from high energy currents due to a drop in velocity	fluvial or estuarine channels	1a, 1c
Sandstone 1e With concretions precipitates	very fine to medium grained sand with rounded millimeter scale non calcareous concretions or precipitates (only in wells 10-28 and 11-28)	around 1.5 meters	massive precipitation from fluid during diagenesis	non indicative	1d
Sandstone 1f Calcrete cemented sands	fine to medium grained sands with white mottled aspect, relates to hydrochloric acid	few centimeters to 1 m	precipitation of cement from calcite rich fluid from the underlying Dupurow Fm during diagenesis	non indicative	1a, 1d
Heterolithic 2a Fining upwards sequence of muds, silts and sands	layers of bitumen saturated rippled to structureless sands interbedded with biturbated sandy silts and laminated or biturbated grey mudstones; sequence repeats itself with an overall decrease in grain size and in the thickness of the coarse grain layers	around one meter	series of waning flows at the end of fine channel fill episode	crevasse channel fill, channel abandonment	1a, 3b, 4c
Heterolithic 2b Slumped sediments	shaped, faulted and fractured sands, silts and mudstones	over 1.5 meters	deposited by mobilization and re-sedimentation in areas of paleo-geographical lows as Karst depressions	non indicative	
Heterolithic 2d Coarsening upwards sequence of mudstones and silty sands	coarsening upwards sequence of laminated, moderately burrowed grey silty mudstones and rippled and parallel bedded silty sands, burrows are scarce, mainly horizontal, some burrows have more than 1 cm in diameter, low bitumen saturation in sands	4 meters	deposited in a mixed energy environment, with flooding or weak currents bringing in the sands	crevasse splay building along the edges of estuarine channels or into bays or shallow lakes	2f, 4c
Heterolithic 2e Interbedded sandy siltstones, sands and mudstones	up to 10 centimeters layers of oil saturated structureless or ripple to laminated sands interbedded with biturbated silts and light grey laminated mudstones, mainly horizontal, moderate biturbation; millimeters to few centimeters, low diversity burrows	less than a meter up to over two meters	alternating episodes of higher energy, settings where currents deposited ripple to laminated cross-laminated sands within a low energy setting where deposition is settling from suspension	channel-proximal overbank deposits (roots are absent probably due to rapid cycles that do not allow the establishment of vegetation)	2f, 1b, 3d

Table 1. Lithofacies summary

Heterolithic 2f Laminated silty mudstone	interlaminated silts and light grey mudstones, some low degree of bioturbation	up to a meter	fallout from suspension during flooding, represents fluctuations in energy within a continuous deposition.	flood plain or distal coastal plain settings	4a, 2c
Heterolithic 2g Burrowed sandy siltstone	sandy silt with some bitumen impregnation, monotonous bioturbation, moderate to abundant, mostly horizontal with some vertical burrows concentrated in some layers, primary sedimentary structures are not visible.	reaches 2-3 meters	suspension fallout in low energy environments where sands are brought in periodically, well-oxygenated bottom conditions	coastal or flood plain settings in the vicinity of the estuarine or fluvial channels	4a
Heterolithic 2h Rippled silty mudstone	thinly laminated, rippled silty mudstone facies not common, thin organic matter lamina commonly present	half a meter	short episodes of flooding	flood or coastal plains	1a, 1d
Mudstone 3a Dark grey mudstones	dark grey massive or fissile shale with organic matter	feet of centimeters to 3 meters	deposited from suspension in oxygen deprived environment	non-marine to paralic or marine settings	3d, 4a, 4b
Mudstone 3b Light grey mudstone	light grey to grey mudstone, massive or fissile, some bioturbation present	centimeters up to 3 meters	deposited from suspension fallout in a low energy regime in a oxidized environment	flood plain, abandoned channels, and coastal plain settings	4a, 4b
Mudstone 3c Burrowed dark grey mudstone.	dark grey laminated mudstone with abundant mainly horizontal burrows	centimeters to 4 meters	deposited in an oxygenated organic rich environment	Lagoon, marsh, marine	4b, 1c
Mudstone 3d Burrowed light grey mudstone	light grey mudstone with mainly horizontal burrows, bioturbation moderate to abundant, primary sedimentary structures are not recognized, diversity is moderate and abundance varies from low to moderate	centimeters to over two meters	deposited from suspension	marginal marine (lagoons, protected brackish bay, abandoned estuarine channels) to marine	associated to many lithofacies
Siltstone, 3e Siltstone, Coal 4a Coal	rare, facies consist of mainly massive siltstone with rare bioturbation black, crumbly coal, occasional yellow spots and bands (sulfur), submetallic lustre	centimeters	rapid suspension fallout during flooding events	coastal plains or flood plains	2g and 3d
Mudstone 4b Coal; mudstone	blackish massive mudstone occasional yellow (possibly sulfur) spots	up to 1.5 m	generated from organic matter in a oxygen deprived environment	peats in a marginal marine setting	4b, 3a, 3b, 2g
Siltstone 4c Coaly and/or rooted siltstone	light grey massive, mottled and rooted Thin carbonaceous laminations are present in some cases. Vertical to sub-vertical roots of up to 12 centimeters long are present	reaches 50 cm little over a meter	suspension fallout in a oxygen deprived environment, with abundant organic matter developed in vegetated areas of coastal plain or floodplain areas, indicates periods of slow sedimentation and subaerial exposure.	non-marine to paralic environments, distal coastal plain with marshes, paleosol	4a 4a and 4b

Cont. Table 1

#### 4.14 List of Figures

**Figure 1.** Location map of the Winter Field in west-central Saskatchewan. The dotted polygon outlines the area of the oil sands and heavy oil reservoirs in the Western Canadian Sedimentary Basin. The study area corresponds to the rectangle shown in the figure.

**Figure. 2.** Correlation chart of the Lower Cretaceous deposits in the Western Canadian Sedimentary Basin (modified from Christopher, 2003). Stratigraphic nomenclature for west-central Saskatchewan is under the Lloydminster Area column. The units under examination, the Cummings and Dina Members of the Mannville Group, are highlighted in the figure.

**Figure. 3.** Type log of the Lower Mannville deposits within the Winter Field. The reservoir located on top of the Duperow Carbonates is within the undifferentiated Dina-Cummings Members of the Cantuar Formation. The GR log signature indicates the thick reservoir sand. The oil/ water contact is observed in the resistivity log.

**Figure. 4.** Base map outlining the Winter 3-D survey showing the locations of the 17 wells used in this study. The locations of seismic transects B-B', E-E', C-C', F-F', D-D' and A-A' are indicated by the dotted lines.

**Figure. 5.** The workflow of the two phases of the study is shown in the diagram. Box A shows the workflow of the first phase, which is described in detail in chapter 3. The workflow for the second phase, which is described in this chapter, is displayed in Box B.

**Figure. 6.** Uninterpreted and interpreted seismic transect A-A'. The seismic profiles show the stratigraphic surfaces interpreted in this study. Note the thinning of the interval between surfaces W and Y observed in this eastern region of the study area. The GR log of Well 04-31 observed at the western edge indicates the presence of coarse sandy deposits overlying the DPRW unconformity.

**Figure. 7.** Seismic transect and corresponding stratigraphic cross section B-B'. The seismic and well-log profiles show the horizons interpreted in this study. Location of the B-B' is shown in Figure 4. The maximum flooding surface MFS is the datum (dashed lines) and the well picks that correspond to the seismic horizons are shown in the stratigraphic cross section. The equivalence between the formal stratigraphic nomenclature and the units defined in this study is indicated in the stratigraphic cross section. Note that not all the well picks have a corresponding interpreted seismic horizon.

**Figure. 8.** A time-slice through the amplitude volume at 688 ms showing a series of elongated features. The outline of these features was used in conjunction with the reflection character of the seismic vertical transects to interpret stratigraphic features in the area.

**Figure. 9.** Example of how the time slices and vertical transects are combined to generate the detailed interpretation. The time slice at 700 ms is displayed at the same scale with interpreted and non-interpreted views of vertical transect C-C'.

Location of transect B-B' is indicated in the time slice and the location of the 700 ms time slice is shown in the vertical transect. The time slice and the vertical transects are interpreted by combining the information observed in both images. Vertical lines (in red) that show the location where the horizon interpretation intersects the time slice (horizontal dashed line shown in white at 700 ms) were used as guides for the interpretation.

**Figure 10.** Interpreted and un-interpreted time slice showing the distribution of units S to Z at 694 milliseconds. Dashed lines highlight the elongated features interpreted from the distribution of amplitudes.

**Figure 11.** Stratal slice showing the distribution of amplitudes at 8 ms above the top of the Duperow and seismic transect B-B'. The vertical transect shows the GR logs of the wells that penetrate the stratigraphic section. Dashed lines outline the elongated features also observed in the rest of the time-slices analyzed. The yellow horizon, shown in vertical transect B-B', indicates the location of the stratal slice which is imaging the basal reservoir sands.

**Figure 12.** List and examples of the lithofacies observed in the cores analyzed in this study.

**Figure 13.** Seismic transects E-E', D-D' and B-B' show the architecture of units S to Z though the study area. Note that several incised valleys cut the deposits at several levels within the interval of interest. Displayed in the figure are the GR

logs of several boreholes that penetrate the stratigraphic section. Also in the figure are the lithofacies of the deposits sampled by the four cores that sampled the Lower Mannville deposits. Figure 14 shows the details of the core lithofacies interpretation.

**Figure 14.** The log signatures and the core descriptions of the four wells shown in the seismic transects in Figure 13. The legend for the different facies is shown in Figure 12. The tops of the formal stratigraphic units are displayed together with the units defined in this study.

**Figure 15.** The map displays facing GR logs within the Dina-Cummings interval for several wells in the region of the Winter Field. Outlined in black is a possible channel or fluvial valley running through the area (at the base of the interval). The red box shows the approximate size of our study area and why only part of the system would be imaged in the 3D seismic survey analyzed in this study.

**Figure 16.** Outlines of the features observed in the time-slices at 688, 694 and 700 ms, interpreted as fluvial incisions. The incisions are colored according to their fill. Note that some incisions were re-incised and re-filled with deposits of different units.

**Figure 17.** A Chesapeake Bay type of microtidal estuary system is interpreted for the study area. If the system had the same size as the modern analog the white square would indicate the size of our seismic survey. Note the dimensions of the

feature that could be imaged with our seismic survey. The satellite image of Chesapeake Bay was manipulated to simulate the N-S orientation of the deepest incision observed in the area.

**Figure 18. a.** Vertical transect B-B' through the gamma-ray (GR) volume with the pseudo-lithologies shown in different colors. Superimposed over the gamma-ray information are the amplitudes traces in gray. Low GR values corresponding to the reservoir sands are shown in yellow, intermediate GR values of the non-reservoir finer deposits in brown and the high GR shales in green. Also shown are the GR logs of the four wells that penetrate the section. **b.** Vertical transect B-B' through the amplitude volume with the units interpreted in this study. Two of the four wells that penetrate the location have cores that sample these deposits; details of the cores are shown in Figure 13.

**Figure 19.** Four data slices through the GR volume show the distribution of the predicted lithologies through time. Low GR (reservoir sands) values are shown in yellow, intermediate GR (non-reservoir deposits) values in brown and the high GR (reservoir regional seal) in green. The outline of the incisions is superimposed onto the GR time-slices to show the type of sediment that is predicted to have filled them.

**Figure 20. A.** Vertical GR and corresponding seismic amplitude transect F-F' displaying the distribution of lithologies within the units. Note Well 07-33 located within a sinkhole generated by collapse of the Duperow carbonates. Note towards

the west in unit W the mud (green) filled incision that corresponds to the SW-NE feature on the plan-view images. B. Vertical GR and corresponding seismic amplitude transect G-G' that show the location where the SW-NE incision coincides with another sinkhole in the area. Location of the vertical transects is shown in Figure 4.

**Figure 21.** A summary diagram showing the stratigraphy and distribution of reservoir facies. The complex stratigraphy was unraveled and lithologies were predicted with the integration of seismic and borehole data.

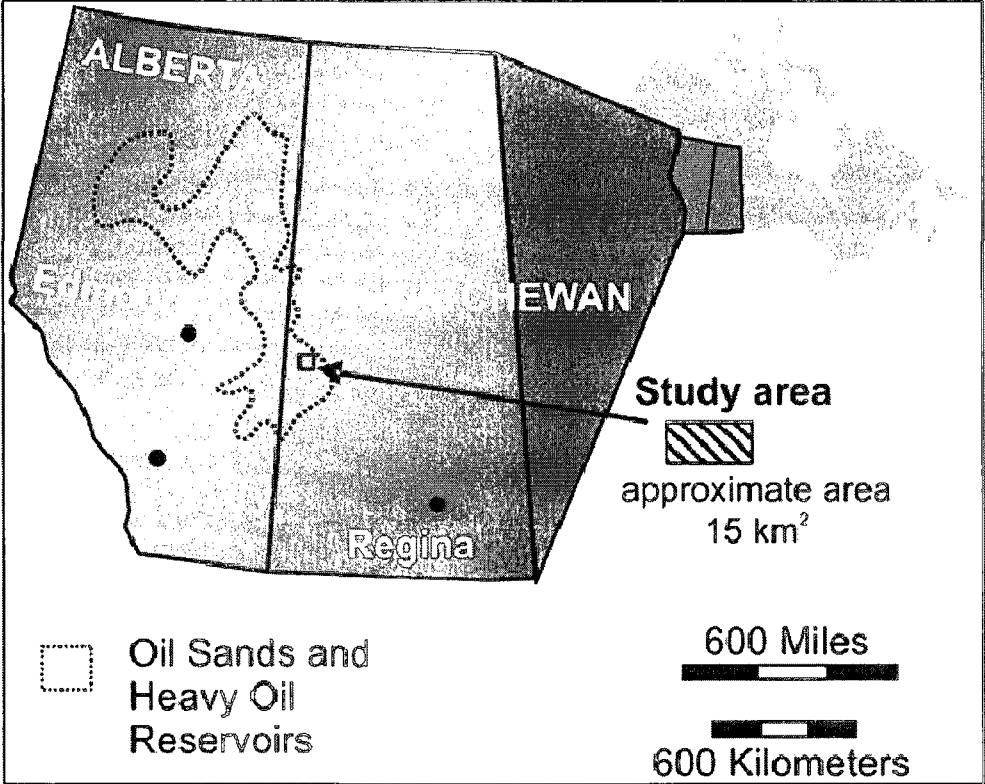


Fig 1

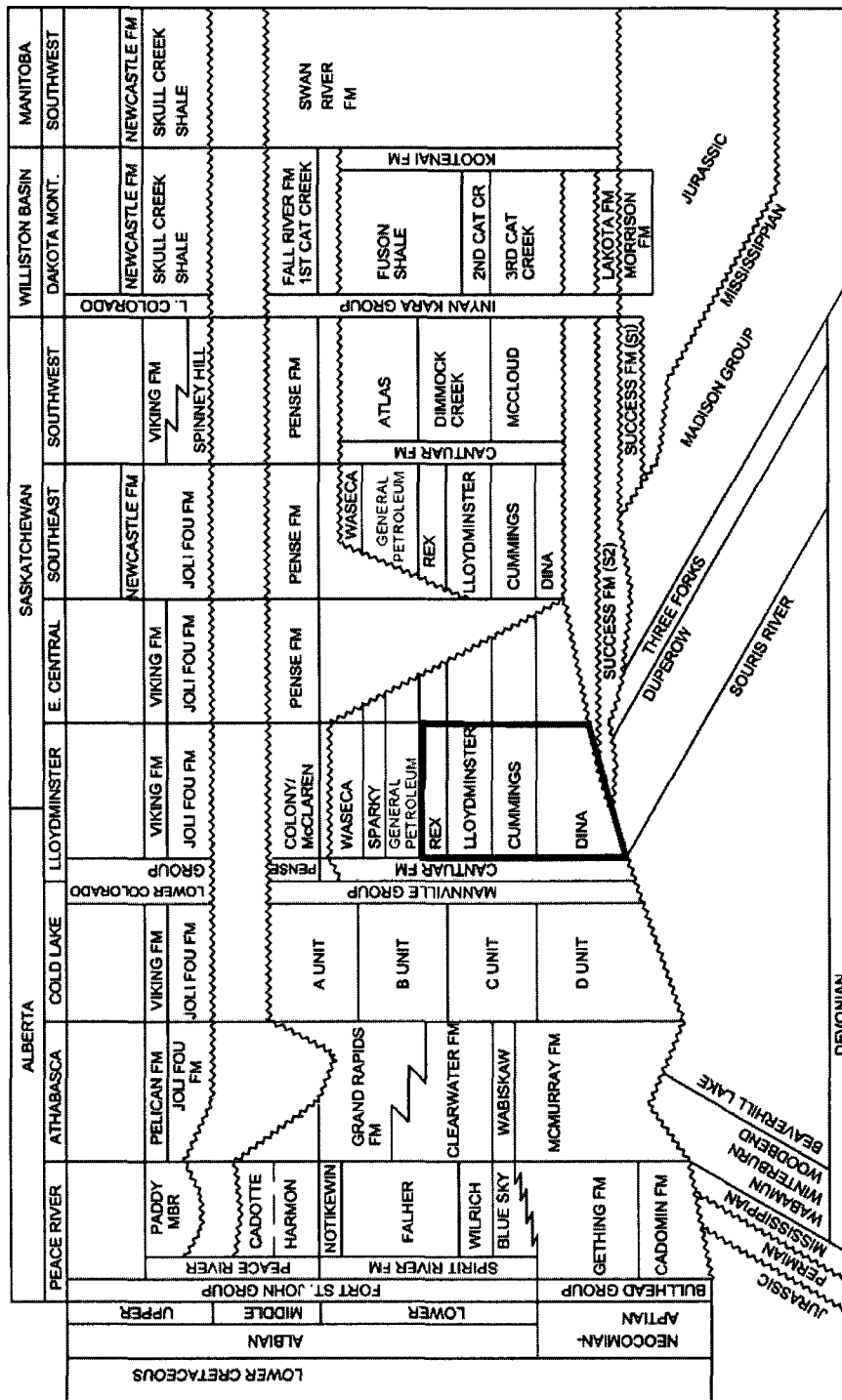


Fig 2

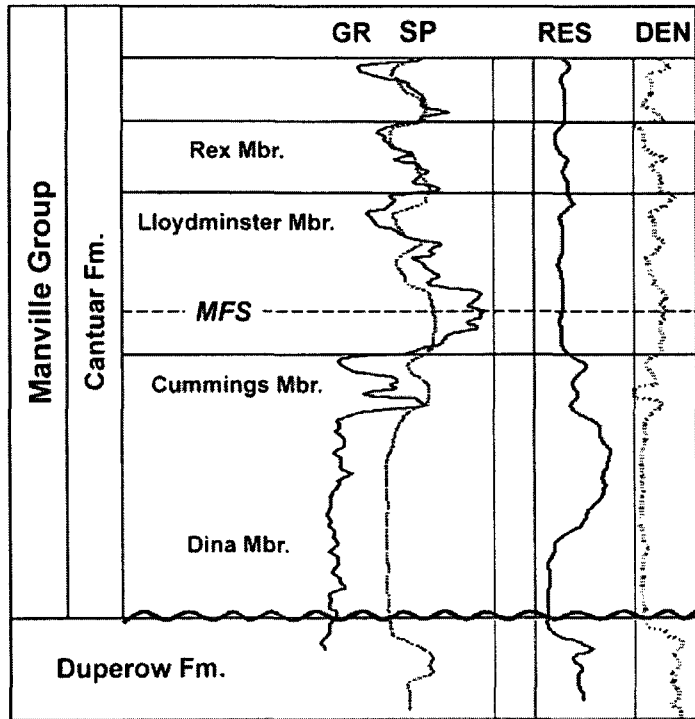


Fig 3

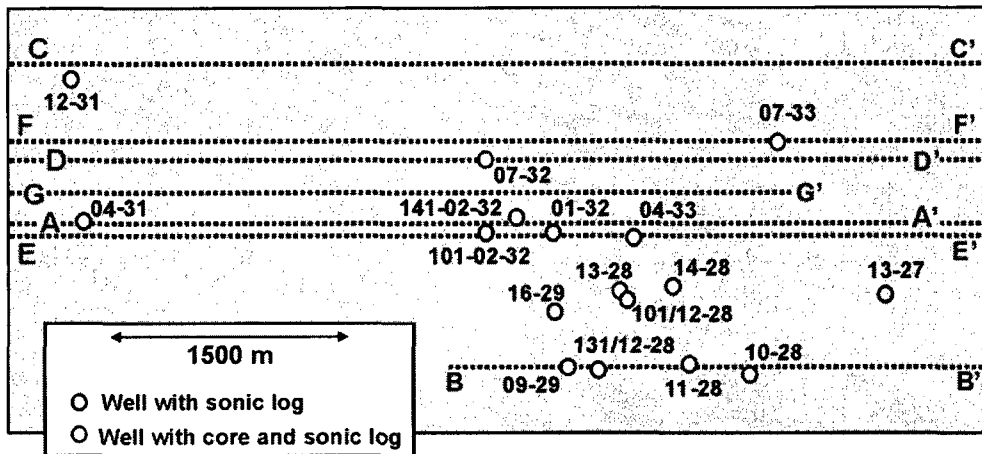


Fig 4

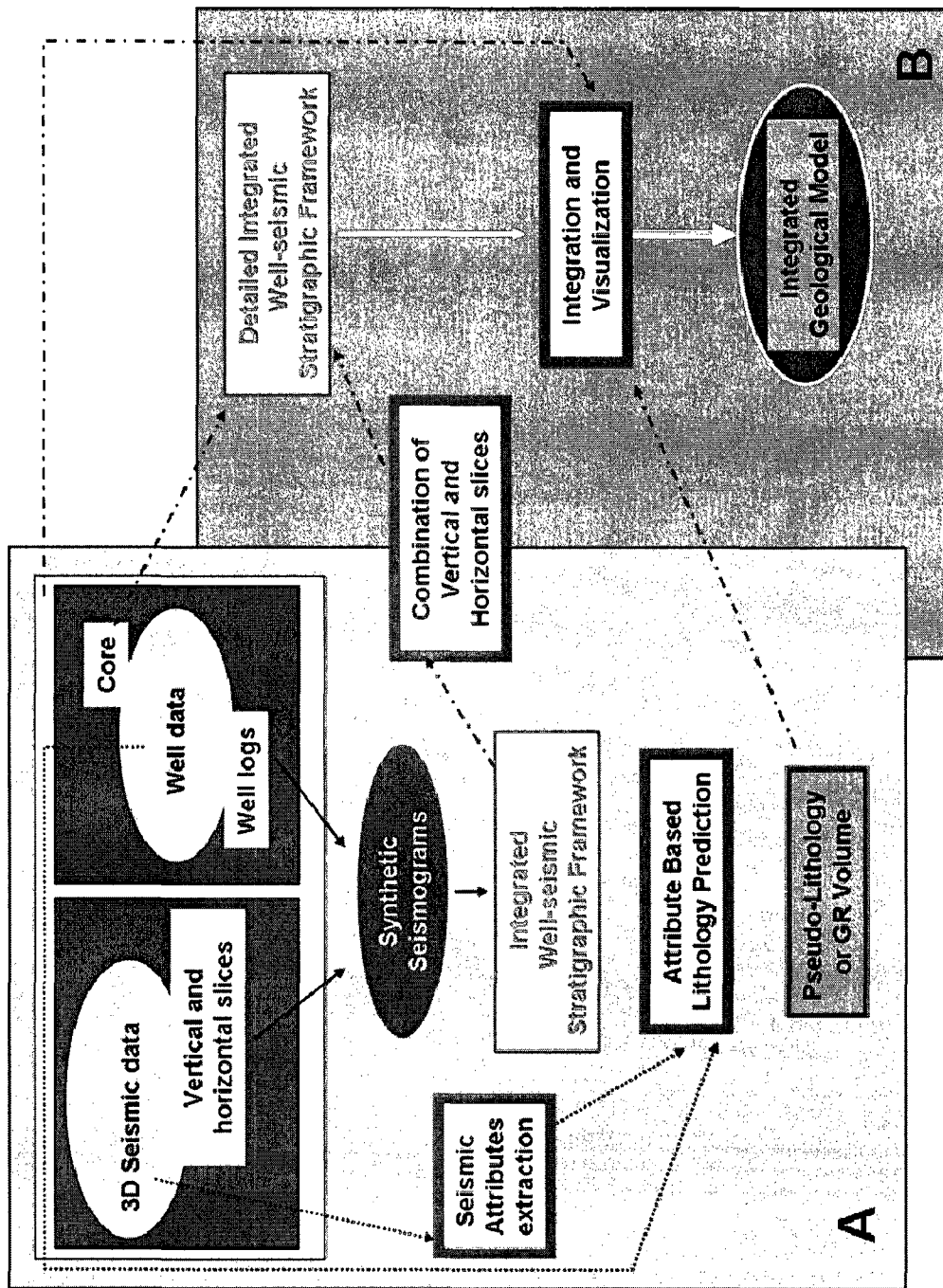


Fig 5

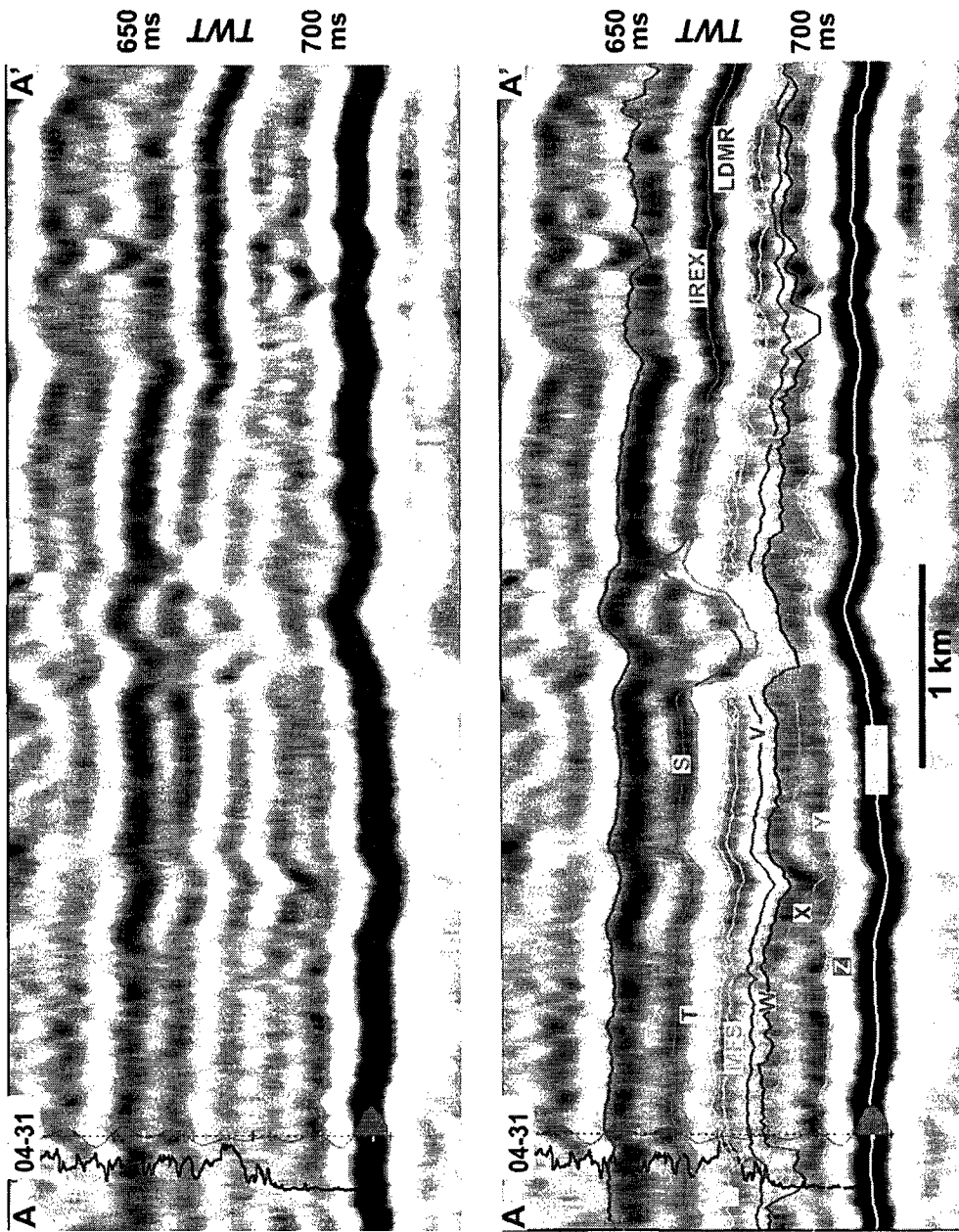


Fig 6

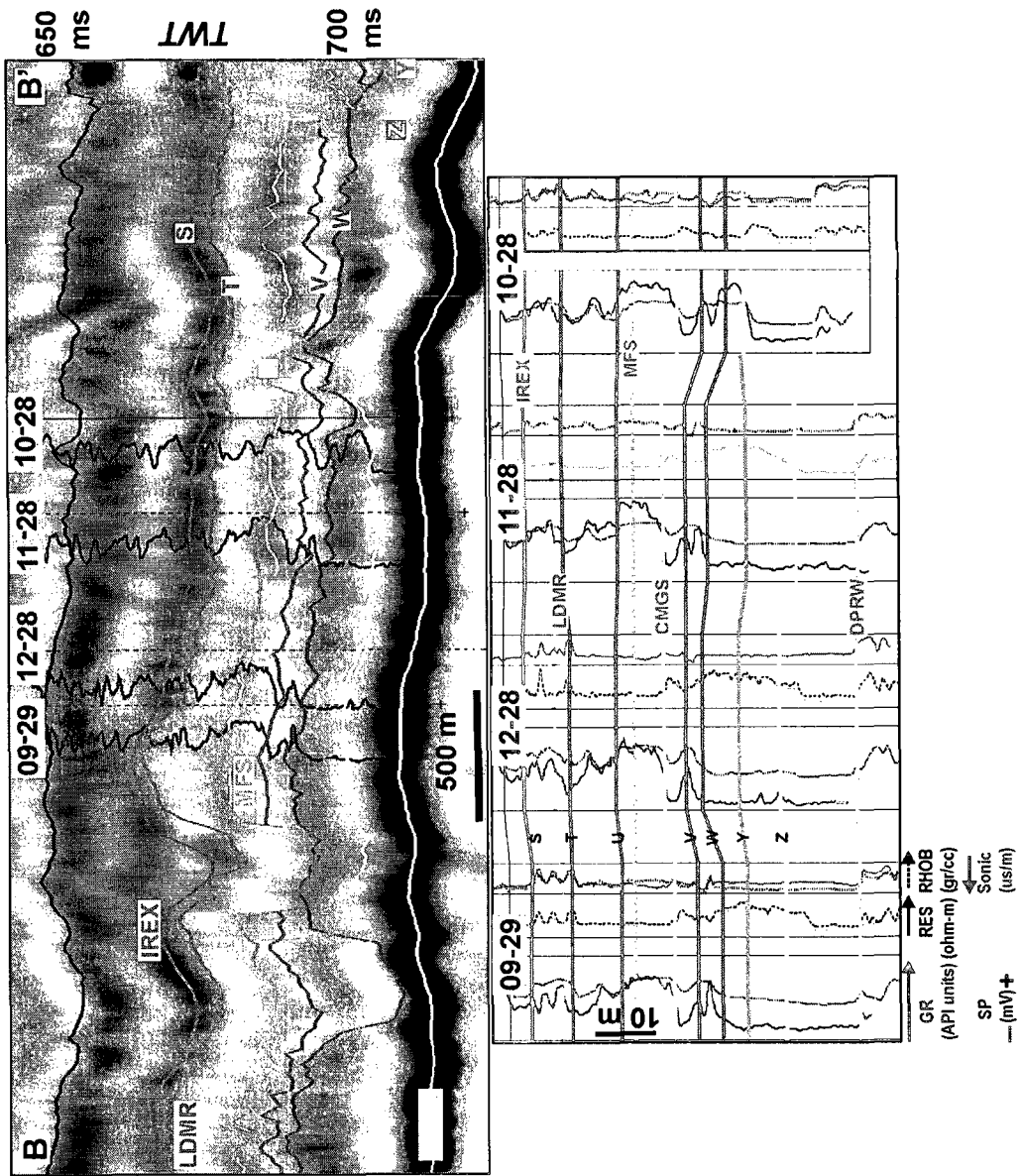


Fig 7

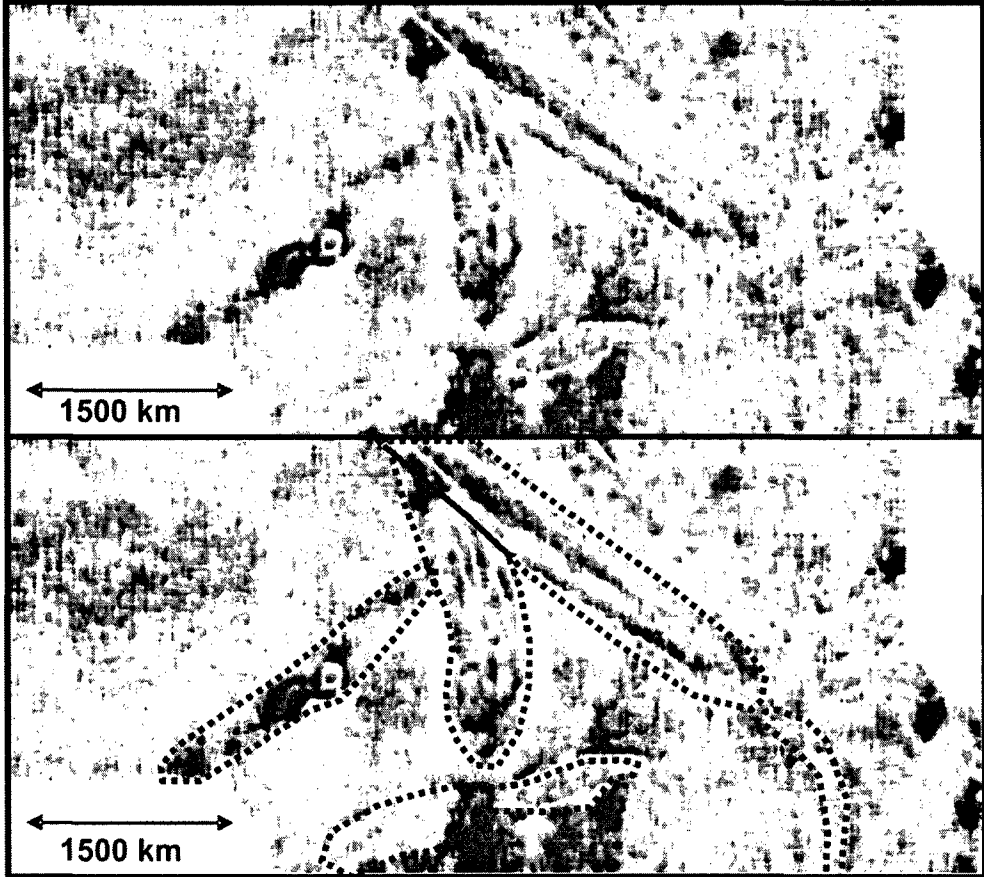


Fig 8

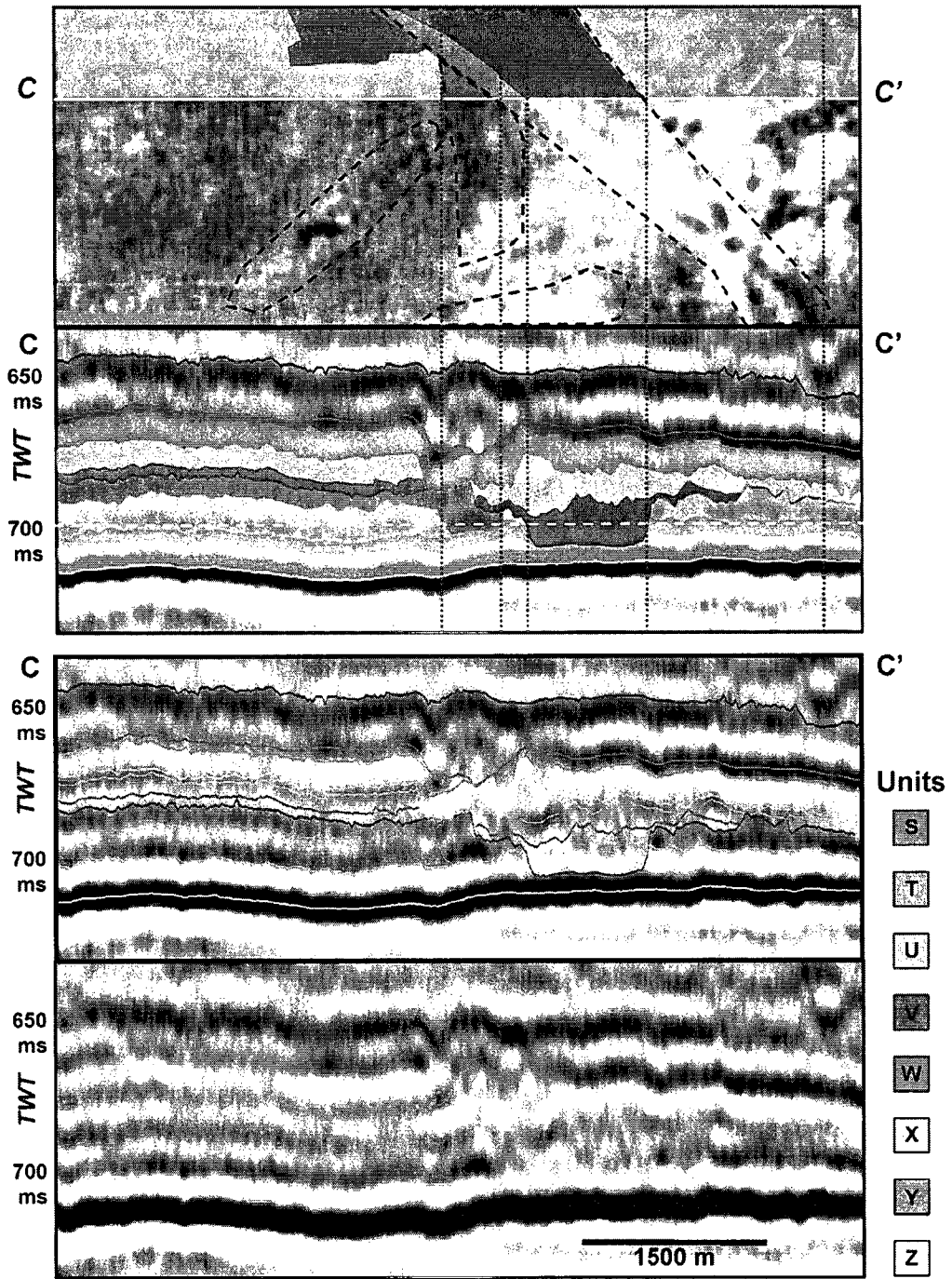


Fig 9

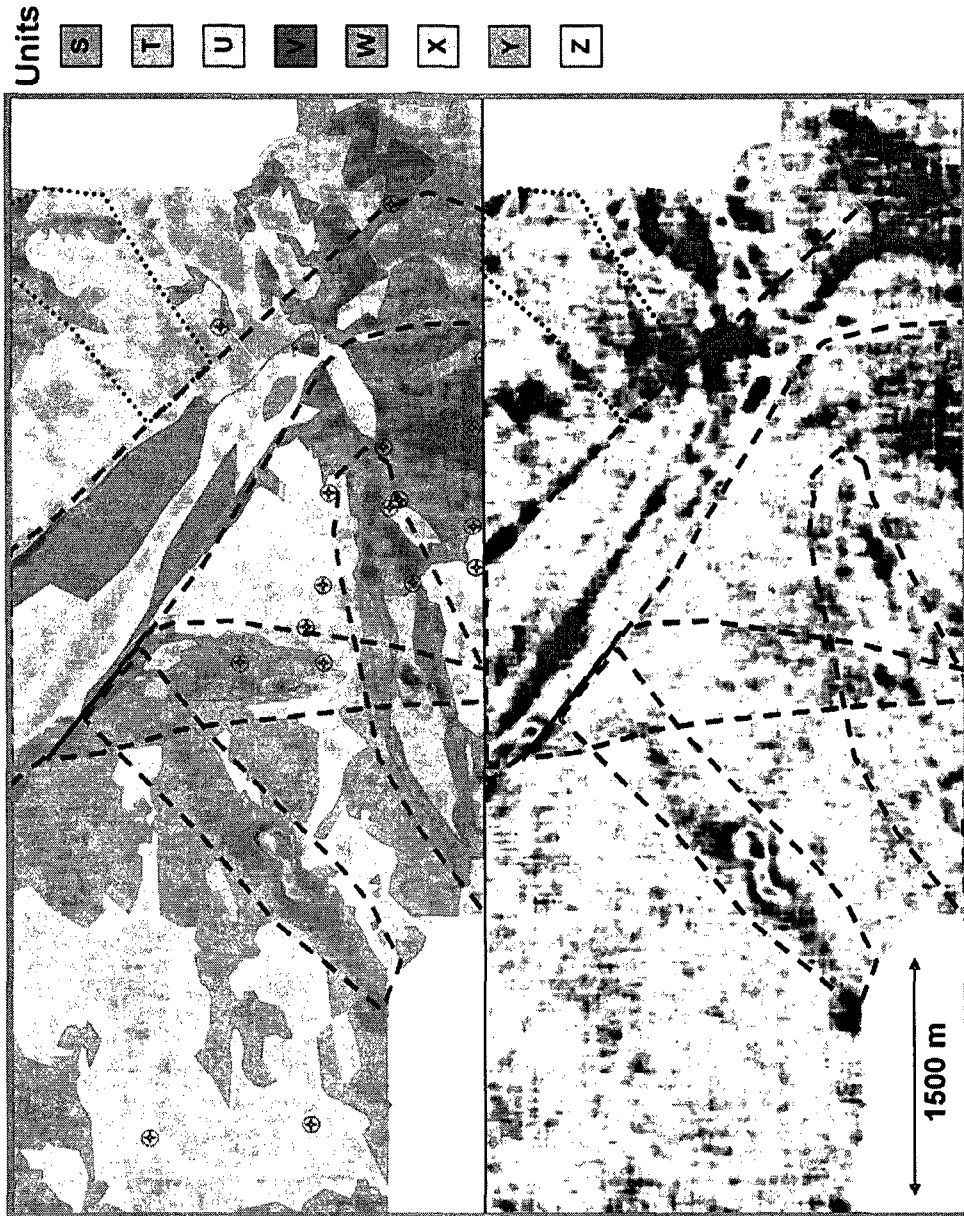


Fig 10

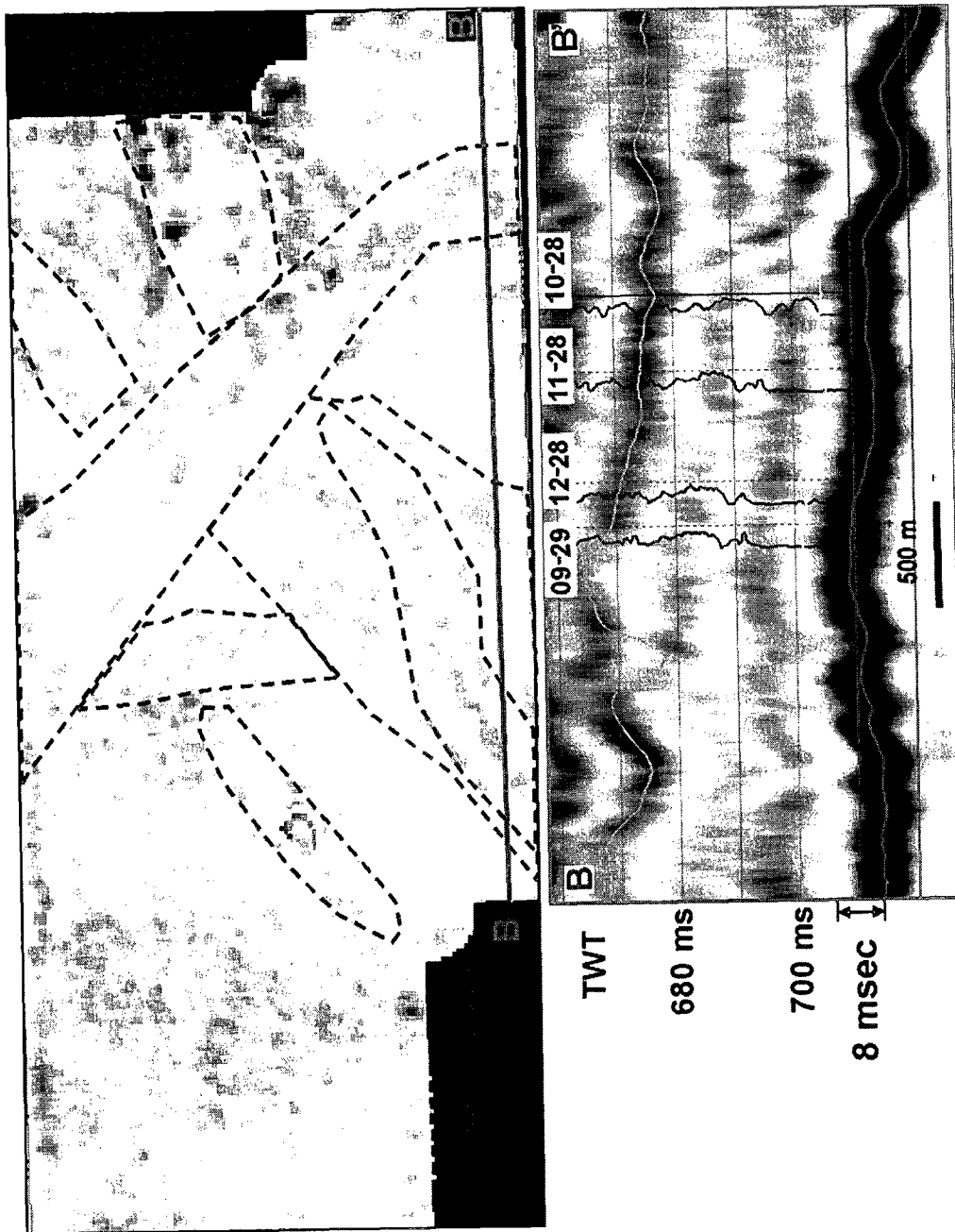


Fig 11

### Lithofacies Legend

#### Facies 1- Sands

- 1a  Cross-stratified sands
- 1b  Parallel laminated to rippled sands
- 1c  Parallel laminated or bedded sands
- 1d  Structureless sands
- 1e  Moderately Bioturbated sands
- 1f  Sands with concretions
- 1g  Mud-clast breccia
- 1h  Calcite cemented sands

#### Facies 2- Heterolithic

- 2a  Fining upwards sequence of muds, silts and sands
- 2b  Slumped sands, silty mudstones and sandy siltstones
- 2c  Inclined interbedded mudstones and rippled to crossbedded sands
- 2d  Coarsening upwards sequence of mudstones and silty sands
- 2e  Interbedded sandy siltstones and silty mudstones

- 2f  Laminated silty mudstone
- 2g  Burrowed sandy siltstone
- 2h  Rippled silty mudstone

#### Facies 3- Mudstones and silts

- 3a  Dark grey mudstone
- 3b  Light grey mudstone
- 3c  Dark grey burrowed mudstone
- 3d  Light grey burrowed mudstone
- 3e  Siltstone

#### Facies 4- Coal, Coaly mudstone and siltstone

- 4a  Coal
- 4b  Coaly mudstone
- 4c  Coaly and/or rooted siltstone

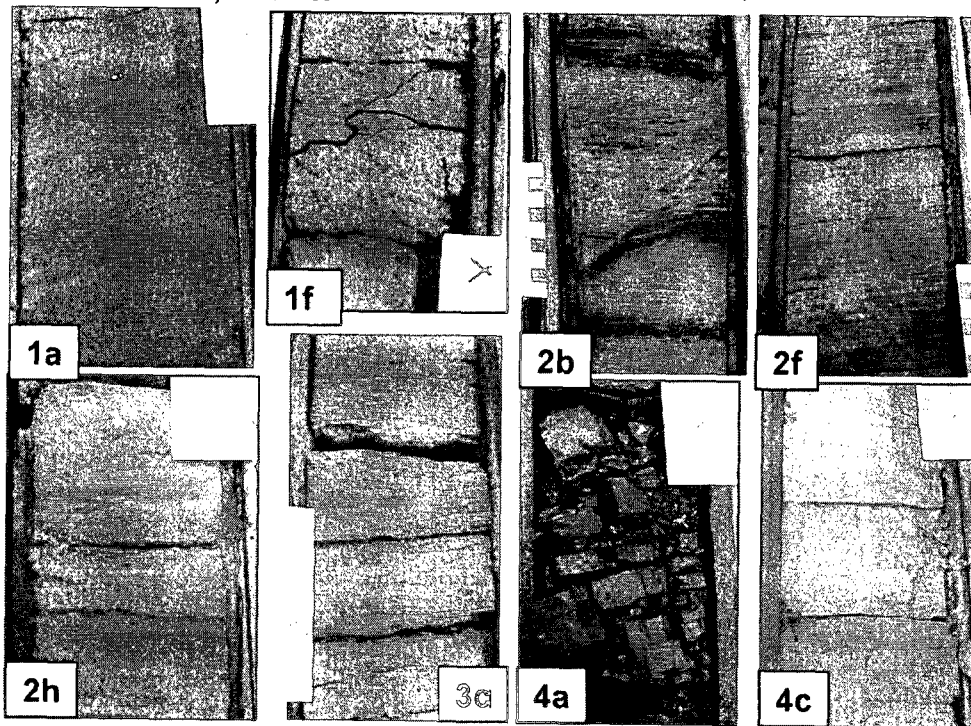


Fig 12

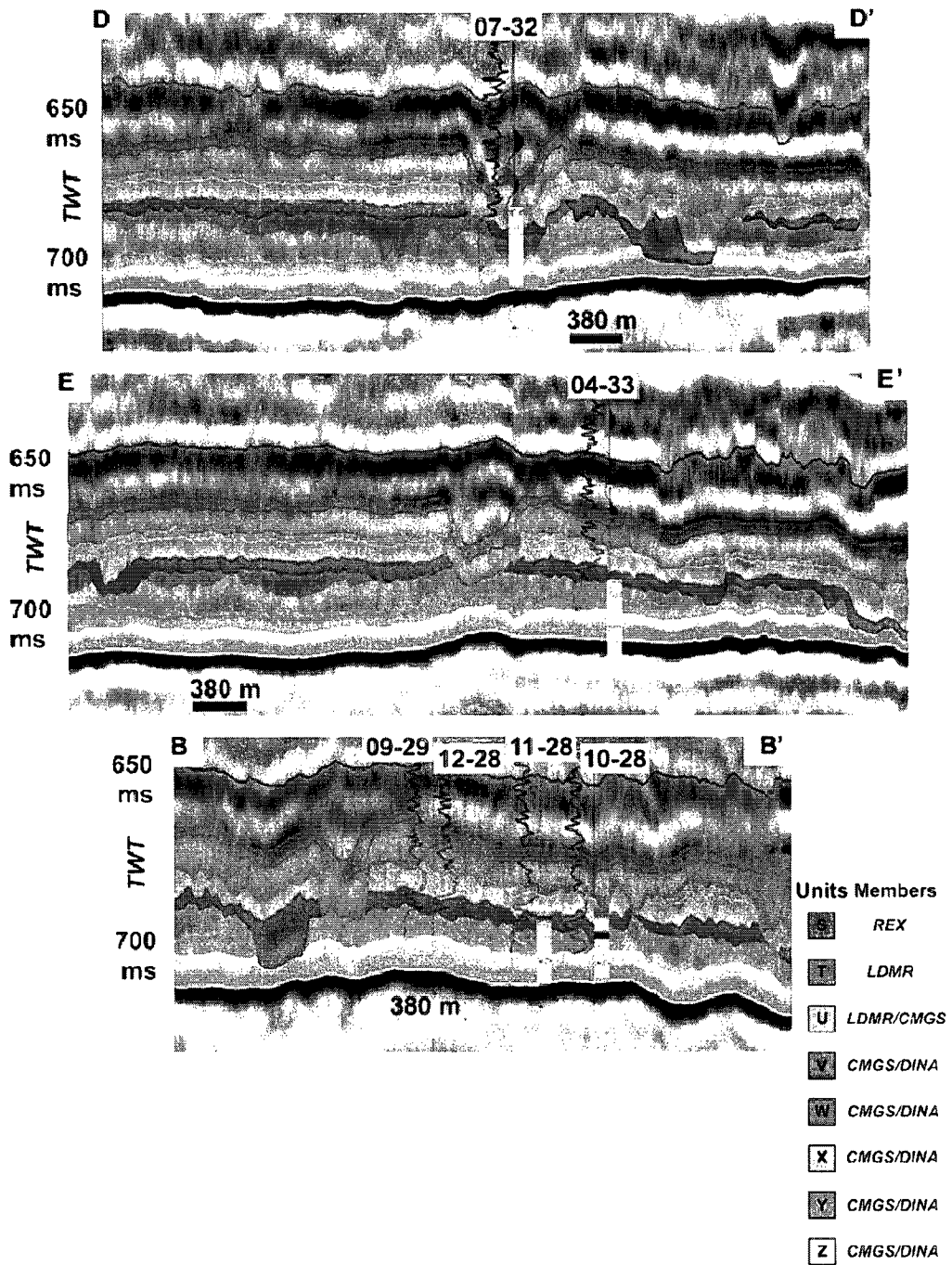


Fig 13

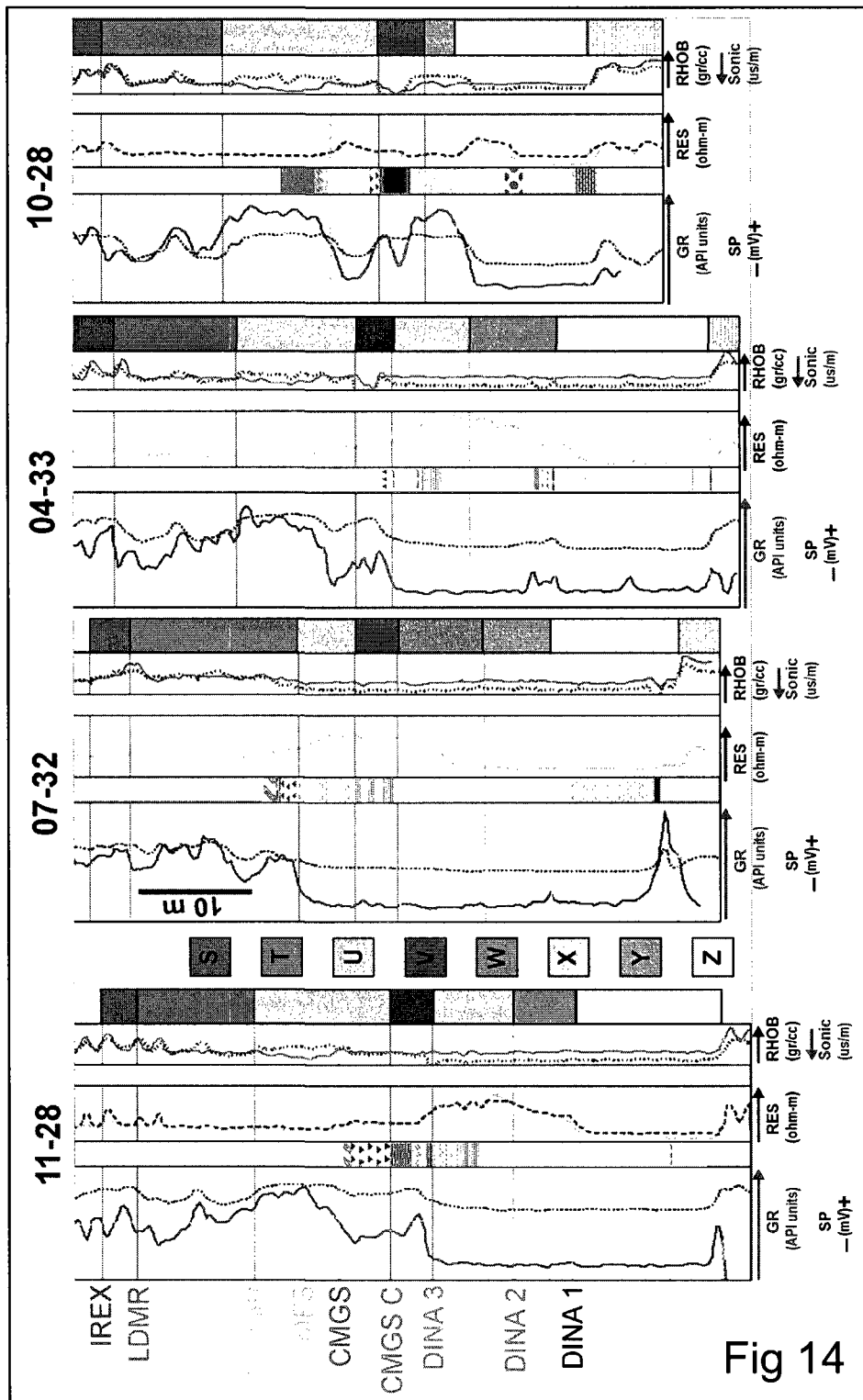


Fig 14

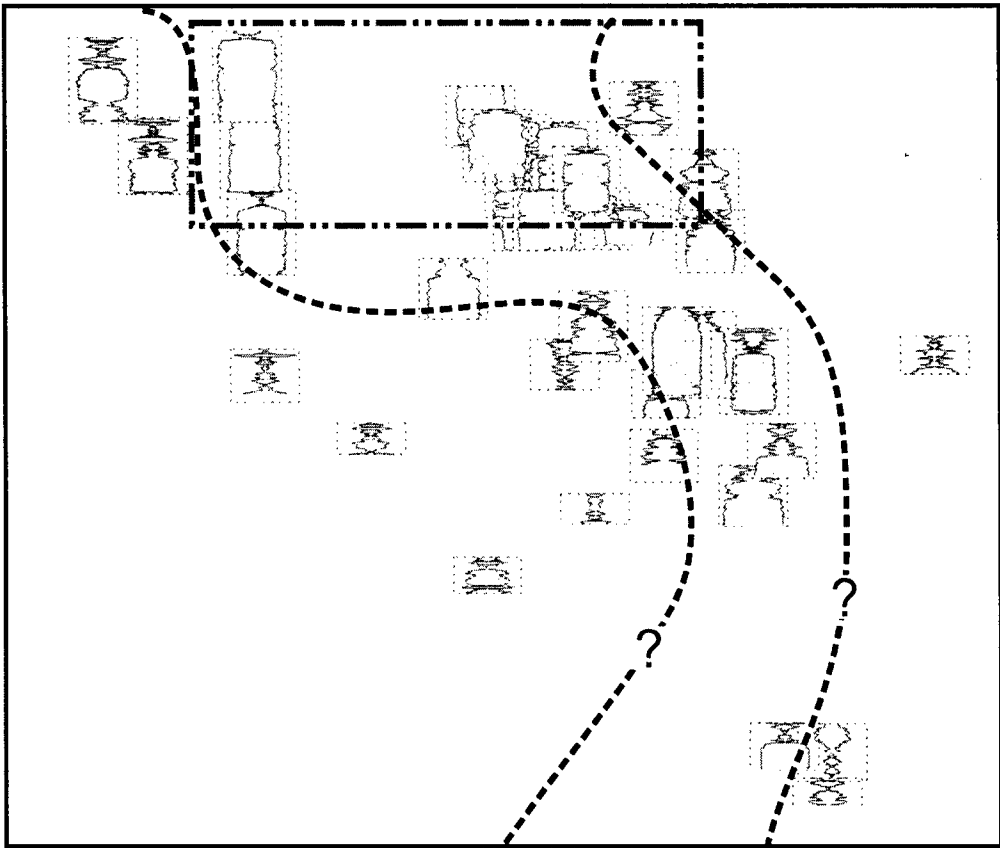


Fig 15

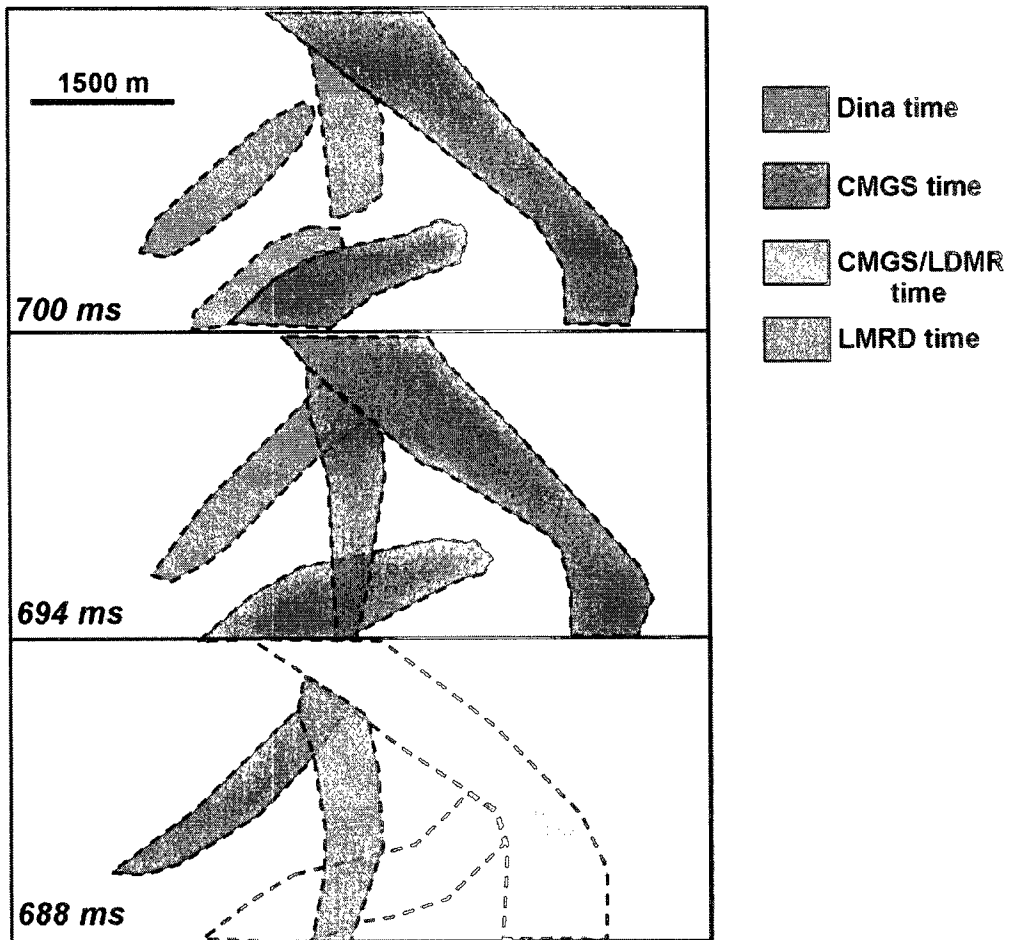


Fig 16

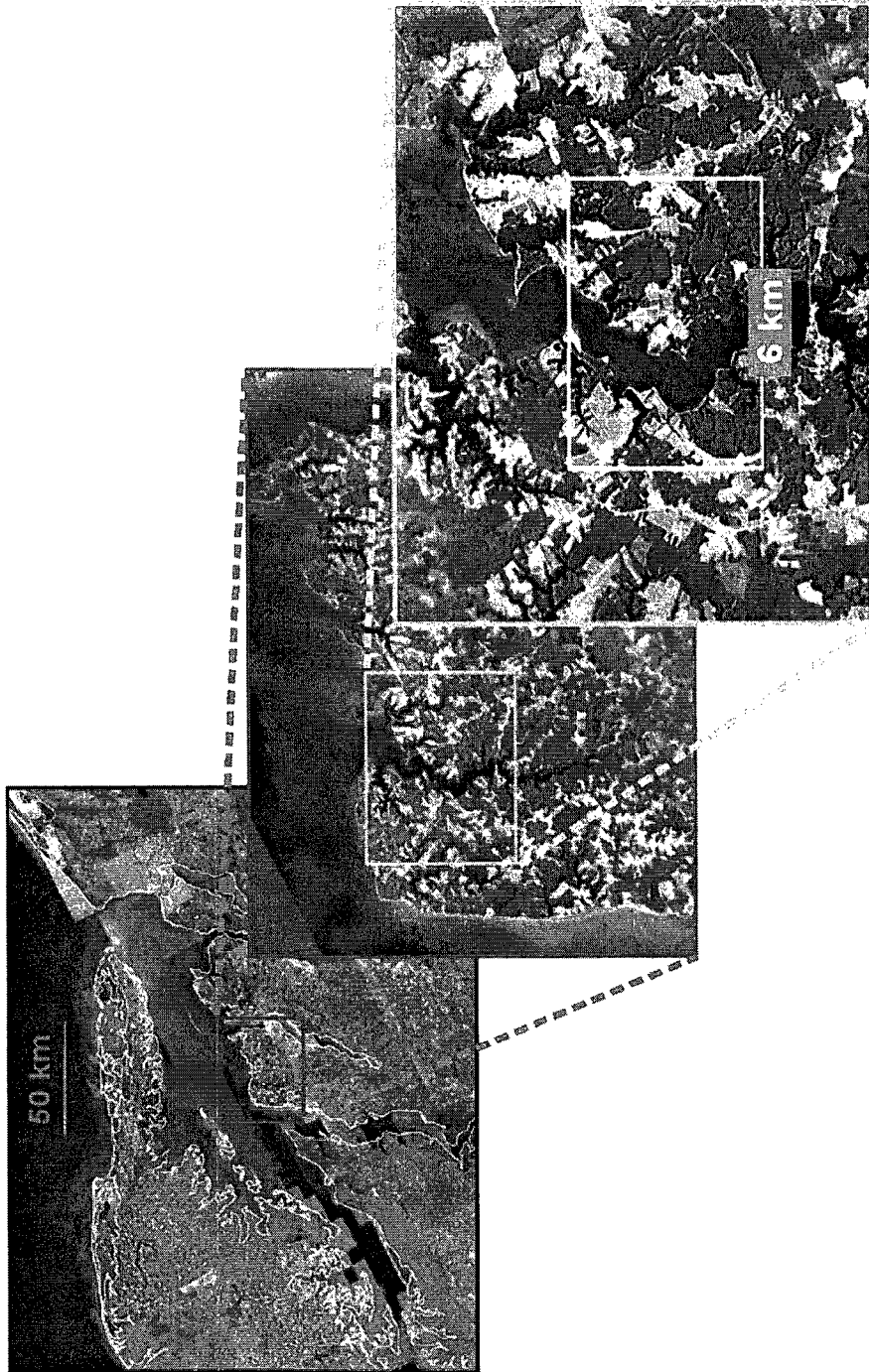


Fig 17

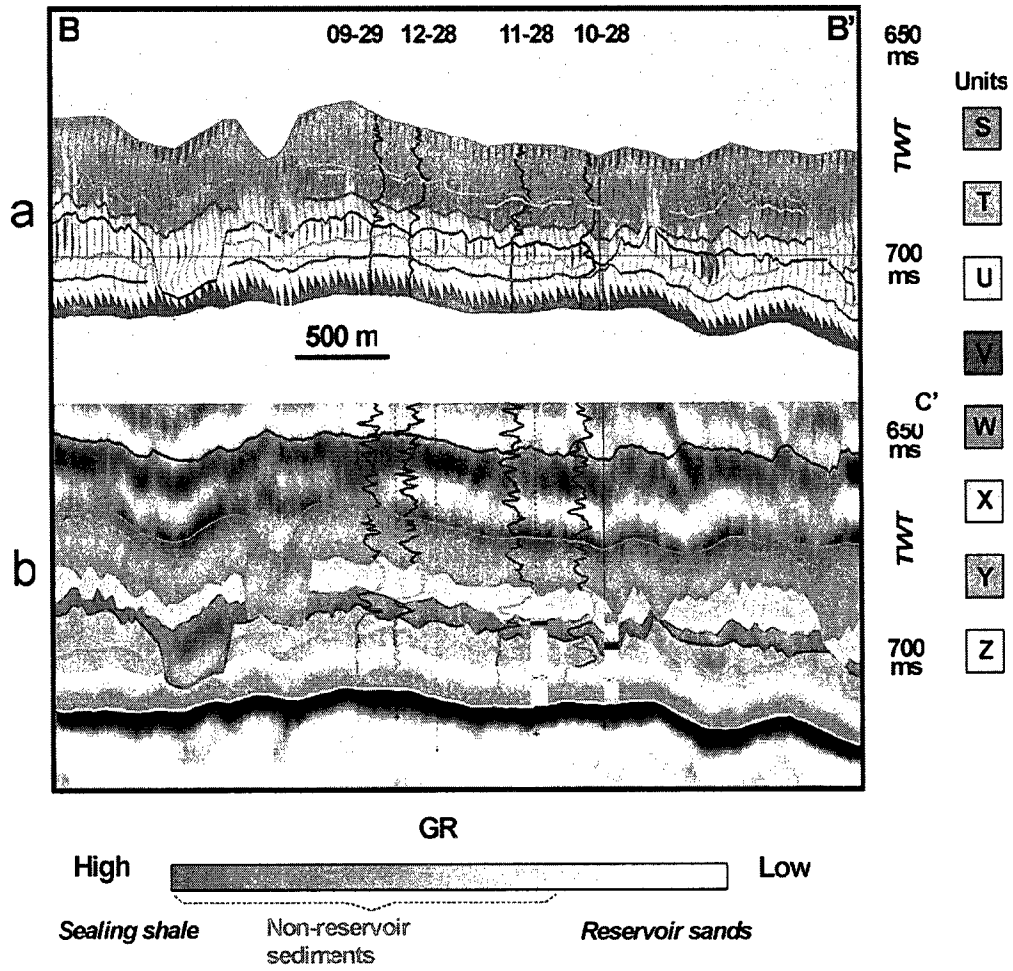
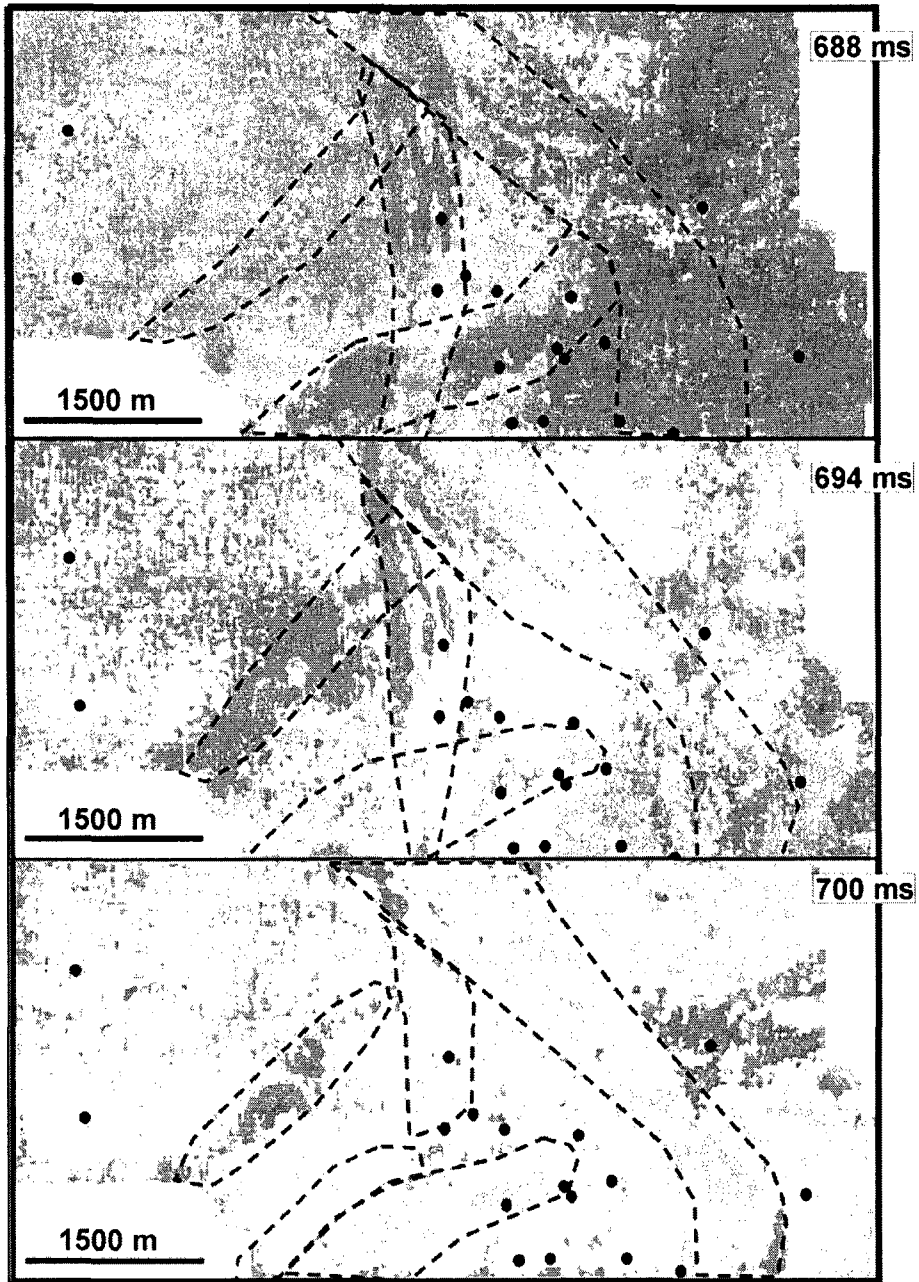


Fig 18



GR

High  Low

*Sealing shale*

*Non-reservoir  
sediments*

*Reservoir sands*

Fig 19

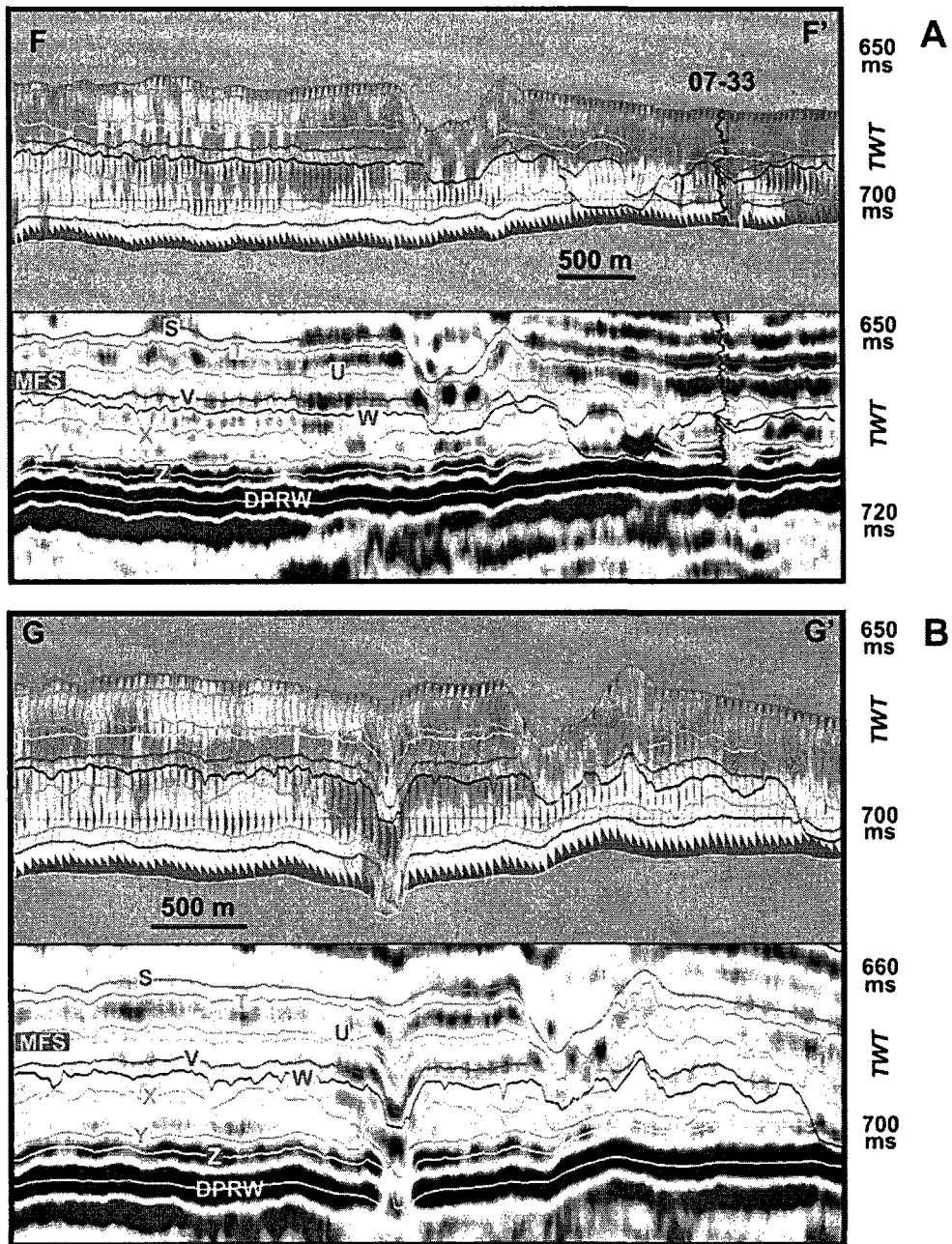


Fig 20

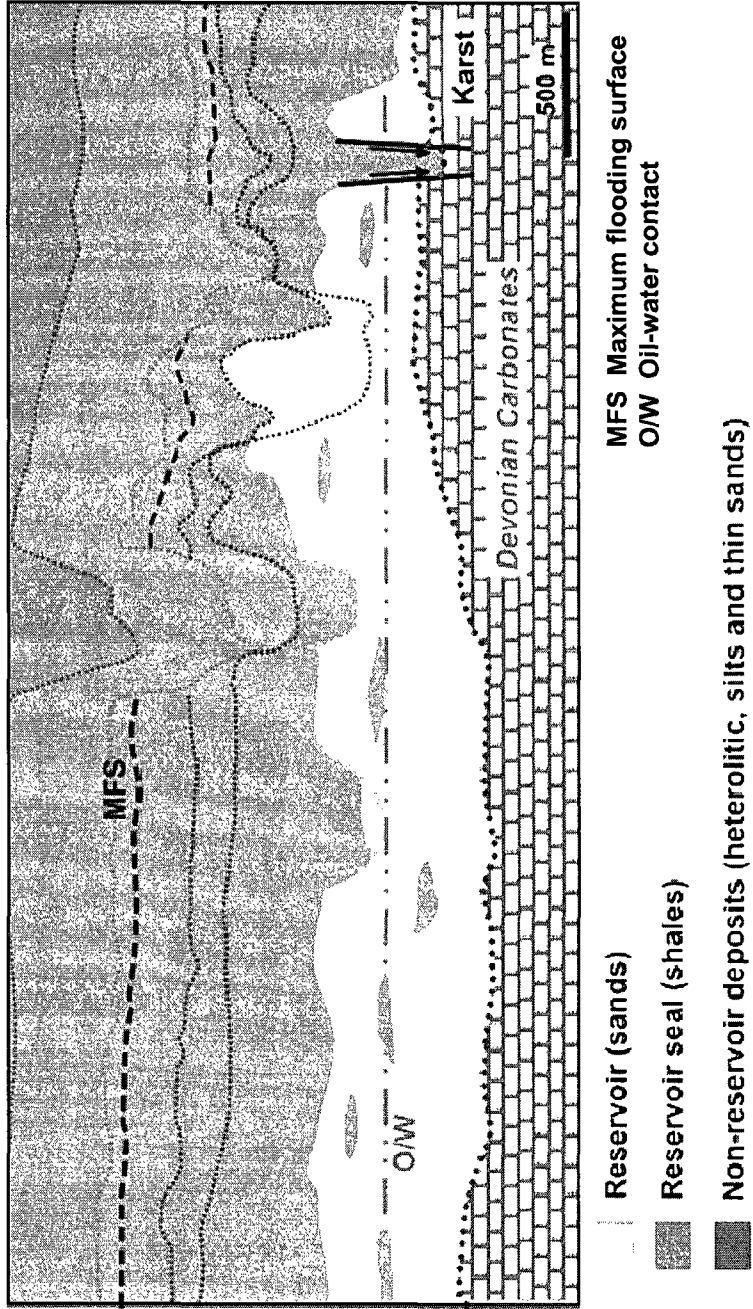


Fig 21

## **5- Conclusions and Recommendations**

This thesis demonstrates that the integration of 3-D seismic and well-log data proved to be an excellent tool to display and interpret the complex stratigraphy of the Mannville Group in several regions of Saskatchewan. Seismic stratigraphy, seismic geomorphology, lithofacies analysis, attribute analysis, including multiattribute analysis and neural network training were all used to generate the models presented in this study. The ability to visualize the 3-D seismic data in a variety of ways, including arbitrary lines and stratal or horizon slicing techniques helped us to define stratigraphic features that would affect fluid flow in hydrocarbon-producing areas. Seismic and well-log data were integrated to generate a GR (pseudo-lithology) volume that seeks to capture the distribution of reservoir and non-reservoir deposits in the study area. The integration of this detailed stratigraphic interpretation with the attribute-based lithological prediction was crucial to proposing a depositional setting and depositional history in order to generate a coherent geological model of the area.

In the first study (Chapter 2), we recognized and mapped unconformities and flooding surfaces in the Mannville Group and adjacent stratigraphic units. Definition of these surfaces allowed us to divide the Mannville into three stratigraphic units, with the S2 Member of the Success Formation forming a fourth unit. Seismic facies from the vertical displays (traces and arbitrary lines) were combined with seismic geomorphology analysis of features seen in the horizontal slices (time slices and stratal slices) and log facies to interpret

depositional features. The channels, point bars, unconformities and other stratigraphic features identified in this study can affect the distribution and movement of fluids in the subsurface. Detecting and mapping similar features is especially important in heavy oil areas where enhanced recovery techniques are employed to stimulate production from the Mannville. Although the primary goal of this study was to focus on reservoir-scale definition of stratigraphic features, our results have significance for the stratigraphy of the Mannville Group in this area. The surfaces and units we defined using our integrated dataset do not correspond exactly to those defined through regional mapping. Although it is possible that seismic-resolution problems prevent us from identifying and mapping existing stratigraphic units, it is also possible that the stratigraphic framework of the Mannville in this area needs to be revisited.

The second study (Chapter 3) shows how seismic attributes were used to predict the lithology distribution in the study area, a portion of the Winter Field in west-central Saskatchewan. The multiattribute neural network study generated a GR (pseudo-lithology) volume. Stepwise linear regression and validation testing indicated that a combination of three attributes, integrated trace, apparent polarity and a band pass filter of 25/30-35/40, would best predict lithology from the seismic data. The use of a neural networks, rather than multivariate linear regression, resulted in an improved lithology prediction for the area. The physical relationship between the attributes (selected using stepwise linear regression) and the lithology was found but was not considered strong. We can conclude that, at least in this study, it is the mathematical combination of attributes and not their physical relationship with the searched property that is responsible of the resulting

GR prediction. This conclusion is based on examination of the 3-D volumes of the three attributes (Integrate, Apparent polarity and Filter 25/30-35/40) and an empirical analysis of their combination. The neural network transform was applied to the seismic volume to generate a geologically reasonable GR (pseudo-lithology) volume. Combination of the GR, seismic amplitude and semblance volumes allows assigning lithologies to stratigraphic features (e.g., fluvial channels) and a more confident interpretation of the architecture of the reservoir. We also concluded that the resultant GR (pseudo-lithology) volume, which predicts the distribution of lithologies away from the well control, does not resolve small features (e.g., shale partings) but can be used to interpret distribution and configuration of larger features (e.g., channel incisions) within the reservoir. A detailed correlation of both seismic data and well logs integrated with core information is necessary at this stage to combine with the GR volume in order to generate a robust stratigraphic model of the area and understand the reservoir behavior.

In the third paper (Chapter 4) a geological model of part of the Winter Field in west-central Saskatchewan was generated through the integration of the geological data (well logs and cores) and geophysical data (amplitude and gamma-ray volumes). A particular way of interpreting the combined vertical and planar views of the seismic amplitude volume was used to generate a detailed stratigraphic correlation of the study area. Several stratigraphic units were defined in this study and correlated throughout the area. Lithology was assigned to these units using borehole and core information together with the attribute-based lithology prediction. According to my interpretation, the base of the reservoir was

deposited by fluvial processes and formed part of a large system that could not be completely imaged due to survey size limitations. We were able to describe the depositional history of the deposits by analysis of the seismic images and integrating them with the lithology prediction and the lithofacies interpretation. An overall transgression occurs from the bottom to the top of the reservoir and all the way to the shales containing the maximum flooding surface, which constitutes a regional seal. Some surfaces have regional sequence stratigraphic significance, such as the DPRW (Sequence Boundary) and the MFS, while others are local erosional surfaces tied to autocyclic processes.

The complex interpretation done in these studies would have been difficult to achieve using only vertical transects without the planar views and even more so with the sole use of well logs. The incorporation of borehole information and lithology prediction to the seismic interpretation tells us that some of the incisions were filled with sands at the bottom and non-reservoir deposits towards the top, and some were filled only with fine-grained sediments. These incisions filled with impermeable deposits do not constitute barriers in this area because of their relatively small vertical and lateral extent. Unfortunately, the location of other possible reservoir barriers, such as thin shale partings within the sandy packages, was beyond the resolution of the seismic data in this study. Integration of all the available information resulted in a comprehensive geological model for the area and contributed to the knowledge of the Lower Mannville stratigraphy and depositional history. Geoscientists working in any area with similar information can apply the methodology demonstrated in this study to generate their applicable geological model.

## Contributions to Knowledge

The following are the most significant contributions to knowledge from this thesis:

1. This study documents the most comprehensive investigation of the deposits of the Mannville Group in Saskatchewan by integrating seismic and borehole data.
2. This study presents a thorough discussion of the use of seismic attributes in predicting pseudo-lithology in the form of a gamma-ray volume.
3. This study presents an innovative methodology to unravel stratigraphy and demonstrates that only through the simultaneous detailed interpretation of vertical and horizontal slices can complex geology can be understood..
4. This study presents a methodology that can be applied by geoscientist working in any area with similar geological and geophysical information.

## **Future Research directions**

Test and improve the integrated geological model generated in this study by incorporating horizontal well lithological data. Determine true reservoir compartmentalization or areas that behave as independent reservoirs by including pressure and production data into the model.

Generate a static reservoir model that can be used for reservoir simulation by incorporating petrophysical data (porosity, permeability, water saturation etc.) to the geological model.

Extend the stratigraphic interpretation to the surrounding 3D surveys, including regional calibration, in order to generate a complete sequence stratigraphic model for the reservoir.

Use other geophysical techniques to predict lithology such as AVO in order to test and complement the interpretation done in this study.



**Appendix 1:**

Core Description

**Appendix 1**

**Core Descriptions  
Wells**

101/07-32-42-25W3

141/07-33-42-25W3

111/04-33-42-25W3

101/13-28-42-25W3

101/11-28-42-25W3

121/10-28-42-25W3

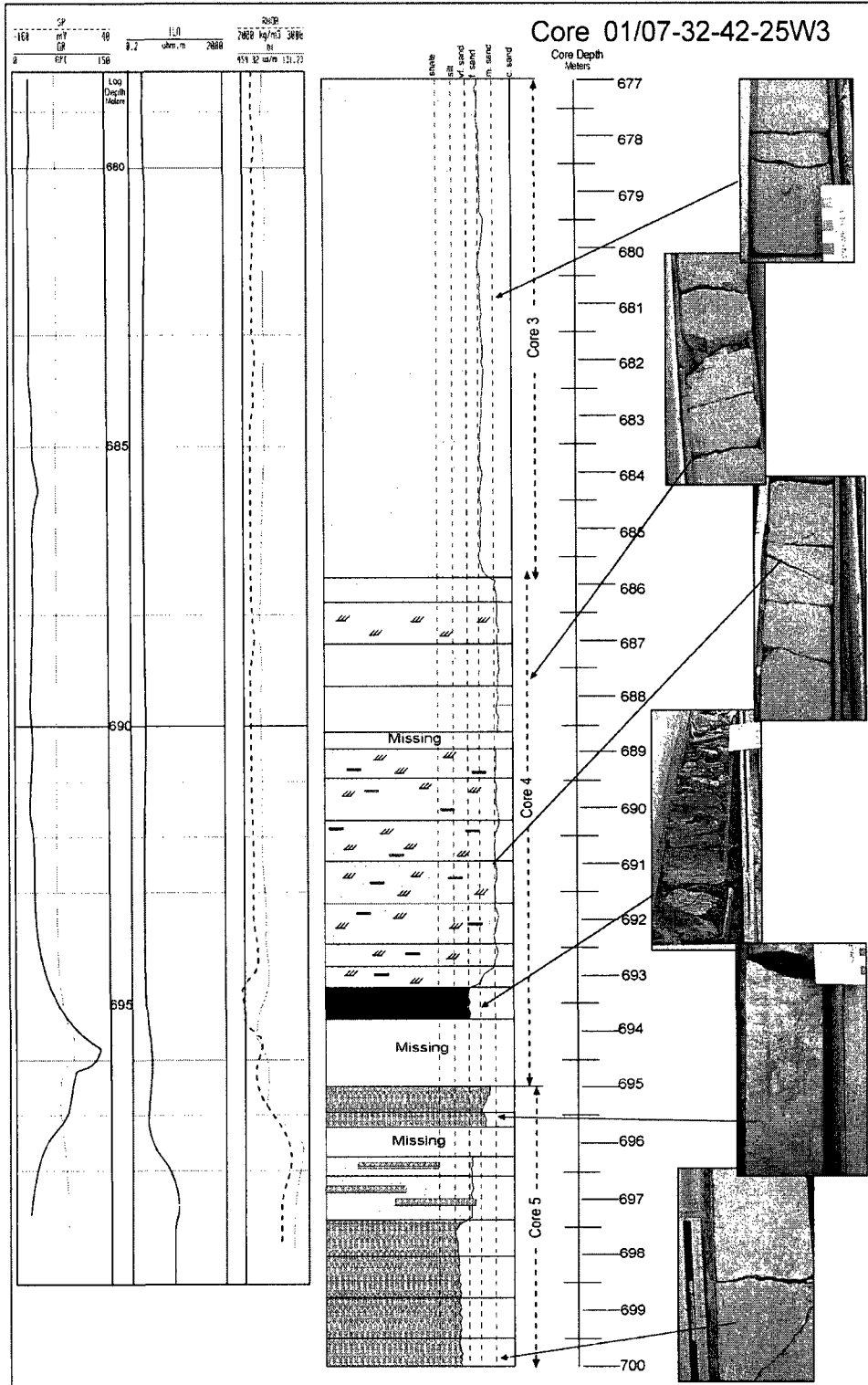
# Legends

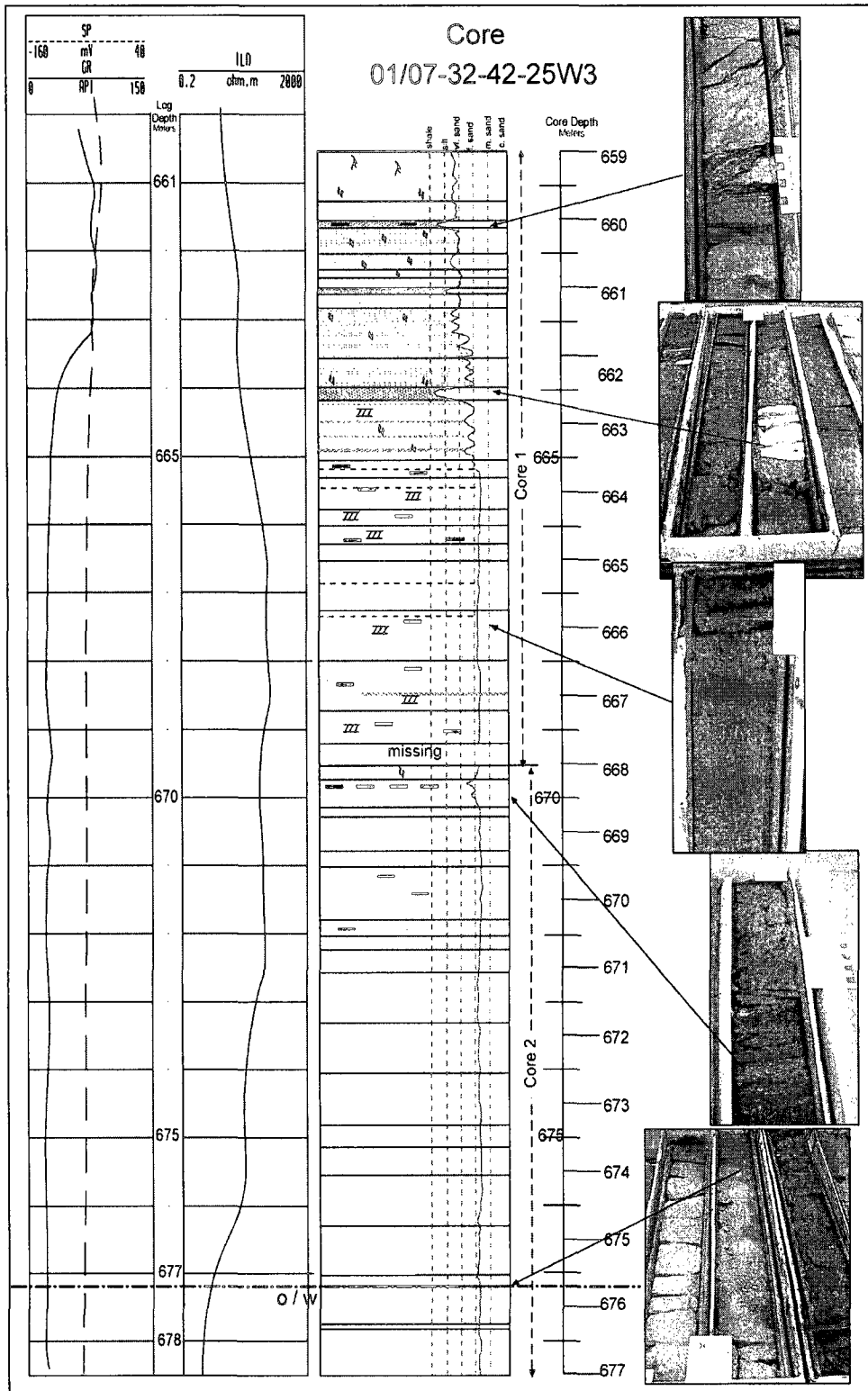
## Lithology

-  Silty shale
-  Silt
-  Silty sand
-  Sand
-  Sandy silt
-  Silty sand & sand
-  Silty shales & sands
-  Interbedded sands & silts
-  Interbedded sands & shales
-  Interbedded sands, shales & silts
-  Interbedded shales & silts
-  Interlaminated sands, shales & silts
-  Interlaminated shales & silts
-  Interlaminated sands & shales
-  Interlaminated sands & silts
-  Shale
-  Limestone
-  Carbonate Cemented sand
-  Marl
-  Coal

## Sedimentary structures

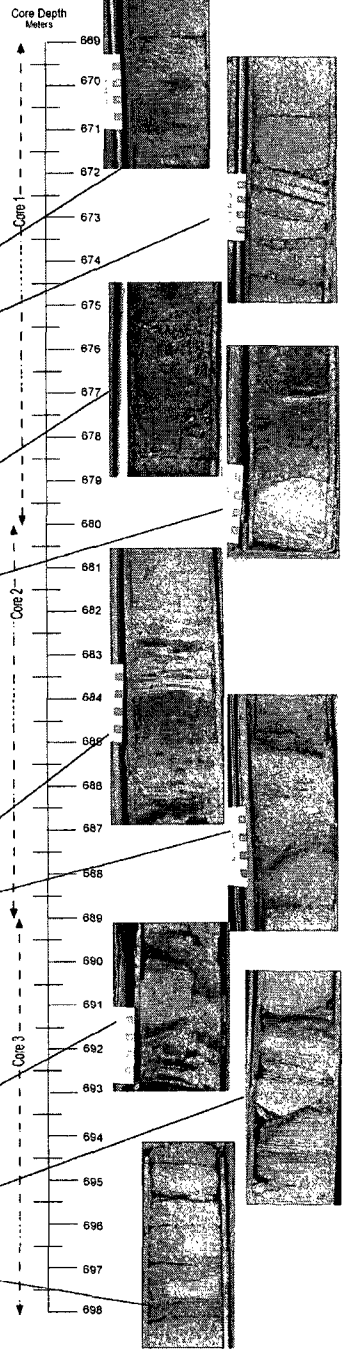
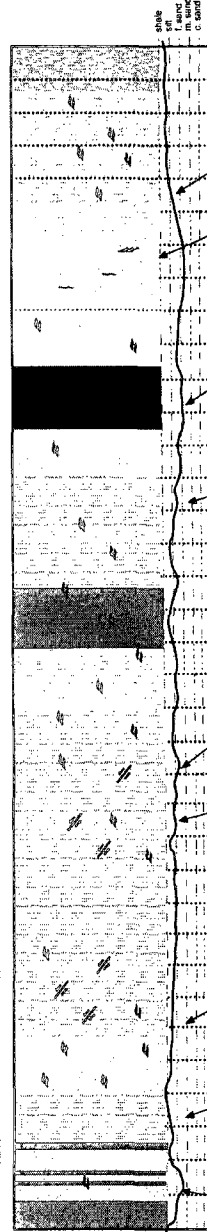
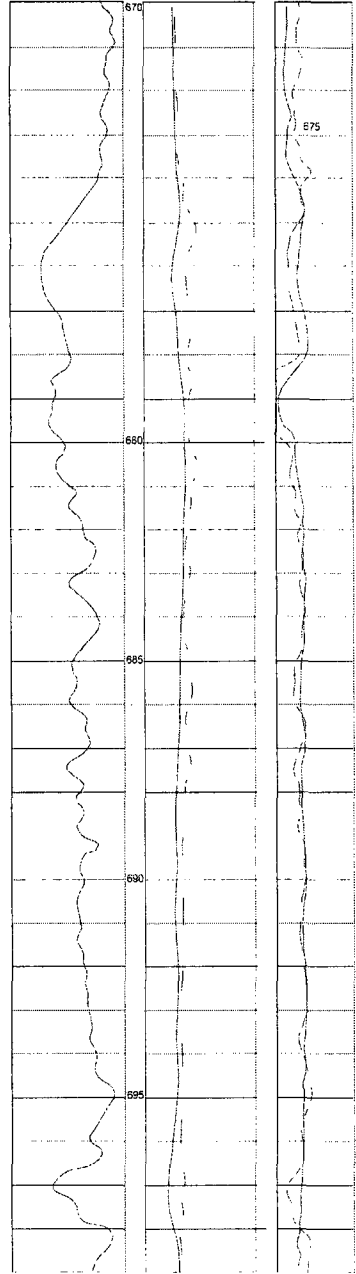
-  Planar bedding
-  Planar cross bedding
-  Wavy lamination
-  Trough cross bedding
-  Flaser
-  Ripples
-  Disturbed bedding
-  Climbing ripples
-  Pyrite
-  Bioturbation
-  Roots
-  Sand lenses
-  Carbonaceous material
-  Shale clasts
-  Carbonaceous lamination
-  Shale lamination
-  Oil/water contact





# Core 141/07-33-42-25W3

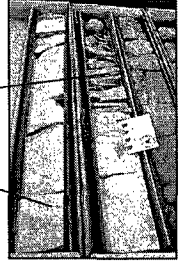
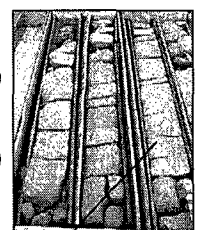
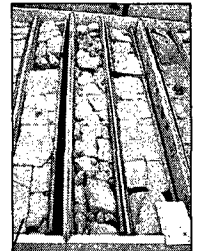
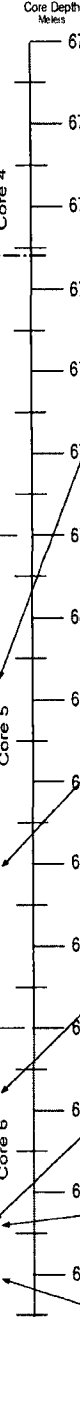
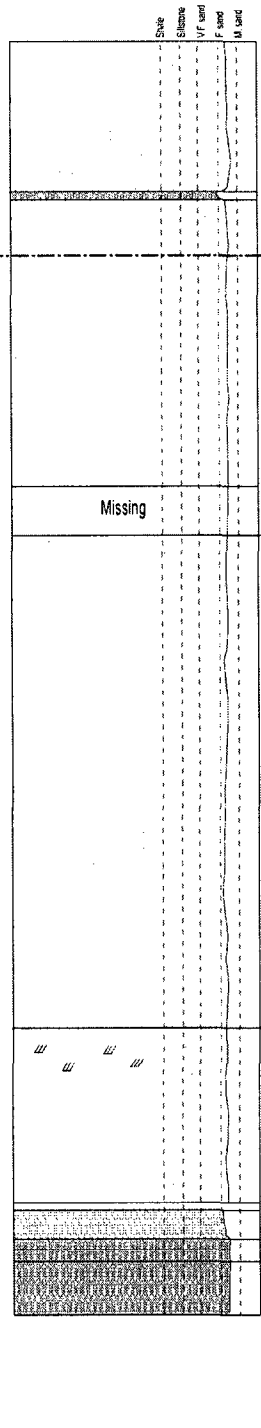
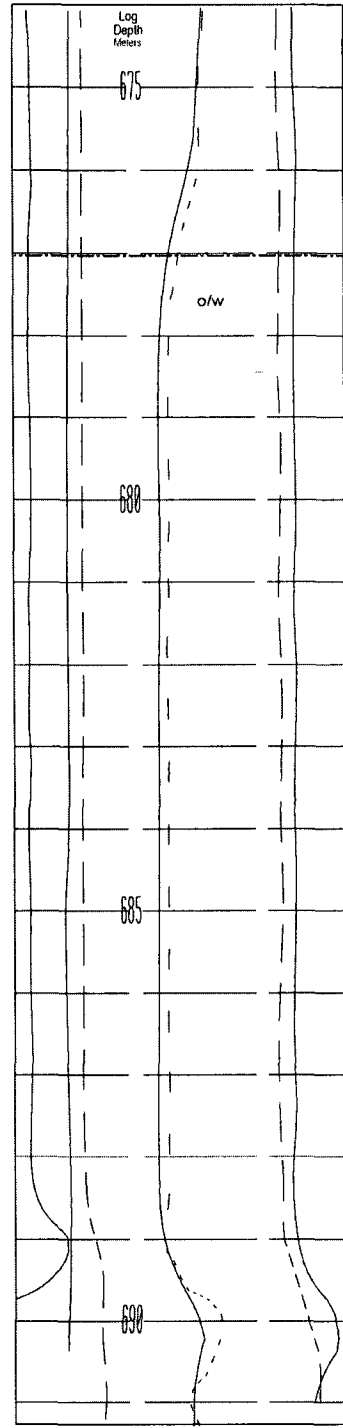
SP  
mV  
CA 46  
RES  
ohm.m 2888  
R498  
2888 kg/m<sup>3</sup> 3888  
SI  
289.32 g/cm<sup>3</sup> 131.25

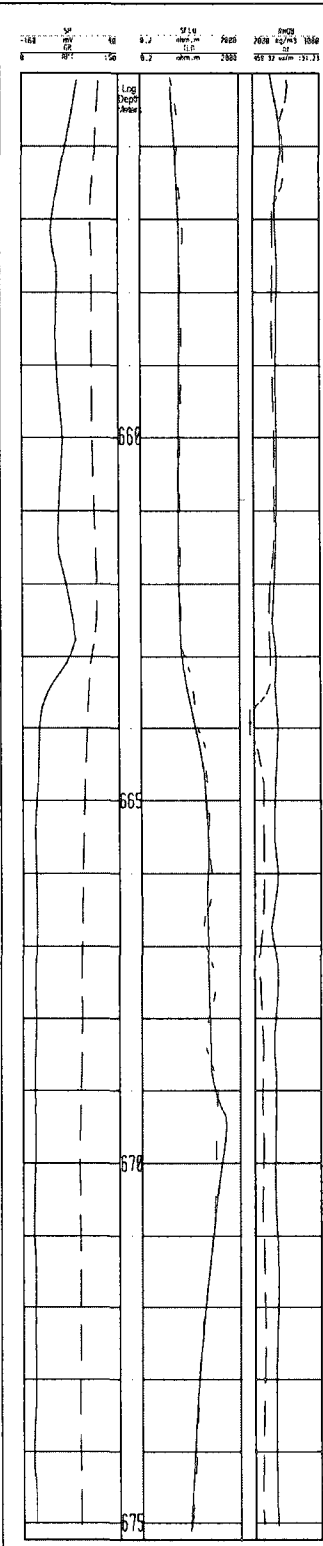




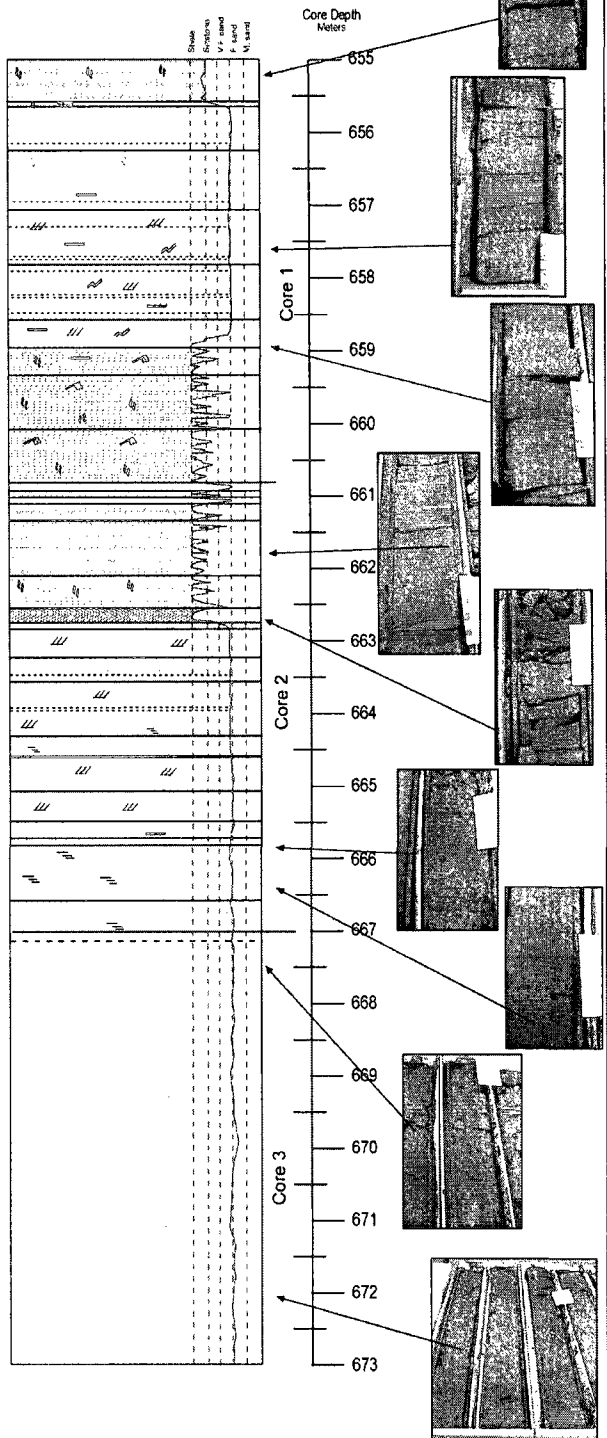
01/13-28-042-25W3/0

SP 11 156 0.2 2000 459.33 459.33 13.1 13.1  
SP 11 156 0.2 2000 459.33 459.33 13.1 13.1  
SP 11 156 0.2 2000 459.33 459.33 13.1 13.1



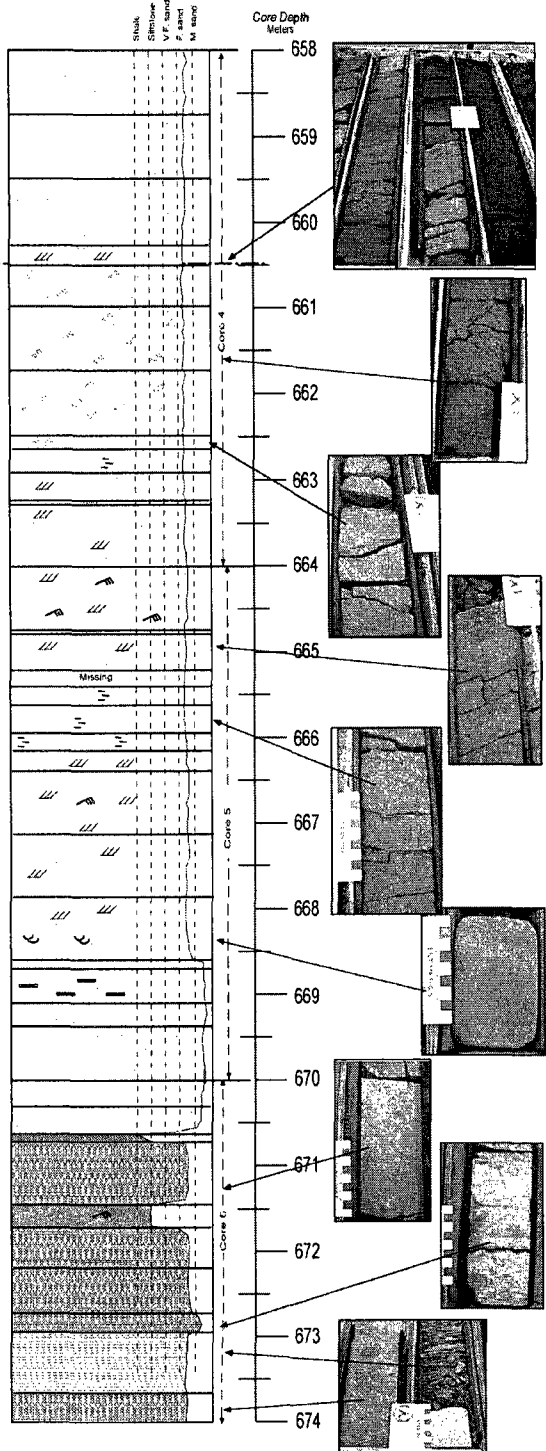
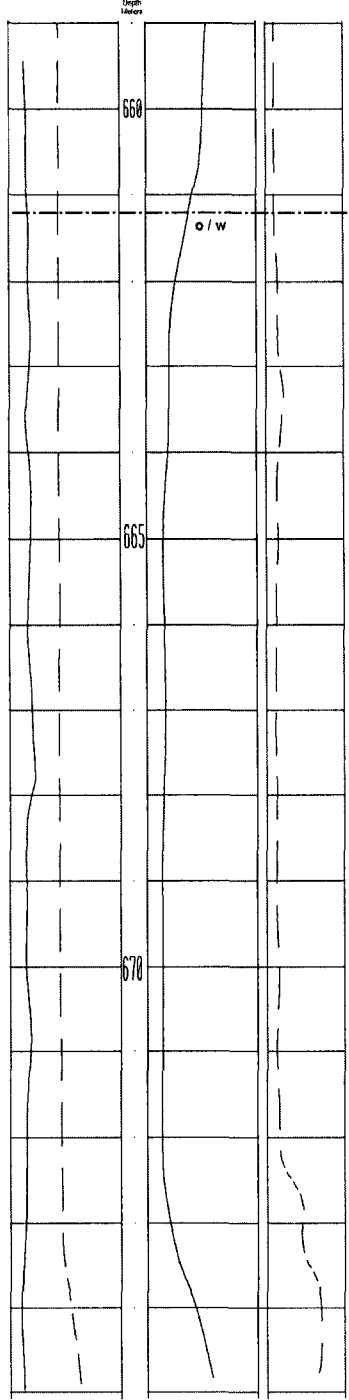


# Core 01/13-28-042-25W3/0

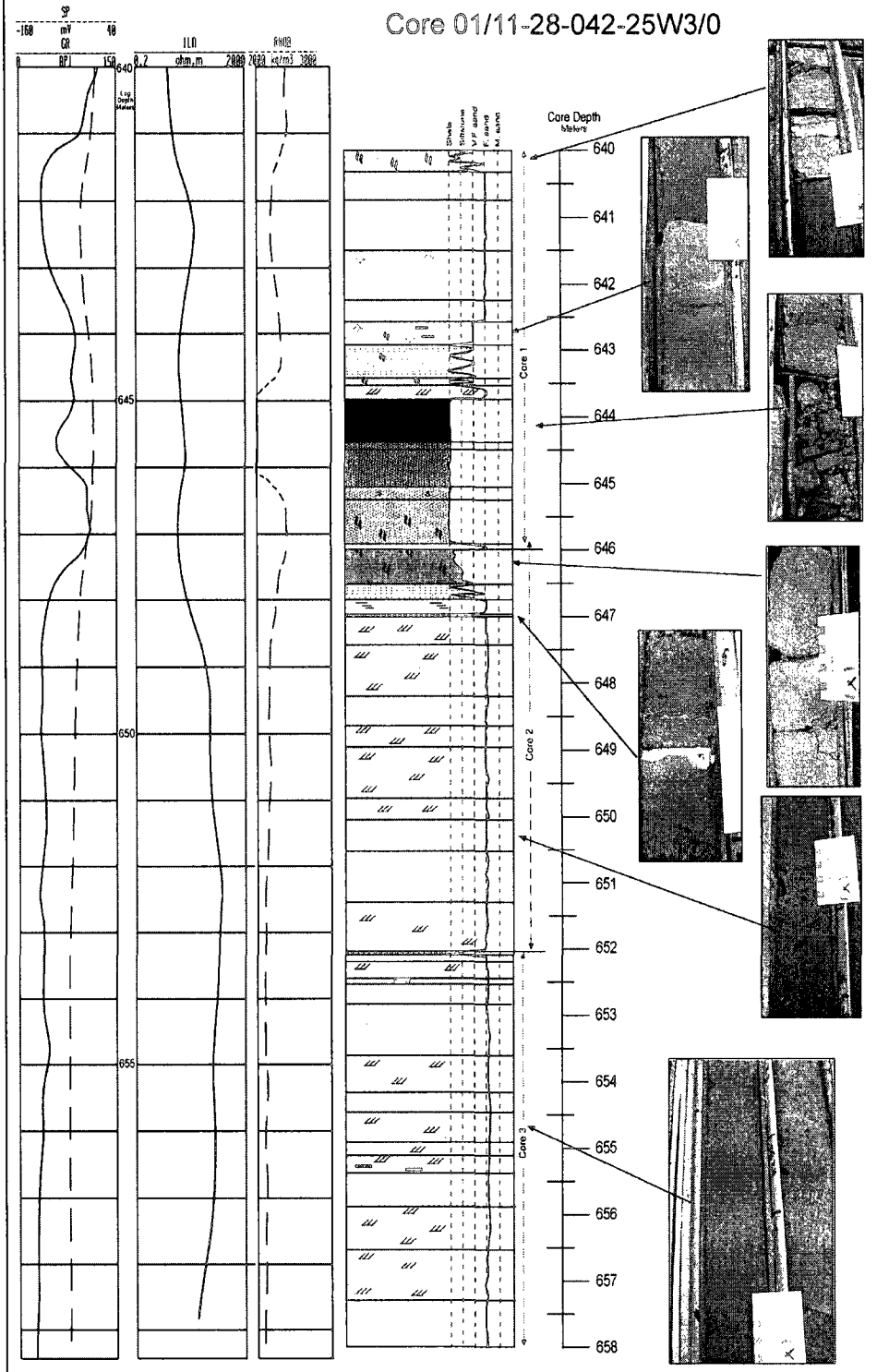


# Core 01/11-28-042-25W3/0

SP 168 40  
 CR 158  
 TLD 2000 2000 kg/m<sup>3</sup> 3000  
 H<sub>2</sub> 158

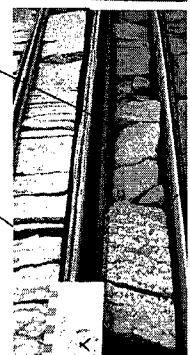
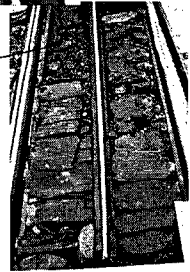
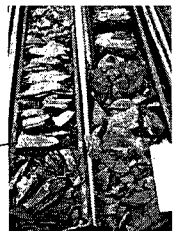
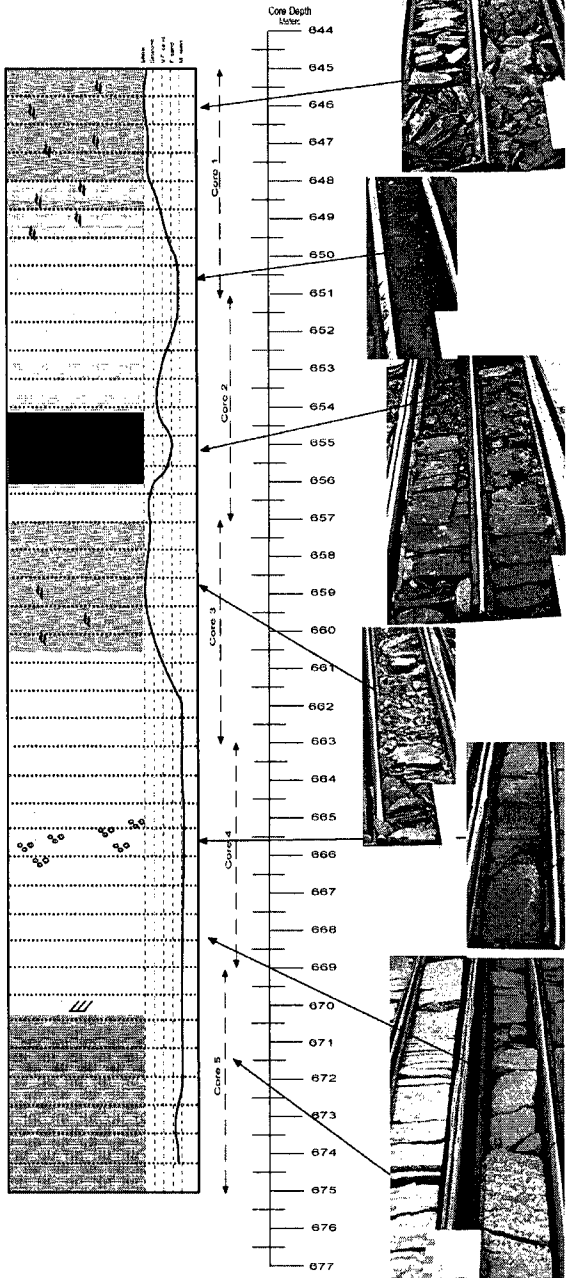
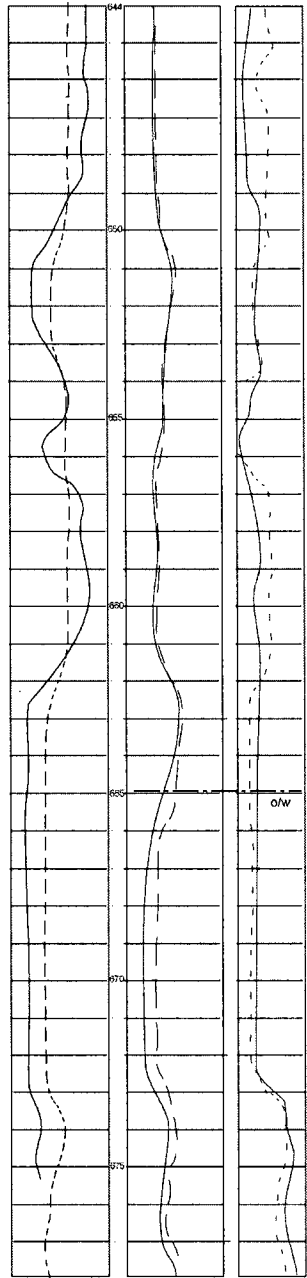


# Core 01/11-28-042-25W3/0



SP	LL	PIG
168	0.2	2880
GR	110	2880
158	0.2	2880
158	0.2	2880
158	0.2	2880

# Core 121/10-28-042-25W3





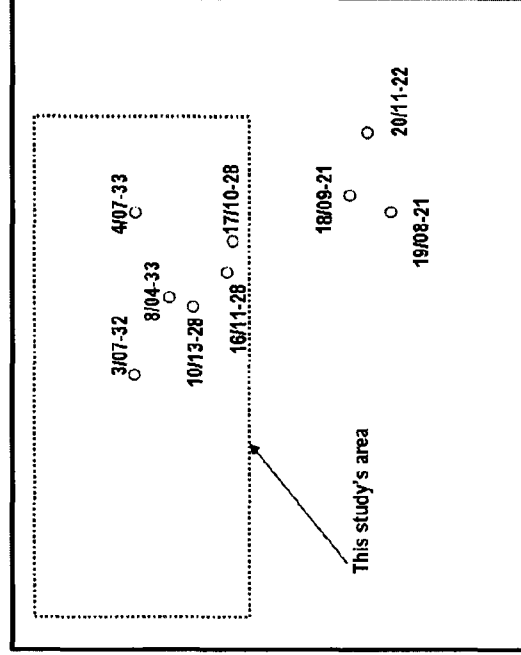
**Appendix 2:**

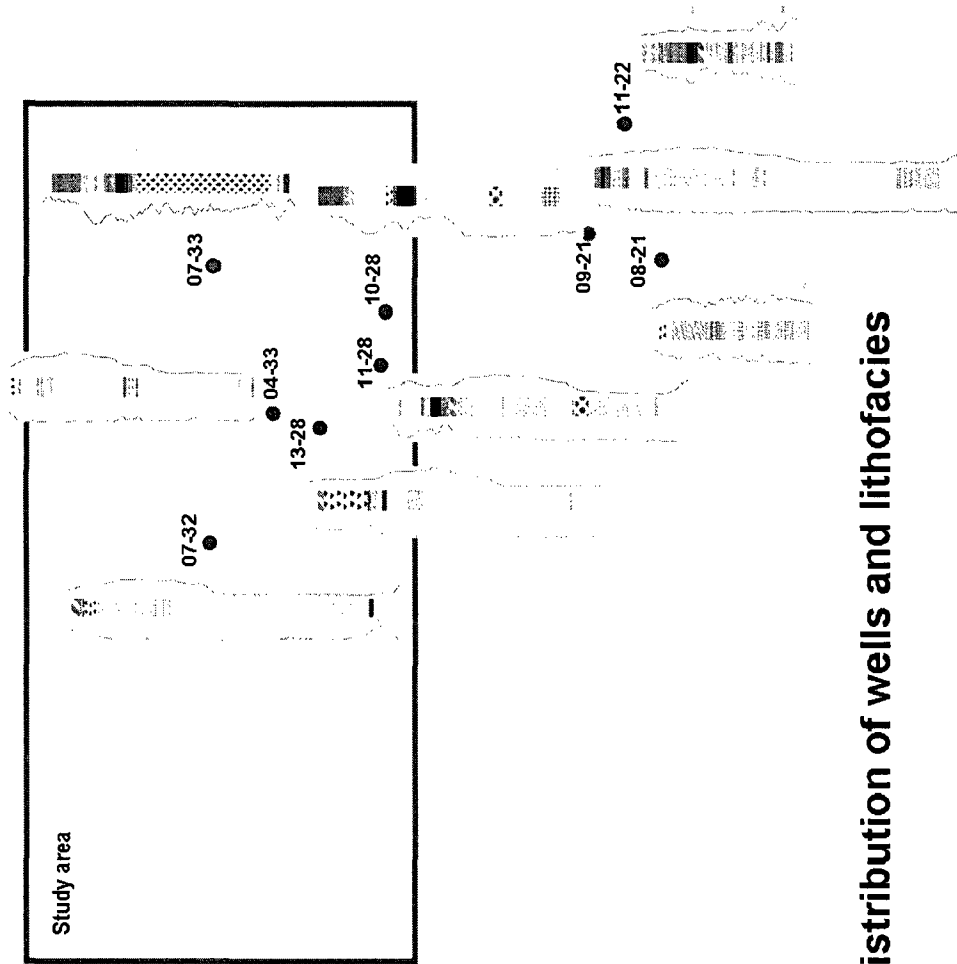
Lithofacies description

## Appendix 2

# Lithofacies description in selected areas of the “Winter pool” West-Central Saskatchewan

Lithofacies Legend	
<b>Facies 1- Sands</b>	
1a	Cross-stratified sands
1b	Parallel laminated to rippled sands
1c	Parallel laminated or bedded sands
1d	Structureless sands
1e	Moderately Bioturbated sands
1f	Sands with concretions
1g	Mud-clast breccia
1h	Calcite cemented sands
<b>Facies 2- Heterolithic</b>	
2a	Fining upwards sequence of muds, silts and sands
2b	Stumped sands, silty mudstones and sandy siltstones
2c	Inclined interbedded mudstones and rippled to crossbedded sands
2d	Coarsening upwards sequence of mudstones and silty sands
2e	Interbedded sandy siltstones and silty mudstones
2f	Laminated silty mudstone
2g	Burrowed sandy siltstone
2h	Rippled silty mudstone
<b>Facies 3- Mudstones and silts</b>	
3a	Dark grey mudstone
3b	Light grey mudstone
3c	Dark grey burrowed mudstone
3d	Light grey burrowed mudstone
3e	Siltstone
<b>Facies 4- Coal, Coaly mudstone and siltstone</b>	
4a	Coal
4b	Coaly mudstone
4c	Coaly and/or rooted siltstone

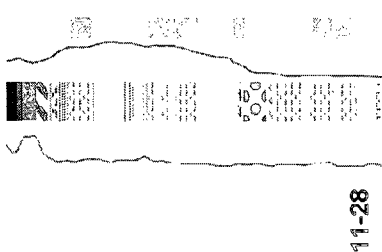




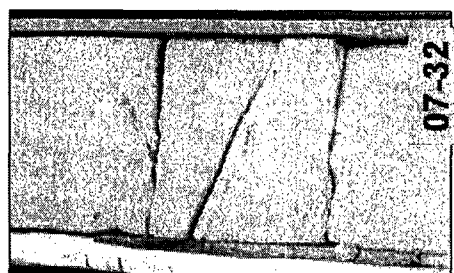
**Distribution of wells and lithofacies**

Lithofacies Legend	
<b>Facies 1. Sands</b>	
1a	Cross stratified sands
1b	Parallel laminated horizontal sands
1c	Parallel laminated or bedded sands
1d	Structureless sands
1e	Moderately bioturbated sands
1f	Sands with concretions
1g	Mud-clast breccia
1h	Caliche cemented sands
<b>Facies 2. Heterolithic</b>	
2a	Fining upwards sequence of muds, silts and sands
2b	Stumpier sands, silty mudstones and sandy siltstones
2c	Inclined rifebedded mudstones and siltstones
2d	Coarsening upwards sequence of mudstones and silty sands
2e	Interbedded sandy siltstones and silty mudstones
2f	Laminated silty mudstone
2g	Burrowed sandy siltstone
2h	Rippled silty mudstone
<b>Facies 3. Mudstones and silts</b>	
3a	Dark grey mudstone
3b	Light grey mudstone
3c	Dark grey burrowed mudstone
3d	Light grey burrowed mudstone
3e	Siltstone
<b>Facies 4. Coal, Coaly mudstone and siltstone</b>	
4a	Coal
4b	Coaly mudstone
4c	Coaly and/or rooted siltstone

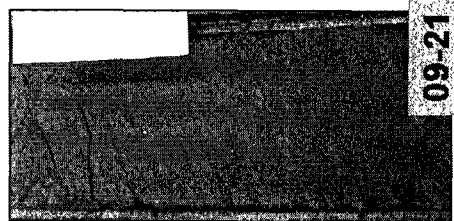
1a—Cross-stratified sands



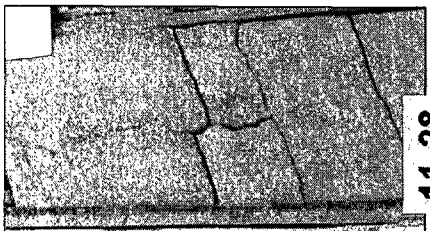
11-28



07-32



09-21



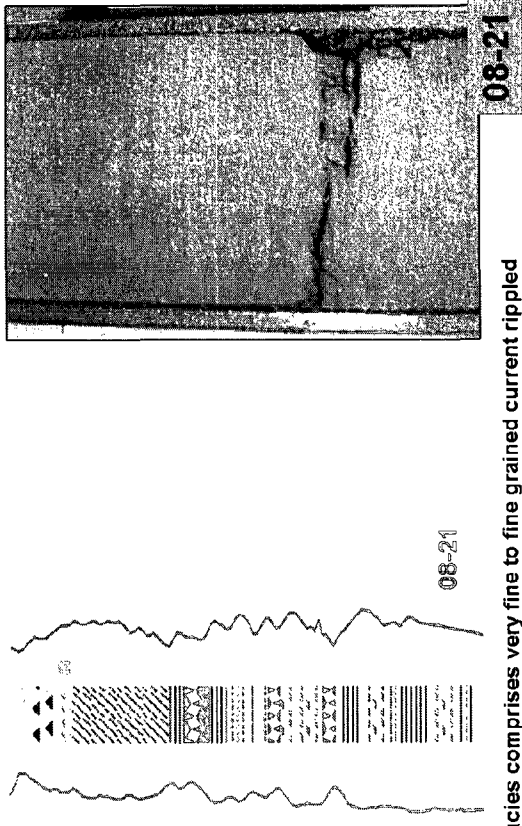
11-28

This facies comprises low to medium angle very fine to medium grained sand with mainly tabular cross-stratified. The unit thickness varies from several centimeters to 10 m. The bases of sets may contain mud clasts. Where bitumen saturation is present it is possible to distinguish heavy saturation in the lamina containing better sorted sands and less saturation in the more poorly sorted sand and silt lamina. In some occasions organic matter lamina is present. No change of grain size with depth is seen in the units containing this facies. This facies is observed in all the cores studied, it is associated with facies 1d and is seen in the basal sandy unit.

This facies corresponds to migrating dunes that can occur in many environments, but the log character and general characteristics would indicate several episodes of channel fill with sands in a fluvial dominated environment. The lack of rhythmic mudstone drapes and extensive bioturbation indicate no marine influence.

Lithofacies Legend	
<b>Facies 1: Sands</b>	
1a	Coarsely stratified sands
1b	Parallel laminated to rippled sands
1c	Parallel laminated or bedded sands
1d	Structureless sand
1e	Moderately bioturbated sands
1f	Sands with concretions
1g	Mud flat breccia
1h	Caliche cemented sands
<b>Facies 2: Heterolithic</b>	
2a	Fining upwards sequence of muds, silts and sands
2b	Stumped sands, silty mudstones and sandy siltstones
2c	Inclined interbedded mudstones and rippled to crossbedded sands
2d	Coarsening upwards sequence of mudstones and silty sands
2e	Interbedded sandy siltstones and silty mudstones
2f	Laminated silty mudstone
2g	Burrowed sandy siltstone
2h	Rippled silty mudstone
<b>Facies 3: Mudstones and silts</b>	
3a	Dark grey mudstone
3b	Light grey mudstone
3c	Dark grey burrowed mudstone
3d	Light grey burrowed mudstone
3e	Siltstone
<b>Facies 4: Coal, Coaly mudstone and siltstone</b>	
4a	Coal
4b	Coaly mudstone
4c	Coaly and/or rooted siltstone

1b- Parallel laminated to rippled

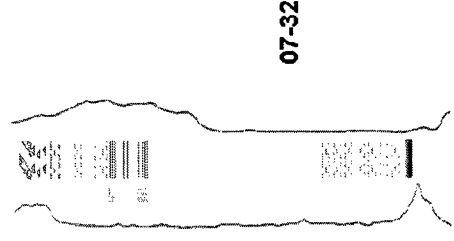
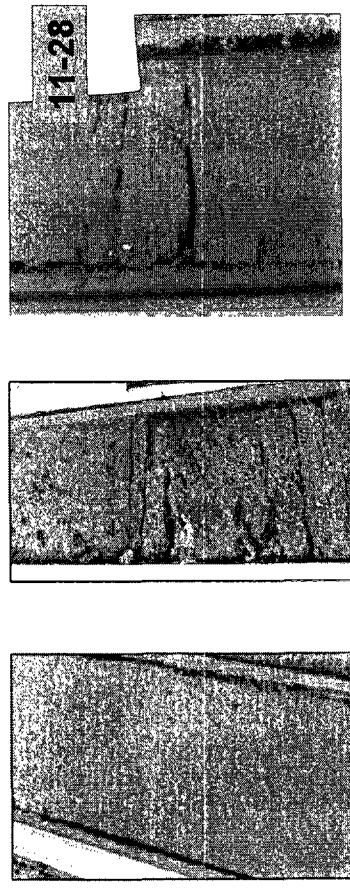


This facies comprises very fine to fine grained current rippled and ripple drift sands associated to parallel laminated sands. The thicknesses vary from few centimeters to around a meter. Bitumen saturation is observed and enhances the view of the sedimentary structures as in the case of the ripple crossbedded sands. This facies is seen within the basal sandy unit and but especially towards the top of the unit associated to heterolithic facies 2a, 2g and 2d.

This facies is interpreted as having been deposited from episodic waning flow in relatively weak slow currents. These types of sands are found in several settings from lagoon, point bar, fluvial channel, overbank, flood channels, so they are not diagnostic of any particular environment by themselves

Lithofacies Legend	
<b>Facies 1- Sands</b>	
1a	Cross-stratified sands
1b	Parallel laminated to rippled sands
1c	Parallel laminated or bedded sands
1d	Structureless sands
1e	Moderately bioturbated sands
1f	Sands with concretions
1g	Mud clast breccia
1h	Calcite cemented sands
<b>Facies 2- Heterolithic</b>	
2a	Fining upwards sequence of muds, silty sand
2b	Slumped sands, silty mudstones and sandy siltstones
2c	Inclined interbedded mudstones and rippled to crossbedded sands
2d	Coarsening upwards sequence of mudstones and silty sands
2e	Interbedded sandy siltstones and silty mudstones
2f	Laminated silty mudstone
2g	Burrowed sandy siltstone
2h	Rippled silty mudstone
<b>Facies 3- Mudstones and silts</b>	
3a	Dark grey mudstone
3b	Light grey mudstone
3c	Dark grey burrowed mudstone
3d	Light grey burrowed mudstone
3e	Siltstone
<b>Facies 4- Coal, Coaly mudstone and siltstone</b>	
4a	Coal
4b	Coaly mudstone
4c	Coaly and/or bedded siltstone

**1c - Parallel laminated to bedded sands**

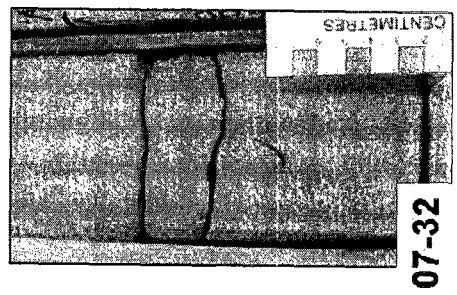
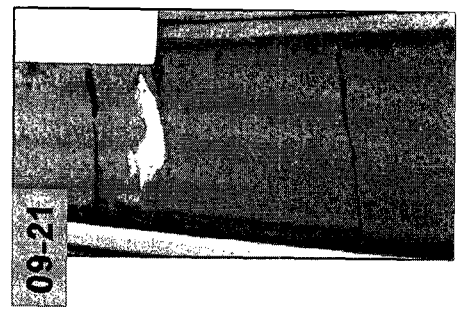
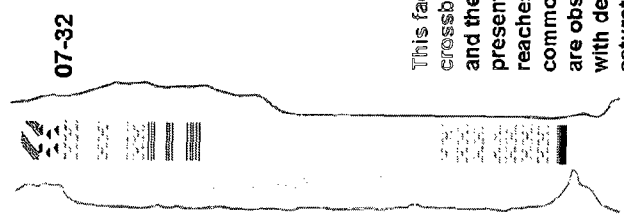


This facies comprises fine grained sands associated to structureless and cross bedded sands. In some cases it has organic matter interlaminated. Bitumen saturation is seen within this facies. The thickness varies from several centimeters to a meter. This facies is seen associated to 1a and 1d. No bioturbation is observed.

This facies because of its grain size and associated lithofacies is interpreted as deposited by high energy currents in fluvial, tidal or coastal settings.

Lithofacies Legend	
<b>Facies 1- Sands</b>	
1a	Cross-stratified sands
1b	Parallel laminated to rippled sands
1c	Parallel laminated or bedded sands
<b>Facies 2- Heterolithic</b>	
2a	Fining upwards sequence of muds, silts and sands
2b	Summed sands, silty mudstones and sandy siltstones
2c	Inclined or interbedded mudstones and rippled to crossbedded sands
2d	Coarsening upwards sequence of mudstones and silty sands
2e	Interbedded sandy siltstones and silty mudstones
2f	Laminated silty mudstone
2g	Burrowed sandy siltstone
2h	Rippled silty mudstone
<b>Facies 3- Mudstones and silts</b>	
3a	Dark grey mudstone
3b	Light grey mudstone
3c	Dark grey burrowed mudstone
3d	Light grey burrowed mudstone
3e	Siltstone
<b>Facies 4- Coal, Coaly mudstone and siltstone</b>	
4a	Coal
4b	Coaly mudstone
4c	Coaly and/or rooted siltstone

**1d- Structureless**

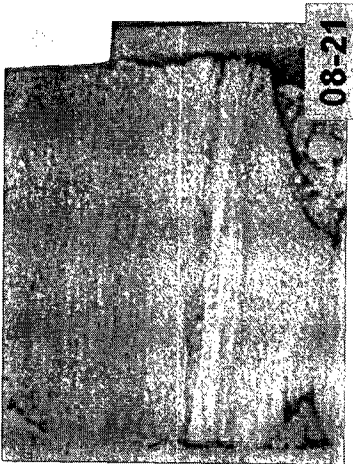
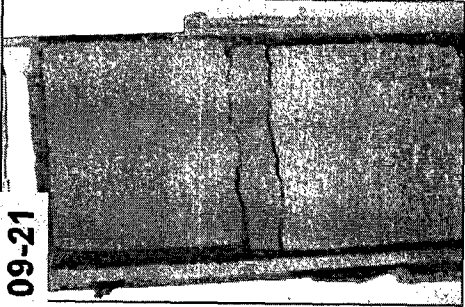


This facies is seen within fine to medium grained sands associated to crossbedded sands. No clear sedimentary structures are distinguished and then appear structureless. It is possible that the oil saturation reaches up to 16 m in thickness but intervals of less than a meter are common towards the top of the basal sandy unit. Isolated mud clasts are observed within this facies in some cores. No change of grain size with depth is seen in the packages containing this facies. Bitumen saturation is observed in this facies. This facies is observed in all the cores studied interbedded with 1a and 1c. It is observed both in the basal sandy unit and in the coarsening upward succession above the coal.

This facies could be interpreted as been deposited rapidly as velocity from strong currents decrease and no equilibrium between bedforms is achieved and hence stratification (Bhattacharya and Walker, 1991). The presence of mud clasts indicates high energy currents.

Lithofacies Legend	
<b>Facies 1- Sands</b>	
1a	Cross-stratified sands
1b	Parallel laminated to rippled sands
1c	Parallel laminated or bedded sands
1d	Structureless sands
<b>Facies 2- Moderately bioturbated sands</b>	
2a	Sands with concretions
2b	Mud-clast breccia
2c	Calcite cemented sands
<b>Facies 3- Heterolithic</b>	
3a	Fining upwards sequence of muds, silts and sands
3b	Slumped sands, silty mudstones and sandy siltstones
3c	Inclined interbedded mudstones and rippled to crossbedded sands
3d	Coarsening upwards sequence of mudstones and silty sands
3e	Interbedded sandy siltstones and silty mudstones
3f	Laminated silty mudstone
3g	Burrowed sandy siltstone
3h	Rippled silty mudstone
<b>Facies 4- Mudstones and silts</b>	
4a	Dark grey mudstone
4b	Light grey mudstone
4c	Dark grey burrowed mudstone
4d	Light grey burrowed mudstone
4e	Siltstone
<b>Facies 5- Coal, Coaly mudstone and siltstone</b>	
5a	Coal
5b	Coaly mudstone
5c	Coaly and/or rootbed siltstone

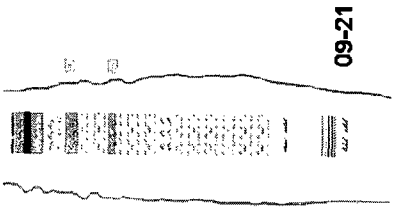
**1e- Moderately bioturbated sands**



This facies comprises very fine to fine sands that are seen at the top of the sandy interval and in some opportunities below the mud-clast breccia. Bitumen saturation is observed and enhances or obscures the trace fossils making them difficult to identify.

It is a rare facies in the cores studied and where found it displays mainly horizontal burrows. In some same cases any primary stratification has been disrupted, it is found as part of a fining upward sequence of facies.

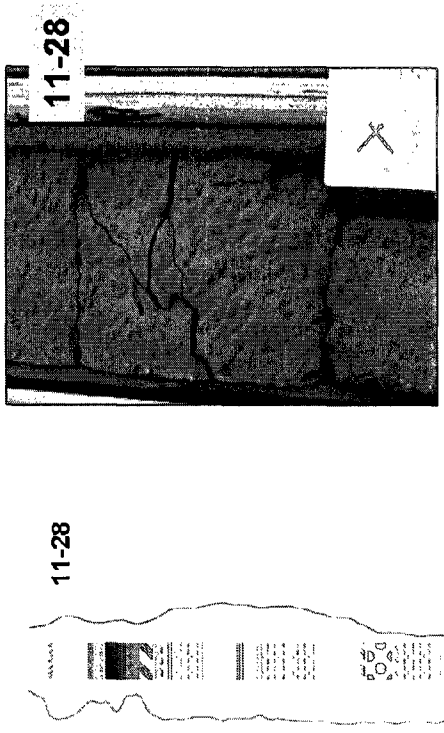
This moderate bioturbation observed in this facies is an indicator of lower sedimentation rates or the presence of more aerobic conditions. This facies could then correspond to a channel abandonment fill or point bar deposit.



09-21

Lithofacies Legend	
<b>Facies 1- Sands</b>	
1a	Cross-stratified sands
1b	Parallel laminated or rippled sands
1c	Parallel laminated or bedded sands
1d	Structureless sands
1e	Micronally Bioturbated sands
1f	Sands with concretions
1g	Mud clast breccia
1h	Calcite cemented sands
<b>Facies 2- Heterolithic</b>	
2a	Fining upwards sequence of muds, silts and sands
2b	Slumped sands, silty mudstones and sandy siltstones
2c	Inclined interbedded mudstones and siltstones
2d	Coarsening upwards sequence of mudstones and silty sands
2e	Interbedded sandy siltstones and silty mudstones
2f	Laminated silty mudstone
2g	Burrowed sandy siltstone
2h	Rippled silty mudstone
<b>Facies 3- Mudstones and silts</b>	
3a	Dark grey mudstone
3b	Light grey mudstone
3c	Dark grey burrowed mudstone
3d	Light grey burrowed mudstone
3e	Siltstone
<b>Facies 4- Coaly mudstone and siltstone</b>	
4a	Coal
4b	Coaly mudstone
4c	Coaly and/or rooted siltstone

1f - With concretions/precipitates



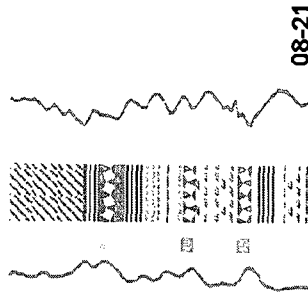
Observed only in wells 10-28 and 11-28 in the study area. It is seen within the basal sandy interval and in both wells measures around 1.5 meters. The concretions do not react to the HCL acid and are spherical to elliptical in shape with a diameter between 2 to 5 mm.

The precipitates encountered within this facies were generated by fluid that penetrated the sands either during their deposition or as part of the subsequent diagenesis. The fact that it is only found in two of the cores of wells located relatively close together indicates that it is an isolated event. Further study of this facies is necessary to establish the nature of the concretions or precipitates.

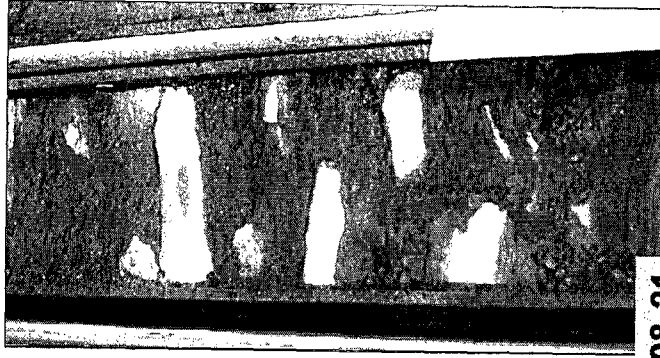
Lithofacies Legend	
<b>Facies 1- Sands</b>	
1a	Cross-stratified sands
1b	Parallel laminated or rippled sands
1c	Parallel laminated or bedded sands
1d	Structureless sands
1e	Moderately bioturbated sands
1f	Sands with concretions
1g	Mud-clast breccia
1h	Caliche cemented sands
<b>Facies 2- Heterolithic</b>	
2a	Fining upwards sequence of muds, silts and sands
2b	Slumped sands, silty mudstones and sandy siltstones
2c	Inclined interbedded mudstones and ripples to crossbedded sands
2d	Coarsening upwards sequence of mudstones and silty sands
2e	Interbedded sandy siltstones and silty mudstones
2f	Laminated silty mudstone
2g	Burrowed sandy siltstone
2h	Rippled silty mudstone
<b>Facies 3- Mudstones and silts</b>	
3a	Dark grey mudstone
3b	Light grey mudstone
3c	Dark grey burrowed mudstone
3d	Light grey burrowed mudstone
3e	Siltstone
<b>Facies 4- Coal, Coaly mudstone and siltstone</b>	
4a	Coal
4b	Coaly mudstone
4c	Coaly and/or rooted siltstone

Matrix supported mud-clast breccia, interbedded between crossbedded, structureless and parallel laminated sands. The elongated sub-angular clasts can get to be as up to the barrel's width (8 cm) and the interval can reach up to half a meter thick. This facies was only observed in well 08-21. Bitumen saturation is observed in the sandy matrix.

This facies is interpreted as product of channel-bank collapse which is part of the normal process of point bar erosion and migration of meandering fluvial or estuarine channels. Groeneveld and Stasiuk observed this facies in the Winter field deposits and interpreted them as part of a tidal channel. They used palynological data that assigns a marine origin for the sands. No indication of marine influence (bioturbation, well sorted sands etc.) was observed in the well that contains three intervals of this facies.



1g - Intraformational Mud-clast breccia



08-21

**Lithofacies Legend**

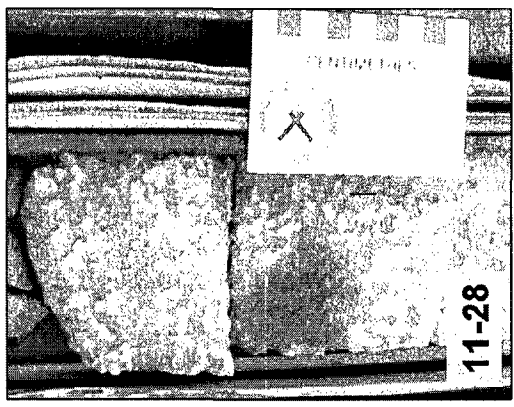
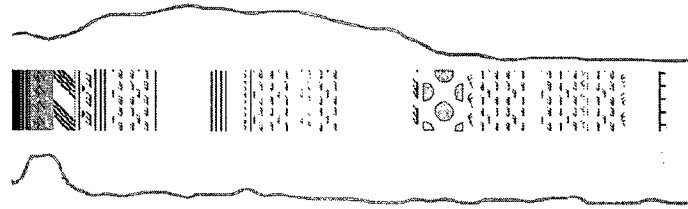
- Facies 1- Sands**
- 1a Cross-stratified sands
  - 1b Parallel laminated to ripple sands
  - 1c Parallel laminated or bedded sands
  - 1d Structureless sands
  - 1e Moderately bioturbated sands
  - 1f Sands with concretions
  - 1g Mud-clast breccia
  - 1h Calcite cemented sands

- Facies 2- Heterolithic**
- 2a Fine upwards sequence of muds, silts and sands
  - 2b Slumped sands, silty mudstones and sandy siltstones
  - 2c Rippled interbedded mudstones and siltstones
  - 2d Coarsening upwards sequence of mudstones and silty sands
  - 2e Interbedded sandy siltstones and silty mudstones
  - 2f Laminated silty mudstone
  - 2g Burrowed sandy siltstone
  - 2h Rippled silty mudstone

- Facies 3- Mudstones and silts**
- 3a Dark grey mudstone
  - 3b Light grey mudstone
  - 3c Dark grey burrowed mudstone
  - 3d Light grey burrowed mudstone
  - 3e Siltstone

- Facies 4- Coal, Coaly mudstone and siltstone**
- 4a Coal
  - 4b Coaly mudstone
  - 4c Coaly and/or rooted siltstone

**1h- Calcite cemented sands**



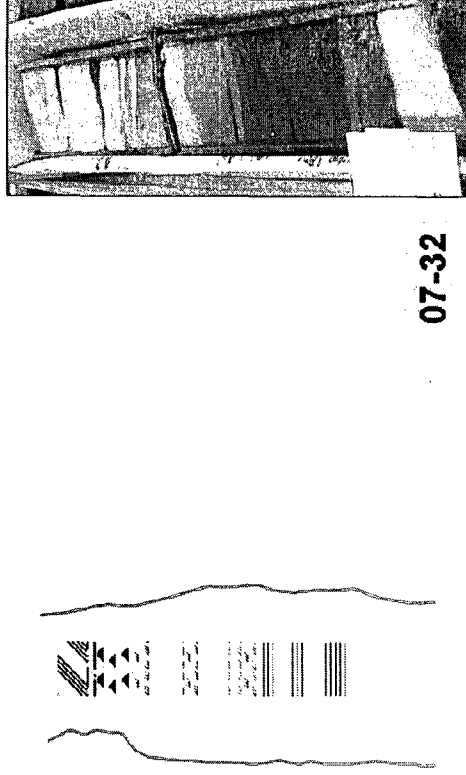
This facies is found at the bottom of the basal sand interval close to or directly above the Sub-Cretaceous unconformity. It has a white mottled aspect and varies from few centimeters less than a meter in thickness.

The cement observed in these sands is most probably an effect of calcareous fluids from the neighboring Duperow facies, which penetrated the sands during or after deposition. More studies are necessary to establish the timing of the cementation.

11-28

Lithofacies Legend	
<b>Facies 1- Sands</b>	
1a	Cross-stratified sands
1b	Parallel laminated to ripple sands
1c	Parallel laminated or bedded sands
1d	Structureless sands
1e	Moderately bioturbated sands
1f	Sands with concretions
1g	Mud about brachiopods
1h	Caliche cemented sands
<b>Facies 2- Heterolithic</b>	
2a	Fining upwards sequence of muds, silts and sands
2b	Slumped sands, silty mudstones and sandy siltstones
2c	Defined interbedded mudstones and ripples to crossbedded sands
2d	Coarsening upwards sequence of mudstones and silty sands
2e	Interbedded sandy siltstones and silty mudstones
2f	Laminated silty mudstone
2g	Burrowed sandy siltstone
2h	Rippled silty mudstone
<b>Facies 3- Mudstones and silts</b>	
3a	Dark grey mudstone
3b	Light grey mudstone
3c	Dark grey burrowed mudstone
3d	Light grey burrowed mudstone
3e	Siltstone
<b>Facies 4- Coal, Coaly mudstone and siltstone</b>	
4a	Coal
4b	Coaly mudstone
4c	Coaly arc/lor rooted siltstone

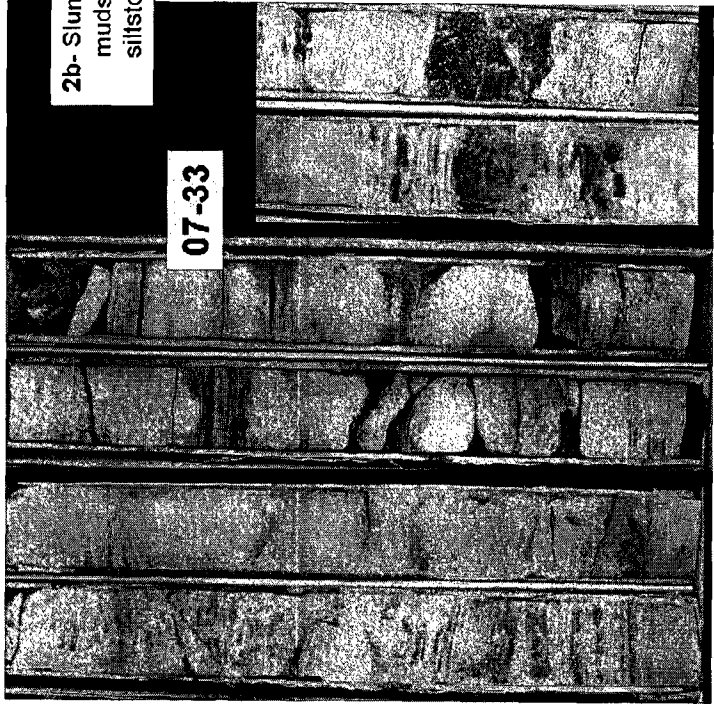
2a- Fining upwards sequence of muds, silts and sands



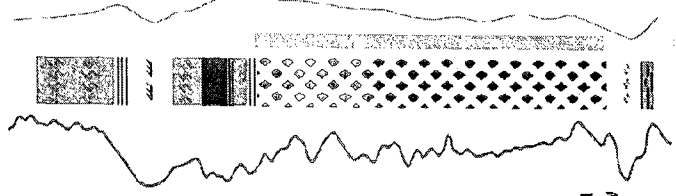
This facies comprises layers of bitumen saturated rippled to structureless sands interbedded with bioturbated sandy silts and laminated or bioturbated grey mudstones. It is found above the basal sandy interval underlying 3b or 4c. The thickness is around one meter. The sequence repeats itself with an overall decrease in grain size and in the thickness of the coarser grain layers. In some cases the contact between the facies is transitional but in other it is abrupt.

This facies that combines sands, silts and muds in an overall fining succession can be interpreted as a series of waning flows at the end of the channel fill episode. This sequence could represent a crevasse channel fill.

Lithofacies Legend	
<b>Facies 1: Sands</b>	
1a	Cross-stratified sands
1b	Parallel laminated to rippled sands
1c	Parallel laminated or bedded sands
1d	Structureless sands
1e	Moderately bioturbated sands
1f	Sands with concretions
1g	Mud slab breccia
1h	Calcite cemented sands
<b>Facies 2: Mafrolithic</b>	
2a	Fining upwards sequence of muds, silts and sands
2b	Stump sands, silty mudstones and silty siltstones
2c	Inclined or bedded mudstones and rippled to crossbedded sands
2d	Coarsening upwards sequence of mudstones and silty sands
2e	Interbedded sandy siltstones and silty mudstones
2f	Laminated silty mudstone
2g	Burrowed sandy siltstone
2h	Rippled silty mudstone
<b>Facies 3: Mudstones and silts</b>	
3a	Dark grey mudstone
3b	Light grey mudstone
3c	Dark grey burrowed mudstone
3d	Light grey burrowed mudstone
3e	Siltstone
<b>Facies 4: Coal, Coaly mudstone and siltstone</b>	
4a	Coal
4b	Coaly mudstone
4c	Coaly and/or rooted siltstone



2b- Slumped sands, silty mudstones and sandy siltstones



This facies comprises slumped, faulted and fractured sands, silts and mudstones. It is a mixture of many lithofacies and is seen only in well-sorted areas where it reaches over 15 meters.

This facies is interpreted to be deposited by mobilization and re-sedimentation in areas of paleo-geographical lows as Karst depressions

07-33

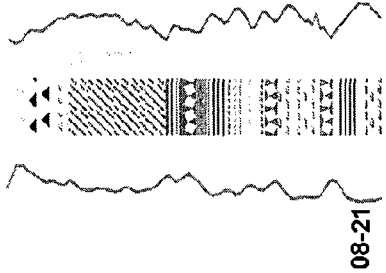
Lithofacies Legend	
<b>Facies 1- Sands</b>	
1a	Cross-stratified sands
1b	Parallel laminated or rippled sands
1c	Parallel laminated or bedded sands
1d	Structureless sands
1e	Moderately bioturbated sands
1f	Sands with concretions
1g	Mud clast breccia
1h	Calcite cemented sands
<b>Facies 2- Heterolithic</b>	
2a	Fining upwards sequence of muds, silts and sands
2b	Stumpier sands, silty mudstones and sandy siltstones
2c	Inclined, ribbed mudstones and rippled to crossbedded sands
2d	Coarsening upwards sequence of mudstones and silty sands
2e	Interbedded sandy siltstones and silty mudstones
2f	Laminated silty mudstone
2g	Burrowed sandy siltstone
2h	Rippled silty mudstone
<b>Facies 3- Mudstones and silts</b>	
3a	Dark grey mudstone
3b	Light grey mudstone
3c	Dark grey burrowed mudstone
3d	Light grey burrowed mudstone
3e	Siltstone
<b>Facies 4- Coal, Coaly mudstone and siltstone</b>	
4a	Coal
4b	Coaly mudstone
4c	Coaly and/or rootlet siltstone

2c- Inclined interbedded mudstones and rippled to crossbedded sands

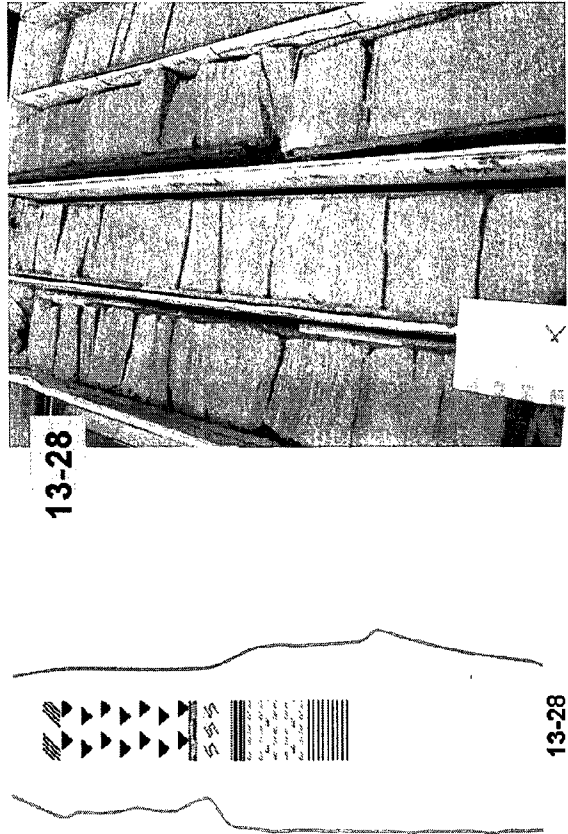


This facies is seen in well 08-21 and reaches 4 meters, lying above the sandy unit containing facies 1g, 1a and 1c interbedded. This facies comprises fine grained oil stained rippled sands interbedded with inclined bedded thin silty muds. Minor bioturbation is observed in this facies.

This facies is interpreted to be lateral accretion deposits formed by unidirectional currents and suspension fallout. These deposits constitute the point bars of meandering fluvial or estuarine systems.



**2d- Coarsening upwards sequence of mudstones and silty sands**



This facies is comprised of laminated, moderately burrowed gray silty mudstones and rippled and parallel bedded silty sands. The burrows observed are scarce, mainly horizontal, some burrows have more than 1 cm in diameter. The sequence of alternating sands and mudstones gets sandier towards the top of the interval. This facies is observed only in well 13-28 where it has a thickness of 4 meters. Bitumen saturation is low in the sandy layers.

The facies is interpreted to be deposited in a mixed energy environment, with flooding or weak currents bringing in the sands. It can be interpreted as crevasse splays building along the edges of estuarine channels or into bays or shallow lakes.

Lithofacies Legend	
<b>Facies 1- Sands</b>	
1a	Cross-stratified sands
1b	Parallel laminated to rippled sands
1c	Parallel laminated o-beded sands
1d	Structureless sands
1e	Moderately bioturbated sands
1f	Sands with concretions
1g	Mud-clast breccia
1h	Calcite cemented sands
<b>Facies 2- Heterolithic</b>	
2a	Fining upwards sequence of muds, silts and sands
2b	Slumped sands, silty mudstones and sandy siltstones
2c	Inclined interbedded mudstones or silts applied to crossbedded sands
2d	Coarsening upwards sequence of mudstones and silty sands
2e	Interbedded sandy siltstones and silty mudstones
2f	Laminated silty mudstone
2g	Burrowed sandy siltstone
2h	Rippled silty mudstone
<b>Facies 3- Mudstones and silts</b>	
3a	Dark grey mudstone
3b	Light grey mudstone
3c	Dark grey burrowed mudstone
3d	Light grey burrowed mudstone
3e	Siltstone
<b>Facies 4- Coal, Coaly mudstone and siltstone</b>	
4a	Coal
4b	Coaly mudstone
4c	Coaly and/or rooted siltstone

### Lithofacies Legend

- Facies 1- Sands**
- 1a Cross-stratified sands
  - 1b Parallel laminated or ripple sands
  - 1c Structureless sands
  - 1d Moderately bioturbated sands
  - 1e Sands with concretions
  - 1f Mud-clast breccia
  - 1g Caliche cemented sands
  - 1h Heterolithic
- Facies 2- Heterolithic**
- 2a Fine upwards sequence of muds, silts and sands
  - 2b Slumped sands, silty mudstones and sandy siltstones
  - 2c Ridged interbedded mudstones and rippled to crossbedded sands
  - 2d Counter-ripping upwards sequence of mudstones and silty sands
  - 2e Interbedded sandy siltstones and silty mudstones
  - 2f Laminated silty mudstone
  - 2g Burrowed sandy siltstone
  - 2h Rippled silty mudstone
- Facies 3- Mudstones and silts**
- 3a Dark grey mudstone
  - 3b Light grey mudstone
  - 3c Dark grey burrowed mudstone
  - 3d Light grey burrowed mudstone
  - 3e Siltstone
- Facies 4- Coal, Coaly mudstone and siltstone**
- 4a Coal
  - 4b Coaly mudstone
  - 4c Coaly siltstone or coaly siltstone

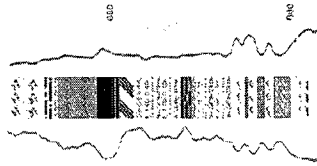
### 2e- Interbedded sandy siltstones, sands and mudstones.



This facies comprises layers from a couple of centimeters to up to 10 centimeters in thickness of oil saturated structureless or ripple to laminated sands interbedded with bioturbated silts and layers of light grey laminated mudstones. It is found overlaying the basal sandy interval associated to facies 2f, 1b and 3d. The thickness varies from less than a meter up to over two meters. The level of bioturbation is moderate and the burrows observed are a mainly horizontal with some vertical occurring in some intervals. The diversity is low and the sizes range from millimeters to a couple of centimeters.

This facies could be interpreted as product of alternating episodes of higher energy settings where currents deposited ripple to laminated cross laminated sands within a low energy setting where deposition is more by settling from suspension. This combination can be interpreted as channel-proximal overbank deposits although the typical roots are absent. This could be due to rapid cycles that do not allow the establishment of vegetation.

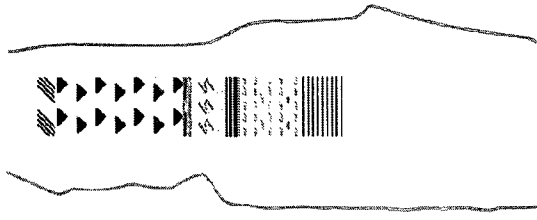
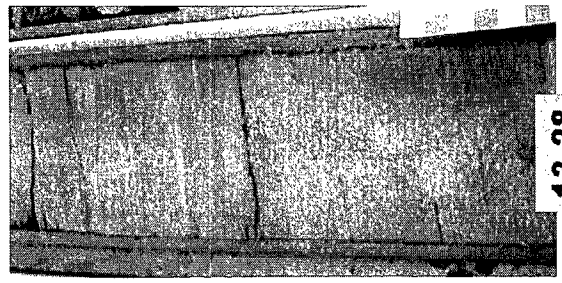
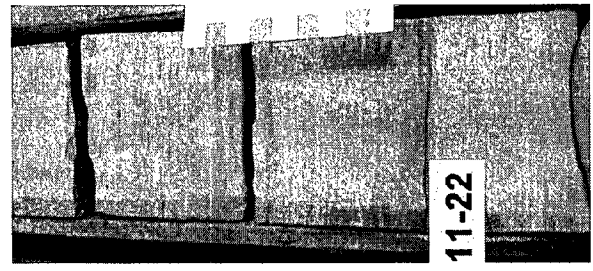
11-22



11-22

Lithofacies Legend	
<b>Facies 1- Sands</b>	
1a	Cross-stratified sands
1b	Parallel laminated to ripple sands
1c	Parallel laminated or bedded sands
1d	Structureless sands
1e	Moderately bioturbated sands
1f	Sands with concretions
1g	Mud clast breccia
1h	Caliche cemented sands
<b>Facies 2- Heterolithic</b>	
2a	Fine upwards sequence of muds, silts and sands
2b	Sumpic sands, silty mudstones and silty siltstones
2c	Inclined or tabbed mudstones and siltstones
2d	Coarsening upwards sequence of mudstones and silty sands
2e	Interbedded sandy siltstones and silty mudstones
2f	Laminated silty mudstone
2g	Burrowed sandy siltstone
2h	Rippled silty mudstone
<b>Facies 3- Mudstones and silts</b>	
3a	Dark grey mudstone
3b	Light grey mudstone
3c	Dark grey burrowed mudstone
3d	Light grey burrowed mudstone
3e	Siltstone
<b>Facies 4- Coal, Coaly mudstone and siltstone</b>	
4a	Coal
4b	Coaly mudstone
4c	Coaly and/or coiled siltstone

**2f- Laminated silty mudstone**

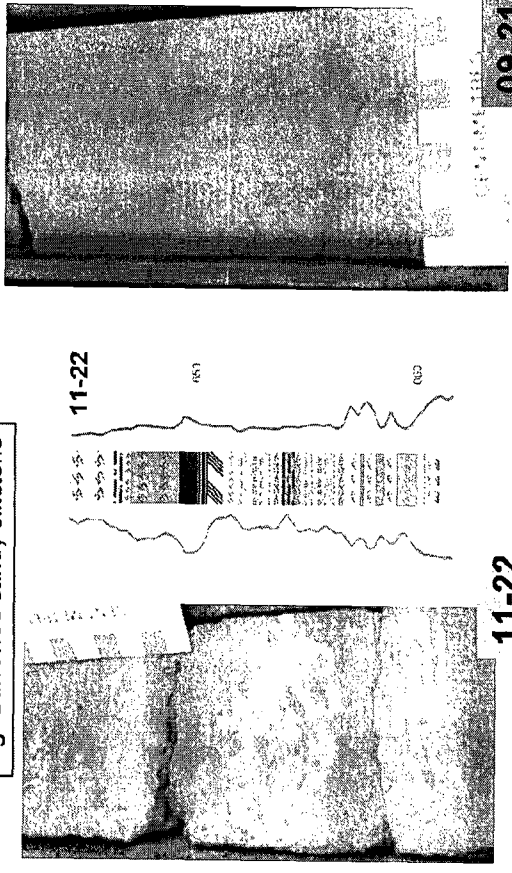


This facies comprises interlaminated silts and light gray mudstones, there is some low degree of bioturbation and the thickness reaches up to a meter. It is observed in the interval overlying 4a and in between 2e.

This facies is interpreted as fallout from suspension during flooding either in flood plain or distal coastal plain settings. It represents fluctuations in energy within a continuous deposition.

Lithofacies Legend	
<b>Facies 1- Sands</b>	
1a	Cross-stratified sands
1b	Parallel laminated or rippled sands
1c	Parallel laminated or bedded sands
1d	Structureless sands
1e	Moderately bioturbated sands
1f	Sands with concretions
1g	Mud-chest breccia
1h	Calcite cemented sands
<b>Facies 2- Heterolithic</b>	
2a	Finning upwards sequence of muds, silts and sands
2b	Slumped sands, silty mudstones and sandy siltstones
2c	Bedded interbedded mudstones and rippled to crossbedded sands
2d	Downward, upward sequence of mudstones and silty sands
2e	Interbedded sandy siltstones and silty mudstones
2f	Laminated silty mudstone
2g	Burrowed sandy siltstone
2h	Rippled silty mudstone
<b>Facies 3- Mudstones and silts</b>	
3a	Dark grey mudstone
3b	Light grey mudstone
3c	Dark grey burrowed mudstone
3d	Light grey burrowed mudstone
3e	Siltstone
<b>Facies 4- Coal, Coaly mudstone and siltstone</b>	
4a	Coal
4b	Coaly mudstone
4c	Coaly and/or rooted siltstone

2g- Burrowed sandy siltstone



09-21

11-22

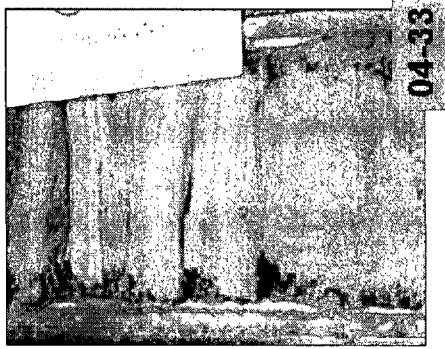
This facies consist of sandy silt with some bitumen impregnation. This facies is found overlying the coal in a couple of wells and reaches the 2.5 meters. Bioturbation is not diverse moderate to abundant, mostly horizontal with some vertical burrows concentrated in some layers. The primary sedimentary structures are not visible. This facies is found overlying 4a or in between sandy layers.

This facies is deposited from suspension fallout in low energy environments where sands in brought in periodically. The environment has well-oxygenated bottom conditions for the biological activity to develop. In the cases where this facies is located over the coal it could have been generated during flooding in either coastal or flood plain settings. When the location of this facies is in between rippled sandy layers at the top of the sandy basal interval it could be interpreted as flood plain deposits in the vicinity of the estuarine or fluvial channels.

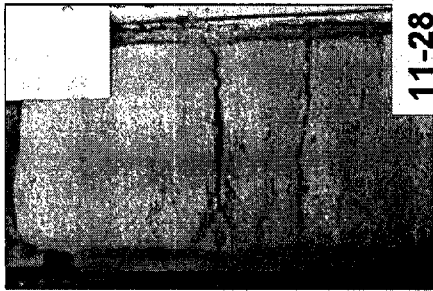
### Lithofacies Legend

- Facies 1- Sands**
- 1a Cross-stratified sands
  - 1b Parallel laminated to rippled sands
  - 1c Parallel laminated or bedded sands
  - 1d Structureless sands
  - 1e Moderately bioturbated sands
  - 1f Sands with rootlets
  - 1g Mud-clast breccia
  - 1h Caliche cemented sands
- Facies 2- Heterolithic**
- 2a Fining upwards sequence of muds, silts and sands
  - 2b Slumped sands, silty mudstones and sandy siltstones
  - 2c Inclined interbedded mudstones and rippled to crossbedded sands
  - 2d Coarsening upwards sequence of mudstones and silty sands
  - 2e Interbedded sandy siltstones and silty mudstones
  - 2f Laminated silty mudstone
  - 2g Burrowed sandy siltstone
  - 2h Rippled silty mudstone
- Facies 3- Mudstones and silts**
- 3a Dark grey mudstone
  - 3b Light grey mudstone
  - 3c Dark grey burrowed mudstone
  - 3d Light grey burrowed mudstone
  - 3e Siltstone
- Facies 4- Coal, Coaly mudstone and siltstone**
- 4a Coal
  - 4b Coaly mudstone
  - 4c Coaly and/or rootlet siltstone

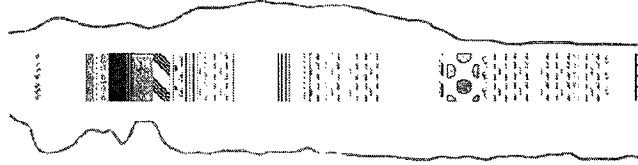
### 2h- Rippled silty mudstone



04-33



11-28



11-28

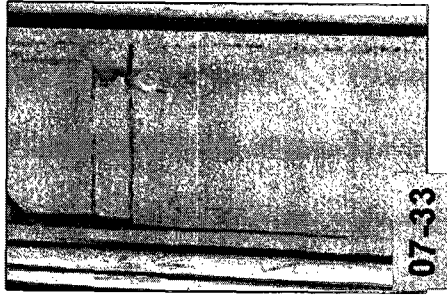
This facies comprised thinly laminated, rippled silty mudstone and is observed overlying the sandy 1a and 1d facies. Its thickness only reaches half a meter and is not found commonly in the area. The presence of thin organic matter lamina is common.

This facies could correspond in some cases to the deposits of short episodes of flooding either in flood or coastal plains.

**Lithofacies Legend**

<b>Facies 1- Sands</b>	
1a	Cross-stratified sands
1b	Parallel laminated to rippled sands
1c	Parallel laminated or bedded sands
1d	Structureless sands
1e	Moderately bioturbated sands
1f	Sands with concretions
1g	Mud ball breccia
1h	Calcite cemented sands
<b>Facies 2- Heterolithic</b>	
2a	Fining upwards sequence of muds, silts and sands
2b	Slumped sands, silty mudstones and sandy siltstones
2c	Inclined interbedded mudstones and rippled to crossbedded sands
2d	Coarsening upwards sequence of mudstones and silty sands
2e	Interbedded sandy siltstones and silty mudstones
2f	Laminated silty mudstone
2g	Burrowed sandy siltstone
2h	Rippled silty mudstone
<b>Facies 3- Mudstones and silts</b>	
3a	Dark grey mudstone
3b	Light grey mudstone
3c	Dark grey burrowed mudstone
3d	Light grey burrowed mudstone
3e	Siltstone
<b>Facies 4- Coal, Coaly mudstone and siltstone</b>	
4a	Coal
4b	Coaly mudstone
4c	Coaly and/or rooted siltstone

**3a- Dark grey mudstones with organic material**



07-33



10-28



10-28

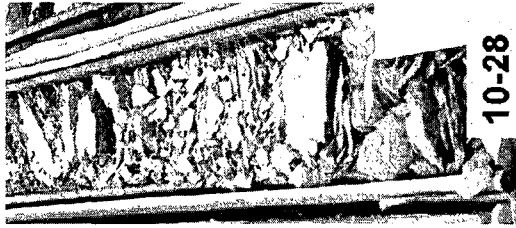
This facies is seen in association with the coaly mudstone and the coal and reaches only a couple of tens of centimeters in thickness. It is also seen not associated to the fissile coal in well 10-28 where it is up to 3 meters in thickness. It is found overlying facies 3d.

This organic rich facies is deposited from suspension in oxygen deprived environment. When associated to the coaly mudstones and coals it is interpreted to be generated in a non-marine to paralic environment. When seen associated with facies 3d the interpretation includes marine environments.

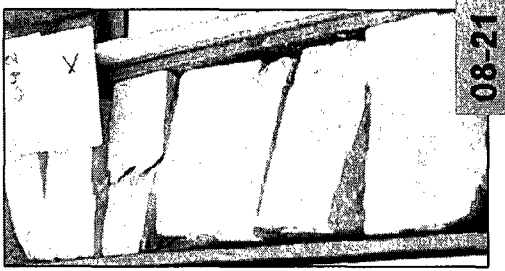
### Lithofacies Legend

<b>Facies 1- Sands</b>	
1a	Cross-stratified sands
1b	Parallel laminated to rippled sands
1c	Parallel laminated or bedded sands
1d	Structureless sands
1e	Mottled or bioturbated sands
1f	Sands with concretions
1g	Mud basal breccia
1h	Caliche cemented sands
<b>Facies 2- Heterolithic</b>	
2a	Fining upwards sequence of muds, silts and sands
2b	Slumped sands, silt mudstones and sandy siltstones
2c	Inclined interbedded mudstones and rippled to crossbedded sands
2d	Coarsening upwards sequence of mudstones and silty sands
2e	Interbedded sandy siltstones and silty mudstones
2f	Laminated silty mudstone
2g	Burrowed serpy siltstone
2h	Rippled silty mudstone
<b>Facies 3- Mudstones and silts</b>	
3a	Dark grey mudstone
3b	Light grey mudstone
3c	Dark grey burrowed mudstone
3d	Light grey burrowed mudstone
3e	Siltstone
<b>Facies 4- Coal, Coaly mudstone and siltstone</b>	
4a	Coal
4b	Coaly mudstone
4c	Coaly and/or rooted siltstone

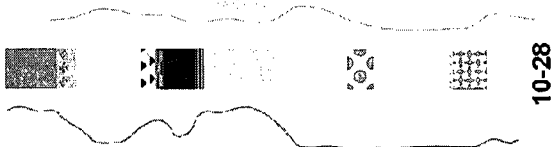
### 3b- Light grey mudstone



10-28



08-21

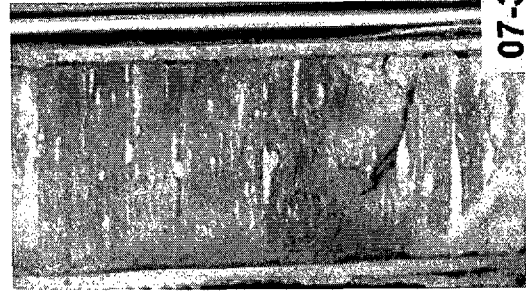


10-28

This facies comprises a light grey to grey mudstone which is also observed massive and fissile. It can measure from centimeters up to 3 meters. It is seen within the basal sandy unit, at the top of the unit and in the unit above the coal. Some bioturbation is present in the facies.

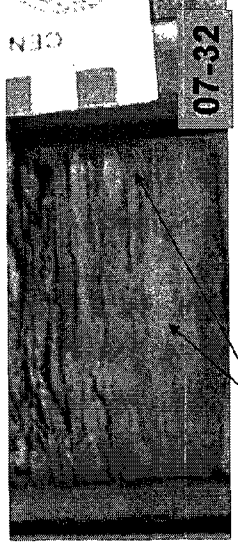
This facies is deposited from suspension fallout in a low energy regime in a more oxidized environment than the black mudstones. This could correspond to flood plain, abandoned channels, and coastal plain settings.

Lithofacies Legend	
<b>Facies 1- Sands</b>	
1a	Cross-bedded sands
1b	Parallel laminated to ripple sands
1c	Parallel laminated or bedded sands
1d	Structureless sands
1e	Moderately bioturbated sands
1f	Sands with concretions
1g	Mud clast breccia
1h	Caliche cemented sands
<b>Facies 2- Heterolithic</b>	
2a	Fining upwards sequence of muds, silts and sands
2b	Sumpier sands, silty mudstones and sandy siltstones
2c	Inclined or interbedded mudstones and rippled to crossbedded sands
2d	Coarsening upwards sequence of mudstones and silty sands
2e	Interbedded sandy siltstones and silty mudstones
2f	Laminated silty mudstone
2g	Burrowed sandy siltstone
2h	Rippled silty mudstone
<b>Facies 3- Mudstones and silts</b>	
3a	Dark grey mudstone
3b	Light grey mudstone
3c	Dark grey burrowed mudstone
3d	Light grey burrowed mudstone
3e	Siltstone
<b>Facies 4- Coal, Coaly mudstone and siltstone</b>	
4a	Coal
4b	Coaly mudstone
4c	Coaly and/or rooted siltstone



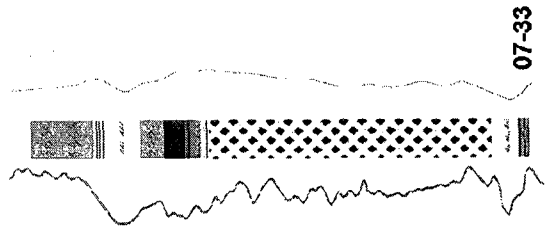
07-33

3c- Burrowed dark grey mudstones.



07-32

Planolites

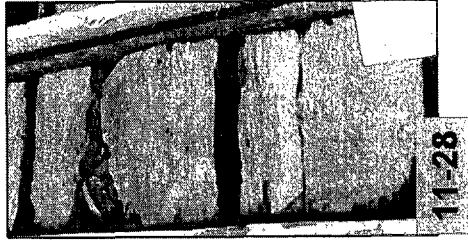


07-33

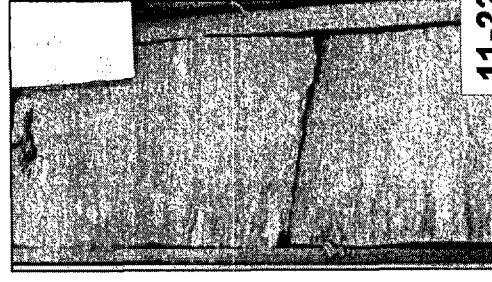
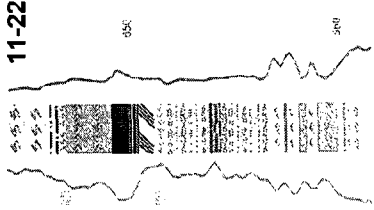
This facies consists of dark grey laminated mudstone with mainly horizontal burrows and is found from centimeters to 4 meters in thickness.

This facies is deposited in an oxygenated organic rich environment. In some cases it is overlying the coaly shale so it can be interpreted as deposited in a lagoon or marsh environment but in other cases that correspond to the thick succession it could correspond to environments that range from marginal marine to marine.

Lithofacies Legend	
<b>Facies 1- Sands</b>	
1a	Cross-stratified sands
1b	Parallel, laminated or rippled sands
1c	Parallel, laminated or bedded sands
1d	Structureless sands
1e	Moderately bioturbated sands
1f	Sands with concretions
1g	Mud-clast breccia
1h	Caliche cemented sands
<b>Facies 2- Heterolithic</b>	
2a	Fining upwards sequence of muds, silts and sands
2b	Slumped sands, silt, mudstones and sandy siltstones
2c	Inclined interbedded mudstones and rippled to crossbedded sands
2d	Coarsening upwards sequence of mudstones and silty sands
2e	Interbedded sandy siltstones and silty mudstones
2f	Laminated silty mudstone
2g	Burrowed silty siltstone
2h	Rippled silty mudstone
<b>Facies 3- Mudstones and silts</b>	
3a	Dark grey mudstone
3b	Light grey mudstone
3c	Dark grey burrowed mudstone
3d	Light grey burrowed mudstone
3e	Siltstone
<b>Facies 4- Coal, Coaly mudstone and siltstone</b>	
4a	Coal
4b	Coaly mudstone
4c	Coaly and/or rooted siltstone



3d- Burrowed light grey mudstone.



This facies consists of light grey mudstone with mainly horizontal burrows. The degree of bioturbation is from moderate to abundant where the primary sedimentary structures are not recognized. The level of diversity is moderate and abundance varies from low to moderate. It is seen associated to many lithofacies at different levels of the cores sections. The thickest interval with this facies is located above the section above the coal in well 11-22 and measures more than two meters.

This facies is deposited from suspension and can be interpreted in a variety of environments from marginal marine (lagoons, protected brackish bay, abandoned estuarine channels) to marine depending on the associated facies and the abundance and diversity of the bioturbation present.

Lithofacies Legend	
<b>Facies 1- Sands</b>	
1a	Cross-stratified sands
1b	Parallel laminated or rippled sands
1c	Parallel laminated or bedded sands
1d	Structureless sands
1e	Moderately bioturbated sands
1f	Sands with concretions
1g	Mud-clast breccia
1h	Calcite cemented sands
<b>Facies 2- Heterolithic</b>	
2a	Fining upwards sequence of muds, silts and sands
2b	Slumped sands, silty mudstones and sandy siltstones
2c	Inclined interbedded mudstones and rippled crossbedded sands
2d	Coarsening upwards sequence of mudstones and silty sands
2e	Interbedded sandy siltstones and silty mudstones
2f	Laminated silty mudstone
2g	Burrowed sandy siltstone
2h	Rippled silty mudstone
<b>Facies 3- Mudstones and siltstones</b>	
3a	Dark grey mudstone
3b	Light grey mudstone
3c	Dark grey burrowed mudstone
3d	Light grey burrowed mudstone
3e	Siltstone
<b>Facies 4- Coal, Coaly mudstone and siltstone</b>	
4a	Coal
4b	Coaly mudstone
4c	Coaly and/or rippled siltstone

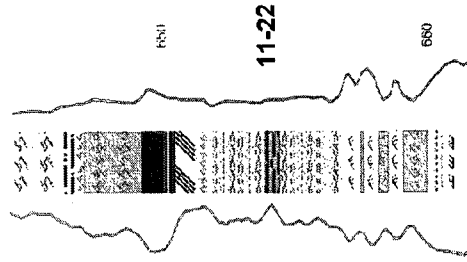
3e- Siltstone.



11-22

This rare facies consist of mainly massive siltstone with rare bioturbation. It centimeters thick and is associated to facies 2g and 3d in the unit above the coal. Minor bitumen staining is observed in some cases. Associated to a fining upward sequence.

This facies could be deposited from rapid suspension fallout during flooding events in coastal plains or flood plains settings.

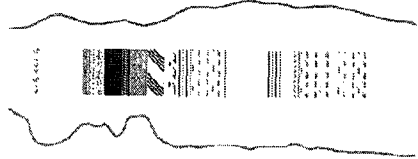


Lithofacies Legend	
<b>Facies 1- Sands</b>	
1a	Cross-stratified sands
1b	Parallel laminated to rippled sands
1c	Parallel laminated or bedded sands
1d	Structureless sands
1e	Moderately bioturbated sands
1f	Sands with compaction
1g	Mud-clast breccia
1h	Calcite oriented sands
<b>Facies 2- Heterolithic</b>	
2a	Fining upwards sequence of muds, silts and sands
2b	Slumped sands, silty mudstones and sandy siltstones
2c	Inclined interbedded mudstones and rippled to crossbedded sands
2d	Coarsening upwards sequence of mudstones and silty sands
2e	Interbedded sandy siltstones and silty mudstones
2f	Laminated silty mudstone
2g	Burrowed sandy siltstone
2h	Rippled silty mudstone
<b>Facies 3- Mudstones and silts</b>	
3a	Dark grey mudstone
3b	Light grey mudstone
3c	Dark grey burrowed mudstone
3d	Light grey burrowed mudstone
3e	Siltstone
<b>Facies 4- Coal, Coaly mudstone and siltstone</b>	
4a	Coal
4b	Coaly mudstone
4c	Coaly eroded rooted siltstone

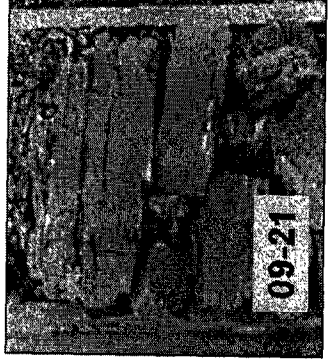
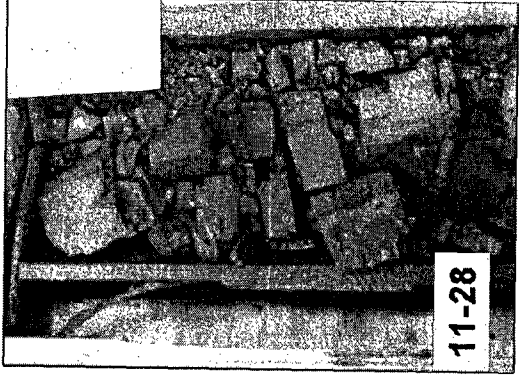
**4a Coal**

This facies consist of up to 1.6 m black, crumbly coal. The coal is thinly banded and shows some carbonaceous shale partings. Yellow spots and bands (sulfur) are observed in some cases. It is commonly associated with an underlying facies 4b.

The coals in the Winter area have been studied by Groeneveld and Stasiuk and bases upon their macerals it was interpreted as formed from marsh peats in a marginal marine setting. Also they determined that it contains very high percentage of mostly organic sulfur.



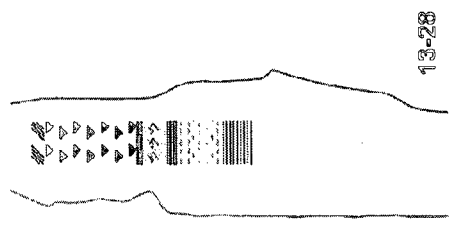
11-28



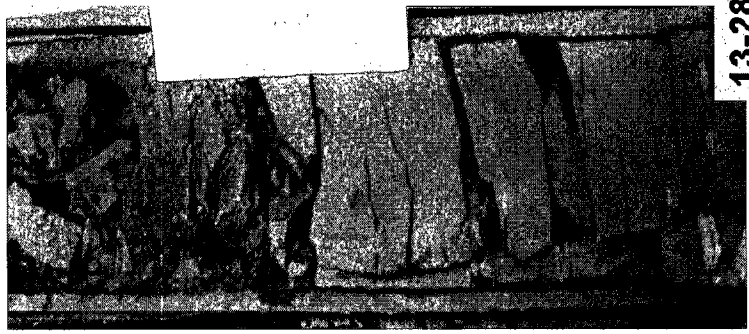
Lithofacies Legend	
<b>Facies 1- Sands</b>	
1a	Cross-stratified sands
1b	Parallel laminated or bedded sands
1c	Structureless sands
1d	Moderately bioturbated sands
1e	Sands with concretions
1f	Mud-clast breccia
1h	Calcite cemented sands
<b>Facies 2- Heterolithic</b>	
2a	Fining upwards sequence of muds, silts and sands
2b	Slumped sands, silty mudstones and sandy siltstones
2c	Inclined interbedded mudstones and siltstones
2d	Coarsening upwards sequence of mudstones and silty sands
2e	Interbedded sandy siltstones and silty mudstones
2f	Laminated silty mudstone
2g	Burrowed serpy siltstone
2h	Rippled silty mudstone
<b>Facies 3- Mudstones and siltstones</b>	
3a	Dark grey mudstone
3b	Light grey mudstone
3c	Dark grey burrowed mudstone
3d	Light grey burrowed mudstone
3e	Siltstone
<b>Facies 4- Coal, Coaly mudstone and siltstone</b>	
4a	Coal
4b	Coaly mudstone
4c	Coaly and/or rooted siltstone

This facies is associated with the coal reaches 50 cm and consist of a blackish massive mudstone. Some locations present yellow spots of possible sulfur. It is normally found associated with 4a but can be seen alone.

This facies is deposited from suspension fallout in non-marine to paralic environments, distal coastal plain with marshes.



4b- Coaly mudstone

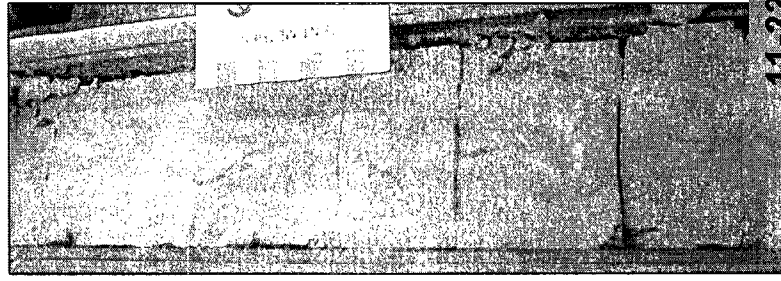
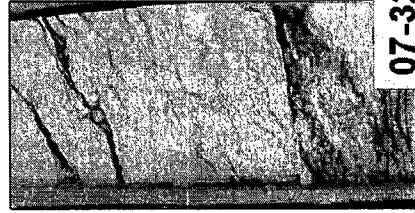
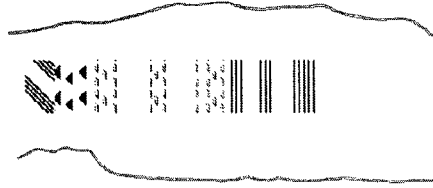


13-28

### Lithofacies Legend

<b>Facies 1- Sands</b>	
1a	Cross-stratified sands
1b	Parallel laminated to rippled sands
1c	Parallel laminated or bedded sands
1d	Structureless sands
1e	Vadically Bioturbated sands
1f	Sands with concretions
1g	Vad. clast breccia
1h	Calcite cemented sands
<b>Facies 2- Heterolithic</b>	
2a	Fining upwards sequence of muds, silts and sands
2b	Stirruped sands, silty mudstones and sandy siltstones
2c	Inclined interbedded mudstones and rippled to crossbedded sands
2d	Coarsening upwards sequence of mudstones and silty sands
2e	Interbedded sandy siltstones and silty mudstones
2f	Laminated silty mudstone
2g	Burrowed sandy siltstone
2h	Rippled silty mudstone
<b>Facies 3- Mudstones and silts</b>	
3a	Dark grey mudstone
3b	Light grey mudstone
3c	Dark grey burrowed mudstone
3d	Light grey burrowed mudstone
3e	Siltstone
<b>Facies 4- Coal, Coaly mudstone and siltstone</b>	
4a	Coal
4b	Coaly mudstone
4c	Coaly and/or rooted siltstone

### 4c- Coaly and/or rooted siltstone



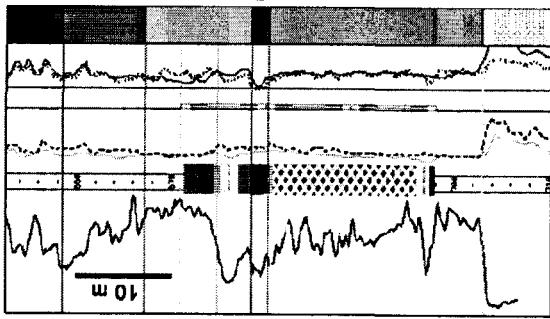
This facies consist of light grey massive, mottled and rooted. Thin carbonaceous laminations are present in some cases. Vertical to sub-vertical roots of up to 12 centimeters long are present. It is commonly found underlying the coaly mudstone and coal and reaches a little over a meter in thickness.

This facies is interpreted as a paleosol that developed in vegetated areas of coastal plain or floodplain areas, and indicates periods of slow sedimentation and subaerial exposure.



**Appendix 3:**

Core and seismic transects



Lithofacies

4a, 4b, 2g, 1c

3c, 1c/1d, 1a, 2g

2b

Unit W

Unit V

07-33

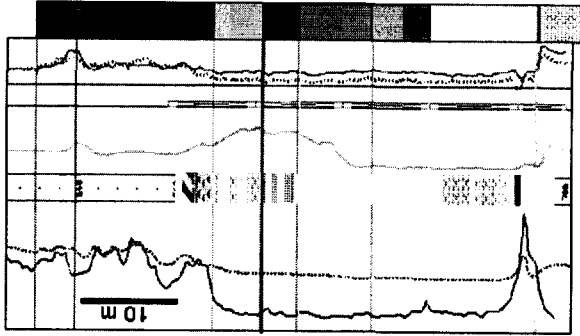


650 ms

700 ms

360 m

Appendix 3



**Lithofacies**

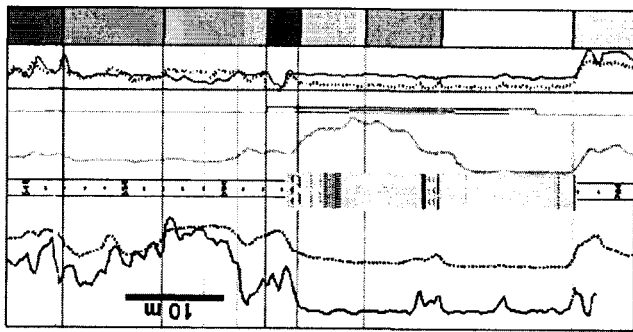
- Unit T 4c,2a
- Unit U 1a,1d
- Unit V 1d,1c
- Unit X 1d
- Unit Y 1d
- Unit Z 1d,1a

07-32



650 ms

700 ms

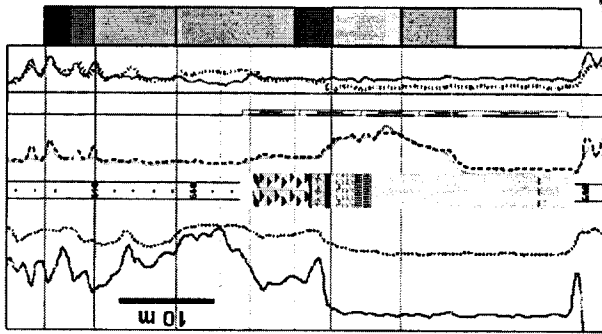


**Lithofacies**

- Unit V  
2a, 3b, 1a
- Unit X  
1d, 1a, 1c
- Unit Y  
1d, 2h, 1b, 3e
- Unit Z  
1d, 1a, 3b



700 ms



**Lithofacies**

- Unit U 2d, 4c
- Unit V 3d, 2d, 2f, 4b, 1a
- Unit X 1a, 1c, 1a, 1d
- Unit Y 1d
- Unit Z 1d, 1a

13-28



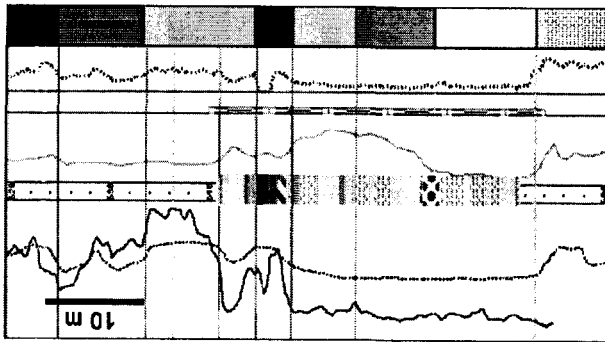
650 ms

700 ms

13-28

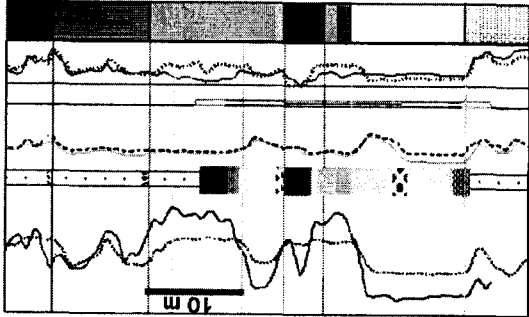
**Lithofacies**

- Unit U 3d, 1d, 2h, 2e
- Unit V 4a, 3c, 4c, 2d, 1a
- Unit X 1c, 1a, 1d
- Unit Y 1a, 1d
- Unit Z 1a, 1f, 1b



11-28





**Lithofacies**

Unit U	3a, 3c/1 a
Unit V	2d, 2f, 4a, 4b, 3b
Unit Y	4a
Unit Z	1d, 1a, 1f, 1h

10-28

